

## **CONTENIDO**

### **PARTE I Publicaciones y trabajos enviados a Congresos y/o Seminarios**

STANDARD SYLLABUS FOR POSTGRADUATE EDUCATIONAL COURSES IN RADIATION PROTECTION AND THE SAFE USE OF RADIATION SOURCES ARGENTINE ADOPTION AND ADAPTATION Arias, C.; Biaggio, A.L. and Nasazzi, N.B.	3
TRAINING ON RADIOISOTOPES TECHNIQUES AND RADIOPROTECTION ASPECTS AT THE SCHOOL OF PHARMACY AND BIOCHEMISTRY OF THE BUENOS AIRES UNIVERSITY (ARGENTINA) Bergoc, R.M.; Rivera, E.S. and Bomben, A.M.	13
RADIOPHARMACEUTICAL ACTIVITIES ADMINISTERED FOR DIAGNOSTIC AND THERAPEUTIC PROCEDURES IN NUCLEAR MEDICINE IN ARGENTINE: RESULTS OF A NATIONAL SURVEY Bomben, A.M. and Chiliutti, C.A.	23
ENVIRONMENTAL RADIOLOGICAL SURVEILLANCE AROUND NUCLEAR POWER PLANTS IN ARGENTINA Ciallella, H.E.; Fernandez, J.A.; Gavini, R.M.; Lewis, E.C. and Quintana, E.E.	33
EVALUATION THROUGH COMET ASSAY OF DNA DAMAGE INDUCED IN HUMAN LYMPHOCYTES BY ALPHA PARTICLES. COMPARISON WITH PROTONS AND CO-60 GAMMA RAYS Di Giorgio, M.; Kreiner, A.J.; Schuff, J.A.; Vallerga, M.B; Taja, M.R.; López, F.O.; Alvarez, D.E.; Saint Martin, G.; Burlón, A.; Debray, M.E.; Kesque, J.M.; Somacal, H.; Stoliar, P.; Valda, A.; Davidson, J.; Davidson, M.; Ozafrán, M.J. and Vázquez, M.E.	41
ASSESSMENT OF INDIVIDUAL RADIOSENSITIVITY IN HUMAN LYMPHOCYTES USING MICRONUCLEUS AND MICROGEL ELECTROPHORESIS "COMET" ASSAYS Di Giorgio, M.; Sardi, M.; Busto, E.; Vallerga, M.B.; Taja, M.R. and Mairal, L.	51
DOSIMETRÍA BIOLÓGICA EN ACCIDENTES DE CRITICIDAD. EJERCICIO DE INTERCOMPARACIÓN EN EL REACTOR SILENE – FRANCIA Di Giorgio, M.; Vallerga, M.B. y Taja, M.R.	61
TELOMERASE AND APOPTOSIS IN HUMAN HEMATOPOIETIC CELL LINES: MODULATION OF THE RADIATION RESPONSE BY PHARMACOLOGICAL INHIBITION OF DNA REPAIR ENZYMES Dubner, D.L.; Pérez, M. del R.; Michelin, S.C.; Bourguignon, M.; Carosella, E.D. and Gisone, P.A.	73
UNA METODOLOGÍA MEJORADA PARA EL ANÁLISIS DE ESPECTROS ALFA Equillor, H.E.	85
RESULTADOS DE LA PARTICIPACIÓN DE LA ARN EN EL PROGRAMA DE GARANTÍA DE CALIDAD DEL EML- DOE PERÍODO 2002-2004 Equillor, H.E.; Serdeiro, N.H.; Fernández, J.A.; Gavini, R.M.; Grinman, A.D.R.; Lewis, E.C. y Palacios, M.A.	95
RADIATION-INDUCED APOPTOSIS OF NEURAL PRECURSORS CELL CULTURES: EARLY MODULATION OF THE RESPONSE MEDIATED BY REACTIVE OXYGEN AND NITROGEN SPECIES (ROS/RNS) Gisone, P.A.; Dubner, D.L.; Robello, E.; Michelin, S.C. and Perez, M. del R.	105
THE ARN CRITICAL DOSIMETRY SYSTEM Gregori, B.N.; Papadópolos, S.; Cruzate, J.A.; Equillor, H.E. and Kunst, J.J.	115
CONCEPTUAL ANALYSIS OF THE FUEL MANAGEMENT STRATEGY FOR THE RA-3 RESEARCH REACTOR AT 10 MW Lerner, A.M.; Madariaga, M.R. and Waldman, R.M.	123

CÓDIGO DE EVALUACIÓN DE DOSIS DEBIDA A LA DESCARGA DE EFLUENTES LÍQUIDOS DE LA CENTRAL NUCLEAR EMBALSE López, F.O.; Boutet, L.I.; Bruno, H.A. y Gavini, R.M.	135
PASSIVE METHOD FOR THE EQUILIBRIUM FACTOR DETERMINATION BETWEEN $^{222}\text{Rn}$ GAS AND ITS SHORT PERIOD PROGENY López, F.O. and Canoba, A.C.	145
1994 – 2004, TEN YEARS OF TOTAL SAFEGUARDS APPLICATION Saavedra, A.D. and Maceiras, E.	155
RETROSPECTIVE BIOLOGICAL DOSIMETRY BY FISH AND ALTERNATIVE TECHNIQUES Nasazzi, N.B.; Mühlmann, M. and Otero, D.	165
LA PROTECCIÓN RADIOLÓGICA DEL PACIENTE: MARCO CONCEPTUAL, NUEVAS RECOMENDACIONES A NIVEL INTERNACIONAL Gisone, P.A. y Perez, M. del R.	175
APOPTOSIS OF NEURAL PRECURSOR CELLS FOLLOWING GAMMA IRRADIATION IS EARLY MODULATED BY FREE RADICALS Robello, E.; Dubner, D.L.; Michelin, S.C.; Perez M. del R.; Puntarulo, S. and Gisone, P.A.	183
NDA MEASUREMENTS FOR ISOTOPIC HOMOGENEITY OF UO <sub>2</sub> POWDER FROM MECHANICAL BLENDING AND RESULTS COMPARISON BETWEEN GAMMA AND MASS SPECTROMETRY Rojas, C.A.; Rojo, M. y Cristallini, O.	191
DOSIMETRÍA INTERNA EN MEDICINA NUCLEAR: DOSIS ABSORBIDA EN EL FETO POR LA ADMINISTRACIÓN DE RADIOFÁRMACOS A LA MADRE Rojo, A.M. y Michelin, S.C.	201
PROCEDIMIENTO PARA LA DETERMINACIÓN DE EMISORES ALFAS EN MUESTRAS DE ORINA Y HECES Serdeiro, N.H.	217
PRIMER EJERCICIO DE INTERCOMPARACIÓN PARA LA ARGENTINA ORGANIZADO POR LA ARN PARA LA DETERMINACIÓN DE URANIO EN MUESTRAS DE AGUA Y ORINA Serdeiro, N.H. y Equillor, H.E.	237
A RAPID METHOD FOR DETERMINATION OF URANIUM, AMERICIUM, PLUTONIUM AND THORIUM IN SOILS SAMPLES Serdeiro, N.H. and Marabini, S.	245
SAFETY ASSESSMENT OF RADIOACTIVE WASTE MANAGEMENT OPERATIONS IN TYPE I FACILITIES Siraky, G. and Medici, M.A.	253
ON THE RADIATION PROTECTION OF THE ENVIRONMENT Sobehart, L.J. ; Clausse, A. and D'Amato, E.	263
THE RADIOACTIVE SOURCES TREATED AS SCRAP - REGULATORY ASPECTS, CONTROL AND SECURITY Truppa, W.A. and Cateriano, M.	273
ATUCHA I NUCLEAR POWER PLANT ACHIEVING A FULL SAFEGUARDS APPROACH Valentino, L.I.; Fernandez Moreno, S.; Llacer, C.D. and Bonino, A.D.	283
CALIBRACIÓN DE UN SISTEMA DE ESPECTROMETRÍA MULTIESFERA PARA CAMPOS DE NEUTRONES Carelli, J.L.; Cruzate; J.A.; Papadópolos; S.; Gregori; B.N. y Ciocci, L	291
CARACTERIZACIÓN DE LOS DETECTORES TERMOLUMINISCENTES LiF:Mg,Cu,P APLICACIONES A LA DOSIMETRÍA AMBIENTAL Ciocci Brazzano, L.; Gregori, B.N.; Papadópolos, S. y Carelli, J.L.	297

**PARTE II**  
**Resúmenes de publicaciones en revistas**

CHROMOSOME ABERRATIONS INDUCED IN HUMAN LYMPHOCYTES BY HEAVY CHARGED PARTICLES IN TRACK SEGMENT MODE Di Giorgio, M.; Edwards, A.A.; Moquet, J.E.; Finnion, P.; Hone, P.A.; Lloyd, D.C.; Kreiner, A.J.; Schuff, J.A.; Taja, M.R.; Vallerga, M.B.; López, F.O.; Burlón, A.; Debray, M.E. and Valda, A.	305
PHARMACOLOGICAL INHIBITION OF DNA REPAIR ENZYMES DIFFERENTIALLY MODULATES TELOMERASE ACTIVITY AND APOPTOSIS IN TWO HUMAN LEUKAEMIA CELL LINES Dubner, D.L.; Perez, M. del R.; Michelin, S.C.; Bourguignon, M.; Moreau, P.; Carosella, E.D. and Gisone, P.A.	306
INTEGRATED SAFEGUARDS: EXPECTATIONS AND REALITIES Fernández Moreno, S.	307
THE EFFECT OF WALL FRICTION IN SINGLE-PHASE NATURAL CIRCULATION STABILITY AT THE TRANSITION BETWEEN LAMINAR AND TURBULENT FLOW Ambrosini, W.; Forgione, N.; Ferreri, J.C.; Bucci, M.	308
THE ROLE OF NITRIC OXIDE IN THE RADIATION-INDUCED EFFECTS IN THE DEVELOPING BRAIN Gisone, P.A.; Dubner, D.L.; Perez, M. del R.; Michelin, S.C. and Puntarulo, S.	309
INCREASED ACTIVITY AND INVOLVEMENT OF CASPASE-3 IN RADIATION-INDUCED APOPTOSIS IN NEURAL CELLS PRECURSORS FROM DEVELOPING RAT BRAIN Michelin, S.C.; Perez, M. del R.; Dubner, D.L. and Gisone, P.A.	310
LISTADO DE AUTORES	311



## **PARTE I**

### **PRESENTACIONES Y TRABAJOS ENVIADOS A CONGRESOS Y/O SEMINARIOS**



# Standard Syllabus for Postgraduate Educational Courses in Radiation Protection and the Safe Use of Radiation Sources

## Argentine Adoption and Adaptation

Arias, C.; Biaggio, A.L. and Nasazzi, N.B.



# **Standard Syllabus for Postgraduate Educational Courses in Radiation Protection and the Safe use of Radiation Sources**

## **Argentine Adoption and Adaptation**

**Arias, C.<sup>1</sup>, Biaggio, A.L.<sup>2</sup> and Nasazzi, N.B.<sup>2</sup>**

<sup>1</sup> Universidad de Buenos Aires

<sup>2</sup> Autoridad Regulatoria Nuclear

**Abstract.** The International Atomic Energy Agency (IAEA) published the Standard Syllabus for Post Graduate Educational Courses in Radiation Protection and the Safety of Radiation Sources in 2002. Along more than two decades, Argentina has obtained valuable experience on building professional knowledge at postgraduate level in Radiation Protection and Nuclear Safety. Such experience made advisable to review the IAEA Standard Syllabus and to modify it accordingly. The whole content of the Standard Syllabus is included in the syllabus developed for the Argentinean Regional Post Graduate Course in Radiation Protection and Safety of Radiation Sources. But a few additional topics were incorporated and changes were introduced in the sequence of subjects. The paper describes those modifications and explains the pedagogic motivations that induce them.

### **1. Introduction**

The International Atomic Energy Agency (IAEA) published the final version of a Standard Syllabus for Post Graduate Educational Courses in Radiation Protection and the Safe Use of Radiation Sources in 2002 [1]. This IAEA Standard Syllabus (SS) is considered to be the model for developing national or regional Post Graduate Courses in the world. This remarkable task started after publication of Safety Series 115 and related Safety Guides includes extensive references and a comprehensive list of practical exercises.

The SS consists of a list of minimum contents in a proposed sequence. It seems that the structure of IAEA Safety Series 115 Publication has influenced the SS conception somehow. It is understood that in adopting the SS the educational institutions would have enough flexibility to determine the most convenient sequence of subjects and, to some extent, their relative relevance.

Argentina has a long tradition in running a Regional Postgraduate Educational Course in Radiation Protection and Nuclear Safety. Significant experience on building professional knowledge at postgraduate level for both national and foreign professionals, coming mainly from other Latin America countries, has been obtained along more than two decades. However, the SS was a convenient input for reconsidering the whole training policy in Argentina.

The last Post Graduate Course in Radiation Protection and Nuclear Safety was run in Buenos Aires in the year 2002, and the SS was directly applied -as it was published by IAEA - to the first part of such course (i.e., the one dealing with Radiation Protection). After reviewing the whole policy regarding the Post Graduate Course during the second half of 2002, it was decided to organize two Post Graduate Courses in Argentina, the first one dealing with Radiation Protection and Safety of Radiation Sources and the second one in Nuclear Safety, starting in 2003 [2] [3].

In order to implement such changes syllabuses for both courses were developed. The SS and the experience obtained since 1980 to 2002 in Argentina, particularly, the analysis of the direct application

<sup>1</sup> Universidad de Buenos Aires, Av. Paseo Colón 850, Dep.de Física, CPA 1063 Buenos Aires, Argentina,

<sup>2</sup> Autoridad Regulatoria Nuclear, Av. del Libertador 8250, CPA C1429BNP, Buenos Aires, Argentina

of SS during 2002 were taken into account for developing the syllabus of the new Post Graduate Course in Radiation Protection and Safety of Radiation Sources.

Consequently, Argentina adopted the SS but modifications were introduced to achieve the best use of resources having in mind the domestic experience. The prevailing criteria for deciding changes were the consideration of student effort and time devoted to every subject, the logic way of linking matters attending to the conceptual hierarchy of knowledge and the optimization of student performance through a gradual and accumulative application of previously imparted knowledge.

## **2. Argentine background in Postgraduate Education in Radiation Protection and Safe use of Radiation Sources**

In 1977 the Regulatory Branch of Atomic Energy Commission (CNEA) decided to create a full time course on Radiation Protection and Nuclear Safety aimed at covering internal needs of the CNEA and related organizations (Operators and Regulators).

By the end of 1978 it was decided to confer a formal academic status to the course. An agreement was then signed between the Engineering School of the University of Buenos Aires, the Ministry of Health and the CNEA. The first Postgraduate Course on Radiation Protection and Nuclear Safety (PGCRPNS) was run in 1980. The International Atomic Energy Agency (IAEA) has supported the course since that year, mainly by granting scholarships to Latin America university graduates.

The role of the regulatory branch of the CNEA in Argentina in running the course was assumed by a new independent organization, the Nuclear Regulatory Authority (ARN), in 1994.

The table below summarizes the number of participants in the PGCRPNS since 1980 to 2002.

Table 1. Number of participants by country in the PGCRPNS, 1980 - 2002

Country	Participants	Country	Participants	Country	Participants
Algeria	4	Argentina	286	Bolivia	23
Brazil	26	Colombia	26	Costa Rica	10
Cuba	38	Chile	25	Ecuador	23
El Salvador	6	Spain	1	Philippine	7
Guatemala	11	Haiti	2	Morocco	1
Mexico	20	Nicaragua	6	Panama	9
Paraguay	11	Peru	40	Poland	1
Dominican Rep	6	Romania	1	Uruguay	19
Yugoslavia	1	Venezuela	29	Vietnam	1
Zaire	2				
<b>Total: 635</b>					

As mentioned, two courses were run in 2003 instead of the original one. One Post Graduate Course in Radiation Protection and Safety of Radiation Sources with an extension of 25 weeks and one Post Graduate Course in Nuclear Safety with an extension of 10 weeks.

During the year 2003, 27 professionals participated in the new Post Graduate Course in Radiation Protection and Safety of Radiation Sources (14 from abroad) and 16 professionals in the new Post Graduate Course in Nuclear Safety (7 from abroad).

### 3. The IAEA Standard Syllabus and the Argentine Adaptation

Table 2. The IAEA Standard Syllabus and the Argentine adaptation (AS)

<b>IAEA STANDARD SYLLABUS</b>	<b>ARGENTINE ADAPTED SYLLABUS</b>
P1- REVIEW OF FUNDAMENTALS	<b>SCIENTIFIC MATTERS</b>
P2- QUANTITIES AND MEASUREMENTS	C1- REVISION OF FUNDAMENTAL CONCEPTS
P3- BIOLOGICAL EFFECTS OF IONISING RADIATIONS	C2- INTERACTION BETWEEN RADIATION AND MATTER
P4- PRINCIPLES OF RADIATION PROTECTION AND THE INTERNATIONAL FRAMEWORK	C3- RADIATION SOURCES
P5- REGULATORY CONTROL	C4- QUANTITIES AND UNITS
P6- ASSESSMENT OF EXTERNAL AND INTERNAL EXPOSURES	C5- BIOLOGICAL EFFECTS OF IONISING RADIATIONS
P7- PROTECTION AGAINST OCCUPATIONAL EXPOSURES	C6- PRINCIPLES OF RADIATION PROTECTION AND INTERNATIONAL FRAMEWORK
P8- MEDICAL EXPOSURES IN DIAGNOSTIC RADIOLOGY, RADIOTHERAPY AND NUCLEAR MEDICINE	<b>GENERIC TECHNICAL MATTERS</b>
P9- EXPOSURE OF THE PUBLIC DUE TO PRACTICES	C7- INSTRUMENTATION AND MEASUREMENTS
P10- INTERVENTIONS IN SITUATIONS OF CHRONIC AND EMERGENCY EXPOSURES	C8- ASSESSMENTS OF EXTERNAL AND INTERNAL EXPOSURE
P11- TRAINING THE TRAINERS	C9- RADIATION PROTECTION AND SAFETY OF SOURCES TECHNOLOGY
(P): Part	<b>SPECIFIC TECHNICAL MATTERS</b>
	C10- RADIATION PROTECTION OF WORKERS
	C11- RADIATION PROTECTION OF PUBLIC
	C12- RADIATION PROTECTION OF PATIENTS
	C13- RADIATION PROTECTION OF WORKERS PUBLIC AND PATIENTS IN SPECIFIC FACILITIES
	C14- INTERVENTION IN PRE-EXISTING EXPOSURES
	<b>REGULATORY MATTERS</b>
	C15- REGULATORY ASPECTS
	C16- TRAINING THE TRAINERS
	(C): Chapter

#### **4. What is different in Argentina Adapted Syllabus (AS)?**

##### ***Classification of knowledge***

When adopting the SS, Argentina considered convenient to modify the distribution of subjects and to open new chapters. However, the overall content of SS is included in Argentine Syllabus (AS).

The classification of knowledge in categories according to their nature helped to order subjects and to decide the opening of new chapters. The categories are the following:

##### **Scientific Matters**

##### **General Technical Matters**

##### **Specific Technical Matters**

##### **Regulatory Matters**

**Scientific Matters** includes all Physical and Biological knowledge on which Radiation Protection is founded. Definition of Quantities and Units are considered here since they are directly related to basic physical and biological aspects of interaction of radiation and matter. The Principles of Radiation Protection are also included because the philosophy of Radiation Protection and Safety has been developed from the scientific knowledge.

**General Technical Matters** refers to basic technology common to every aspect of radiation protection practice irrespective of radiation source and kind of people to protect. It includes Measurements and Instrumentation, Assessment of External and Internal Exposures and Radiation Protection and Source Safety Technology.

**Specific Technical Matters** includes particular considerations on Radiation Protection and Safety of Sources for protection of Workers, members of the Public and Patients in the prevailing circumstances determined by most common radiation sources and facilities.

**Regulatory Matters** refers to regulatory control organization and regulatory responsibilities. Training of Trainers is included here due to its relevance in regulatory control.

##### ***New Chapters***

Pedagogic considerations advised to modify somehow the sequence of subjects presented in the SS. In addition, new chapters were opened for rising the attention to important matters and to include subjects whose significance remains hidden in the SS because, despite of their common nature, they are spread into various chapters. The order of titles helps to describe the logic sequence of ideas and concepts in the education of radiation protection specialists.

The following subjects have deserved specific chapters:

##### **Interaction between Radiation and Matter**

##### **Radiation Sources**

##### **Measurements and Instrumentation**

##### **Radiation Protection Technology**

##### **Radiation Protection in Specific Facilities**

Items included in these chapters are considered in the SS but distributed in different chapters without having a particular entity.

**Interaction between Radiation and Matter** deserves a particular chapter because various fundamental concepts in Radiation Protection are based on a good understanding of how matter and radiation modify themselves when interact. Biological Effects of radiations, definition of Quantities and Units, Radiation Detection and Measurements, Radiation Shielding and the physical aspects of every Radiation Applications are good examples.

**Radiation Sources** deserves a particular chapter because its presentation allows opening the whole spectrum of radiation applications at the beginning of the course. It also allows making the first comments on radiation protection needs. The subject appears again in the Radiation Protection for Specific Facilities Chapter.

**Measurements and Instrumentation.** The specialist in radiation protection has to develop capabilities to carry out measurements in different circumstances using the proper instrumentation. The relevance of these subjects makes advisable to have a specific chapter for it. In such a way Measurements and Instrumentation are studied as a **technical** matter after having considered Quantities and Units as a **scientific** matter. In SS the presentation of Quantities and Units and their Measurement are included in the same Part. The deep comprehension of Quantities and Units is very significant and should not to be disturbed by the study of one of its applications.

**Radiation Protection Technology** The knowledge about technical ways of reducing exposures (external and internal), reducing probabilities of potential exposures, safe transport of radioactive material and safe management of radioactive wastes are spread into various chapters related to protection of workers, members of the public and patients in the SS. It seemed reasonably to congregate all substantial technological knowledge in one chapter before starting to consider the protections of workers, members of the public and patients.

When splitting the old Argentine course in Radiation Protection and Nuclear Safety into the two present courses there was a significant concern about the convenience of including the essential tools of safety for preventing accidents and reducing their consequences in the new syllabus for the Post Graduate Course in Radiation Protection and Safety of Radiation Sources. This subject was considered of outstanding relevance because of the several accidents involving radiation sources with very severe consequences for workers, members of the public and patients occurred in the last 20 years. Although the subject is somehow addressed in the SS, the Argentinean Syllabus (AS) put a significant emphasis in the technology for protecting against potential exposures.

**Radiation Protection in Specific Facilities.** This subject is included in the workers protection chapter of the SS. However, problems of radiation protection can involve workers, members of the public and patients in case of medical facilities. It seems convenient to open a specific chapter for presenting examples of the design and operational factors aimed at protecting workers, members of the public and, patients in case of medical facilities, embracing both normal and potential exposures, for each type of facility.

#### *Modification in the Subject Sequence*

**Regulatory Control** This subject is placed immediately after Principles of Radiation Protection in SS. However, they are of very different nature. Radiation Protection philosophy is directly related to scientific knowledge in Physics and Biology and involves deep concepts in the nature of radiation Risks and the criteria to define the ambition in limiting them. Regulatory Control deals with administrative and technical questions to put into practice the philosophy. There is a big gap between both. To understand the complexities of Regulatory Control students must have some previous knowledge on evaluation of doses and risks and technological methods of dose reduction and safety improvement applied to the specific protection of workers, members of the public and patients.

Therefore, Regulatory Control was placed almost at the end of the course in AS. However, in the Principles of Radiation Protection chapter a brief introduction to the implementation of Radiation Protection is included.

**Protection of Patients:** This chapter is placed between Protection of Workers and Protection of Members of the Public in the SS as it is in Safety Series 115. However there are much more similarities between protection of workers and protection of member of the public despite the magnitudes of allowed doses and methods of control. Protection of patients requires particular interpretation of Principles of Radiation Protection. Therefore, Protection of Patients is presented after Protection of Workers and Protections of members of the Public in the AS.

## 5. Total time and its distribution - Relative weigh in time

The total time assigned to the Course on Radiation Protection and the Safety of Radiation Sources is 25 weeks, five days per week, full time. Time assigned to tutorial activities, evaluations, conferences, technical visits, seminars, opening and ending days and special holydays is around 6 weeks. Table 3 shows the distribution of theoretical classes and practical exercises per Chapter.

Table 3: Time assigned to chapters

Chapter	Weeks	%
1	1.6	8.4
2	1	5.3
3	0.6	3.2
4	0.8	4.2
5	1	5.3
6	0.6	3.2
7	2.2	11.6
8	2	10.5
9	2.2	11.6
10	1.2	6.3
11	0.8	4.2
12	1	5.2
13	1.4	7.3
14	0.8	4.2
15	1	5.2
16	0.8	4.2
Total	19	100

## 6. Formative and Informative Knowledge

The time assigned to each category of knowledge is approximately:

SCIENTIFIC MATTERS	5.6 weeks	(30 %)
GENERAL TECHNICAL MATTERS	6.4 weeks	(33 %)
SPECIFIC TECHNICAL MATTERS	5.2 weeks	(27 %)
REGULATORY MATTERS	1.8 weeks	(10 %)

The first two categories are considered the core of fundamental knowledge for Radiation Protection specialists. The concepts involved are **formative** and to assure their good and deep understanding is of

primary significance in argentine course. The total time devoted to them is 12 weeks or 63 % of total time.

These last two categories provide students with a significant amount of **informative** knowledge whose deep meaning will be fully understood as long as professionals will acquire expertise being actively engaged in Radiation Protection work. The total time devoted to them is 7 weeks or 37 % of total time

## **7. Conclusions**

The SS has been the result of time and effort devoted by many experts in Radiation Protection and Radiation Protection Education along several years. The output is a very comprehensive document and a useful guide to organise postgraduate courses on Radiation Protection and Safe Use of Radiation Sources.

Argentine professionals devoted time and effort to revision of the SS with the purpose of conciliating that expertise with the experience obtained along 23 years in postgraduate educational courses on that subject. This may be an endless task but the present version of argentine adaptation of the SS, it is to say the AS, has already proved to be reasonable good for the Regional Course carried out in Buenos Aires in 2003.

## **References**

1. IAEA, *Standard Syllabus for Post Graduate Educational Courses in Radiation Protection and the Safety of Radiation Sources*, Training Courses Series Nº18 (2002)
2. Argentine Postgraduate Course in Radiation Protection and The Safe Use of Radiation Sources, *Syllabus* (2003)
3. Argentine Postgraduate Course in Nuclear Safety, *Syllabus* (2003)



# Training on Radioisotopes Techniques and Radioprotection Aspects at the School of Pharmacy and Biochemistry of the Buenos Aires University (Argentina)

Bergoc, R.M.; Rivera, E.S. and Bomben, A.M.



## **Training on Radioisotopes Techniques and Radioprotection Aspects at The School of Pharmacy and Biochemistry of the Buenos Aires University (Argentina)**

**Bergoc, R.M.<sup>(1)</sup>; Rivera, E.S.<sup>(1)</sup> and Bomben, A.M.<sup>(2)</sup>**

<sup>(1)</sup> Radioisotopes Laboratory, School of Pharmacy and Biochemistry, Buenos Aires University, 956 Junín St., 1113-Buenos Aires, ARGENTINA. <sup>(2)</sup> Nuclear Regulatory Authority, 8250 Libertador Ave., 1429-Buenos Aires, ARGENTINA. [rmbbergoc@ffyb.uba.ar](mailto:rmbbergoc@ffyb.uba.ar) / [abomben@sede.arn.gov.ar](mailto:abomben@sede.arn.gov.ar)

**Abstract.** The use of ionizing radiation sources and radioisotopes in Argentina takes place at more than 1700 facilities, which operate in Nuclear Medicine, in telecobalotherapy, in Industry, in Biochemistry, and in research. All of these centers have one or more professionals trained in the specific field of radioprotection and they have been authorized by the Nuclear Regulatory Authority. At the School of Pharmacy and Biochemistry of the Buenos Aires University, Argentina, we consider of great interest to teach radioisotopes methodology at different levels, to harmonize the use of these methodologies with environmental preservation and to provide education and training on radioprotection. Currently, the school offers five different courses in all of which the radioprotection is one of the most important subjects: 1) Course on Methodology of Radioisotopes for students at the undergraduate level, in the Biochemistry Career (140 hrs). Since 1960, more than 6000 students have passed their examinations. 2) Course on Methodology of Radioisotopes for post-Graduates in Biochemistry, Biology, Chemists or other related disciplines. 3) Course for Graduates in Medicine. Since 1962, the School delivers every year these two courses. Their syllabus (212 hrs) dedicates a 50% of the time schedule to subjects related to radioprotection aspects. More than 1800 professionals have passed their examinations, many of them from different Latin American countries. 4) Up-date on Methodology of Radioisotopes (100 hrs) a course delivered since 1992 for professionals wishing to up-date their knowledge. 5) Course for Technicians in Nuclear Medicine (more than 200 hrs). At present, this course is the basic level of the Technicians in Nuclear Medicine Career. At the present paper it will be presented statistics regarding the different courses and the experience that has been gathered for the last 40 years organizing courses and carrying out research activity on radiobiology, radioimmunoanalysis, radioreceptors and radiopharmacy.

**1. Introduction.** The application of the techniques employing radioisotopes to cellular and molecular biology, biochemistry and pharmacology for the last 50 years is one of the reasons that explains the notorious advance in these sciences. These techniques have found a field of study particularly promising in the metabolism and biodistribution of pharmaceutical drugs, pharmacodynamics, etc. Besides, radioisotopes and radiation are frequently employed in medicine for diagnosis as well as for therapy of malignant and non-malignant diseases. Radiopharmaceutical and radiations of different types are extensively used for therapeutic protocols. Moreover, radiometric techniques are a methodology routinely employed in human endocrinology and general clinic and, also, in veterinary and agriculture; receptor characterization by radiometric techniques is very important in basic and clinical investigations and their quantification has clinical use in pharmacology and in medicine. Therefore, the importance of the training in different methodologies for the use of radioisotopes has also been growing noticeably.

Early in the 1960s the School of Pharmacy and Biochemistry of the University of Buenos Aires introduced as an optional course the subject Physic III, which provided students with the basis of radioactivity. This Course was given at the Radioisotopes Laboratory and, very soon, it became apparent both for teachers and students that, owing to the growing use of this methodology, this subject should be compulsory for all the biochemistry students. Hence it was added to the syllabus of the Biochemistry Career.

As a result of the researches performed in our Laboratory employing radioisotope techniques and their use in many fields, it has been evident that it is essential for biomedicine graduates to be able to manage radioactive materials prudently and safely.

Thus, the School currently offers five different Courses on Radioisotopes Methodology in which Radiological Protection is focused from different points of view according to the students background, but always as a fundamental subject; the courses are: 1) Course on Methodology of Radioisotopes for undergraduate Biochemistry students; 2) Course on Methodology of Radioisotopes for Biochemistry,

Biology, Chemists (and other related disciplines) post-Graduates; 3) Course for Medicine post-Graduates; 4) Up-date on Methodology of Radioisotopes; 5) Course for Nuclear Medicine Technicians.

The objective of the present paper is to provide a description of the scope and structure of these courses as well as the goals achieved.

## **2. Organization of the Courses and Results.**

### ***2.1. Undergraduate Course.***

This Course started in 1960 as a part of the general subject Physic. It provided students with the basic knowledge on radioactivity and measurement techniques and, owing to changes in the Biochemistry Career syllabus, it became first an optional subject called Radiochemistry and, later, a compulsory one called Radioisotopes Methodology.

The Course is given at the Radioisotope Laboratory of the School of Pharmacy and Biochemistry, University of Buenos Aires, and the students attend to a 140 hour (84 hours of theory and 56 hours of practical work). The theoretical syllabus of the course includes a first part of basic and general concepts and a second part with all the specific applications of radioisotopes to biochemistry. The practical syllabus is focused on the basic and general aspects of radioisotopes but emphasizing those that are of specific significance to biochemistry, both in hospitals and in research, as this will be the students' future working field.

Besides, the objective of the training in radioprotection at undergraduate level in Biochemistry is to give guidelines for the adequate application of radioactive materials and the radioprotection philosophy, with special emphasis on biochemical-clinical practices and on radioisotope techniques utilized in different research areas. Students tend either to neglect or to enhance radiological risks associated with the work with radioisotopes due to lack of knowledge. In this sense, students are led to acquire adequate criteria by the analysis of different practical situations.

One of the most common practices with radioisotopes in Argentina at biochemical level for the diagnosis of different diseases is the labeling of molecules with  $^{125}\text{I}$  and their utilization on different radiometric assays. Then, we analyze the decay scheme of  $^{125}\text{I}$  and give the calculus of estimate dosimetry for workers in different operational situations as radiolabeled of proteins and radiometric assays.

Up to the present, more than 6200 students have been trained in our classrooms (Figure 1).

### ***2.2. Course on Methodology of Radioisotopes for post-Graduates in Biomedicine.***

The Course on Methodology of Radioisotopes for Biomedicine post-Graduates began in 1962.

The basic syllabus includes: Nuclear stability. Binding Energy. Nuclear models. Radioactive decay mechanisms and kinetic equations. Particles and radiation interaction mechanisms. Instrumentation: ionization chamber, proportional counters, Geiger-Müller tubes, mono and bidimensional radiochromatograph analyzers, solid and liquid scintillation spectrometry, solid state detectors, radioautography, activity determination. Detection efficiency. Statistics of radioactivity measurements. The specific syllabus includes: Production of radioisotopes and radiopharmaceutical materials. Purity control criteria. Activation analysis. Biochemical applications of radioisotopes. Radiometry: radioimmunoassay and radioreceptor characterization and determination.

The training in Radiological Protection is theoretical and practical. It encompasses the study of the general principles of radioprotection, quantities, dosimetric units, internal and external dosimetry of nuclides for diagnosis and therapy, with the needed amplitude according to each specialty, barriers to

avoid contamination, shielding, management of radioactive wastes, national and international legislations.

This Course has been designed to enable graduates in biomedicine to:

- Acquire criteria for the adequate application of the radioprotection philosophy, independently of the previous university training the graduates attending the course have, emphasizing the importance of this practice as well as the potential environmental impact that it may have,
- Planning professional practices with an adequate training of the personnel involved in order to keep the doses as low as it is reasonably possible (ALARA principle),
- Adequate the procedures taking into account the elements to be utilized.

Graduates attend 122 hours of theory and 100 hours of practice. They have to pass two partial examinations and a final one, this allows them to apply to the Argentine Nuclear Regulatory Authority for permission to use radioactive materials.

### ***2.3. Course on Methodology of Radioisotopes for post-Graduates in Medicine.***

This Course began simultaneously to the Course for post-Graduates in Biomedicine, in 1962. It shares many characteristics with the latter regarding its organization and contents. Graduates have 122 hours of theory and 100 hours of practice (divided in 20 classes of 5 h. each), and take two partial examinations and a final one.

The basic syllabus includes similar subjects than course 2). The specific syllabus includes: Production of radioisotopes and radiopharmaceutical materials. Purity control criteria. Notions of biochemical applications of radioisotopes as radioimmunoassay and radioreceptor determination. Medical applications of radioisotopes and radiations: radioisotopes and images. Radiopharmaceuticals for diagnosis. Radiopharmaceuticals for treatment. National and international regulations. Radiopharmaceuticals for endocrinology, cardiology, lungs, G.I, kidney and urinary system, hematology, lymphatic system, C.N.S. Radiopharmaceutical employed in Pediatric. Radioisotopes for oncological studies. Radiopharmaceutical for metabolic therapy: basics, different radioisotopes. Therapeutic procedures. Radioisotopes by accelerator. Instrumentation in Nuclear Medicine. Scintillography. Gamma chamber. SPECT. PET. Collimators. Sensitivity and Resolution. Computation in Nuclear Medicine. Image Interpretation. Phantoms. Quality control.

The training in Radiological Protection comprises: Dose; Effective Dose; Equivalent Dose; Collective Equivalent Dose; Compromised Equivalent Dose; Environmental and Directional Equivalent Dose; Kerma; Dose Rate, in all the cases with their correspondent magnitude and unities. Internal and External sources. Shielding. General aspects of Radioprotection: dose justification, optimization and limitation. Biological effects of ionizing radiations. Radiobiology. Working areas classification. Occupational radiological protection. Internal and external contamination. Monitoring. Instrumentation in radioprotection. Management of wastes produced by the practices with radioactive material, with special emphasis in those produced by the medical and biomedical practices. Norms, recommendations and national and international regulations. Transportation regulations for radioactive materials. International and Argentine regulations for the use of radioactive materials. The safety culture.

The practical training makes special emphasis in the:

- Acquisition of criteria for the adequate application of the radioprotection philosophy,
- Planning of professional practices with an adequate training of the personnel involved in order to keep the doses as low as it is reasonably possible (ALARA principle),
- Adequation of the procedures taking into account: elements to be utilized, techniques, time required for the practice, radiological risks for patients and other workers.
- Internal dosimetric calculus, including MIRD methodology.
- External dosimetry.

As Radiological Protection is a key aspect of the Courses 2 and 3), 30% of the theoretical classes and 40% of the practices are devoted to its teaching. The first practice is totally dedicated to the basic principles of radiological protection: justification, optimization of practices and dose limitation. It is explained and analyzed how to work minimizing risks, and concepts that will be developed in each subsequent practice, when the graduates work with radioisotopes of frequent use. Each practice is specifically designed for a particular theme and provides graduates attending the Courses with the tools and skills necessary to successfully manage similar situations in their professional lives. For example, to perform and/or control procedure for decontamination, simple internal and external dosimetry and shielding calculus, etc.

At the end of the Course, to pass the final examination -open-book type- it is essential to plan and carry out an experiment employing radioisotopes, taking into account, very particularly, the radioprotection organization. The basic idea of this approach is to consider that any one who has done this Course and is consequently authorized by the Argentine Nuclear Regulatory Authority must be able to resolve the Radiological Protection matters arising in their respective laboratories, being it for medical applications (Nuclear Medicine) or biomedical (Radiopharmacy, Protein labeling, Radioreceptor determination, Radioimmunoanalysis, Radiopharmacodinamyc, others.)

In total, more than 1900 graduates have attended Courses 2) and 3) from all over Argentina and from different Latin American countries as Uruguay, Chile, Peru, Bolivia, Venezuela, Mexico, and have passed their examinations.

The fluctuation in the proportion of graduates from different careers attending Courses is a sensible mirror of the labor demand in Argentina. In the 1970s, the introduction of radioimmunoassay in the biochemist diagnose made a great number of biochemists train in that technology. Early in the 1980s an important surge in the medical application of radioisotopes made the proportion of physicians attending the Courses rise. In the same way the need of biologists able to set-up molecular biology in diagnostic laboratories increased their attendance to the Courses. An important trend for the application of radiopharmaceutical in equines, which practically is a non-exploited field till present in Argentine, is arising, as well as a greater application in the agronomic area as consequence of the current economic situation (Figure 2).

#### ***2.4. Up-date on Methodology of Radioisotopes.***

This Course has been given since 1992 and provides graduates the opportunity to up-date not only the general and specific knowledge on methodology techniques with radioisotopes but also this concerning their professional activities. The Course is divided in modules. The Radioprotection module is mandatory and encompasses around 50% of the total time-load.

Up to now many graduates from different biomedical areas have taken this Course at our Laboratory.

#### ***2.5. Technicians in Nuclear Medicine.***

For thirty-five years technicians attended the Course simultaneously with the Graduates, although some specific items were covered separately.

In 1997 an special Course for technicians was started. It is given at the Radioisotopes Laboratory of the School of Pharmacy and Biochemistry, and is applied at Nuclear Medicine centers.

This Course was the basis for the Technicians in Nuclear Medicine Career and, from 2003, it is called the Superior Technologist in Nuclear Medicine Career. The basic knowledge of this new career is given at our Laboratory and its application is impaired at approved Nuclear Medicine Centers of Buenos Aires; in total, students must attend 2000 hours of theoretical and practice sessions. The objective is to provide knowledge with the focus on specific practices they will fulfill once graduated in this career.

Our experience is that it is extremely important the acquisition of the knowledge on radiological protection needed by this population occupationally exposed by their tasks in radiopharmaceutical, fractioning of radioactive materials, etc., and that they must be adequately trained for it.

However, the need of professional technical assistance in Nuclear Medicine Services has led to the setting of an Interdisciplinary Commission at Ministerial level with the objective to create the Superior Technologist in Nuclear Medicine Career. Our Laboratory has actively participated in the creation of this career, whose incumbencies, minimal contents, time-load, jurisdiction areas, matriculation, etc., have been extensively analyzed by the Interdisciplinary Commission. The Commission is formed by members of the Argentine National Regulatory Authority, Argentine Association of Technicians in Nuclear Medicine and Argentine Association of Biology and Nuclear Medicine. As of this year our Laboratory offers students the possibility of following this Career at our premises

### **3. Conclusions.**

The use of radioisotopes and radiations in different professional activities is currently a common practice in research and applications, in special in the biomedical field. However, these activities are acceptable only in a context of radiological safety, with personal appropriately trained and with full awareness of the need of harmonizing these tasks with the environmental preservation. The Courses described in this paper have been conceived and organized with these purposes in mind, and a background of more than 40 years of constant teaching and up-dating in the thematic area. The students must show to have the conceptual clarity and theoretical/practical fitness needed for the safe and efficient manipulation of radioactive tools in their respective field to pass the final exams. The results are amply satisfactory: more than 95% of the applicants have succeeded in their exams at their respective levels.

We think that the experience in our Laboratory, the only one of its kind in the University of Buenos Aires with more than 40 years of experiences in research and teaching this topic, a teaching staff of more than 20 professors, most of them with the maximum academic degree given by the University of Buenos Aires (Ph.D.), and the participation of specialists from the National Nuclear Regulatory Authority, the Nuclear Medicine, and others, allow us to offer a level of excellence to those who take some of our courses. Since 1975 Pharmacy students have also been taught some elemental notions of radioactivity in the Physics syllabus at our Department. Our present goal is the preparation of the syllabus of a new subject that we considered indispensable, Radiopharmacy, to be offered in the Pharmacy cycle.

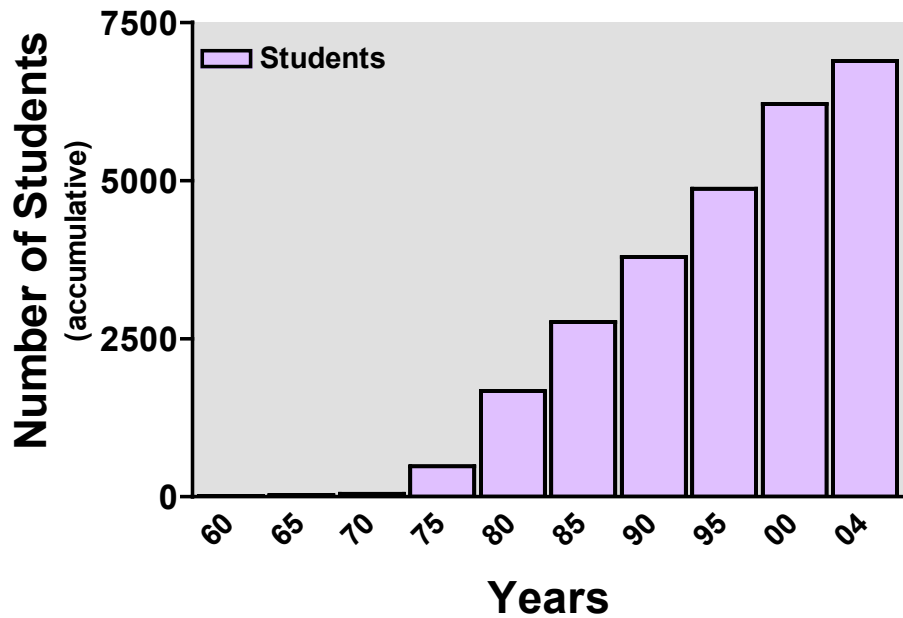


FIG 1. Undergraduate Course. Number of students per quinquennium (accumulated).

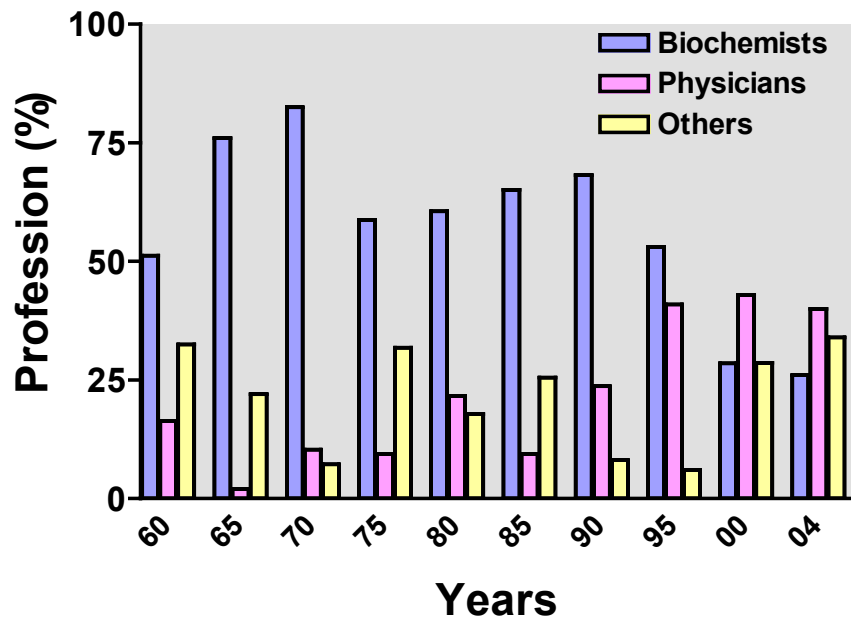


FIG 2. Post-graduate Courses. Percentage of professionals per quinquennium.

## References

1. Dutreix, J., Desgrez, A., Bok, B., Chevalier, C. *Física y Biofísica: radiaciones*. Edited by AC, Madrid, (1980).
2. Sprawls, P., Jr. *Physical Principles of Medical Imaging*. P. Aspen Publishers Inc., Maryland, USA, (1987).
3. Tubiana, M., Dutrieux, J., Wambersie A. *Introduction to Radiobiology*. Edited by Taylor & Francis, London, New York, Philadelphia, (1990).
4. Annals of the ICRP. Published on behalf of the International Commission of Radiological Protection, (1989-1993)
5. Statkiewicz-Sherer, M. A., Visconti, P. J., Ritenour, E. R. *Radiation Protection in Medical Radiography*. Mosby Inc. St. Louis, Missouri, (1998).
6. ElBaradei, M., IAEA. Edited by Micharl F. L'Annunziata, (1998).
7. Saha, G. *Fundamentals of Nuclear Pharmacy*, Pringer-Verlag, New York, (1998).

**Corresponding author:** Prof. R.M. Bergoc, Radioisotopes Laboratory, Faculty of Pharmacy and Biochemistry, Junin 956 St.-1113 Buenos Aires, ARGENTINA.

Fax: +54 (11) 4 964 8204; Tel: +54 (11) 4 964 8277

E-mail: [rmbergoc@ffyb.uba.ar](mailto:rmbergoc@ffyb.uba.ar) [rmbergoc@arnet.com.ar](mailto:rmbergoc@arnet.com.ar)

**Keywords:** capacitation, radiological protection, post-grade, technicians, biomedicine, nuclear medicine.



# Radiopharmaceutical Activities Administered for Diagnostic and Therapeutic Procedures in Nuclear Medicine in Argentine: Results of a National Survey

Bomben, A.M. and Chiliutti, C.A.



# **Radiopharmaceutical Activities Administered for Diagnostic and Therapeutic Procedures in Nuclear Medicine in Argentine: Results of a National Survey**

**Bomben, A.M. and Chiliutti, C.A.**

Autoridad Regulatoria Nuclear, Av. del Libertador 8250 (1429) Buenos Aires, Argentina  
E-mail: abomben@sede.arn.gov.ar

**Abstract.** Nuclear medicine in Argentine is carried out at 292 centres. With the purpose of knowing the activity levels of radiopharmaceuticals that were administered to patients for diagnostic and therapeutic procedures, a national survey was conducted, during 2001 and 2002. Nuclear medicine physicians in 107 centres voluntarily answered this survey. There were 37 nuclear medicine procedures, chosen among those most frequently performed, that were included in the survey. There were included tests for: bone, brain, lung, thyroid, kidney, liver, gastrointestinal tract and cardiovascular system. The nuclear medicine physicians reported the different radiopharmaceutical activities administered to typical adult patients. In this paper are presented the average radiopharmaceutical activity administered for each of the diagnostic and therapeutic procedures included in the survey and the range and distribution of values. In order to place these data in a frame of reference, these average values were compared to the guidance levels for diagnostic procedures in nuclear medicine. From this comparison it was observed that the activities administered in the 40 % of the diagnostic procedures included in the survey were between  $\pm 30$  % of the reference values. As a result of this study, it is important to point out the need to continue the gathering of data in a wider scale survey to increase the knowledge about national trends. It is also essential to widely spread the results of this type of surveys, with the purpose of creating awareness of the need for procedures optimization that will result in a better radiation protection of patients.

## **1. Introduction**

When nuclear medicine procedures are carried out, the radiopharmaceutical activities administered to the patients are very important factors to take into account to optimize the radiation protection of the patient.

With the purpose of knowing the activity levels of radiopharmaceuticals that were administered to patients for diagnostic and therapeutic procedures in nuclear medicine in Argentine, a national survey was conducted, during 2001 and 2002. The survey was prepared and carried out by personnel of the Department of Radioactive Installations and Radiation Source of the Nuclear Regulatory Authority of Argentina.

Nuclear medicine in Argentina is carried out at 292 centres, distributed all over the country, mainly concentrated in the provinces capital cities. The survey was distributed during the regulatory inspections and was answered voluntarily by nuclear medicine physicians which were responsible for radiation safety in 107 centres, that means the 37 % of all the nuclear medicine centres of the country.

The nuclear medicine centres included in the survey were selected to cover all the country. Seven geographical regions were defined and they are shown in FIG 1. The number of nuclear medicine centres for each region that were included in the survey are shown in Table I.

Table I: Centres of nuclear medicine included in the survey, by region

Region	Number of NM centres in Argentina	Number of NM centres included in the survey
City of Buenos Aires (Capital Federal)	68	29
Province of Buenos Aires	109	34
Northeast	10	7
Northwest	20	7
Pampeana	56	25
Cuyo	16	4
Patagonia	13	1



FIG 1. *Geographical regions of Argentina*

To gather information that reflects the general panorama of the nuclear medicine practice, in the survey were not only included centres where all type of diagnostic tests are carried out but also there were included specialized nuclear medicine centres where only cardiovascular, endocrinological or oncological diagnostic procedures are performed.

The nuclear medicine centres included in the survey have different type of equipment. The centres that only have single photon emission computerized tomographs (SPECT) are 51 %, those that only have gamma camera are 27%, and those that only have scintiscanner are 6 %. The centres that have SPECT and gamma camera are 11%, with SPECT and scintiscanner 1% and those with gamma camera and scintiscanner are 4 %.

The radiopharmaceutical activity administered to a patient to conduct a diagnostic or therapeutic procedure in nuclear medicine depends on several characteristics of the patient (physical contexture, age, health state, etc.) and also on the type of medical equipment of the centre. In order to try to reduce the variables, it was asked to the nuclear medicine physicians to report the radiopharmaceutical activities administered to typical adult patients.

## 2. Results

In the survey were included 37 nuclear medicine procedures chosen among those most frequently performed. The radionuclides included were  $^{99m}\text{Tc}$ ,  $^{201}\text{Tl}$ ,  $^{67}\text{Ga}$  and  $^{131}\text{I}$ , with their different chemical forms. In those diagnostic procedures were included tests for: bone, brain, lung, thyroid, kidney, liver, gastrointestinal tract and cardiovascular system.

In Tables II to X, are shown the results of the survey. The data corresponding to 32 diagnostic procedures are reported. The other 5 nuclear medicine tests included in the survey have been answered by less than the 10 % of the participants and as the data obtained were not considered representative, the results of these procedures are not presented in this paper. These procedures are: salivary gland imaging with  $^{99m}\text{Tc}$  as  $\text{TcO}_4^-$ , sentinel lymph nodes detection with  $^{99m}\text{Tc}$  nanocolloid, red cell survival and red cell volume with  $^{51}\text{Cr}$ -labelled normal erythrocytes and breast imaging with  $^{99m}\text{Tc}$ -sestamibi.

The information related to the different diagnostic procedures, the radionuclides and their chemical forms as well as the number of nuclear medicine centres that have reported data for each test are shown in the Tables II to X. The range of radiopharmaceutical activities administered to patients, the average administered activities and the reference levels, for each test are also shown. When the data for a diagnostic test was reported as a range of administered activities, instead of reporting a single value, the average administered activity for that nuclear medicine centre was estimated as the mean between the lowest and highest activities reported, taking into account the lack of information on the characteristics of the distribution of the administered activities to the patients. In addition, for each diagnostic test, the average value of the radiopharmaceutical administered activity was calculated as the arithmetic mean considering either the single data reported or the mean values estimated for each centre.

To place these data in a frame of reference, these average values were compared to the guidance levels for diagnostic procedures in nuclear medicine mentioned at the Safety Series N° 115 [1]. For the tests not included in this publication, the data were compared to values published by UNSCEAR [2], corresponding to countries with health-care level I, or compared to ARSAC recommended values [3].

From the analysis of the collected data, it was observed that in the 40 % of the diagnostic tests included in the survey the average administered activities were within  $\pm 30\%$  of the reference values considered. The average administered activities for thyroid imaging, thyroid uptake tests and thyroid metastases after ablation using  $^{131}\text{I}$  as iodide are significantly below the reference level values. Whereas other average administered activities are significantly above of the recommended values, so it is the case of liver imaging with  $^{99m}\text{Tc}$ -labelled colloid, lung perfusion with  $^{99m}\text{Tc}$ -macroaggregated albumin and the myocardial imaging with  $^{99m}\text{Tc}$ -MIBI, all of them by gamma camera.

In Figures 2 to 7 are shown the frequency distribution of ranges of administered activities for some of the diagnostic procedures included in the survey that have been selected as representative of each group of tests.

In spite of the fact that reference levels for therapeutic procedures are not appropriate because the radiopharmaceutical activity to administer is a matter of clinical judgment and must be determined case by case by the nuclear medicine physician responsible for the administration, some therapeutic procedures with unsealed sources were included in the survey just to know the national trends. Taking into account this consideration, it was asked to the participants to report the activity of  $^{131}\text{I}$ , as sodium iodide, administered to patients for two therapeutic practices. In the case of nuclear medicine therapy for hyperthyroidism, 55 nuclear medicine centres reported data, the average administered activity was 340 MBq with a range of activities of 74-650 MBq. For the thyroid carcinoma therapy, the average administered activity was 5 GBq, considering the 58 nuclear medicine centres that reported data, and the range of values was 1,95-7,4 GBq.

### **3. Conclusions**

As a result of this study, it is important to point out the need to continue the gathering of data in a wider scale survey, including all the nuclear medicine centres of Argentina, to increase the knowledge about national trends. In order to identify tendencies, it appears necessary to gather information about the type of medical equipment, its age, its calibration and other characteristics of the centres. It is also essential to widely spread the results of this type of surveys (i.e. courses, congresses, professional societies meetings, etc.), with the purpose of creating awareness of the need for procedures optimization, that will result in a better radiation protection of patients.

#### 4. References

1. International Atomic Energy Agency, *International Basic Safety Standards for Protection against Ionizing Radiation and for the Safety of Radiation Sources*, Safety Standards, Safety Series No. 115, IAEA, Vienna (1996).
2. United Nations Committee on the Effects of Atomic Radiation, *Sources and Effects of Ionizing Radiation*, UNSCEAR 2000 Report to the General Assembly, with Scientific Annexes. Volume I: Sources, United Nations, New York.
3. National Radiological Protection Board. Administration of Radioactive Substances Advisory Committee, *Notes for Guidance on the Clinical Administration of Radiopharmaceuticals and Use of Sealed Radioactive Sources*. ARSAC, December 1998.

Table II. Diagnostic procedures for bone

Test	Radio-nuclide	Chemical form	Number of nuclear medicine centres	Range of administered activities (MBq)	Average administered activities (MBq)	Reference administered activities (MBq)
<b>Bone imaging (GC)</b>	<sup>99m</sup> Tc	Phosph. compound (*)	97	500-1295	860	600 [1]
<b>Bone imaging (SPECT)</b>	<sup>99m</sup> Tc	Phosph. compound (*)	56	555-1390	990	800 [1]
<b>Bone marrow imaging</b>	<sup>99m</sup> Tc	Labelled colloid	13	185-925	700	400 [1]

(\*) Phosphonate and phosphate compounds

Table III. Diagnostic procedures for brain

Test	Radio-nuclide	Chemical form	Number of nuclear medicine centres	Range of administered activities (MBq)	Average administered activities (MBq)	Reference administered activities (MBq)
<b>Brain imaging (GC)</b>	<sup>99m</sup> Tc	TcO <sub>4</sub> <sup>-</sup> / DTPA (*)	31	370-1110	710	500 [1]
<b>Brain imaging (SPECT)</b>	<sup>99m</sup> Tc	TcO <sub>4</sub> <sup>-</sup> / DTPA (*)	44	370-1290	850	800 [1]
<b>Cerebral blood flow</b>	<sup>99m</sup> Tc	HM-PAO (○)	30	92,5-1110	640	500 [1]

(\*) Diethylenetriaminepentaacetic acid

(○) Hexamethyl propylene amine oxime

Table IV. Diagnostic procedures for lung

Test	Radio-nuclide	Chemical form	Number of nuclear medicine centres	Range of administered activities (MBq)	Average administered activities (MBq)	Reference administered activities (MBq)
<b>Lung ventilation imaging</b>	<sup>99m</sup> Tc	DTPA-aerosol	83	296-1850	938	662 [2]
<b>Lung perfusion imaging (GC)</b>	<sup>99m</sup> Tc	Human albumin (*)	38	37-740	200	100 [1]
<b>Lung imaging (SPECT)</b>	<sup>99m</sup> Tc	MAA (○)	59	37-925	280	200 [1]

(\*) Macroaggregates

(○) Macroaggregated albumin

Table V. Diagnostic procedures for thyroid

Test	Radio-nuclide	Chemical form	Number of nuclear medicine centres	Range of administered activities (MBq)	Average administered activities (MBq)	Reference administered activities (MBq)
Thyroid imaging	<sup>131</sup> I	I <sup>-</sup>	59	0,74-18,5	4,7	17 [2]
Thyroid imaging	<sup>99m</sup> Tc	TcO <sub>4</sub> <sup>-</sup>	85	18,5-555	210	200 [1]
Thyroid uptake	<sup>131</sup> I	I <sup>-</sup>	72	0,17-7,4	1,9	3,1 [2]
Thyroid metastases (after ablation)	<sup>131</sup> I	I <sup>-</sup>	67	74-425	180	400 [1]
Parathyroid imaging	<sup>99m</sup> Tc	MIBI(*)/TcO <sub>4</sub> <sup>-</sup>	53	7,4-1110	470	900 [3]
Parathyroid imaging	<sup>201</sup> Tl	Tl <sup>+</sup> chloride	28	37-185	80	80 [1]

(\*) Isonitriles

Table VI. Diagnostic procedures for kidney

Test	Radio-nuclide	Chemical form	Number of nuclear medicine centres	Range of administered activities (MBq)	Average administered activities (MBq)	Reference administered activities (MBq)
Renal imaging /renography	<sup>99m</sup> Tc	DTPA	94	18,5-830	220	350 [1]
Renal imaging	<sup>99m</sup> Tc	DMSA(*)	89	37-740	230	160 [1]

(\*) Dimercaptosuccinic acid

Table VII. Diagnostic procedures for liver

Test	Radio-nuclide	Chemical form	Number of nuclear medicine centres	Range of administered activities (MBq)	Average administered activities (MBq)	Reference administered activities (MBq)
Liver imaging (GC)	<sup>99m</sup> Tc	Labelled colloid	22	74-370	210	80 [1]
Liver imaging (SPECT)	<sup>99m</sup> Tc	Labelled colloid	45	85-555	220	200 [1]

Table VIII. Diagnostic procedures for gastrointestinal tract

Test	Radio-nuclide	Chemical form	Number of nuclear medicine centres	Range of administered activities (MBq)	Average administered activities (MBq)	Reference administered activities (MBq)
Gastrointestinal bleeding	<sup>99m</sup> Tc	Labelled colloid	71	148-1480	720	400 [1]
Oesophageal Transit and reflux	<sup>99m</sup> Tc	Labelled colloid	54	3,7-370	53	40 [1]

Table IX. Diagnostic procedures for cardiovascular system

Test	Radio-nuclide	Chemical form	Number of nuclear medicine centres	Range of administered activities (MBq)	Average administered activities (MBq)	Reference administered activities (MBq)
<b>Myocardial imaging (GC)</b>	<sup>99m</sup> Tc	MIBI (*)	21	185-925	560	300 [1]
<b>Myocardial imaging (SPECT)</b>	<sup>99m</sup> Tc	MIBI (*)	51	185-1110	600	600 [1]
<b>Myocardial imaging (GC)</b>	<sup>201</sup> Tl	Tl <sup>+</sup> chloride	27	55,5-111	85	100 [1]
<b>Myocardial imaging (SPECT)</b>	<sup>201</sup> Tl	Tl <sup>+</sup> chloride	46	74-370	146	100 [1]
<b>Myocardial imaging (GC)</b>	<sup>99m</sup> Tc	Phosph. compound (○)	17	555-1110	740	600 [1]
<b>Myocardial imaging (SPECT)</b>	<sup>99m</sup> Tc	Phosph. compound (○)	21	460-1110	700	800 [1]
<b>Cardiac imaging</b>	<sup>99m</sup> Tc	Labelled RB (+)	82	555-1390	880	800 [1]
<b>First pass blood flow studies (lower limbs)</b>	<sup>99m</sup> Tc	MAG3 (#)	51	37-1110	400	400 [1]
<b>First pass blood flow studies (upper limbs)</b>	<sup>99m</sup> Tc	MAG3 (#)	35	37-740	310	400 [1]

(\*) Isonitriles

(○) Phosphonate and phosphate compounds

(+) Labelled normal red blood cells

(#) Macroaggregated globulin 3

Table X: miscellaneous

Test	Radio-nuclide	Chemical form	Number of nuclear medicine centres	Range of administered activities (MBq)	Average administered activities (MBq)	Reference administered activities (MBq)
<b>Lymph node imaging</b>	<sup>99m</sup> Tc	Labelled colloid	46	18,5-740	150	80 [1]
<b>Tumour or abscess imaging</b>	<sup>67</sup> Ga	Citrate	48	74-500	190	300 [1] 150 [3]

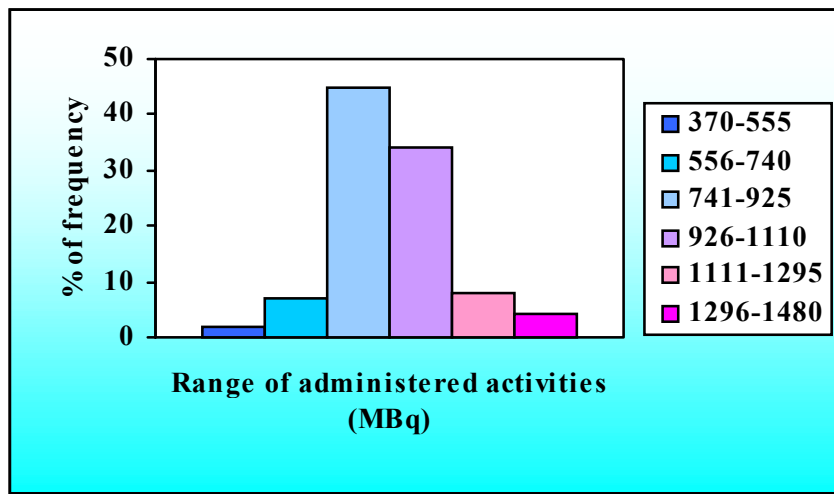


FIG. 2. Frequency distribution of ranges of administered activities for bone imaging by SPECT, with  $^{99m}\text{Tc}$ -MDP.

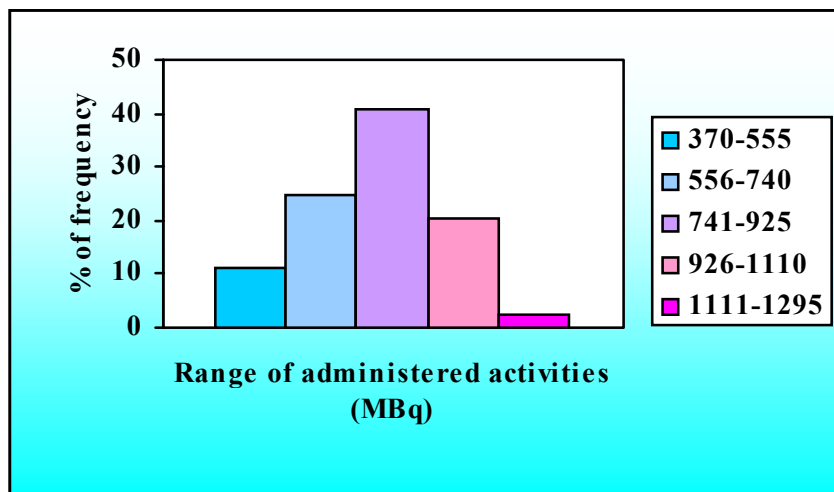


FIG. 3. Frequency distribution of ranges of administered activities for brain imaging by SPECT, with  $^{99m}\text{Tc}$ -DTPA.

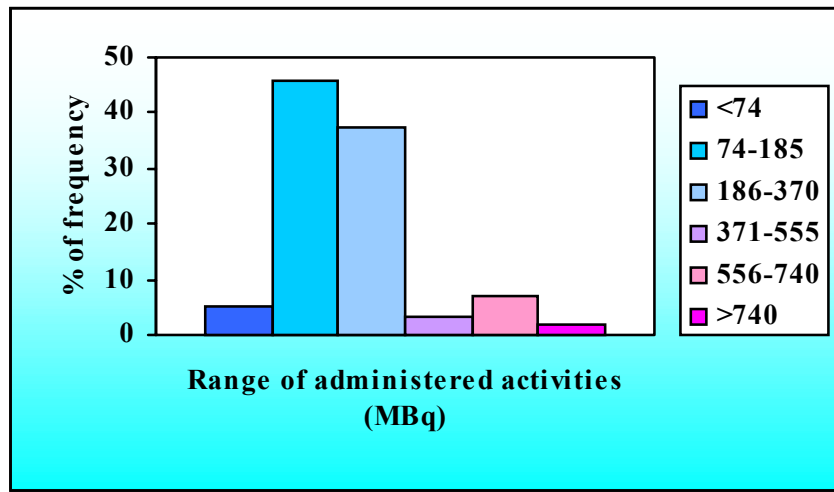


FIG. 4. Frequency distribution of ranges of administered activities for lung imaging by SPECT, with  $^{99m}\text{Tc}$ -MAA.

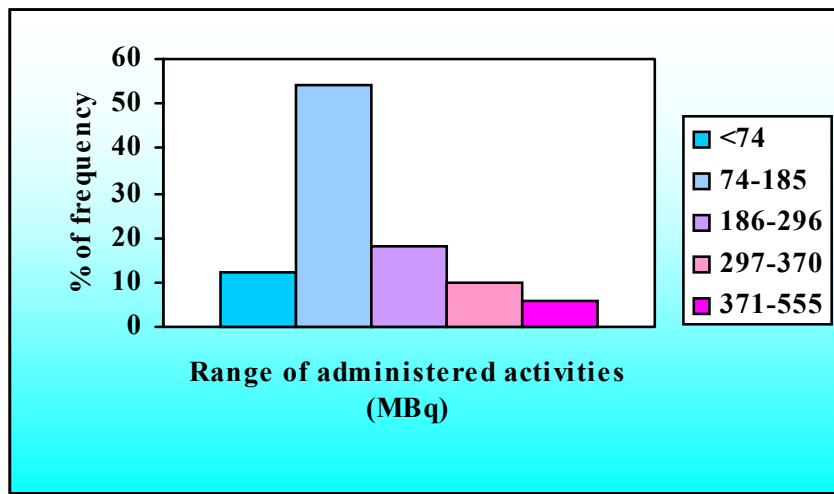


FIG. 5. Frequency distribution of ranges of administered activities for thyroid imaging, with  $^{99m}\text{TcO}_4^-$ .

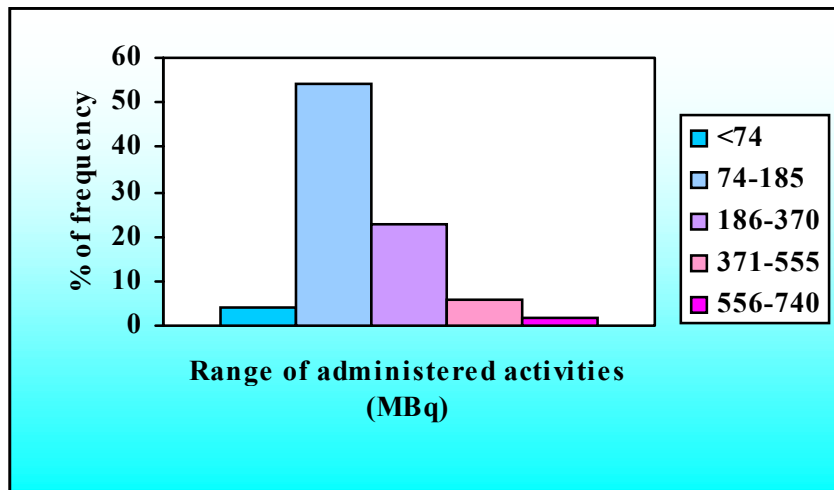


FIG. 6. Frequency distribution of ranges of administered activities for renal imaging by SPECT, with  $^{99m}\text{Tc}$ -DMSA.

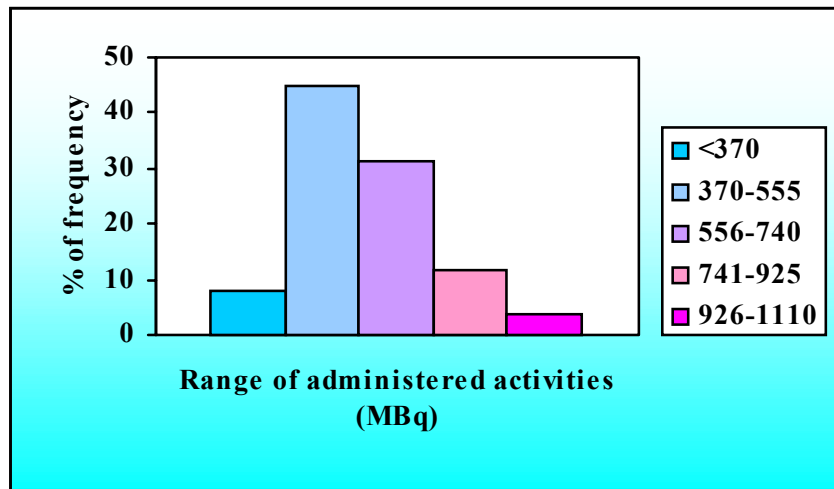


FIG. 7. Frequency distribution of ranges of administered activities for myocardial imaging by SPECT, with  $^{99m}\text{Tc}$ -MIBI.

# Environmental Radiological Surveillance Around Nuclear Power Plants in Argentina

Ciallella, H.E.; Fernandez, J.A.; Gavini, R.M.;  
Lewis, E.C. and Quintana, E.E.



# **ENVIRONMENTAL RADIOLOGICAL SURVEILLANCE AROUND NUCLEAR POWER PLANTS IN ARGENTINA**

**Ciallela, H.E.; Fernandez, J.A.; Gavini, R.M.; Lewis, E.C. and Quintana, E.E.**  
**Autoridad Regulatoria Nuclear**  
**Argentina**

## **ABSTRACT**

During the last five years of operation of Atucha I Nuclear Power Plant (CNA I) and Embalse Nuclear Power Plant (CNE), a field team from the Environmental Radioactivity Division of Nuclear Regulatory Authority (NRA) has carried out surveillance programs in the surroundings of these facilities, in order to estimate the radiological impact.

The argentine nuclear power plants use natural uranium as fuel and heavy water as refrigerant and moderator. During normal operation, radionuclides are released to the environment through liquid and gaseous discharges; mainly tritium which is generated from the neutron activation of heavy water deuterium.

One of the environmental radioprotection requirements for a nuclear facility licensing is the compliance of the dose limit (1 mSv/year) to the most exposed members of the public (critic group). The authorised annual dose limits established for NRA, to control the release of radioactive effluents are 50 and 100 µSv/year for CNA I and CNE respectively.

The surveillance programs carried out around the mentioned nuclear facilities included the radionuclide analysis of H-3, Cs-137, Co-60, I-131 and Sr-90. The matrixes analysed were milk, grass, diet, fish and groundwater, surface and tap water. The results, including the dose assessment, are presented.

The measured results of the radionuclides mentioned above were, in general, below the detection limit (except for tritium). The doses estimated for both, liquid and gaseous discharges, varied from 4 to 5 µSv/year for each nuclear power plant, since 1998 to 2002. This implies that the population living in the vicinity of these areas receives no significant exposure.

Key words: environmental surveillance, nuclear power plants, H-3, Cs-137, Co-60, I-131, Sr-90

## **I. INTRODUCTION**

Argentine has in operation Atucha I (CNA I) and Embalse (CNE) nuclear power plants. CNA I is in operation since june 1974, it is located nearby Paraná de las Palmas river, in Buenos Aires province, 100 km north-east from Buenos Aires city. CNE, whose operation started in January 1984, is located in the south coast of Embalse de Río Tercero, in Córdoba province, 110 km south-east from Córdoba city.

CNA I has a heavy water pressure reactor (HWPR) from Germany, of 357 electric net power megawatts (MWe) and uses natural uranium as fuel. The reactor core has 253 fuel elements, which contain uranium dioxide ( $\text{UO}_2$ ) pellets. This arrangement is immersed in 500 t of heavy water, which acts as moderator and refrigerant.

CNE has a pressure tubes reactor, CANDU model from Canada, of 648 electric net power megawatts (MWe) and also uses natural uranium as fuel and heavy water as refrigerant and moderator. The core is horizontally penetrated by 380 fuel elements.

In normal operation conditions, this type of reactor has a tritium production rate of  $7,4 \cdot 10^{13}$  Bq/MWe. This is due to the neutron activation of heavy water deuterium. A fraction of this tritium is released to the environment as gaseous discharge through the power plant stack due to the degassed of the primary circuit [1].

There are liquid discharges also. CNA I releases liquid discharges to the Paraná de las Palmas river and CNE to the Embalse de Río Tercero lake. In this kind of reactor tritium is the main radionuclide released to the environment, and has a great importance from the radiological point of view because is the main contributor to the effective and collective dose to the public.

The ARN performs surveillance programs in the surroundings of nuclear power plants, fully independent from the monitoring carried out by the facilities themselves, in order to estimate the radiological impact [2,3].

The environmental monitoring carried out in both facilities has several objectives, one of them is to obtain information of the correlation between discharges and environmental levels (that allows to implement predictions) and additionally, to know about the radionuclide behaviour in the biosphere.

## II. EXPERIMENTAL METHOD:

The surveillance programs carried out around the mentioned nuclear facilities included representative samples that were taken from the different radionuclide transfer compartments. In order to evaluate the environmental impact of the liquid discharges, river, lake water and fish samples were collected and analysed. To assess the environmental impact of the gaseous emissions, samples of locally produced food, such as milk, vegetables and diet, were taken and analysed. Grass was analysed as an indicator of radioactive material deposition. Additionally, tap water (groundwater and surface water) samples were taken. From the radiological point of view, the radionuclides analysed were mainly fission products (Cs-137, Sr-90 and I-131) and neutron activation products (H-3 and Co-60).

The population in the surroundings of Atucha I nuclear power plant is low and is conformed principally by farmers. In the case of Embalse nuclear power plant, the population lives in small areas around the facility and is basically dedicated to tourist activities.

In Figures 1 and 2 are shown the selected points around CNA I and CNE respectively.

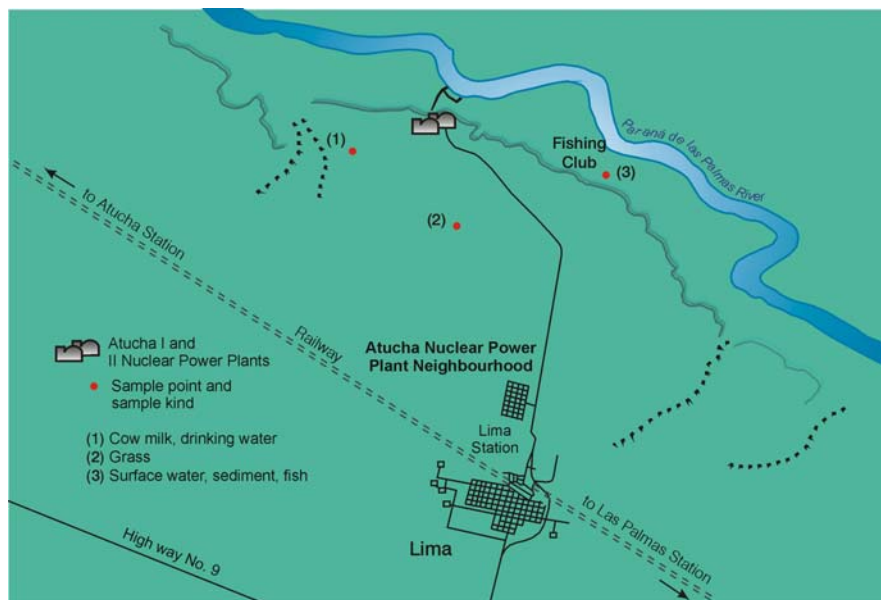


Figure No. 1: The map shows the environmental sample points around CNA I



Figure No. 2: The map shows the environmental sample points around CNE

The samples were processed at the NRA environmental laboratories localised at the Centro Atómico Ezeiza, located in Ezeiza, province of Buenos Aires.

The Sr-90 determination was performed over the concentrated samples or the ashes obtained from the burnt samples. After digestion in different acids, a final Y-90 in equilibrium extraction with HDEHP is used. A liquid scintillation measurement is carried out using the Cerenkov emission. Tritium is measured directly over a sample aliquot by liquid scintillation [4]. Cs-137 and Co-60 determination were performed by gamma spectrometry, using GeHp of high efficiency and resolution. Liquid samples were evaporated till 30 cm<sup>3</sup> geometry and were directly measured over the detector: The ashes were measured with a 60 g pellet geometry. I-131 was measured directly by gamma spectrometry over fresh samples [4].

### III. RESULTS

For both nuclear power plants the experimental results were obtained from nearly 100 quarterly samples of different sample points, between 1998-2002 [5].

In Table 1 is presented the activity concentration in the different analysed samples from CNA I.

Table 1  
Activity concentration in CNA I environmental samples

<b>Environmental sample</b>	<b>Radio-Nuclide</b>	<b>1998</b>	<b>1999</b>	<b>2000</b>	<b>2001</b>	<b>2002</b>
Surface water (Bq/L)	H-3	3.1	2.1	1.3	0.5	0.8
	Cs-137	<0.002	<0.0012	<0.002	<0.002	<0.002
	Co-60	<0.0025	<0.0021	<0.002	<0.006	<0.002
	Sr-90	0.0012	<0.0004	<0.0002	<0.0002	<0.0002
Freshwater fish (Bq/kg)	Cs-137	<0.04	<0.03	<0.06	<0.02	<0.02
	Co-60	<0.04	<0.02	<0.02	<0.02	<0.02
	Sr-90	0.25	<0.05	0.04	0.037	0.07
Grass (Bq/m <sup>2</sup> )	I-131	<0.6	<4.5	<3.3	<3.4	<2.5
	Cs-137	<1.0	<4.7	<3.8	<3.3	<2.8
	Co-60	<0.9	<3.1	<4.4	<2.8	<2.6
Drinking water (Bq/L) (groundwater)	H-3	1.5	<0.3	0.2	0.2	0.2
	Cs-137	<0.0025	<0.0023	<0.001	<0.0015	<0.001
	Co-60	<0.002	<0.002	<0.0008	<0.0015	<0.009
	Sr-90	<0.0012	<0.0003	<0.0003	<0.0002	<0.0002
cow milk (Bq/L)	I-131	<0.2	<0.2	<0.3	<0.2	<0.2
	Cs-137	<0.01	<0.002	<0.01	<0.009	<0.009
	Sr-90	<0.08	<0.02	<0.016	<0.017	<0.017
diet (Bq/kg)	Cs-137	---	---	---	<0.02	<0.01
	Co-60	---	---	---	<0.02	<0.02
	Sr-90	---	---	---	<0.03	<0.06

In Table 2 is presented the activity concentration in the different analysed samples from CNE.

Table 2  
Activity concentration in CNE environmental samples

<b>Environmental sample</b>	<b>Radio-Nuclide</b>	<b>1998</b>	<b>1999</b>	<b>2000</b>	<b>2001</b>	<b>2002</b>
Surface water (Bq/L)	H-3	170	33	30	53	71
	Cs-137	<0.0035	<0.001	<0.001	<0.07	<0.002
	Co-60	<0.004	<0.001	<0.001	<0.05	<0.002
	Sr-90	<0.003	<0.0005	0.0005	<0.0003	<0.0005
Freshwater fish (Bq/kg)	Cs-137	<0.09	<0.08	<0.06	<0.03	<0.04
	Co-60	<0.04	<0.03	<0.03	<0.02	<0.02
	Sr-90	0.25	<0.04	0.03	0.05	<0.03
Grass (Bq/m <sup>2</sup> )	I-131	<4.0	<5.0	<5.0	<4.1	<2.7
	Cs-137	<0.8	<6.7	<4.7	<4.5	<3.1
	Co-60	<0.5	<4.7	<3.5	<3.1	<2.7
Drinking water (Bq/L)	H-3	170	33	24	44	51
	Cs-137	<0.004	<0.002	<0.001	<0.002	<0.002
	Co-60	<0.003	<0.001	<0.001	<0.002	<0.0007
	Sr-90	<0.002	<0.0004	<0.0003	<0.003	<0.0004
cow milk (Bq/L)	I-131	<0.2	<0.3	<0.3	<0.2	<0.1
	Cs-137	<0.01	<0.01	<0.01	<0.02	<0.01
	Sr-90	<0.04	<0.01	<0.02	<0.02	<0.02
diet (Bq/kg)	Cs-137	---	---	---	<0.02	<0.03
	Co-60	---	---	---	<0.01	<0.02
	Sr-90	---	---	---	<0.01	<0.03

Moreover, to assess the environmental impact of the emissions, effective doses to the most exposed members of the public (critic group) were calculated. The concentration levels of the radionuclides in the environmental samples were used to calculate the effective doses of the critic group. The doses were calculated taking into account the critical exposition pathways and considering that the population consume local products. In Table 3 are shown the results [6].

The critic group in Atucha I is located 1 km West from the stack of the nuclear power plant. In the case of Embalse nuclear power plant the critic group is 1 km South.

Table 3  
Effective doses from Nuclear Power Plants

Year	Doses (mSv/year)	
	CNA I	CNE
1998	<0.0036	<0.005
1999	<0.0025	<0.0045
2000	<0.0025	<0.0045
2001	<0.002	<0.0025
2002	<0.002	<0.0024

## CONCLUSIONS:

The measured results of the radionuclides mentioned above were, in general, below the detection limit of used techniques (except for tritium).

In the case of CNA, positive H-3 levels were detected in aqueous matrixes, but near environmental concentration. The Sr-90 fish determinations deserve an explanation where positive results were obtained. These low activity levels obtained were basically produced by residual fall out coming from nuclear weapons test carried out in the seventies. The positive values were probably obtained by concentration effect of the mentioned matrix.

In the case of CNE, H-3 activity levels in tap and surface water were detected attributable to the nuclear power plant operation. The activity levels presented in drinking and lake water were practically the same because the tap water was coming from the Embalse de Río Tercero lake. The rest of radionuclides gave similar results that the concentration levels founded in the surroundings of CNA I.

One of the environmental radioprotection requirements for a nuclear facility licensing is the compliance of the dose limit (1 mSv/year) to the most exposed members of the public (critic group). The authorised annual dose limits established for NRA, to control the release of radioactive effluents are 50 and 100 µSv/year for CNA I and CNE respectively.

The resulting doses estimated to individuals of the critic group for both, liquid and gaseous discharges, varied from 4 to 5 µSv/year for each nuclear power plant since 1998 to 2002. These values are far of the dose constraint and only represent less than 0.5% of the annual dose limit. This implies that the population living in the vicinity of these areas receives no significant exposure.

## REFERENCES:

- [1] National Council on Radiation Protection and Measurements. Tritium in the Environment. NCRP, NCRP Report No. 62; 1979.
- [2] "Monitoraje ambiental en la zona de emplazamiento de la Central Nuclear de Atucha". Menossi, C. A., Ciallella N. R., Bruno H. A., Escribano T. L.; Comisión Nacional de Energía Atómica. NT 8/78, Argentina (1978).
- [3] "Monitoreo ambiental en los alrededores de las centrales nucleares de la República Argentina realizado en los años 1996 y 1997". Canoba, A. C., López, F. O., Bruno, H. A.; 4o Congreso Regional de Seguridad Radiológica y Nuclear (IRPA). La Habana, Cuba. Octubre 1998. Memorias, Tomo 4, tema 14, pág. 9-12, 1998.
- [4] Laboratory Techniques Manual (2002). Nuclear Regulatory Authority, Argentina.
- [5] Annual Reports (1998 – 2002). Nuclear Regulatory Authority, Argentina.
- [6] Safety Reports Series No.19, Generic Models for in assessing the impact of discharges of radioactive substances to the environment. IAEA (2001).

# Evaluation Through Comet Assay of DNA Damage Induced in Human Lymphocytes by Alpha Particles. Comparison with Protons and Co-60 Gamma Rays

Di Giorgio, M.; Kreiner, A.J.; Schuff, J.A.; Vallerga, M.B; Taja, M.R.; López, F.O.; Alvarez, D.E.; Saint Martin, G.; Burlón, A.; Debray, M.E.; Kesque, J.M.; Somacal, H.; Stolar, P.; Valda, A.; Davidson, J.; Davidson, M.; Ozafrán, M.J. and Vázquez, M.E.



# Evaluation through comet assay of DNA damage induced in human lymphocytes by alpha particles. Comparison with protons and Co-60 gamma rays

<sup>1</sup> Di Giorgio, M.; <sup>2,3,4</sup>Kreiner, A.J.; <sup>2</sup>Schuff, J.A.; <sup>1</sup>Vallerga, M.B.; <sup>1</sup>Taja, M.R.; <sup>1</sup>López, F.O.;  
<sup>1</sup>Alvarez, D.E.; <sup>2</sup>Saint Martin, G.; <sup>2,3</sup>Burlón, A.; <sup>2,3</sup>Debray, M.E.; <sup>2</sup>Kesque, J.M.; <sup>3</sup>Somacal, H.;  
<sup>2,3</sup>Stolar, P.; <sup>3</sup>Valda, A.; <sup>4</sup>Davidson, J.; <sup>4</sup>Davidson, M.; <sup>2</sup>Ozafrán, M.J. and <sup>2</sup>Vázquez, M.E.

<sup>1</sup>Autoridad Regulatoria Nuclear, Av. Del Libertador 8250, CP: C1429BNP, Ciudad de Buenos Aires,  
ARGENTINA. mdigiorg@cae.arn.gov.ar

<sup>2</sup>Comisión Nacional de Energía Atómica, , Av. Gral. Paz 1499, CP: 1650, Villa Maipú, ARGENTINA.

<sup>3</sup>Escuela de Ciencia y Tecnología, UNSAM, Alem 3901, CP: 1653, Villa Ballester, ARGENTINA.

<sup>4</sup>CONICET, Rivadavia 1917, Ciudad de Buenos Aires, ARGENTINA.

## Abstract

### *Background and purpose:*

Several techniques with different sensitivity to single-strand breaks and/or double strand breaks were applied to detect DNA breaks generated by high LET particles. Tests that assess DNA damage in single cells might be the appropriate tool to estimate damage induced by particles, facilitating the assessment of heterogeneity of damage in a cell population. The microgel electrophoresis (comet) assay is a sensitive method for measuring DNA damage in single cells.

The objective of this work was to evaluate the proficiency of comet assay to assess the effect of high LET radiation on peripheral blood lymphocytes, compared to protons and Co-60 gamma rays.

*Materials and methods:* Irradiations of blood samples were performed at TANDAR laboratory (Argentina). Thin samples of human peripheral blood were irradiated with different doses (0 – 2.5 Gy) of 20.2 MeV helium-4 particles in the track segment mode, at nearly constant LET. Data obtained were compared with the effect induced by 4 MeV protons and Co-60 gamma rays. Alkaline comet assay was applied. Comets were quantified by the Olive tail moment.

*Results:* Distribution of the helium-4 particles and protons were evaluated considering Poisson distribution in lymphocyte nuclei. The mean dose per nucleus per particle result 0.053 Gy for protons and 0.178 Gy for helium-4 particles. When cells are exposed to a dose of 0.1 Gy, the hit probability model predicts that 43 % of the nuclei should have experienced an alpha traversal while with protons, 85% of the nuclei should be hit. The experimental results show a biphasic response for helium-4 particles (0.1 Gy), indicating the existence of two subpopulations: unhit and hit. Distributions of tail moment as a function of fluence and experimental dose for comets induced by helium-4 particles, protons and Co-60 gamma rays were analyzed. With helium-4 irradiations, lymphocyte nuclei show an Olive tail moment distribution flattened to higher tail moments as dose increase. However, for irradiations with protons and gamma rays, at increasing doses the tail moments are shifted towards high values with the same distribution, characterized by its asymmetry.

*Conclusions:* The comet assay allowed to observe differences in the patterns of DNA damage induced by helium-4 particles compared to protons and gamma rays, indicating that the mean dose and the hit distribution in the lymphocyte population influence the damage induction.

## INTRODUCTION

The double aim of optimizing clinical efficacy of hadrontherapy and determining radiation risk estimates for space research, converges on the assessment of the biological effects of charged particles on cells. This effect depends on the spatial distribution of ionizing events. With high LET, the ionizations are deposited in tracks and so are non-randomly distributed both within a cell and among the cells.

The relative biological effectiveness (RBE) for many end points, including mutations, cell killing and chromosome aberrations, increases as LET increases reaching a maximum around 100 keV/ $\mu$ m and decreasing at higher LET values. Nevertheless, RBE for double strand break induction remains around 1.0 for all radiation qualities studied. An accepted explanation is that high LET radiation tracks produce highly localized clustered damage within the DNA and also spatially separated sites of damage along the path of the radiation track. Lesions are concentrated in localized areas and are more complex due to the larger number and size of multiply damage sites when compared to low LET radiation.

Ion irradiation is heterogeneous, a single particle traversal of a cell yields a high dose and when a moderately high dose is given to a blood sample there will be cells traversed by 0, 1, 2 etc tracks. Several techniques with different sensitivity to single-strand breaks and/or double strand breaks were applied to detect DNA breaks generated by high LET particles. Tests that assess DNA damage in single cells might be the appropriate tool to estimate damage induced by particles, facilitating the assessment of heterogeneity of damage in a cell population. The microgel electrophoresis (comet) assay is a sensitive method for measuring DNA damage in single cells.

The objective of this work was to evaluate the proficiency of comet assay to assess the effects of high LET radiation on peripheral blood lymphocytes, compared to protons and Co-60 gamma rays. The experience was based on the changes in the distribution of the Olive tail moment (OTM), which is considered as a sensitive indicator of DNA breakage.

## MATERIALS AND METHODS

### Radiation beams

The irradiations of blood samples used the apparatus described previously [1] with some modifications [2]. The helium-4 ions and proton beams were obtained from the TANDAR 20 MV electrostatic tandem accelerator of the Atomic Energy Commission in Buenos Aires. In brief, negative helium-4 atoms were generated by a radio-frequency charge exchange source and pre-accelerated to the main accelerator. They were further accelerated to a positive high voltage where passage through a thin carbon foil stripped off the electrons to make positive ions, which were then accelerated to ground potential. A magnetic analyzer selected the required energy and the particles were focused on the detection zone and then entered the beam line. On entry the beam energy was 29.6 MeV with currents from 1 to 5 nA.

The experimental beam line consists of two vacuum chambers linked by a 10 cm diameter stainless steel tube approximately 8 m long. The beam first passes through a gold scattering foil of  $12.0 \pm 0.5 \mu\text{m}$  in thickness, located in the first chamber. A system of anti-scatter collimators in the second chamber defines the maximum size of the beam. Scintillator screens, located in both chambers, helped to locate the beam. The system was designed to produce a beam profile homogeneous within  $\pm 1\%$ , sufficiently wide to cover a blood specimen holder.

The energies of the produced beams were 20.2 MeV for helium-4 particles and 4 MeV for protons. Both, helium-4 ions and protons passed to the same irradiation chamber. In the irradiation chamber, the beam monitor consists of a thin ( $25\mu\text{m}$ ) aluminium-coated Mylar film from which backscattered electrons are collected on a ring held at +120 V. The backscatter current is proportional to the beam current. Finally, the beam passes out of the accelerator tube through a vacuum window of  $100 \mu\text{m}$  Mylar.

Uniformity achieved at the TANDAR generator was measured with a parallel plate ionization chamber Capintec PS-033 with a copper shield containing an aperture of 1.5 mm diameter.

### Dosimetry

Different parallel plate ionization chambers were used to calibrate the beam monitor in terms of dose: a Capintec PS-033 for alpha particles and a Scanditronix NACP-01 for protons, previously calibrated for low energy protons in Orsay Protontherapy Center, France.

The ionization chambers were calibrated according to an IAEA standard [3]. In both cases the beam monitor and ionization chamber currents were recorded remotely.

The ionization chambers were located at the position of the blood samples with additional absorbers to simulate dose at the blood mid-plane.

The energy spectrum of the helium-4 beam is measured using a silicon surface barrier detector. The beam energy is 20.2 MeV with an energy width (FWHM) of 0.6 MeV.

An additional monitor calibration was performed using a Faraday cup, placed at the target position.

The dose was obtained through the following expression

$$D_t = \left( \frac{N}{A} \right) \left( \frac{S}{\rho} \right)_t \left( 1.602 \times 10^{-10} \right) \quad (1)$$

$D_t$  is the calculated dose in Gy, N is the number of particles, A is the effective area of the beam (in  $\text{cm}^2$ ) and  $(S/\rho)t$  is the ICRU Report 49 [4] mass stopping power (in  $\text{MeV.cm}^2.\text{g}^{-1}$ ) for alpha particles in water at the beam energy, all quantities corresponding to the irradiation position.

The ionization chambers and the Faraday cup calibrations agreed within 2%.

### Blood irradiation

Thin samples of human peripheral blood were irradiated with 20.2 MeV helium-4 particles and 4 MeV protons, in the track segment mode, avoiding rapid changes in dose along the track associated with the Bragg peak. Thus, irradiations have been carried out at nearly constant LET [2]. Cells were also irradiated with Co-60 gamma rays at a dose rate of 0.49 Gy/min.

Freshly-drawn, heparinized blood obtained from healthy adults, was dispensed onto plastic discs with a circular inner trough of 26.46 mm in diameter and 60 – 70  $\mu\text{m}$  in depth. The blood sample was held in position by a Mylar foil 4  $\mu\text{m}$  thick. The sample-holding discs were placed in a sample wheel, which rotated at 10 revolutions per minute. Each position on the wheel passed through the beam for the same number of times. They passed about 2.5 cm from the beam exit window. Between the samples and the window there was a pneumatically operated shutter (4 bar of pressure) and a beam shaper with a 4° angle, used at 0.05 Gy and 0.1 Gy helium ions and protons from 0.1 to 1.5 Gy. The beam shaper was replaced by a 10° angle for helium doses from 0.5 Gy to 3 Gy and protons of 2 Gy. The doses, shown in the table of results, were given in less than 5 minutes.

### Comet assay

Alkaline Comet assay was performed according to Singh [5] and Tice [6] technique with modifications. A layer of 1.5% normal melting agarose was prepared on microscope slides. After cell irradiation,  $\approx$ 25,000 cells in 50  $\mu\text{l}$  were mixed with 120  $\mu\text{l}$  of 0.5% low melting agarose. The suspension was pipetted onto the precoated slides. Slides were immersed in cold lysis solution at pH 10 (2.5 M NaCl, 100 mM Na<sub>2</sub>EDTA, 10 mM Tris pH 10, 1% Triton X-100, 10% DMSO) and kept at 4 °C for 60 min. To allow denaturation of DNA, the slides were placed in alkaline electrophoresis buffer at pH 13 (1mM Na<sub>2</sub>EDTA / 300 mM NaOH) and left for 25 min. Subsequently, were transferred to an electrophoresis tank with fresh alkaline electrophoresis buffer and electrophoresis was performed at a field strength of 1.33 V/cm for 25 min at 4 °C (20 V – 125 mA). Slides were neutralized in 0.4 M Tris pH 7.5 for 5 min and stained with 20  $\mu\text{g}/\text{ml}$  ethidium bromide. For visualization of DNA damage, observations were made using a 20x objective on a epifluorescent microscope equipped with an excitation filter of 510-560 nm and a barrier filter of 590 nm. One to two hundred comets on duplicated slides were analyzed. Images were captured with a digital camera with networking capability and analyzed by an image analysis software, CASP [7]. DNA damage was quantified by the Olive tail moment (OTM) [8], whose distribution was adjusted by a two-parameter Weibull model [9]. OTM is the product of the distance (in x direction) between the center of gravity of the head and the center of gravity of the tail and the percent tail DNA.

## RESULTS AND DISCUSSION

Dosimetric data of the lymphocyte irradiations are shown in Table I., being  
 Fluence [ $\text{particles}/\text{cm}^2$ ] =  $D[\text{Gy}] / (\text{Stopping power}[\text{MeV.cm}^2/\text{g}] \times 1.602 \times 10^{-10})$

The mean number of impacts per nucleus,  $\lambda = (D[\text{Gy}] \times \text{Lymphocyte nucleus area} [\text{cm}^2]) / (1.602 \times 10^{-10} \times \text{Stopping power} [\text{MeV.cm}^2/\text{g}])$ .

The mean dose per nucleus per particle was calculated assuming a spherical cell nucleus of 6  $\mu\text{m}$  diameter, a mean lymphocyte radius crossed by one ion ( $= 4/3 r$ ) and a density of water  $\rho=1$ ; the mean dose per particle in Gy is  $0.00566L$ , where L (LET) is in  $\text{keV}\mu\text{m}^{-1}$ .

The mean dose per nucleus per particle resulted **0.053 Gy for protons and 0.178 Gy for helium-4 particles.**

Experimental dose = “accumulated dose”[counts] (beam monitor)/ calibration factor [counts/Gy], where: calibration factor = accumulated dose/ (ionizing chamber dose x geometric factor) and the geometric factor = 4/360 or 10/360, according to the beam shaper angle.

Table I. Dosimetric data for protons and helium-4 particles used for lymphocyte irradiations

Ion	Energy [MeV]	Stopping Power [MeV*cm <sup>2</sup> /g]	LET [keV/ $\mu$ m]	Fluence [particles/cm <sup>2</sup> ]	Mean ion/ Nucleus ( $\lambda$ )	Mean dose/ Nucleus [Gy]	Experimental dose [Gy]
$H^+$	4	94.04	9.4	$7.45 \times 10^6$	2.1	0.112	0.112
				$2.05 \times 10^7$	5.8	0.309	0.309
				$4.69 \times 10^7$	13.3	0.707	0.707
				$6.72 \times 10^7$	19	1.013	1.013
				$10^8$	28.4	1.515	1.515
				$1.33 \times 10^8$	37.7	2.011	2.011
${}_4He^{2+}$	20.2	314	31.4	$1.01 \times 10^6$	0.3	0.051	0.051
				$2.07 \times 10^6$	0.6	0.104	0.104
				$1.01 \times 10^7$	2.9	0.511	0.511
				$2.01 \times 10^7$	5.7	1.010	1.010
				$4.07 \times 10^7$	11.5	2.050	2.050
				$5.02 \times 10^7$	14.2	2.526	2.526

Hit probability calculations were evaluated assuming Poisson distribution in lymphocyte nuclei:

$$P(n) = (e^{-\lambda} \lambda^n) / n!$$

where,  $P(n)$  is the probability for one nucleus to be hit by  $n$  ions and  $\lambda$  is the mean number of impacts per nucleus.

Table II. Calculated hit probability for lymphocyte nuclei receiving a 0.1 Gy (4 MeV) proton dose

Number of nuclei hits	Hit fraction (%)
0	15
1	29
2	27
3 or more	29
Nuclei hit (%)	<b>85</b>

Table III. Calculated hit probability for lymphocyte nuclei receiving a 0.1 Gy  $\alpha$  particle dose

Number of nuclei hits	Hit fraction (%)
0	57
1	32
2	9
3 or more	2
Nuclei hit (%)	<b>43</b>

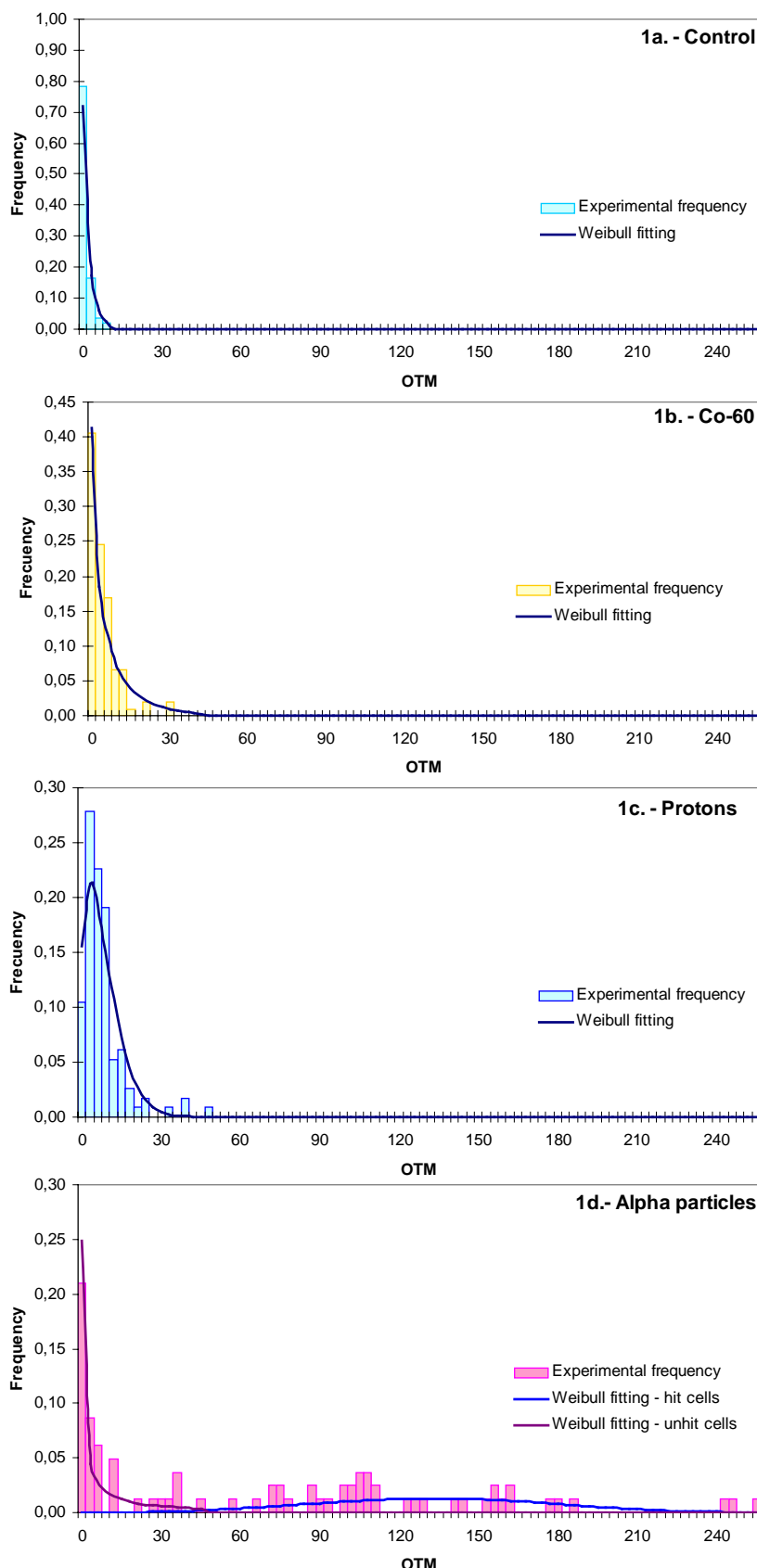


Figure 1. Probability distribution of OTM for unirradiated lymphocytes and exposed to 0.1 Gy

As the histograms obtained from the comet assay data (OTM) show a distinctive asymmetry, Weibull distributions were applied to fit comet experimental data obtained from lymphocytes exposed to 0.1 Gy of helium-4 particles, protons and Co-60 gamma rays (Figure 1). The two-parameter Weibull model implies that the probability density function has the following dependence:

$$f(x) = \left( \frac{\beta \cdot x^{\beta-1}}{\alpha^\beta} \right) \cdot e^{-\left(\frac{x}{\alpha}\right)^\beta} \quad (2)$$

where,  $\alpha$  is the scale parameter or characteristic value of the variable  $x$ , here the OTM, and  $\beta$  is the shape parameter. The integral of the probability density function  $f(x)$  is the probability distribution  $P(x)$ . The probability distribution is normalized so that the total area under the curve equals one. Figure 1a shows the probability distribution for unirradiated lymphocytes (control), Figure 1b to 1d represent the probability distribution for lymphocytes irradiated with 0.1 Gy of Co-60 gamma rays, protons and alpha particles.

When cells are exposed to a dose of 0.1 Gy, the hit probability model predicts that 43 % of the nuclei should have experienced an alpha traversal (Table III) while with protons, 85% of the nuclei should be hit (Table II). The comet experimental results show a biphasic response for 0.1 Gy helium-4 particles, indicating the existence of two subpopulations: unhit and hit, that is consistent with the predictions. In Fig. 1d, the first profile (area under the curve) indicates that 51% of the lymphocytes corresponds to the unhit subpopulation (control, see Fig. 1a), the second profile shows that 49% are hit cells.

Histograms in Fig. 2 represent the distributions of OTM as a function of the experimental dose for comets induced by helium-4 particles, protons and Co-60 gamma rays irradiations.

For irradiations with gamma rays, at increasing doses the tail moments are shifted towards high values with the same distribution, which is characterized by its asymmetry. When cells are irradiated with 4 MeV protons (9.4 KeV/ $\mu$ m), the comet distribution profiles follow a similar pattern but with higher dispersion of comet distributions. Fluences of  $7.45 \times 10^6$  and  $2.05 \times 10^7$ , involving doses of 0.112 and 0.309 Gy respectively, do not induce a significant change in DNA damage distribution compared with control. With fluences of  $6.72 \times 10^7$ ,  $10^8$  and  $1.33 \times 10^8$  (doses: 1.013, 1.515 and 2.011 Gy) a significant shift to higher OTM is observed.

After irradiations with 20.2 MeV helium-4 particles (31.4 KeV/ $\mu$ m), the shift to higher OTM at increasing mean dose is more pronounced and a broadening in comet distribution is observed.

As an example, 19 hits per nucleus are required for 4 MeV protons to produce a 1 Gy dose. For the same mean dose, 5.7 hits 20.2 MeV alpha particles cause a significant increase in DNA damage, evaluated through OTM of lymphocytes comets (see Fig.2). Thus, this indicates that for exposures to an ion of moderate LET, the mean dose and the hit distribution in the lymphocyte population influence the damage induction.

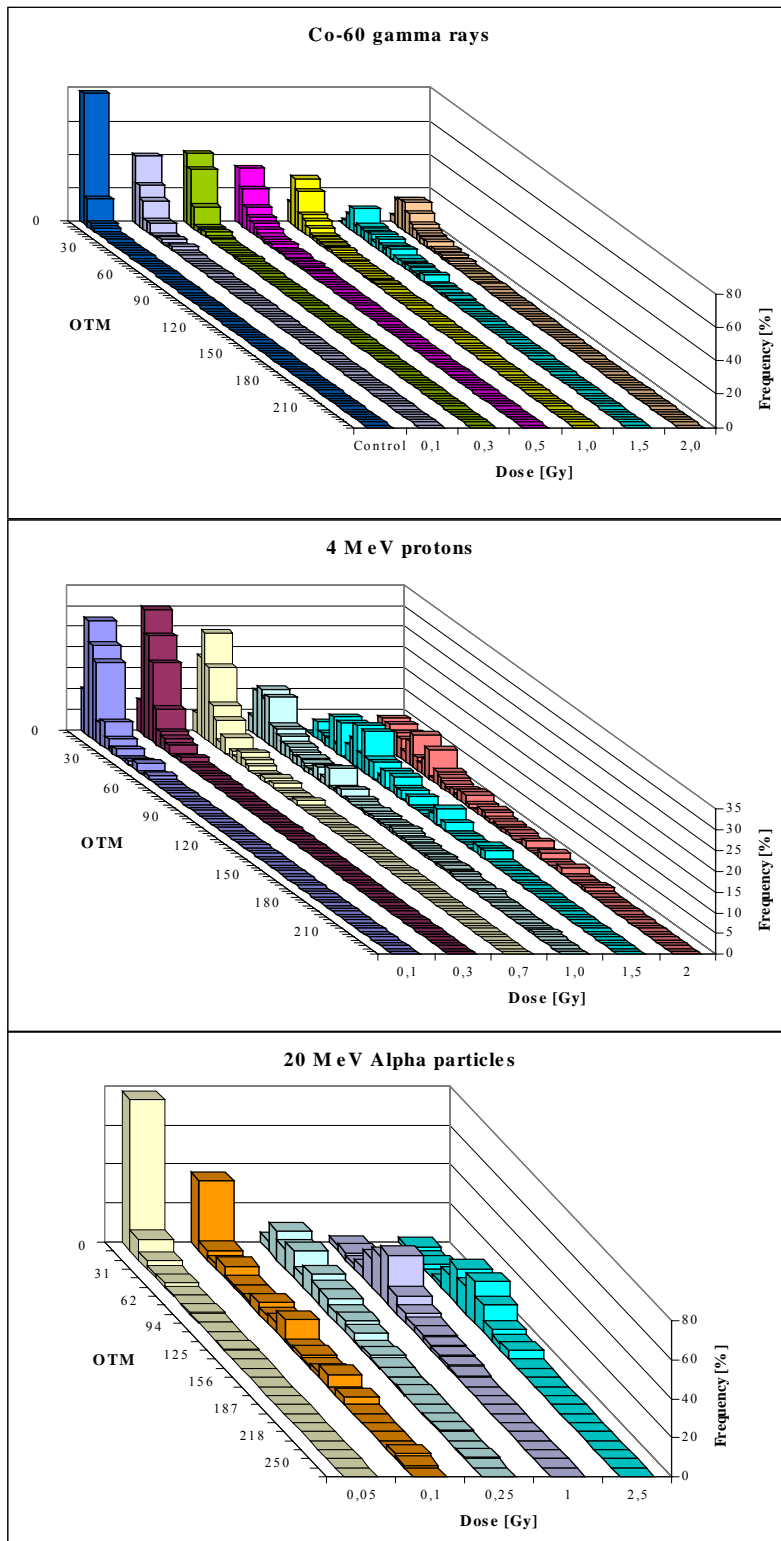


Figure 2. Distribution of OTM as a function of the mean dose for comets of human lymphocytes irradiated with Co-60  $\gamma$  rays, 4 MeV protons and 20.2 MeV  $\alpha$  particles

## CONCLUSIONS

At present, few studies have applied comet assay to evaluate the effects of high LET ions on cells [10]. The comet assay provided information of the heterogeneity of DNA damage induced by alpha particles in single human lymphocytes, allowing to identify and quantify hit and unhit subpopulations at low doses (0.1 Gy).

With helium-4 irradiations, it was observed a clear shift and dispersion (broadening) of comet distributions towards high OTMs with increasing fluence and mean dose. These marked variations in DNA damage suggest that each lymphocyte nucleus might be crossed by different number of particles, and thus, receive different doses. However, such a dispersion was not observed after irradiations with low LET radiation (Co-60 gamma rays) because increasing doses induce more breaks in every cell, resulting in a shift of comet distribution with the same profile.

The comet assay allowed to observe differences in the patterns of DNA damage induced by helium-4 particles compared to protons and gamma rays, indicating that for exposures to an ion of moderate LET, the mean dose and the hit distribution in the lymphocyte population influence the damage induction.

## REFERENCES

1. Edwards A. A., Lloyd D. C., Prosser J. S., Finnon P. and Moquet J. E. *Chromosome aberrations induced in human lymphocytes by 8.7 MeV protons and 23.5 MeV helium-3 ions*. Int. J. Radiat. Biol. 50, 137-145 (1986).
2. M. Di Giorgio, A.A. Edwards, J.E.Moquet, P.Finnon, P.A. Hone, D.C. Lloyd, A.J. Kreiner, J.A. Schuff, M.R.Taja, M.B Vallerga, F.O. López, A.Burlón, M.E.Debray, A. Valda, *Chromosome aberrations induced in human lymphocytes by heavy charged particles in track segment model*. Radiat. Prot. Dosim., in press, (2004).
3. International Atomic Energy Agency. *Absorbed Dose Determination in External Beam Radiotherapy*. Tech. Rept. Series 398 (Vienna, IAEA) (2000).
4. ICRU INTERNATIONAL COMMISSION ON RADIATION UNITS AND MEASUREMENTS, *Stopping Powers and Range for Protons and Alpha Particles*. ICRU Report 49, Bethesda, MD: ICRU (1993).
5. Singh N.P, Mc Coy MT, Tice RR., Schneider EL. *A simple technique for quantitation of low levels of DNA damage in individual cells*. Exp. Cell Res., 175: 184-191 (1988).
6. Tice RR. *The single cell gel/comet assay: a microgel electrophoretic technique for the detection of DNA damage and repair in individual cells*. Environmental mutagenesis. D.H.Phillips and S.Venitt, eds. Oxford, 315-339 (1995).
7. Końca K, Lankoff A, Lisowska H, Kuszewski T, Góźdż S, Koza Z, Wojcik A. *A cross-platform public domain PC image-analysis program for the comet assay*. Mutat. Res., 534: 15-20 (2003).
8. Olive PL, Banáth JB, Durand RE. *Heterogeneity in radiation induced DNA damage and repair in tumor and normal cells measured using the comet assay*. Radiat. Res., 122: 86-94 (1990).
9. Ejchart A, Sadlej-Sosnowska N. *Statistical evaluation and comparison of comet assay results*. Mutat. Res., 534: 85-92 (2003).
10. Testard I., Sabatier L. *Assessment of DNA damage induced by high-LET ions in human lymphocytes using the comet assay*. Mutat. Res., 448: 105-115 (2000).

# Assessment of Individual Radiosensitivity in Human Lymphocytes using Micronucleus and Microgel Electrophoresis "Comet" Assays

Di Giorgio, M.; Sardi, M.; Busto, E.; Vallerga, M.B.;  
Taja, M.R. and Mairal, L.



# **Assessment of individual radiosensitivity in human lymphocytes using micronucleus and microgel electrophoresis “Comet” assays**

**<sup>1</sup>Di Giorgio, M.; <sup>2,3</sup>Sardi, M.; <sup>2</sup>Busto, E.; <sup>1</sup>Vallerga, M.B.; <sup>1</sup>Taja, M.R. and<sup>3</sup>Mairal, L.**

**<sup>1</sup>Autoridad Regulatoria Nuclear, Av. Del Libertador 8250, CP: C1429BNP  
mdigorg@cae.arn.gov.ar**

**<sup>2</sup>Hospital Italiano, Gascón 450, CP: C1181ACH**

**<sup>3</sup>Mevaterapia, Tte. Gral. J. D. Perón 3937, CP: 1198  
Ciudad de Buenos Aires – ARGENTINA**

## **Abstract**

**Background and purpose:** Individual radiosensitivity is an inherent characteristic, associated with an increased reaction to ionizing radiation on the human body. Individuals show marked differences in radiation sensitivity, which has consequences in the fields of both radiation protection and radiation therapy. It is suggested that DNA repair mechanisms are involved. Consequently, the characterization of DNA repair in lymphocytes through cytokinesis blocked micronucleus (MN) and alkaline single-cell microgel electrophoresis (comet) assays could be suitable approaches to evaluate individual radiosensitivity in vitro.

The aims of this study were: 1) to assess the in vitro radiosensitivity of peripheral blood lymphocytes from two groups of cancer patients (prospectively and retrospectively studied), using MN and comet assays, in comparison with the observed clinical response and 2) to test the predictive potential of both techniques.

**Materials and methods:** 38 cancer patients receiving radiation therapy were enrolled in this study. The tumor sites were: head and neck ( $n = 25$ ) and cervix ( $n = 13$ ). 19 patients were evaluated prior, mid-way and on completion of treatment (prospective group) and 19 patients were evaluated about 2-480 month after radiotherapy (retrospective group). Cytogenetic data from the prospective group were analyzed using a mathematical model to evaluate the attenuation of the cytogenetic effect as a function of the time between a single exposure and blood sampling, estimating a cytogenetic recovery factor  $k$ . In the retrospective group, blood samples were irradiated in vitro with 0 (control) or 2 Gy and evaluated using MN test. Cytogenetic data were analyzed comparing expected MN frequencies (calibration curve from healthy donors) with values observed after in vitro irradiation. One over-reactor and patients that did not develop late effects were also evaluated through comet assay. DNA damage and repair capacity were quantified by the Olive tail moment. Lymphocytes of healthy individuals were used as reference sample.

**Results:** In the prospective evaluation, factor  $k$  correlated with the individual radiosensitivity. Patients with low recovery from the cytogenetic effect ( $k$  tending to zero) developed late toxicity (fibrosis and actinic rectitis). In the retrospective evaluation, lymphocytes of 3 from 4 patients that had developed late reactions were significantly more radiosensitive than lymphocytes from the rest of the patients and normal donors. The individual cytogenetic response suggested a correlation with the maximum grade of late reaction (osteonecrosis, fibrosis and trismus). A patient with severe late reactions showed reduced DNA repair capacity, measured by comet assay.

**Conclusions:** MN and comet tests could be suitable predictive assays to evaluate individual radiosensitivity in vitro. The identification of sub-groups with high radiosensitivity should be relevant for radiation protection and radiation therapy purposes. However, further studies are required to confirm the validity of these tests.

## **INTRODUCTION**

Individual radiosensitivity is an inherent characteristic, associated with an increased reaction to ionizing radiation on the human body. Individuals show marked differences in radiation sensitivity, which has consequences in the fields of both radiation protection and radiation therapy. After a radiation accident the physical dose and the individual radiosensitivity will determine the outcome for the exposed person.

The purpose of radiation protection remains to prevent deterministic effects of clinical significance and limit stochastic effects to acceptable levels. At the moment, current dose limits for occupational exposure are based on the assumption that the human population is homogeneous in its radiosensitivity; thus, individuals with high radiation sensitivity would suffer an increased incidence of both deterministic and stochastic effects. In radiotherapy, patients receiving identical radiation treatments have different impacts on normal tissues, varying from undetectable to sever.

Clinical studies have suggested that a large part of the spectrum of normal tissue reaction may be due to differences in individual radiosensitivity. The identification of such sub-groups should be relevant for radiation protection and radiation therapy purposes.

Radiation-induced damage to DNA can produce radiobiological effects such as cell inactivation and neoplastic processes. Nevertheless, in certain conditions the cell is able to modulate the damage by means of enzymatic repair mechanisms (homologous and illegitimate recombination). Biological endpoints such as clonogenic survival, chromosome aberration formation and repair capacity of radiation-induced damage have been applied to evaluate individual radiosensitivity *in vitro*.

The present study focused on the assessment of predictive *in vitro* assays for the evaluation of individual radiosensitivity in radiotherapy research, as an indicator of the extent of a patient's normal tissue reaction. This knowledge would provide further applications on radiation protection field.

Around 5%-7% of cancer patients develop adverse side effects to radiation therapy in normal tissues within the treatment field, which are referred as "clinical radiation reactions" and include acute effects, late effects and cancer induction [1]. It has been hypothesized that the occurrence and severity of these reactions are mainly influenced by genetic susceptibility to radiation [2]. Additionally, the nature of the genetic disorders associated with hypersensitivity to radiotherapy (mutations in the ATM and NBS gene associated with Ataxia Telangiectasia and Nijmegen breakage syndromes, respectively) suggests that DNA repair mechanisms are involved. Consequently, the characterization of DNA repair in lymphocytes through cytokinesis blocked micronucleus (MN) and alkaline single-cell microgel electrophoresis (comet) assays could be suitable approaches to evaluate individual radiosensitivity *in vitro*.

The MN assay is an established cytogenetic technique to evaluate intrinsic cell radiosensitivity in tumor cells and lymphocytes; the comet assay is a sensitive and rapid method for measuring DNA damage and repair in individual cells.

The aims of this study were: 1) to assess the *in vitro* radiosensitivity of peripheral blood lymphocytes from two groups of cancer patients (retrospectively and prospectively studied), using MN and comet assays, in comparison with the observed clinical response and 2) to test the predictive potential of both techniques.

## MATERIALS AND METHODS

38 cancer patients receiving radiation therapy were enrolled in this study. The tumor sites were head and neck ( $n = 25$ ) and cervix ( $n = 13$ ). 19 patients were evaluated prior, mid-way and on completion of treatment (prospective group) and 19 patients were evaluated 2-480 month after radiotherapy (retrospective group). Patient recruitment started in October 2000.

Cytogenetic data from the prospective group were analyzed using a mathematical model [3] to evaluate the attenuation of the cytogenetic effect,  $F(MN)$ , as a function of the time,  $d_i$ , between a single exposure and blood sampling, estimating a cytogenetic recovery factor  $k$  and its correlation with the clinical response.

$$F(MN) = \sum (MN_i \cdot e^{-d_i k}) \quad (1)$$

$k$  values are positive and vary between 0 and 1, if  $k$  tends to zero, the  $F(MN)$  value approaches the *in vitro* calibration curve, which indicates low recovery from the cytogenetic effect (high radiosensitivity); increasing values of  $k$  are proportional to increasing recovery from the cytogenetic effect (low radiosensitivity) as a function of time.

Integral doses were determined from isodose curves of each patient, obtained through the evaluation by tomography. The equivalent whole-body dose was calculated dividing the integral dose by the individual body weight.

In the retrospective group, blood samples were irradiated *in vitro* with 0 (control) or 2 Gy of Co-60  $\gamma$  rays and evaluated using MN test. This 2 Gy dose was selected as it resulted in negligible cell killing and measurable MN yield. Cytogenetic data were analyzed comparing the expected MN frequencies (calibration curve from healthy donors) with the values observed after *in vitro* irradiation, using  $\chi^2$  test.

#### *Micronucleus test*

0.8 – 1 ml whole blood samples were cultured in 8.5 ml RPMI 1640 growth medium (Gibco) supplemented with 25% fetal calf serum (Gibco). The cultures were stimulated with 3% phytohaemagglutinin M (Gibco) and incubated at 37 °C in a 5% CO<sub>2</sub> atmosphere for 72-74 hours. Cytochalasin B (Sigma) was added to a final concentration of 6 µg/ml 44 hours after addition of phytohaemagglutinin, to inhibit cytokinesis. After a further 28-30 hours of incubation cells were collected by centrifugation, treated with hypotonic solution, according to Iskandar method (0.9% NaCl / 0.075 M KCl 9 : 1) to preserve the cell cytoplasm, fixed with methanol/acetic acid (3 : 1 v/v), and stained with Giemsa. MN frequencies were assessed scoring 500 – 1000 binucleate cells applying Fenech, M. criteria [4] for selecting binucleate cells and MN.

#### *Comet assay*

Alkaline Comet assay was performed according to Singh [5] and Tice [6] technique with modifications. A layer of 1.5% normal melting agarose was prepared on microscope slides. After cell irradiation, ≈25,000 cells in 50 µl were mixed with 120 µl of 0.5% low melting agarose. The suspension was pipetted onto the precoated slides and cover with a cover slip. The agarose was allowed to cool down for 5 min in a refrigerator, the cover slip was removed and the microscope slide was immersed in cold lysis solution at pH 10 (2.5 M NaCl, 100 mM Na<sub>2</sub>EDTA, 10 mM Tris pH 10, 1% Triton X-100, 10% DMSO) and kept at 4 °C for 60 min. To allow denaturation of DNA, the slides were placed in alkaline electrophoresis buffer at pH 13 (1mM Na<sub>2</sub>EDTA / 300 mM NaOH) and left for 25 min. Subsequently, slides were transferred to an electrophoresis tank with fresh alkaline electrophoresis buffer and electrophoresis was performed at a field strength of 1.33 V/cm for 25 min at 4 °C (20 V – 125 mA). Slides were neutralized in 0.4 M Tris pH 7.5 for 5 min, stained with 20 µg/ml ethidium bromide, covered with a cover slip and incubated for 5 min in dark.

After adding the cells to the slides until the end of the electrophoresis, direct light irradiation was avoided and all steps were performed at 4 °C to prevent additional DNA damage.

For visualization of DNA damage, observations were made using a 20x objective on a epifluorescent microscope equipped with an excitation filter of 510-560 nm and a barrier filter of 590 nm. The slides were analyzed by an image analysis software called CASP [7]. Olive tail moment (OTM) [8] was used as a measure of DNA damage. OTM is the product of the distance (in x direction) between the center of gravity of the head and the center of gravity of the tail and the percent tail DNA.

One over-reactor and patients with normal late toxicity were also evaluated through comet assay. Lymphocytes of healthy individuals were used as reference sample. Blood samples were in vitro irradiated with 2 Gy and DNA repair capacity was evaluated for initial damage and after 5, 10, 20, 30, 50 and 80 minutes of incubation at 37 °C, 5% CO<sub>2</sub>. DNA damage and repair capacity were quantified by the Olive tail moment, whose distribution was adjusted by a two-parameter Weibull model [9]. The Weibull alpha parameter was applied to describe DNA damage at the mentioned repair times after irradiation. 80-100 comets were evaluated per point.

A non linear regression analysis and curve fitting program (NLREG) was applied to asses the repair profiles of patients and healthy donors.

Late toxicity in normal tissues, within the treatment field, was evaluated and correlated with the in vitro radiosensitivity derived from the application of MN and comet assays.

## RESULTS

#### *Prospective evaluation*

Figure 1. shows that MN frequency increases linearly with the equivalent whole-body dose ( $R^2 = 0.9$  ;  $P = 0.015$ ). This correlation demonstrates the suitability of the MN assay as a biological dosimeter for the evaluation of ionizing radiation exposure *in vivo*. The comparison of spontaneous MN frequency in healthy subjects ( $0.013 \pm 0.008$ ) with those in cancer patients prior to radiotherapy ( $0.0285 \pm 0.0047$ ) reveals significant difference.

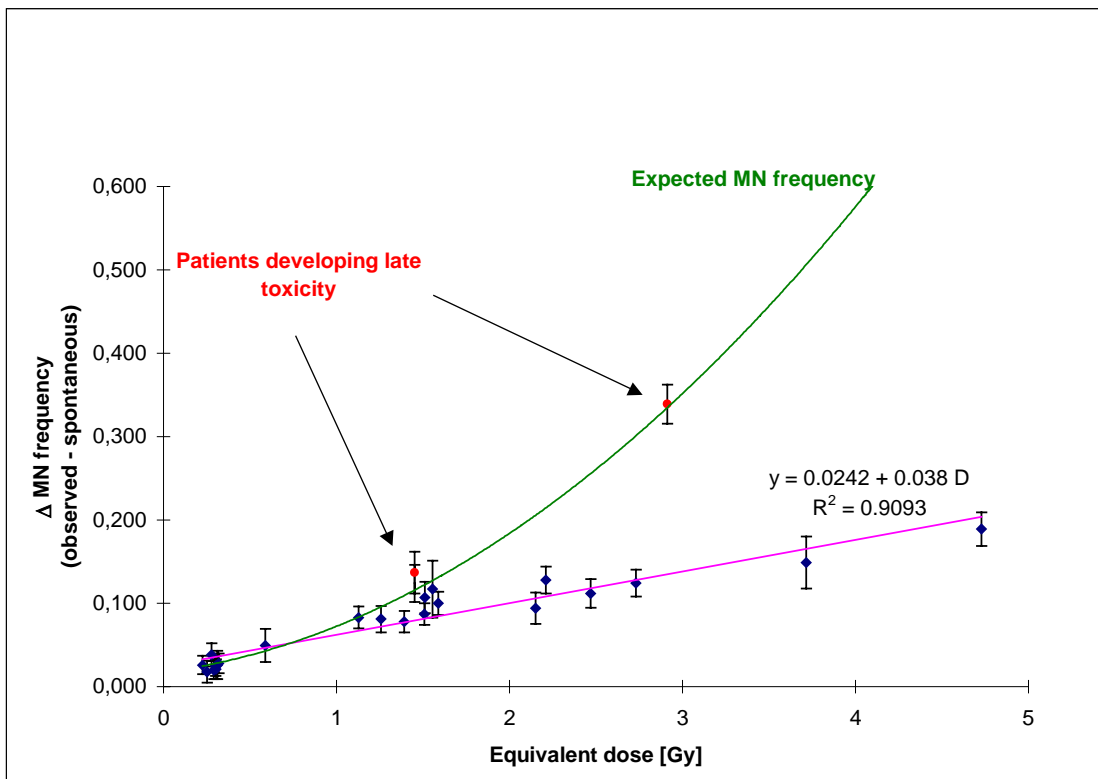


Figure 1. Correlation between the MN frequency and the equivalent whole-body dose in 19 cancer patients undergoing radiotherapy

Patient data tend to fall below the calibration curve (expected frequency) over 2 Gy equivalent dose. This phenomenon could be attributed to fractionation of the dose rather to the condition of partial irradiation. For fractionated treatment on parts of the body having a large blood volume and flow it is suggested that lymphocyte remixing contributes to a final homogenization of the total absorbed dose. Therefore, it can be assumed that with fractionated irradiation there exists a partial cytogenetic recovery from the effect induced by a single exposure as a function of time between exposure and blood sampling. The individual recovery from the cytogenetic effect can be measured in the range between 2 – 5 Gy of equivalent whole- body dose, where a substantial difference is found between patients data and the calibration curve.

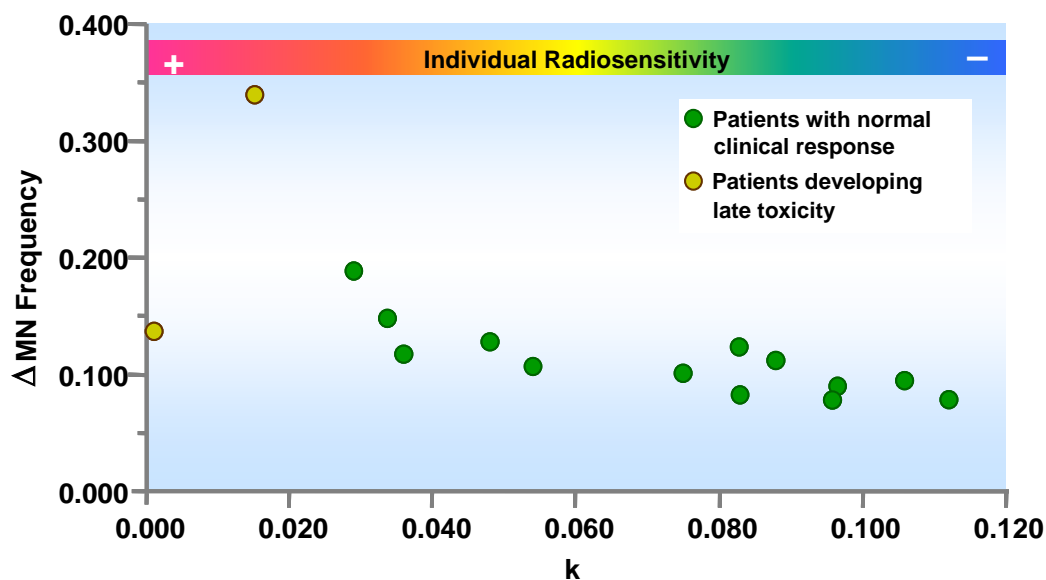


Figure 2.  $\Delta$  MN frequency vs. cytogenetic recovery factor k

In 2 out of the 19 prospectively evaluated patients, the MN frequencies approach the calibration curve. This indicates low recovery from the cytogenetic effect and high radiosensitivity of the patients. Factor k correlates with the individual radiosensitivity (Figure 2). Patients with low recovery from the cytogenetic effect (k tending to zero) develop late toxicity (fibrosis and actinic rectitis).

#### *Retrospective evaluation*

Patient	Dose = 0Gy		Dose = 2Gy	
	Observed Frequency	$\chi^2$ Test	Observed Frequency	$\chi^2$ Test
1	0,0423	36,15	0,3412	134,06
2	0,0095	3,52	0,1694	1,17
3	0,0216	1,05	0,1984	1,11
4	0,0128	1,15	0,2012	1,59
5	0,0132	0,97	0,2053	2,44
6	0,0138	0,70	0,1240	19,60
7	0,0398	29,26	0,3450	140,62
8	0,0119	1,71	0,2041	2,18
9	0,0102	2,91	0,1358	12,67
10	0,0136	0,79	0,1600	3,15
11	0,0123	1,45	0,1780	0,20
12	0,0098	3,27	0,1920	0,34
13	0,0200	0,42	0,2082	3,15
14	0,0080	5,00	0,1478	7,15
15	0,0136	0,80	0,1319	14,82
16	0,0112	2,15	0,1346	13,30
17	0,0134	0,88	0,1369	12,10
18	0,0272	5,71	0,1790	0,14
19	0,0287	7,51	0,3272	111,23

Table I. Spontaneous MN frequencies and radiation induced MN frequencies, after in vitro irradiation with 2 Gy of Co-60, analyzed using  $\chi^2$  test

Cytogenetic data, comparing expected MN frequencies (derived from the calibration curve of healthy donors) with values observed after in vitro irradiation, were analyzed using  $\chi^2$  test. Values  $> 3,84$  (DF = 1;  $p < 0.05$ ) indicate statistically significant differences between observed and expected MN frequencies and thus, individual radiosensitivity or radioresistance (Table I).

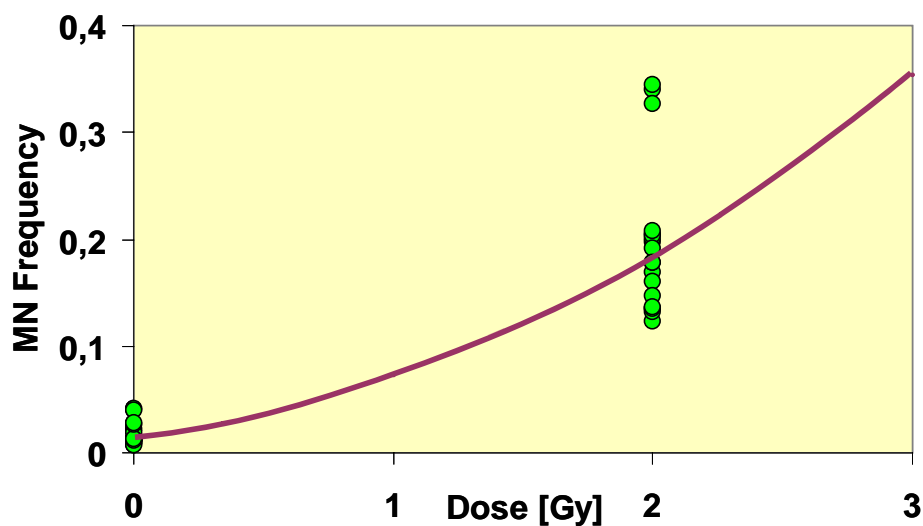


Figure 3. Cytogenetic data comparing expected MN frequencies with values observed after in vitro irradiation, retrospective analysis

In the retrospective evaluation, lymphocytes of 3 from 4 patients that had developed late reactions were significantly more radiosensitive than lymphocytes from the rest of the patients and normal donors (Figure 3). The individual cytogenetic response suggests a correlation with the maximum grade of late reaction (osteonecrosis, fibrosis and trismus).

One patient with sever late reaction in normal tissue (osteonecrosis) and patients with normal late toxicity were also evaluated through comet assay, applying CASP program (Figure 4).

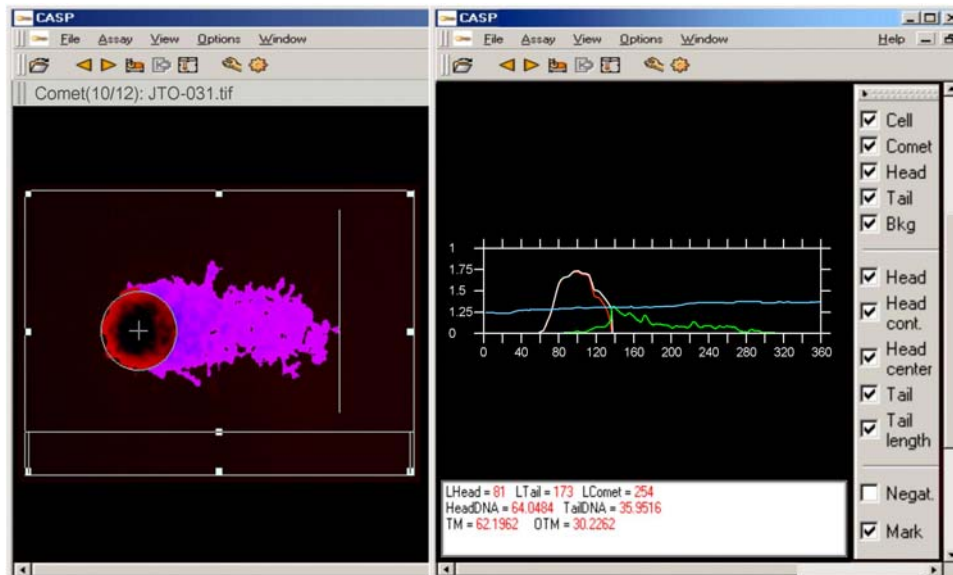


Figure 4. View of CASP program windows: On the left window the comet image with the measurement frame is visible, head and tail marked. In the right window the intensity profiles are plotted

Figure 5. shows the repair kinetics in lymphocytes of patients and healthy controls. The extent of DNA damage was measured up to 80 minutes. Olive tail moment (OTM) data were fitted by a mono-exponential function:

$$OTM(t) = TM_0 \cdot e^{-\left(\frac{t \cdot \ln 2}{\tau_{1/2}}\right)} + TM_R \quad (2)$$

where,

$OTM$  = Olive Tail moment

$TM_0$  =  $OTM$  initial damage

$TM_R$  =  $OTM$  residual damage

$\tau_{1/2}$  = repair half time

$t$  = incubation time after in vitro irradiation

The mean half-times, i.e., the time required for lymphocytes to restore 50% of the initial DNA damage, for over-reactor patient, patients with normal late toxicity and controls were 22.9, 5.9 and 1.2 minutes, respectively. DNA damage of the patient developing osteonecrosis resulted about 9.5 times higher than that of the healthy controls, evaluated 10 minutes post irradiation.

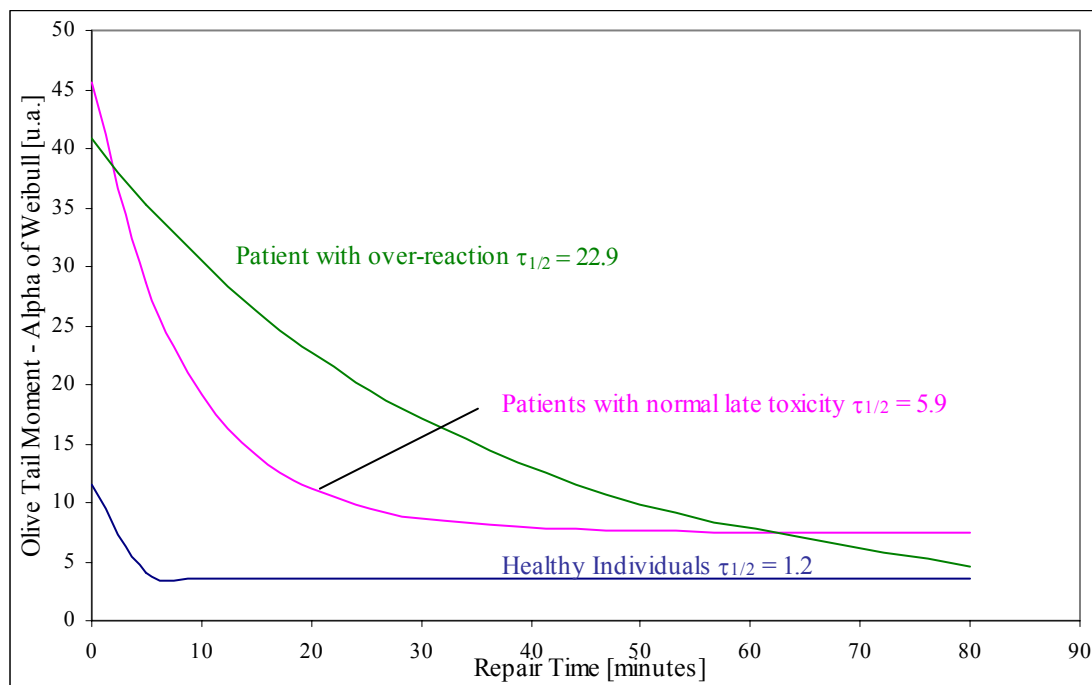


Figure 5. Repair kinetics in lymphocytes determined by the comet assay.

## CONCLUSIONS

The cytogenetic data demonstrate that the cytokinesis blocked micronucleus assay is suitable for the evaluation of individual cytogenetic response to radiotherapy in body areas having a large blood volume and flow or including bone marrow. Thus, suggesting that lymphocyte remixing contributes to a final homogenization of the total absorbed dose.

In the prospective evaluation, the cytokinesis blocked micronucleus assay (in vitro) correlated with the clinical late toxicity (in vivo) over 2 Gy equivalent whole-body dose, in agreement with other studies [10]. Therefore, the predictive potential of MN assay results limited by the requirement to accumulate 2 Gy equivalent whole-body dose (more than 10 fractions) in order to find a substantial difference in the DNA repair capacity, measured through  $k$  parameter. Low values of  $k$  indicate high radiosensitivity of the lymphocyte pool and thus, a patient with low recovery from the cytogenetic effect.

No correlation with clinical acute toxicity was observed.

In the retrospective evaluations, both, spontaneous and in vitro radiation-induced micronucleus frequencies were significantly increased, compared with the expected values from the calibration curve, in those patients who had developed late tissue reactions.

The retrospective evaluation with micronucleus assay would allow predicting the late toxicity in patients that would require re-irradiation treatment.

The assessment of the repair kinetics in lymphocytes of the patient with sever late effects supports the comet assay as a useful indicator for individual radiosensitivity. Comet assay permitted to determine the initial DNA damage, the speed of repair (repair half life) and the amount of residual DNA damage after a specific time of repair (80 minutes). The test provides not only the information on mean values (alpha parameter of Weibull distribution for the Olive tail moment), but also the representation of distributions (frequency histograms) based on the results on the single cell level.

MN and comet tests could be suitable predictive assays to evaluate individual radiosensitivity in vitro, contributing with the detection of patients that develop late adverse reactions.

These studies would contribute with radiosensitivity tests of current use but applying rapid methodologies easy to implement in a routine clinical laboratory. However, further studies are required to confirm the validity of these tests. This knowledge would provide further applications on the radiation protection field.

In the radiation therapy field, the identification of radiosensitive patients will allow the individualization of patient treatment. Normal tissue radiosensitivity testing could be used to dose-escalate or dose-reduce without compromising tumor control rates.

## REFERENCES

1. Twardella D, Chang-Claude J. *Studies on radiosensitivity from an epidemiological point of view – overview of methods and results*. Radiother Oncol, 62: 249-260 (2002).
2. Popanda O, Ebbeler R, Twardella D et al. *Radiation-induced DNA damage and repair in lymphocytes from breast cancer patients and their correlation with acute skin reactions to radiotherapy*. Int. J. Radiation Oncology Biol. Phys., 55 (5): 1216 – 1225 (2003).
3. Catena C, Conti D, Parasacchi P et al. *Micronuclei in cytokinesis-blocked lymphocytes may predict patient response to radiotherapy*. Int. J. Radiat. Biol., 70 (3): 301 – 308 (1996).
4. Fenech, M. *The in vitro micronucleus technique*. Mutat. Res., 455: 81-95 (2000).
5. Singh N.P, Mc Coy MT, Tice RR., Schneider EL. *A simple technique for quantitation of low levels of DNA damage in individual cells*. Exp. Cell Res., 175: 184-191 (1988).
6. Tice RR. *The single cell gel/comet assay: a microgel electrophoretic technique for the detection of DNA damage and repair in individual cells*. Environmental mutagenesis. D.H.Phillips and S.Venitt, eds. Oxford, 315-339 (1995).
7. Końca K, Lankoff A, Lisowska H, Kuszewski T, Góźdż S, Koza Z, Wojcik A. *A cross-platform public domain PC image-analysis program for the comet assay*. Mutat. Res., 534: 15-20 (2003).
8. Olive PL, Banáth JB, Durand RE. *Heterogeneity in radiation induced DNA damage and repair in tumor and normal cells measured using the comet assay*. Radiat. Res., 122: 86-94 (1990).
9. Ejchart A, Sadlej-Sosnowska N. *Statistical evaluation and comparison of comet assay results*. Mutat. Res., 534: 85-92 (2003).
10. Catena C, Parasacchi P, Conti D, Sgura A, Trenta G, Righi E, Trinci MM Trinci M. *Peripheral blood lymphocyte decrease and micronucleus yields during radiotherapy*. Int. J. Radiat. Biol., 72(5): 575-585 (1997).

# Dosimetría biológica en accidentes de criticidad. Ejercicio de intercomparación en el reactor Silene – Francia

Di Giorgio, M.; Vallerga, M.B. y Taja, M.R.



# DOSIMETRÍA BIOLÓGICA EN ACCIDENTES DE CRITICIDAD. EJERCICIO DE INTERCOMPARACIÓN EN EL REACTOR SILENE – FRANCIA

Di Giorgio, M.; Vallerga, M.B. y Taja, M.R.

Autoridad Regulatoria Nuclear  
Argentina

**Abstract:** BIOLOGICAL DOSIMETRY AFTER CRITICALITY ACCIDENTS. INTERCOMPARISON EXERCISE IN THE SILENE REACTOR-FRANCE

The Institute of Radiation Protection and Nuclear Safety (IRSN) organized an international biological dosimetry intercomparison, at the SILENE experimental reactor (Valduc, France), simulating different criticality scenarios: bare source 4 Gy, lead shield source 1 and 2 Gy and gamma pure  $^{60}\text{Co}$  source 2 Gy. Fifteen laboratories were involved in this exercise, including the biological dosimetry laboratory from Argentina. The purposes of the intercomparison were: I) to compare the unstable chromosome aberration (UCA) frequency observed by the different laboratories and 2) to compare the dose estimation for gamma rays and neutrons. The objects of the present work were: I) to compare the mean frequency of UCA observed by Argentina-laboratory with the mean frequency observed by the participant laboratories as a whole. II) to compare the dose estimates performed by Argentina-lab with those estimated by the other laboratories involved in the second stage of the intercomparison.

Overall, the mean frequencies of UCA and the correspondent 95% confidence limits obtained by the Argentina-lab were consistent with the results obtained by the laboratories as a whole. For the gamma pure scenario, less variations were observed among laboratories in terms of dose ( $CV=18,2\%$ ) than in terms of frequency ( $CV=30,1\%$ ). For the mixed field scenarios, only four laboratories, including Argentina-lab, estimated gamma and neutron components of the total dose and just two (Argentina lab and lab 12) were in agreement with the given physical doses. The 1 Gy experiment presented less variations both in terms of frequency and dose than the other two scenarios. For the 4 and 2 Gy experiments, variations in neutron dose were more significant than variations in gamma dose, related to the magnitude of the dose.

The results suggest that intercomparison exercises jointly with the accreditation of biological dosimetry by cytogenetic service laboratories, in compliance with ISO/IEC 17025, would allow to unify the protocols applied regarding: techniques, metaphase selection and scoring process. Thus, improving the dosimetric response in accidental overexposures that would require cooperation among countries.

## Introducción

El Instituto de Radioprotección y Seguridad Nuclear (IRSN) de Francia organizó un ejercicio de intercomparación internacional en dosimetría accidental, entre 15 laboratorios, en junio de 2002 – 2003, en el cual participó el Laboratorio de Dosimetría Biológica de la Autoridad Regulatoria Nuclear. En esta intercomparación estuvieron involucradas las dosimetrías física y biológica.

Desde el punto de vista de la dosimetría biológica, se evaluó la respuesta en campos mixtos neutrón-gamma por ser de gran interés en caso de accidentes de criticidad. Si bien estos accidentes no son frecuentes resultan complejos en su evaluación como lo revelan los ocurridos en Oak Ridge (1958, accidente de criticidad planta Y-12) [1], Vinca (1958, accidente de criticidad en un reactor experimental) [2], Hanford (1962, accidente de criticidad Recuplex) [3], Buenos Aires (1983, RA-2 Centro Atómico Constituyentes, accidente en una facilidad crítica) [4], Chernobyl (1986, accidente en una planta nuclear) [5], Tokai-mura (JCO) (1999, accidente de criticidad en una planta de procesamiento de uranio) [6]. Este último accidente ha recibido particular atención por ser el primer caso en el cual un considerable número de personas fue expuesta a neutrones. Previamente, las bombas atómicas de Hiroshima y Nagasaki constituyeron las bases para la evaluación de las consecuencias para la salud de la exposición de poblaciones humanas a neutrones, aunque estas bases biológicas fueron relegadas luego de la re-evaluación dosimétrica DS86 que estimó que las dosis de neutrones fueron muy pequeñas en ambas ciudades [7].

La eficiencia biológica relativa (RBE) de los neutrones del espectro de fisión y de la radiación gamma es muy diferente: la penetración de la radiación gamma en el organismo es más profunda que la de los neutrones, pero los neutrones poseen una mayor RBE. El espectro de energía de neutrones al que un individuo puede estar expuesto varía ampliamente, dependiendo de la fuente de neutrones y su moderación en blindajes, incluyendo el cuerpo. La importancia de estos efectos depende de la variación de la RBE en el rango de energía de interés.

La Dosimetría Citogenética, basada en la estimación de la frecuencia de aberraciones cromosómicas inestables (ACI) radioinducidas a partir de cultivos de linfocitos obtenidos de una muestra de sangre venosa, es el método de rutina más ampliamente utilizado en la evaluación biodosimétrica de las sobreexposiciones accidentales. Esta dosimetría complementa a las dosimetrías física y clínica y, en ciertos casos, por falta de registros físicos de la dosis o por imprecisa reconstrucción del escenario de sobreexposición, constituye la única evaluación posible.

La estimación biológica de la dosis se basa en el recuento de ACI (dicéntricos y anillos). La dosis media es determinada a partir de la frecuencia observada, utilizando curvas dosis-efecto realizadas para distintas calidades de radiación. Estas curvas de calibración están influenciadas por los protocolos utilizados por cada laboratorio.

Diversos factores pueden influenciar la estimación de la dosis: condiciones de cultivo, las relaciones dosis-respuesta establecidas y los criterios de selección de metafases y de recuento de aberraciones cromosómicas. En la presente intercomparación se evaluaron los efectos de los criterios de selección de metafases y del recuento de aberraciones cromosómicas.

Los objetivos de la intercomparación fueron: 1) comparar las frecuencias de ACI observadas por los distintos laboratorios y 2) comparar la estimación de la componente gamma y neutrones de la dosis total, determinada a partir de la frecuencia de ACI observada en campos mixtos.

Los objetivos del presente trabajo fueron: I) comparar la frecuencia media de dicéntricos más anillos por célula observada por el laboratorio de la ARN-Argentina respecto de la frecuencia media obtenida por todos los laboratorios en su conjunto y II) comparar la estimación dosimétrica realizada por el laboratorio de la ARN-Argentina respecto de la estimada por cada uno de los laboratorios participantes en esta segunda etapa de la intercomparación.

## Materiales y métodos

*Condiciones de la exposición:* A fin de simular el efecto neutrón/gamma en el organismo, muestras de sangre entera fueron irradiadas en tubos heparinizados adheridos a un fantoma humano, junto con los dosímetros físicos. Las irradiaciones de las muestras de sangre fueron realizadas en el reactor experimental SILENE (Valduc, Francia), excepto la irradiación con gamma puro de  $^{60}\text{Co}$  que fue realizada en LCIE, Fontenay-aux roses, Francia. Se utilizaron tres tipos de exposición a neutrones, correspondientes a diferentes relaciones neutrón/gamma o diferentes dosis que se resumen en la Tabla 1.

*Cultivos celulares:* Antes del inicio del cultivo, las muestras de sangre se incubaron a 37°C durante 2 horas para permitir la reparación del ADN.

Los cultivos celulares fueron realizados en Francia por el laboratorio organizador con la ayuda del National Radiological Protection Board del Reino Unido.

Los cultivos de linfocitos fueron establecidos de acuerdo con las recomendaciones de la OIEA [8]. Brevemente, 0,5 ml de sangre entera fueron mezclados con 5 ml de medio de cultivo RPMI 1640, adicionado con suero bovino fetal 10%, L-glutamina 1%, hepes

1%, penicilina-estreptomicina 1%, bromodeoxiuridina 1%, piruvato de sodio 1% y 150 µl de fitohemaglutinina. Después de 46 horas de cultivo a 37°C, se añadieron 0,5 µg de colcemida y la mitad de los cultivos se incubaron durante 2 horas y la otra mitad, durante 4 horas. Las células fueron cosechadas, tratadas con solución hipotónica (0,075 M KCl) y fijadas en tres pasos de fijación con metanol: ácido acético (3:1, v/v).

Luego, los vidrios ya preparados (sembrados) o suspensiones celulares en fijador (sin sembrar) fueron enviados a los distintos laboratorios, de acuerdo a lo requerido. El laboratorio de la ARN solicitó vidrios ya sembrados para evitar el deterioro del material, en previsión de la ocurrencia de demoras en el transporte de las suspensiones celulares.

La frecuencia de ACI fue establecida por todos los participantes evaluando alrededor de 500 células o 100 ACI para las muestras control e irradiadas, respectivamente. El laboratorio de la Argentina aplicó los criterios de selección de metafases y la nomenclatura establecidos en Technical Report 260/405, OIEA [8, 9] y ISCN 1995 [10].

## Resultados

Para los escenarios 1, 2 y 3 (campos mixtos), la irradiación con gama puro de  $^{60}\text{Co}$  y los correspondientes controles, los resultados citogenéticos obtenidos por el laboratorio de la ARN-Argentina se muestran en la Tabla 2.

El análisis de la distribución de dicéntricos + anillos fue realizado según Papworth [11 Papworth 1970] utilizando la relación varianza/media ( $\sigma^2/y$ ) y el parámetro de sobredispersión  $\mu$ . Para los escenarios de campos mixtos no hubo evidencia de sobredispersión significativa respecto de la distribución de Poisson, indicando que las irradiaciones fueron homogéneas y sugiriendo el uso de la distribución de Poisson para la estimación de las incertezas.

I) Se comparó la frecuencia media de ACI (dicéntricos más anillos por célula) observada por el laboratorio de la ARN-Argentina respecto del obtenido por todos los laboratorios en forma conjunta (Tabla 3.).

Para la fuente desnuda (4 Gy -  $\gamma/n= 1,2$ ), 13 laboratorios participaron en el recuento de ACI. La frecuencia media para el laboratorio de la ARN-Argentina (lab. 4) fue: 2,105 ACI/célula con un intervalo de confianza del 95% entre 1,849 – 2,360. El valor medio para todos los laboratorios resultó  $2,27 \pm 0,68$  (DS) ACI/célula. Sólo 3 laboratorios mostraron una frecuencia media no incluida en este intervalo. El mínimo valor observado en este escenario fue 1,16 ACI/célula y el máximo valor, 3,70 ACI/célula ( $\Delta=2,54$  ACI/célula).

Para la fuente blindada con plomo (2 Gy -  $\gamma/n=0,19$ ), 13 laboratorios estuvieron involucrados en este experimento. La frecuencia media para el laboratorio de la ARN-Argentina fue: 1,488 ACI/célula con un intervalo de confianza del 95% entre 1,230 – 1,746. La frecuencia media de dicéntricos más anillos para todos los laboratorios fue  $1,67 \pm 0,39$  ACI/célula. Dos laboratorios mostraron frecuencias medias próximas a los 2 valores extremos y otros 4 laboratorios, frecuencias medias próximas al intervalo pero fuera del mismo. Sin embargo la diferencia observada entre el valor más alto (2,44 ACI/célula) y el más bajo (1,18 ACI/célula), ( $\Delta=1,26$  ACI/célula), resultó menor que la observada en el experimento anterior (fuente desnuda 4 Gy).

El último experimento en campo mixto neutrón/gamma involucró también una fuente blindada con plomo pero con una dosis de 1 Gy, entregada en aproximadamente 30 minutos. Once laboratorios participaron en este experimento. La frecuencia media para el laboratorio de la ARN-Argentina fue: 0,656 ACI/célula con un intervalo de confianza del 95% entre 0,534 – 0,778. La frecuencia media de dicéntricos más anillos para todos los laboratorios fue  $0,81 \pm 0,12$  ACI/célula. Para este experimento, 4 laboratorios

presentaron frecuencias medias que resultaron fuera de este intervalo. Nuevamente, la diferencia observada entre el valor más alto (1,04 ACI/célula) y el más bajo (0,62 ACI/célula), ( $\Delta=0,42$  ACI/célula), fue menor que la observada para la experiencia con fuente desnuda.

Para el escenario de irradiación con 2 Gy (gama puro de  $^{60}\text{Co}$ ), 12 laboratorios estuvieron involucrados en este experimento. La frecuencia media para el laboratorio de la ARN-Argentina fue: 0,279 ACI/célula con un intervalo de confianza del 95% entre 0,231 – 0,326. La frecuencia media de dicéntricos más anillos para todos los laboratorios fue  $0,28 \pm 0,08$  ACI/célula. Tres laboratorios presentaron frecuencias medias que resultaron fuera de este intervalo. La diferencia observada entre el valor más alto (0,450 ACI/célula) y el más bajo (0,156 ACI/célula) fue  $\Delta=0,294$  ACI/célula.

Para los escenarios de campos mixtos, las mayores diferencias en las frecuencias medias observadas entre laboratorios, cuyos coeficientes de variación fueron: 29,9% (4 Gy); 23,1% (2 Gy) y 15,1% (1 Gy), correspondieron al escenario de 4 Gy, fuente desnuda.

## II) Se compararon las estimaciones dosimétricas.

Las estimaciones dosimétricas debidas a radiación gamma y a neutrones, administradas a las muestras evaluadas por el laboratorio de la ARN-Argentina, fueron realizadas con referencia:

- 1)Curva de calibración del laboratorio para radiación gamma de  $^{60}\text{Co}$  (0,70 Gy/min)  

$$y = 0,0005 + 0,0168D + 0,0556D^2$$

- 2)Curva de neutrones del espectro de fisión (0,7 MeV), Technical Report 260/405, OIEA [8, 9]

$$y = 0,0005 + 0,832D$$

Donde  $y$  es la frecuencia de aberraciones cromosómicas (dicéntricos más anillos), y  $D$  es la dosis en Gy.

Resultados obtenidos por nuestro laboratorio en un estudio previo [12] permiten aplicar esta curva de calibración para la estimación biológica de la dosis en un escenario de criticidad.

Para el escenario de gamma puro (2 Gy), el cálculo de dosis fue realizado por 12 laboratorios (Figura 1). Las líneas horizontales representan la dosis física administrada a las muestras  $(2\text{Gy}) \pm \text{el } 20\%$ . Las estimaciones dosimétricas para todos los laboratorios, excepto 2, se encontraron en este rango. La dosis media estimada por el lab. de la ARN-Argentina fue 2,17 Gy con una dosis máxima de 2,36 Gy y una dosis mínima de 1,96 Gy (intervalo de confianza del 95%).

Para los escenarios de campos mixtos, el lab. de la ARN-Argentina estimó ambas componentes de la dosis total (dosis gamma y dosis de neutrones) a partir de las frecuencias de aberraciones observadas y conociendo la relación gamma/neutrón ( $\gamma/n$ ), proveniente de mediciones por dosimetría física. Se aplicó un proceso iterativo de acuerdo al método propuesto en los Reportes Técnicos del OIEA 260/405 [8, 9], postulando que ambas calidades de radiación son aditivas en la inducción de aberraciones cromosómicas y que la distribución de aberraciones no muestra sobredispersiones respecto a la distribución de Poisson.

Sólo 4 laboratorios estimaron ambas componentes de la dosis (Tabla 4.).

El escenario de 1 Gy mostró menos variaciones que los otros dos. Para los escenarios de 4 Gy y 2 Gy, la variación entre el valor de dosis de neutrones más alto y el más bajo se encuentra en el mismo rango: 1 Gy y 1,2 Gy, respectivamente. Estas variaciones son importantes teniendo en cuenta las dosis involucradas en estos escenarios. Sólo las dosis estimadas por los laboratorios 4 (ARN) y 12 fueron consistentes con las dosis físicas administradas. Respecto a la componente gamma de la dosis total, excepto para el

escenario de 4 Gy, las variaciones fueron menos importantes, nuevamente relacionado con las dosis involucradas.

## Discusión y conclusiones

### Etapa I:

Las frecuencias medias de aberraciones y los correspondientes intervalos de confianza del 95% obtenidos por el lab. de la Argentina son consistentes con los resultados obtenidos por todos los laboratorios en su conjunto. Las variaciones entre laboratorios en el recuento de aberraciones pueden provenir de la calidad de radiación utilizada ya que la mayoría de los citogenetistas están más familiarizados con el recuento de aberraciones en células expuestas a radiación de baja transferencia lineal de energía (LET) que a alta LET. Con alta LET, algunas células pueden resultar altamente dañadas, produciendo dificultades en el recuento. Los criterios utilizados por cada laboratorio en la selección de las metafases a analizar pudo haber diferido.

### Etapa II:

Para el escenario de gamma puro (2 Gy), se observaron menos variaciones entre los laboratorios cuando se compararon las dosis ( $CV = 18,2\%$ ) que cuando se compararon las frecuencias ( $CV = 30,1\%$ ). Esto confirma que algunas condiciones experimentales, tales como el recuento de dicéntricos y anillos, son laboratorio dependientes. Resultados similares fueron presentados en una intercomparación realizada en 1995 involucrando 5 laboratorios latinoamericanos, en la que también participó el lab. de la ARN de la Argentina: de las 15 estimaciones dosimétricas, 11 estuvieron dentro de  $\pm 30\%$  de la dosis [13].

Para los escenarios de campos mixtos, los resultados tendieron a mostrar mayores variaciones a altas dosis. Dado que las frecuencias observadas por los 4 laboratorios se encuentran dentro de la franja comprendida por la frecuencia media y su desviación estándar para todos los laboratorios en conjunto, las diferencias en las dosis estimadas pueden deberse a las curvas de calibración aplicadas, principalmente a la curva de neutrones del espectro de fisión, o inconsistencias en el proceso iterativo para el cálculo dosimétrico.

Los resultados precedentes sugieren que los ejercicios de intercomparación, junto con la acreditación de los laboratorios de dosimetría biológica, bajo la norma ISO 17025, permitirían unificar los protocolos utilizados por los distintos laboratorios, tanto en lo referido a las técnicas aplicadas como a los criterios de selección de metafases, recuento de aberraciones cromosómicas y cálculo dosimétrico. Esta unificación de los criterios y cuantificación de la respuesta de los laboratorios permitiría: 1) utilizar curvas de calibración internacionales, dado que no siempre es posible disponer de fuentes para distintas calidades de radiación, a fin de realizar las curvas de calibración propias del laboratorio y 2) mejorar la respuesta en situaciones accidentales que requieran asistencia mutua entre países.

## Bibliografía

1. Bender, M. A.; Gooch, P.C. *Persistent chromosome aberrations in irradiated human subjects*. Radiat. Res., 16: 44-53 (1962).
2. Pendić, B.; Barjaktarović, N.; Kostić, V. *Chromosomal Aberrations in Persons Accidentally Irradiated in Vinča 19 Years Ago*. Radiat. Res. 81: 478-482 (1980).
3. Bender, M. A.; Gooch, P.C. *Somatic Chromosome Aberrations Induced by Human Whole Body Irradiation: The "Recuplex" Criticality Accident*. Radiat. Res. 29: 568-582 (1966)
4. Giménez, J. C.; Couto, S. L.; Del Río, M. R.; Nazazzi, N.; Taja, M. R.; Caamaño, J. *Dosimetría Biológica del Personal involucrado en un accidente de criticidad*, 12<sup>ava</sup> Reunión Científica de la Asociación Argentina de Tecnología Nuclear, Buenos Aires, Argentina (1984).

5. Salassidis, K.; Georgiadou-Schumacher, V.; Braselmann, H.; Müller, P.; Peter, R. U.; Bauchinger, M. *Chromosome painting in highly irradiated Chernobyl victims: a follow-up study to evaluate the stability of symmetrical translocations and the influence of clonal aberrations for retrospective dose estimation.* Int. J. Radiat. Biol. 68 N°3: 257-262 (1995).
6. Sasaki, M.S.; Hayata, I.; Kamada, N.; Kodama, Y.; Kodama S. *Chromosome Aberration ANALYSIS IN Persons Exposed to Low-level Radiation from JCO Criticality Accident in Tokai-mura.* J. Radiat. Res. 42, SUPPL.: S107-S116 (2001).
7. RERF US-Japan Joint Reassessment of Atomic Bomb Radiation Dosimetry in Hiroshima and Nagasaki, Final Report, Vol 1 y 2, Roesch, W. C., ed., Radiation Effects Research Foundation, Hiroshima (1987).
8. IAEA. *Biological Dosimetry: Chromosomal Aberration Analysis for Dose Assessment* Technical Report Series n° 260. International Atomic Energy Agency, Vienna (1986).
9. IAEA. *Cytogenetic analysis for radiation dose assessment: a manual. Technical Report series n°405.* International Atomic Energy Agency, Vienna (2001).
10. ISCN (1995): *An International System for Human Cytogenetic Nomenclature*, Mitelman, F. (ed); S. Karger, Basel (1995)
11. Savage, J. R. K., *Sites of radiation induced chromosome exchanges.* Current Topics in Radiation Research, 6: 129-194 (1970).
12. Nasazzi, N.; Taja, M. R.; Di Giorgio, M.; Barrios, L.; Gregori B. N.; Kunst, J. J. *Biological Dosimetry of Mixed Neutron - Gamma ray Field.* 10th International Congress of The International Radiation Protection Association, Hiroshima, Japón (mayo 2000).
13. Garcia, O. F., Ramalho, A. T., Di Giorgio, M. D., Mir, S. S., Espinoza, M. E., Manzano, J., Nasazzi, N; Lopez, I. *Intercomparison in cytogenetic dosimetry among five laboratories from latin america.* Mutat. Res. 327: 33-39 (1995).

**DOSIMETRÍA BIOLÓGICA EN ACCIDENTES DE CRITICIDAD. EJERCICIO DE INTERCOMPARACIÓN EN EL REACTOR SILENE – FRANCIA**

<b>Tipo de escenario</b>	<b>Dosis total a 4 m</b>	<b>Tasa de dosis máxima</b>	<b>Tipo de irradiación</b>	<b>Modo de operación</b>
1. Accidente de criticidad	4 Gy en < 3 min.	4 Gy/s	Campo mixto ( $\gamma/n = 1,2$ )	Evolución libre Fuente desnuda
2. Accidente de criticidad	2 Gy en < 3 min.	2 Gy/s	Neutrón ( $\gamma/n = 0,19$ )	Evolución libre Fuente blindada con plomo
3. Reactor en operación	1 Gy en ~30 min.	0,004 Gy/s	Neutrón ( $\gamma/n = 0,19$ )	Modo estado estacionario Fuente blindada con plomo
4. Reactor en parada	2 Gy en ~20 min.	0,1 Gy/min.	$\gamma$ puro ( $^{60}\text{Co}$ )	Fuente gamma . NO en el reactor SILENE

Tabla 1. Condiciones de irradiación de las muestras de sangre

<b>Escenario de irradiación</b>	<b>Nº L.P.<sup>†</sup></b>	<b>Frecuencia media [ACI/cél] (ARN)</b>	<b>Intervalo de confianza del 95% (ARN)</b>	<b>Frecuencia media [ACI/cél] (todos los laboratorios)</b>	<b>Coeficiente de Variación [%]</b>
Fuente desnuda 4 Gy - $\gamma/n = 1,2$	13	2,105	1,849 – 2,360	$2,27 \pm 0,68^*$	29,9
Fuente blindada con plomo 2 Gy - $\gamma/n = 0,19$	13	1,488	1,230 – 1,746	$1,67 \pm 0,39^*$	23,1
Fuente blindada con plomo 1 Gy - $\gamma/n = 0,19$	11	0,656	0,534 – 0,778	$0,81 \pm 0,12^*$	15,1
$\gamma$ puro ( $^{60}\text{Co}$ ) 2 Gy	12	0,279	0,231 – 0,326	$0,28 \pm 0,08^*$	30,1

Tabla 3. Comparación de la frecuencia media observada por el laboratorio de la ARN-Argentina respecto del obtenido por todos los laboratorios en su conjunto

<sup>†</sup>Número de laboratorios participantes

\*desviación estándar

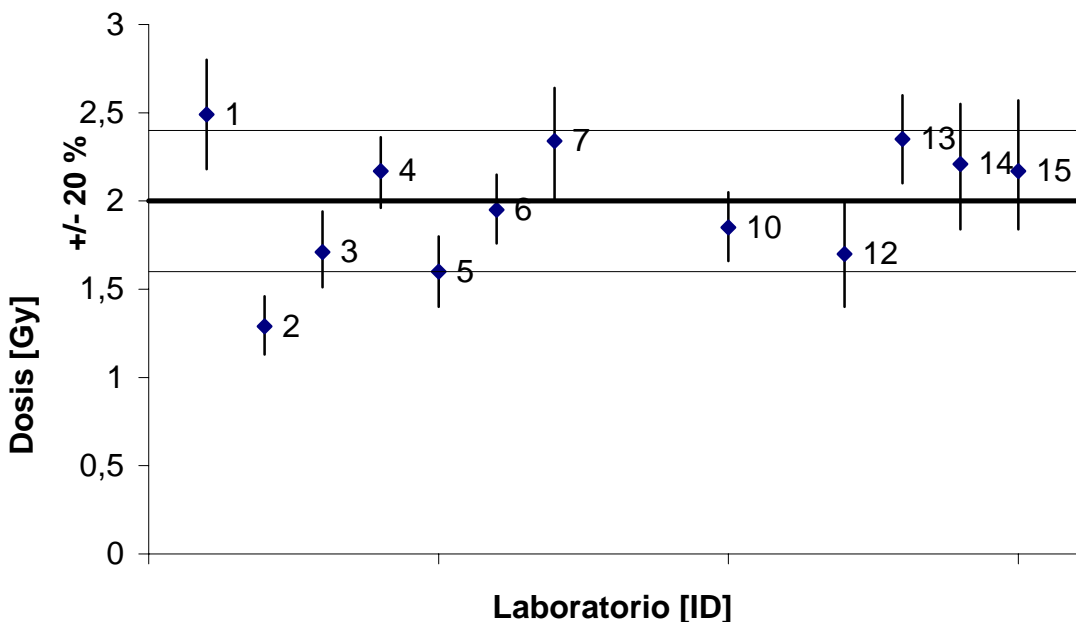


Figura 1. Comparación de las dosis estimadas por los laboratorios para el escenario de 2 Gy (gamma puro de  $^{60}\text{Co}$ ). Cada punto corresponde a la dosis estimada  $\pm$  intervalo de confianza del 95%

ID	Fuente desnuda (4 Gy)		Fuente blindada (2 Gy)		Fuente blindada (1Gy)	
	Dosis Neutrones [Gy]	Dosis Gamma [Gy]	Dosis Neutrones [Gy]	Dosis Gamma [Gy]	Dosis Neutrones [Gy]	Dosis Gamma [Gy]
ARN	2,07 (1,85–2,28)*	2,48 (2,22–2,74)*	1,77 (1,47–2,08)*	0,34 (0,28–0,39)*	0,78 (0,64–0,93)*	0,15 (0,12–0,18)*
10	2,56	3,07	2,63	0,5	1,08	0,21
12	1,8	2,1	1,7	0,3	1	0,2
13	2,78	3,34	2,89	0,55	1,19	0,23

Tabla 4. Comparación de la estimación dosimétrica entre los 4 laboratorios participantes.

\* intervalo de confianza del 95% [Gy]

Escenario de irradiación	Muestra	Nº de células evaluadas	Nº de dicéntricos	Nº de anillos céntricos	Exceso de acéntricos	Distribución de células conteniendo dicéntricos + anillos							$\sigma^2/y$	$\mu$
						0 dic	1 dic	2 dic	3 dic	4 dic	5 dic	6 dic		
$\gamma/n = 1,2$	C	500	0	0	4	0	0	0	0	0	0	0	-	-
$4 \text{ Gy}$ $\gamma/n = 1,2$	I	124	240	21	117	18	28	34	22	13	7	2	1,03	0,27
$\gamma/n = 0,19$	C	500	0	0	3	0	0	0	0	0	0	0	-	-
$2 \text{ Gy}$ $\gamma/n = 0,19$	I	86	121	7	74	21	29	17	13	4	2	0	1,09	0,57
$\gamma/n = 0,19$	C	500	0	0	2	0	0	0	0	0	0	0	-	-
$1 \text{ Gy}$ $\gamma/n = 0,19$	I	169	100	11	106	94	48	19	7	1	0	0	1,18	1,65
$\gamma(\text{Co}^{60})$	C	500	0	0	4	0	0	0	0	0	0	0	-	-
$2 \text{ Gy}$ $\gamma(\text{Co}^{60})$	I	470	123	8	113	363	87	16	4	0	0	0	1,15	2,32

Tabla 2. Resultados citogenéticos obtenidos a partir de muestras de sangre irradiadas con: fuente desnuda (4 Gy -  $\gamma/n=1,2$ ); fuente blindada con plomo(2 Gy -  $\gamma/n=0,19$  y 1 Gy -  $\gamma/n=0,19$ ); 2 Gy  $\gamma$  puro  $^{60}\text{Co}$  y controles



# Telomerase and Apoptosis in Human Hematopoietic Cell Lines: Modulation of the Radiation Response by Pharmacological Inhibition of DNA Repair Enzymes

Dubner, D.L.; Pérez, M. del R.; Michelin, S.C.; Bourguignon, M.;  
Moreau, P. ; Carosella, E.D. and Gisone, P.A.



# Telomerase and apoptosis in human hematopoietic cell lines: modulation of the radiation response by pharmacological inhibition of DNA repair enzymes

Dubner, D.L.<sup>1</sup>; Pérez, M. del R.<sup>1</sup>; Michelin, S.C.<sup>1</sup>; Bourguignon, M.<sup>2,3</sup>; Moreau, P.<sup>2</sup>;  
Carosella, E.D.<sup>2</sup> and Gisone, P.A.<sup>1,2</sup>

<sup>1</sup>Autoridad Regulatoria Nuclear, Gerencia de Apoyo Científico, Laboratorio de Radiopatología, Avenida del Libertador 8250, (C1429BNP) Buenos Aires, Argentina

TEL: 54 11 43 79 83 86; FAX: 54 11 43 79 84 60 E-mail: ddubner@cae.arn.gov.ar

<sup>2</sup>Commissariat à l' Energie Atomique, Hôpital Saint-Louis, Service de Recherches en Hémato-Immunologie, 1 avenue Claude Vellefaux, 75475 Paris cedex 10, France

<sup>3</sup>Faculté de Médecine de Paris-Île-de France Ouest et DGSNR, 6 place de Colonel Bourgoin, 75572 Paris cedex 12, France

**Abstract.** Telomeres play an important role in genome stability maintenance and have been related to radiation sensitivity. Telomerase is a ribonucleoprotein involved in telomere maintenance and cell survival. DNA-repair enzymes might be selective targets for enhancing radiation sensitivity of tumor cells. We investigated the effect of wortmannin and 3-aminobenzamide (3-AB) on telomerase activity (TA) and apoptosis in two human leukemia cell lines. MOLT-4 (*p53*-wild type) and KG1a (*p53*-null) cells were irradiated with  $\gamma$ -rays (3 Gy at 1.57 Gy/min). Cell cultures were treated with 1 $\mu$ M wortmannin, an inhibitor of phosphatidylinositol-3 kinase (PI 3-K) and 10mM 3-AB, a poly(ADP-ribose) polymerase (PARP) inhibitor. TA was measured by PCR and the expression of *hTERT*, *hTR* and *TP1* was assessed by RT-PCR. Apoptosis was evaluated by fluorescence microscopy and flow cytometry, which also allowed to analyze cell cycle distribution.. A radiation-induced up-regulation of TA was observed from 4h-post-irradiation (p.i.) in both cell lines. This up-regulation was abrogated by wortmannin and 3-AB. TA was maximal 24h p.i., coinciding with an accumulation of *hTERT* mRNA. Apoptosis and G2/M arrest were evident from 4h p.i. in MOLT-4 cells. KG1a cells exhibited G2/M block at 24h-p.i. and apoptosis increased thereafter. Three-AB abolished G2/M blockage and enhanced radiation-induced apoptosis in both cell lines. While wortmannin increased early apoptosis in MOLT-4 cells, it did not radiosensitize KG1a cells. This study demonstrates that ionizing radiation induces a transient up-regulation of TA in MOLT-4 and KG1a cell lines. Our findings indicate the participation of post-transcriptional mechanisms in the regulation of TA during the first hours p.i., whereas transcriptional activation of *hTERT* seems to be contributing to the peak of TA observed later. We provide evidence that , besides their known roles as PI3K and PARP inhibitors, wortmannin and 3-AB also inhibit both constitutive and up-regulated TA, with different consequences on the radiation induced apoptotic cell death of MOLT-4 and KG1a cells.

## 1. Introduction

Eukaryotic chromosomes are capped by telomeres, structures composed by proteins and a tandem repeat of a guanine-rich sequence that protect them from DNA degradation and prevent illegitimate recombination[1] (Greider and Blackburn 1996, Preston 1997, Blackburn 2001, Poole *et al.* 2001).. Telomeres progressively shorten in each round of DNA synthesis. A specialized polymerase called telomerase catalyzes the synthesis and extension of telomeric DNA thereby compensating for this telomere loss (Blackburn 2001). Telomeres have been related to radiation sensitivity [2-3]. In a previous study we observed a radiation induced up-regulation of TA in KG1a cells which was influenced by the dose, dose-rate and radiation quality [4]. Disregulation of apoptotic cell death may contribute to the abnormal expansion of malignant cells and may account for cell resistance to radio and chemotherapy. It has been suggested that telomerase could play an anti-apoptotic role and that down-regulation of *hTERT* increases apoptosis in mammalian cells [5].

Wortmannin is a fungal metabolite that potentiates cellular radiosensitivity by its highly specific inhibition of phosphatidylinositol-3 kinase (PI3K), a cytoplasmic signal transducer involved in the cellular response to genotoxic stress [6]. It also inhibits PI3K-related proteins, such as DNA-dependent protein kinase (DNA-PK) and ataxia-telangiectasia-mutated (ATM). Wortmannin has been widely used for *in vitro* cell radio and chemosensitization [7].

Three-aminobenzamide (3-AB) is a potent poly(ADP-ribose) polymerase (PARP) inhibitor which retarded the rejoicing of DNA strand breaks rendering cells more sensitive to genotoxic stress. The clinical utility of PARP inhibitors as adjuvant therapeutics for the treatment of various forms of cancer has been proposed [8].

The purpose of the present study was to assess the effects of wortmannin and 3-AB on telomerase activity (TA) and apoptosis following gamma-irradiation of two human leukemia cell lines differing in their *p53*-status.

## 2. Material and methods

### 2.1 Cell lines and cultures

MOLT-4 is a cell-line derived from a human acute lymphoblastic T-cell leukemia that exhibits increased levels of p53 protein after exposure to ionizing radiation. These cells were grown in RPMI 1640 medium (Gibco<sup>TM</sup>-BRL) supplemented with 10% fetal bovine serum (Gibco<sup>®</sup>-BRL), at 37°C in a humidified atmosphere containing 5% CO<sub>2</sub>.

KG1a is a *p53*-deficient subclone of the KG1 cell-line isolated from a human acute myelogenous leukemia, with an immune phenotype very similar to that of primitive hematopoietic stem cells (Clave *et al.* 1996). These cells were grown in Iscove's modified Eagle's medium (Gibco<sup>TM</sup>-BRL) supplemented with 10% fetal bovine serum (Gibco<sup>TM</sup>-BRL), at 37°C in a humidified atmosphere containing 5% CO<sub>2</sub>.

### 2.2 Irradiation of cell cultures

Exponential-phase growing cells were suspended in normal growth medium and irradiated with 3 Gy at a dose rate of 1.5 Gy/min at room temperature, at least in three separate experiments, using a teletherapy gamma unit (<sup>60</sup>Co). One equilibrium-thickness of water-equivalent material was included in order to provide secondary electron equilibrium. Control samples were sham-irradiated.

### 2.3 Evaluation of telomerase activity and telomerase-related gene expression

TA was determined at least in three separate experiments, using a PCR-based telomeric repeat amplification protocol (TRAPeze Intergen<sup>TM</sup> C #S7700-Kit) as previously described [4]. TA in the irradiated samples was expressed as relative to the control.

Telomerase is composed of two proteins, a catalytic subunit (human telomerase reverse transcriptase, hTERT), a telomerase-associated protein (TP1) and an internal RNA template (hTR). The mRNA level of these telomerase-related genes was evaluated by RT-PCR as previously described ( Pérez *et al* 2003) . The thermal cycling protocols applied for each PCR-assay are presented in table 1. The results in irradiated samples were expressed relative to the control.

Table 1 Thermal cycling conditions applied for PCR amplification of hTERT, hTR, and TP1

	<b>hTERT</b>	<b>hTR</b>	<b>TP1</b>	<b>β-actine</b>
General conditions	94°C/5 min + «n»cycles [94°C/30 sec; 60°C/40 sec; 72°C/40 sec] + 72°C 7 min	94°C/5 min + «n» cycles [94°C/30 sec; 64°C/40 sec; 72°C/40 sec] + 72°C 7 min	94°C/5 min + «n» cycles [94°C/30 sec; 58°C/40 sec; 72°C/40 sec] + 72°C 7 min	94°C/5 min + «n» cycles [94°C/30 sec-58-64°C (*)/40 sec; 72°C/40 sec] + 72°C 7 min
N° of cycles KG1a	32	32	28	18
N° of cycles MOLT4	26	24	28	18

(\*) adapted to temperature conditions of each primer

### 2.4 Evaluation of apoptosis and cell-cycle distribution

Samples were collected at different time-points and assessed for apoptosis and cell-cycle distribution by flow cytometry (FACStar Plus Becton Dickinson<sup>®</sup>). Briefly, 1x10<sup>6</sup> cells previously fixed in 70% ethanol were washed and resuspended in PBS containing RNase 50µg/ml and propidium iodide (IP) 40 µg/ml. Apoptotic cells were identified in a DNA histogram as a sub-G<sub>1</sub> hypodiploid population.

In order to verify flow cytometric findings apoptosis was also evaluated by fluorescence microscopy. A mixture containing 2µg/ml of Hoechst 33342 (H), 15µg/ml of fluorescein diacetate (FDA) and 5 ug/ml of IP was prepared in PBS pH7.4. Ten µL of this fluorescent mix was added to 500µL aliquots of cell suspensions (3 x 10<sup>6</sup> cells/ml). After 5 min incubation at 37°C and one wash, samples were dropped onto slides and observed by fluorescence microscopy (Carl Zeiss<sup>TM</sup> MC 80 DX). Early

(living) and late (dead) apoptotic cells were distinguished by the presence of nuclear condensation and of spotted blue (H) or red (IP) bodies, respectively.

### 2.5 Incubation with chemical agents

Wortmannin (Sigma<sup>®</sup>), was dissolved in anhydrous dimethyl sulfoxide (DMSO) at a stock concentration of 10mM and stored at -80°C until use. A working solution was prepared in culture medium, sterilized by filtration, and added to cell cultures at a 1µM final concentration 60 min prior to irradiation. Dilutions of 3-AB (Sigma<sup>TM</sup>) were prepared in culture medium, sterilized by filtration, and added to cell cultures 30 minutes prior to irradiation, at a final concentration of 10mM.

The media containing these products were replaced by simple culture medium 24h-p.i. Optimal conditions for assays were chosen after testing cell viability at different final concentrations and incubation times.

## 3. Results

### 3.1 Time-course of telomerase activity after irradiation

The time-course of TA following irradiation with 3 Gy at a dose-rate of 1.5 Gy/min was evaluated over a 72-hour period. As shown in figure 1, TA early (4h-p.i.) increased in MOLT-4 and KG1a cells. A similar temporal pattern was observed thereafter for both cell-lines: maximal activation up-to around 4-fold control values at 24h-p.i., followed by a decline toward basal values by 72h-p.i.

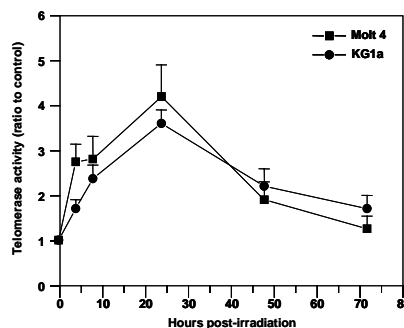


FIG.1. Time-course of telomerase activity following gamma-irradiation.

### 3.2 Effect of wortmannin and 3-AB on radiation-induced telomerase activation

We next evaluated the effect of pre-treatment with PI3K and PARP inhibitors on TA for a 24-h time period, corresponding to maximal radiation-induced up-regulation of TA. As seen in figure 2, wortmannin and 3-AB inhibited radiation induced up-regulation of TA in both cell lines. Constitutive TA was reduced by about 50% in sham-irradiated samples following 24-hour-incubation with wortmannin and 3-AB (data not shown).

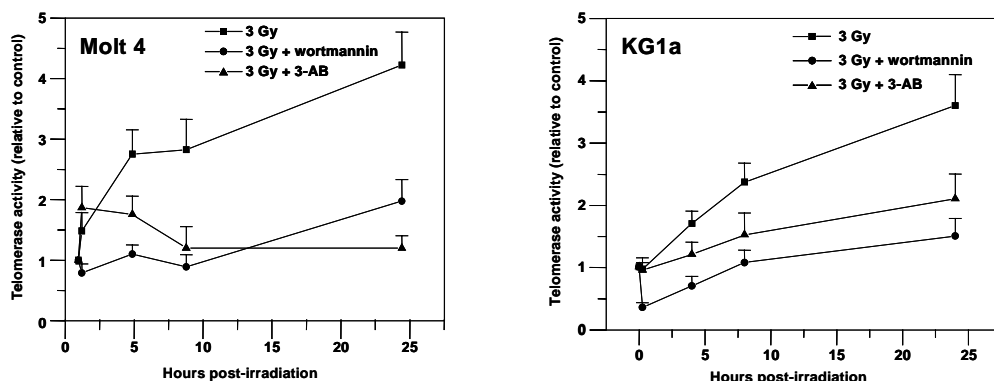


FIG. 2. Effect of PI3K and PARP inhibitors on telomerase activity, following gamma-irradiation

### 3.3 Telomerase-related gene expression after irradiation

To determine whether the radiation-induced increase in TA was due to changes in telomerase-related gene expression, hTERT, hTR, and TP1 mRNA levels were quantified by RT-PCR for 24 hours following irradiation, the time-period during which TA increased maximally. As seen in figure 3, an accumulation of hTERT mRNA was observed at 24h-p.i. in both cell-lines. The hTR mRNA level did not reveal a significant alteration in the response to ionizing radiation in either of the two cell-lines during the period studied. While the level of TP1 mRNA did not significantly change in MOLT-4 cells, a decrease was observed during the first 8h-p.i. in KG1a cells.

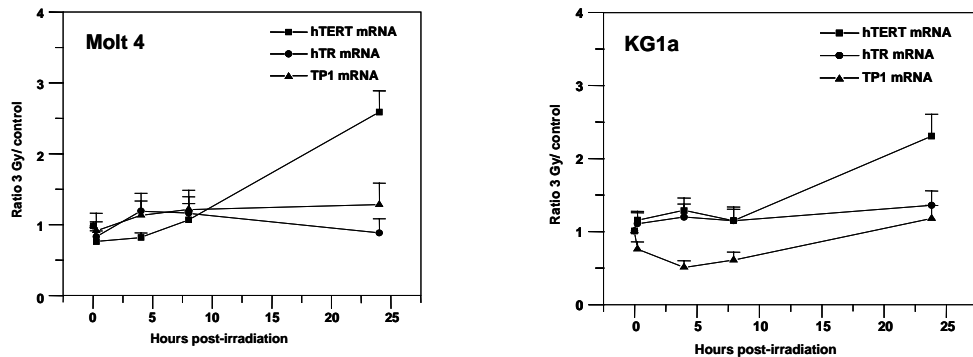


FIG 3. Time-course of telomerase-related gene expression following gamma-irradiation

### 3.4 Effects of wortmannin and 3-AB on telomerase-related gene expression

We next evaluated the effect of PI3K and PARP inhibitors on telomerase-related gene expression at 24h-p.i. As shown in figure 4, wortmannin abolished radiation-induced hTERT mRNA accumulation only in MOLT-4 cells, without modifying hTR or TP1 mRNA levels in either of the two irradiated cell-lines. PARP inhibition by 3-AB did not modify hTERT, hTR, and TP1 mRNA levels in irradiated cell-lines

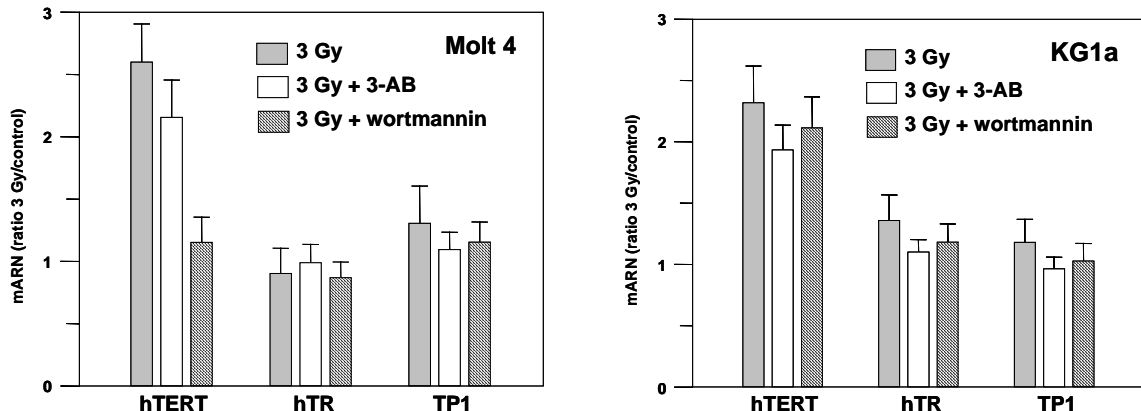


FIG. 4. Effect of PI3K and PARP inhibitors on telomerase-related gene expression 24 hours p.i.

### 3.5 Kinetics of apoptotic cell-death and the cell-cycle upon irradiation

The kinetics of the appearance of apoptotic cells was followed by flow cytometry and fluorescence microscopy over a 72-hour-period after irradiation. As seen in figure 5, the time-course of radiation-induced apoptosis differed in the two cell-lines. The induction of apoptosis following irradiation of MOLT-4 cells, already evident at 4h-p.i., attained maximal values within the first 48h-p.i. In contrast, KG1a cells did not die by apoptosis during the first 24h-p.i. However, apoptotic cell death became evident later, between 48h and 72h-p.i. Fluorescence microscopy confirmed these flow cytometry findings. The kinetics of G2/M accumulation following irradiation is presented in figure 6. In MOLT-4 cells, early G2/M blockage was already evident by 4h-p.i., and reached a maximum at 8h-p.i., decreasing thereafter. Exposure of KG1a cells to ionizing radiation induced a G2/M arrest at 24h-p.i. that disappeared at 48h-p.i.

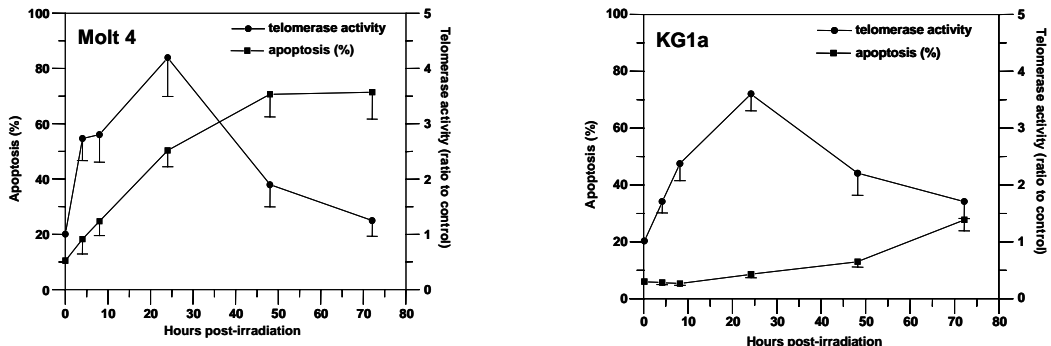


FIG. 5. Kinetics of apoptosis and its temporal correlation with telomerase activity following gamma-irradiation

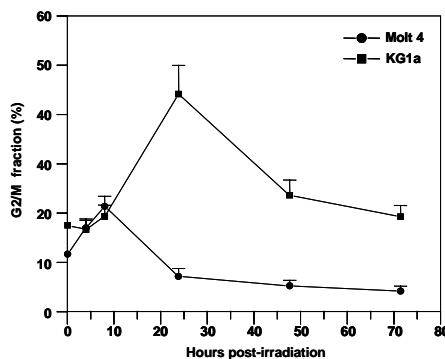


FIG. 6. G2/M progression upon gamma-irradiation

### 3.6 Effect off wortmannin and 3-AB on apoptosis and on the G2/M checkpoint

The effect of wortmannin and 3-AB on apoptotic cell-death following irradiation was studied over the same 72-h period. To determine whether these pharmacological products were cytotoxic *per se*, apoptosis was also evaluated in control sham-irradiated cells treated under the same conditions. No cytotoxic effects were observed following treatment with wortmannin alone, whereas the apoptotic cell fraction of both cell types increased in non-irradiated cells treated with 3-AB.

As shown in figure 7, PI3K inhibition by wortmannin induced a significant increase in the radiation-induced apoptotic cell fraction during the first day p.i. in Molt4 cells, whereas it did not modify radiation-induced apoptotic cell-death in KG1a cells.

PARP inhibition by 3-AB enhanced radiation-induced apoptosis in both cell lines, as seen in figure 8. While this effect was observed between 8 to 24h-p.i. in Molt4 cells, it was evident later (after 24h-p.i.) in KG1a cells.

We next evaluated the effects of 3-AB and wortmannin on radiation-induced G2/M arrest. PARP inhibition by 3-AB abolished radiation-induced G2/M blockage in both cell-lines. Cell cycle flow cytometric profiles corresponding to one representative experiment are presented in figure 9.

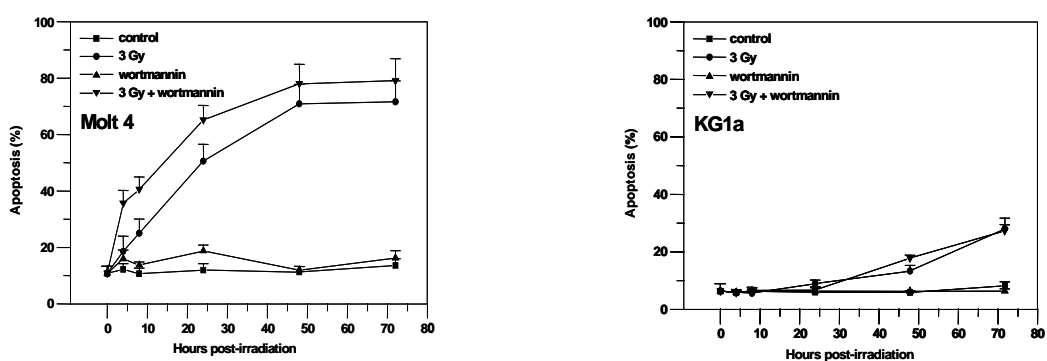


FIG. 7. Effect of wortmannin on apoptotic cell death following gamma-irradiation

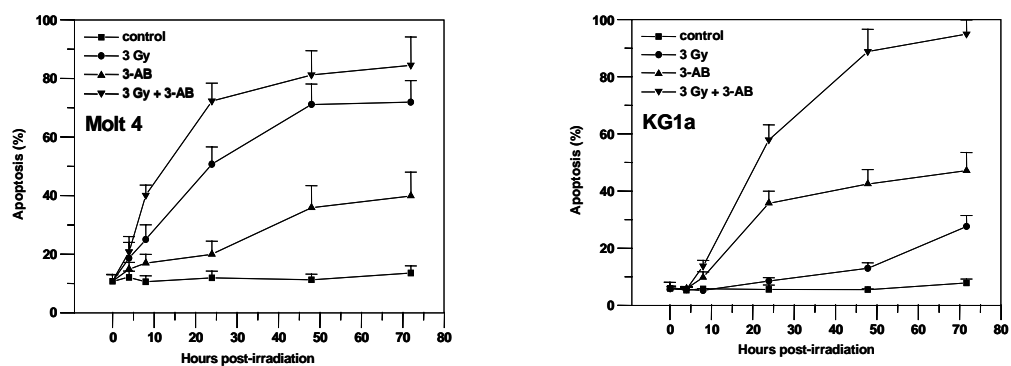


FIG. 8. Effect of 3-aminobenzamide (3-AB) on apoptotic cell-death, following gamma-irradiation

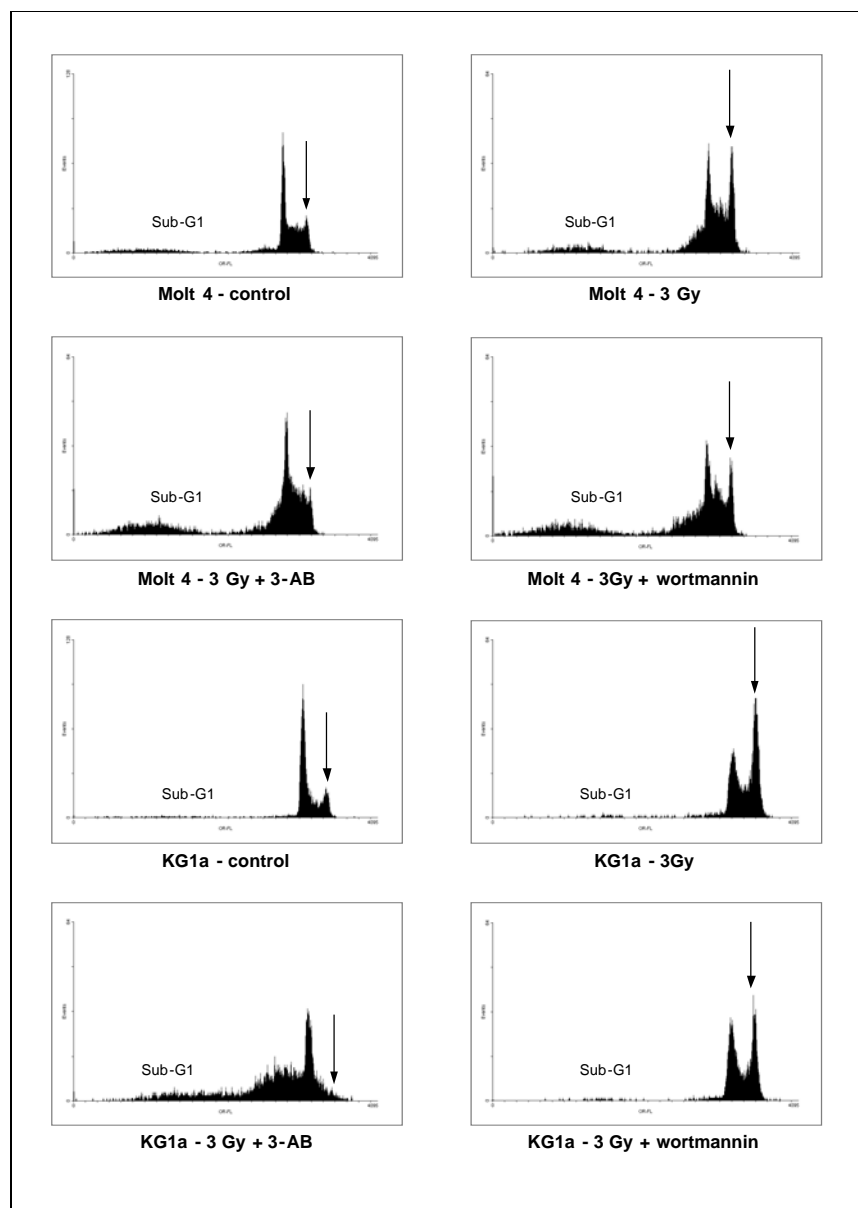


FIG. 9. Apoptotic cell fraction and cell cycle redistribution following gamma-irradiation

## 4. Discussion

### 4.1 Radiation-induced up-regulation of TA

We found that ionizing radiation up-regulated TA in both cell lines during the first days p.i., indicating a transient radiation-dependent modulation. The present report represents the first observation of TA regulation by ionizing radiation in MOLT-4 cells. The 24h-peak of TA coincided with an accumulation of hTERT mRNA, which was not observed at earlier time-points. These findings suggest the participation of post-transcriptional mechanisms in the regulation of TA during the first hours p.i., whereas transcriptional activation of *hTERT* seems to be contributing to the peak of TA observed later. Several pathways for radiation-induced post-transcriptional regulation of TA may be proposed. Protein kinase B (Akt/PKB), one of the downstream targets of PI3K, activates hTERT by phosphorylation and the PI3K/Akt signal transduction pathway is activated by ionizing radiation. Ionizing radiation may also modulate TA by inducing translocation of telomerase within the cell [9]. Concerning the radiation-induced transcriptional activation of TA, the *hTERT* promoter contains several binding sites for ionizing radiation-inducible transcription factors involved in telomerase activation, such as c-myc, NF- $\kappa$ B, and Ap1[10].

### 4.2 Inhibition of telomerase by wortmannin and 3-AB

The inhibition of PI3K could account for the early TA decrease observed within the first 15 minutes p.i. after pre-treatment with wortmannin , which abolishes Akt-dependent hTERT activation by phosphorylation. When MOLT-4 cells had been previously incubated with wortmannin, the radiation-induced hTERT mRNA accumulation did not occur. In contrast, wortmannin did not modify the time-course of hTERT mRNA in KG1a cells following irradiation. Thus, the inhibition of TA by wortmannin occurred both at the transcriptional and post-transcriptional levels in MOLT-4 cells, whereas in KG1a cells it seems to be only a post-transcriptional phenomenon.

Our results provide evidence that the decrease of TA by 3-AB is not mediated by transcriptional down-regulation of hTERT in either MOLT-4 or KG1a cells. The inhibition of TA by 3-AB may result from post-transcriptional modifications, a hypothesis reinforced by the fact that 3-AB inhibits protein kinase C (PKC), an enzyme that participates in the regulation of telomerase [11-12]

### 4.3 Effects of wortmannin and 3-AB on apoptosis and cell cycle kinetics

The timing of radiation-induced apoptosis initially coincided with G2/M blockage in MOLT-4 cell-line. Apoptotic cell death occurred in KG1a cells after they were released from G2/M blockage as observed in other *p53*-deficient cell-lines. Our findings demonstrate that in spite of their different *p53* status, both MOLT-4 and KG1a cells exhibited G2/M arrest following exposure to ionizing radiation indicating that this effect may be *p53*-independent.

Wortmannin enhanced early radiation-induced apoptosis in MOLT-4 cells. Although wortmannin has been reported to sensitize cells to ionizing radiation, it is noteworthy that in the present study it did not radiosensitize KG1a cells. Similar results were recently observed in a human glioblastoma cell line [13].

Because of its involvement in cell recovery from DNA damage, PARP operates as a survival factor. In the presence of PARP inhibitors, the DNA repair process is not completely blocked, but is very much slower. Indeed, we found that 3-AB enhanced radiation-induced apoptosis in both cell lines. We also found that 3-AB abolished radiation-induced G2/M blockage in both cell lines. It has been demonstrated that 3-AB down-regulates genes involved in cell cycle control. The lack of radiation-induced G2/M arrest was accompanied by an increase in apoptosis, a finding previously described [14].

### 4.4 Telomerase and apoptosis

By stabilizing broken DNA-ends by chromosome healing, telomerase could allow cells to survive for a short time. Since chromosome healing does not provide legitimate DNA repair, it may lead to chromosomal aberrations which could trigger apoptosis at later time-points.

Our study demonstrated that in MOLT-4 cells the radiation-induced up-regulation of TA temporally coincided with the beginning of apoptosis, indicating that maintenance of higher levels of TA does not avoid triggering of apoptotic cell death in this cell line. Although wortmannin and 3-AB inhibited TA and significantly enhanced apoptosis within the first 24-p.i. in MOLT-4 cells, these results do not

allow to conclude that TA plays an anti-apoptotic role in this cell line. Methods to regulate specifically hTERT should be applied in order to confirm this hypothesis.

Regarding KG1a cells, the present study showed that radiation-induced apoptosis was triggered once TA had returned toward basal values. However, the inhibition of TA by wortmannin did not increase radiation-induced apoptotic cell death thus precluding the involvement of TA in the modulation of late apoptosis in this cell line.

#### 4.5 Concluding comments

We provide evidence that, besides their known roles as PI3K and PARP inhibitors, wortmannin and 3-AB also inhibited both constitutive and up-regulated TA, with different consequences on radiation-induced apoptotic cell death of MOLT-4 and KG1a cells. This study also demonstrated that ionizing radiation induced a transient up-regulation of TA in MOLT-4 and KG1a cell lines. DNA-repair enzymes might be selective targets for enhancing radiation response of tumor cells provided that the pharmacological agents to be applied were carefully selected according to the specific cell type. Further investigations should be carried out in order to determine the criteria which could guide such selection.

### 5. References

- [1] Blackburn, E.H., *Switching and signaling at the telomere*, Cell, 106:661-673,(2001)
- [2] Bouffler, S. D., Blasco, M. A., Cox, R. and Smith, P. J., *Telomeric sequences, radiation sensitivity and genomic instability*. International Journal of Radiation Biology, 77:995-1005, (2001).
- [3] Sharma, G.G., Gupta, A., Wang, H., Scherthan, H., Dhar, S., Gandhi, V., Iliakis, G., Shay, J.W., Young, C.S. and Pandita, T.K., *hTERT associates with human telomeres and enhances genomic stability and DNA repair*. Oncogene, 22 : 131-146 (2003).
- [4] Pérez, M. R, Dubner, .., D., Michelin, S., Leteurtre, F., Gisone, P. A. and Carosella., E. D., *Radiation-induced up-regulation of telomerase activity in KG1a cells is dependent of the dose-rate and radiation quality*. International Journal of Radiation Biology, 78:1175-1183 (2002).
- [5] Cao, Y., Li, H., Deb, S. and Liu, J. P., *TERT regulates cell survival independent of telomerase enzymatic activity*. Oncogene, 21:3130-3138 (2002).
- [6] Roberts, E. C., Shapiro, P. S., Nahreini, T. S, Pages, G., Pouyssegur, J., and Ahn, N. G., *Distinct cell cycle timing requirements for extracellular signal-regulated kinase and phosphoinositide 3-kinase signaling pathways in somatic cell mitosis*. Molecular and Cellular Biology, 22:7226-7241 (2002).
- [7] Klejman, A., Rushen, L., Morrione, A., Slupianek, A. and Skorski , T., *Phosphatidylinositol-3 kinase inhibitors enhance the anti-leukemia effect of ST1571*. Oncogene, 21:5868-5876,(2002).
- [8] Virag, L. and Szabo, C, *The therapeutic potential of poly(ADP-ribose) polymerase inhibitors*. Pharmacological Reviews, 54:375-429, (2002).
- [9] Wong, J. M., Kusdra, L., and Collins, K., *Subnuclear shuttling of human telomerase induced by transformation and DNA damage*. Nature Cell Biology, 4:731-736, (2002).
- [10] Kyo, S., and Inoue, M., *Complex regulatory mechanisms of telomerase activity in normal and cancer cells: how can we apply them for cancer therapy?* Oncogene, 21:688-697,(2002).
- [11] Ricciarelli, R., Palomba, L., Cantoni, O. and Azzi, A., *3-Aminobenzamide inhibition of protein kinase C at a cellular level*. FEBS Letters, 431:465-467, ( 1998).
- [12] | Sheng, W.Y., Chien, Y.L. and Wang, T.C., *The dual role of protein kinase C in the regulation of telomerase activity in human lymphocytes*. FEBS Letters 540 : 91-95, (2003).
- [13] Yoshida, M., Hosoi, Y., Miyachi, H., Ishii, N., Matsumoto, Y., Enomoto, A., Nakagawa, K., Yamada, S., Suzuki, N., and Ono, T., *Roles of DNA-dependent protein kinase and ATM in cell-cycle-dependent radiation sensitivity in human cells*. International Journal of Radiation Biology, 78:503-512, (2002).
- [14] Strunz, A. M., Peschke, P., Waldeck, W., Ehmann, V., Kissel, M., and Debus, J., *Preferential radiosensitization in p53-mutated human tumour cell lines by pentoxifylline-mediated disruption of the G2/M checkpoint control*. International Journal of Radiation Biology, 78:721-732, (2002).

## **6. Acknowledgements**

The authors thank François Leteurtre for his technical expertise concerning telomerase activity and telomerase-related gene expression measurements, as well as for helpful discussions. We also thank Alicia Carregado for her collaboration with literature research. This work was partially supported by the French *Ministère des Affaires Etrangères* and the *Direction des Sciences du Vivant* of the *Commissariat à l'Energie Atomique*, within the framework of Project 3T-005.



# Una metodología mejorada para el análisis de espectros alfa

Equillor, H.E.



# **UNA METODOLOGÍA MEJORADA PARA EL ANÁLISIS DE ESPECTROS ALFA**

Equillor, H.E.

Autoridad Regulatoria Nuclear  
Argentina

En este trabajo se describe una metodología, desarrollada en los últimos años, para el análisis de espectros de emisores alfa, obtenidos con detectores semiconductores de silicio de ión implantado, que tiende a resolver algunos de los variados problemas que presentan este tipo de espectros. Esta es una metodología mejorada respecto de la presentada en una anterior publicación<sup>[1]</sup>. El método se basa en la aplicación de una función matemática que permite modelar la cola de un pico alfa, para evaluar la parte del pico que no se ve, en los casos de superposición parcial con otro pico. Asimismo, un programa de cálculo que trabaja de manera semiautomática, es decir con posibilidad de intervención interactiva del analista, ha sido desarrollado simultáneamente y se describe con detalle.

## **1. INTRODUCCIÓN**

En espectrometría alfa es muy frecuente encontrar el solapamiento de dos o más picos entre sí, a pesar de los avances logrados en las últimas décadas en la resolución de los detectores. Esto hace que el cálculo del área de un pico no sea siempre una cuestión simple.

Varios factores inciden para esta situación: uno de ellos es la necesidad que existe en el área ambiental y ocupacional de medir muy cerca del detector o con detectores grandes, para obtener el máximo de sensibilidad, lo cual disminuye la resolución; otro factor es el hecho de que la preparación de la muestra, para poder ser medida, requiere un importante y a veces prolongado tratamiento químico previo, pudiendo dar como resultado un incremento en el ancho de los picos, así como también la aparición de trazas de otros emisores alfa, producto de una deficiente separación; además la necesidad de incluir en la muestra radionucleidos trazadores para poder evaluar el rendimiento del proceso aumenta el número de picos y por lo tanto la superposición entre los mismos.

Una metodología que permite reducir la cola de los picos y mejorar la separación entre ellos es la que utiliza un electropulido previo. Sin embargo, en la mayor parte de los casos existe algún grado de superposición y por ello es necesario recurrir a un modelo matemático que permita la correcta evaluación del área de cada uno de los picos. Muchos autores han reportado diversas metodologías con distinto grado de complejidad y eficacia<sup>[2-11]</sup>.

La metodología que en este trabajo se propone, se basa en una función matemática exponencial simple que permite la interpretación de la cola de los picos alfa, desde las cercanías del centroide, hasta un considerable número de canales hacia la zona de bajas energías.

Asimismo fue necesario desarrollar un programa de computación para hacer posible el cálculo de las áreas y el ensayo de diversas condiciones de análisis del solapamiento de los picos. El programa consiste en una presentación gráfica del espectro donde puede visualizarse y modificar la curva que permite evaluar la forma de los picos.

## **2. MATERIALES**

- Espectrómetro Octete PC de EG&G Ortec.
- Detectores de ión implantado ULTRA de EG&G Ortec, desde 300 mm<sup>2</sup> a 900 mm<sup>2</sup>.
- Fuente de electrodeposición de corriente constante.
- Electrodos de alambre de platino.
- Discos de acero inoxidable 316L, de 2 cm de diámetro.

### 3. METODOLOGÍA DE ANÁLISIS PARA UN PICO ALFA

$$Y = \frac{e^{\left[ \frac{1}{e^{(p \cdot X + b)}} \right]}}{f} \quad (1)$$

La expresión analítica de la función utilizada es:

donde  $X$  es el número de canal,  $Y$  corresponde a las cuentas acumuladas en el canal  $X$ , mientras que  $p$  y  $b$  son constantes cuyos valores cambian según las características de cada espectro, es decir la forma, la posición y la altura de los picos. Asimismo,  $f$  es un parámetro que permite corregir la forma de la curva en la zona de baja energía. Reordenando y tomando logaritmos en base e, obtenemos:

$$\ln(Y \cdot f) = \frac{1}{e^{(p \cdot X + b)}}$$

Luego, reordenando y tomando logaritmos nuevamente, llegamos a la expresión:

$$p \cdot X + b = \ln \left[ \frac{1}{\ln(Y \cdot f)} \right]$$

donde se observa que los parámetros  $p$  y  $b$  pueden ser fácilmente obtenidos por regresión lineal, para un valor dado de  $f$ . En la figura 1 se representa una curva sobre un espectro de pico único, donde se aprecia su grado de coincidencia con la cola del pico.

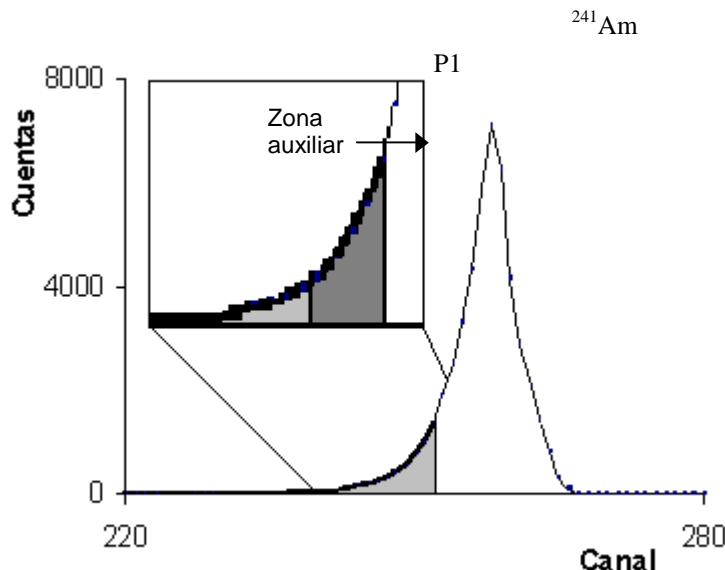


**Figura 1.** Espectro de  $^{241}\text{Am}$  con curva modelo (en línea más negra), y detalle de la curva.

#### 4. EL PROGRAMA PROALFA

El programa fue desarrollado en Visual Basic versión 6, es decir que cuenta con interfase gráfica y el soporte de Windows 95-2000. La figura 2 muestra la pantalla de Proalfa donde se aprecian los comandos principales.

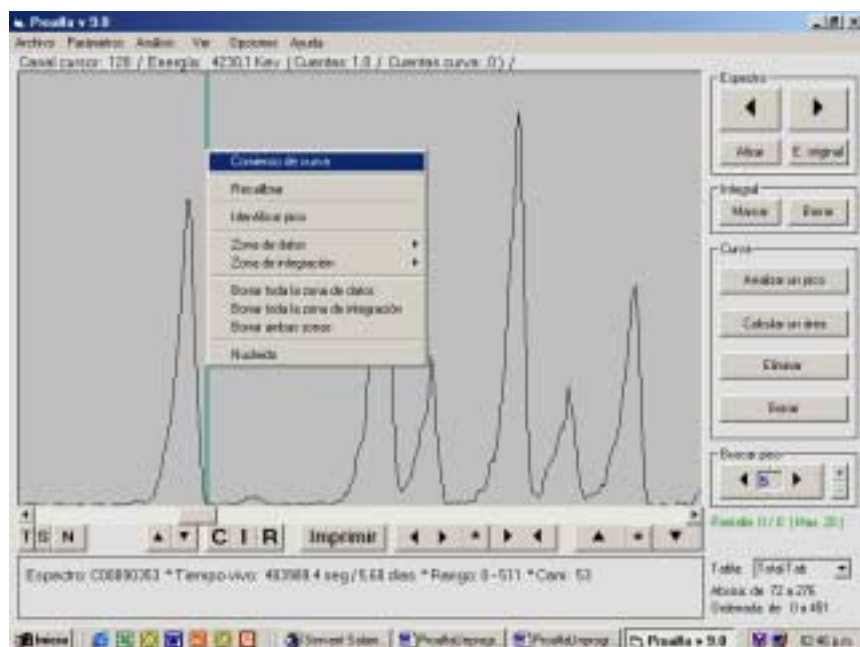


Figura 2. Proalfa 9, pantalla principal con espectro.

**4.1 La presentación gráfica.** El espectro es desplegado en forma gráfica utilizando puntos unidos por líneas, sobre un cuadro cuyo eje horizontal corresponde a número de canal, o energía en el caso en que exista una calibración, mientras que el eje vertical corresponde a cuentas. Adicionalmente, fuera del cuadro y arriba, se muestran datos de número de canal, energía, contaje en el canal, contaje de la función modelo en el canal y radionucleido probable. En el sector inferior se detalla el nombre del espectro, tiempo de medición, rango de canales del espectro, el número de cámara e integral en una zona, cuando una zona de integración está marcada. Un conjunto de menús en la parte superior del cuadro permite acceder a diversos comandos, mientras que una serie de botones facilitan el rápido acceso a las funciones de uso frecuente.

**4.2 Gestión de archivos.** Permite visualizar tres tipos de archivos de espectros, a través de una pantalla clásica de selección de archivos de Windows: archivos "CHN" desarrollados por Ortec, archivos "CNF" desarrollados por Canberra, y archivos de caracteres legibles y encolumnados. Asimismo el programa permite descontar un espectro de fondo, corregido por tiempo de medición, luego de cargar el espectro de la muestra.

**4.3 Comandos de MCA.** Se encuentran como una serie de botones de acceso directo, inmediatamente bajo el cuadro gráfico. Están disponibles todos los comandos clásicos de una interfaz multicanal, como ser variación de escalas horizontal, vertical y auto escala, expandir, contraer y auto escala, así como la posibilidad de movilizar, por medio de botones o del mouse, un cursor o marcador representado por una línea vertical que atraviesa el cuadro. Otra de las funciones clásicas de multicanal es la de marcar una región de integración, o borrarla. Un botón permite alisar el espectro y otro retrotrae al espectro original.

**4.4 Comandos de análisis.** Otra serie de botones corresponden a los comandos de análisis de un pico y generación de la curva que modela la cola: *analizar un pico*, *calcular un área*, *eliminar* y *borrar la curva*. Un comando relacionado se encuentra ubicado en el menú que aparece sobre el cuadro gráfico cuando se pulsa el botón derecho del mouse y permite realizar un análisis automático del pico estableciendo el *comienzo de curva* en la posición en que se encuentra el cursor. Dos botones adicionales permiten aumentar o reducir la altura de la cola, para poder hacer un último ajuste visual.

Cada vez que se pulsan cualquiera de los botones *alisar*, *eliminar* o *espectro original*, el programa cambia de pantalla, las que van siendo almacenadas en memorias, hasta un numero de 20. Existen dos botones en el ángulo superior derecho que permiten avanzar o retroceder con el número de pantalla como si fueran paginas de un libro.

**4.4.1 Análisis automático.** El análisis de un pico alfa se activa cuando se pulsa el botón *analizar un pico*, o cuando se accede a la opción *comienzo de curva* en el menú contextual que aparece sobre el cuadro gráfico al pulsar el botón derecho del mouse. El análisis consiste en encontrar los parámetros mas adecuados para la función modelo que ayuden a interpretar la parte del pico que no se halla explicitada por estar incluida en el pico siguiente. En el análisis automático, la curva es construida sobre dos canales, de la siguiente forma:

- 1) El primer canal se elige a la izquierda del centroide, como aquel cuya altura es de aproximadamente 20% (el usuario puede variarlo) de la altura máxima del pico (punto *P1* de la figura 1). Desde este punto hasta el punto más extremo del pico, a la derecha, pasando por el centroide, el contaje se obtiene como integral de las cuentas reales.
- 2) Se define una zona *auxiliar* de hasta 10 canales, que va desde *P1* hacia la izquierda.
- 3) El segundo canal para el cálculo de la curva (punto *P2*) estará ubicado a la izquierda, a 100 canales de distancia del primero, su altura es virtual y quedará definida como aquella que haga que la curva se ajuste lo mejor posible a los valores reales de la zona auxiliar definida en el punto 2.
- 4) El valor de *f* se calcula como  $f = K / Y_2$  (2), donde *K* es una constante experimental que por lo común lleva un valor de 10 e *Y<sub>2</sub>* es el valor de la altura en el punto *P2*.

El análisis del pico se realiza sobre un espectro alisado, lo que permite analizar también aquellos picos que poseen escaso contaje. El número de veces que se alisa el espectro se determina como  $10 / h$ , donde *h* es la altura del pico. Esto significa que cuanto menor es la altura del pico, mayor es el número de veces que se alisa el espectro.

**4.4.2 Comienzo de curva.** A veces la elección automática del comienzo de curva no es satisfactoria dado que la forma estadística del pico no siempre es regular, encontrándose protuberancias o depresiones que afectan al análisis. Otras veces, la aparición de trazas de otros radionucleidos, producto de una deficiente separación radioquímica, provoca deformaciones que dificultan el análisis automático. Esta opción permite entonces elegir el comienzo de curva a criterio del analista, de modo que con un solo toque se obtiene el análisis automático basado en los criterios del punto 4.4.1, pero con fijación manual del comienzo de curva.

**4.4.3 Retoque manual de la curva.** La curva puede ser retocada manualmente mediante dos botones que permiten aumentar o reducir su altura. Esto se logra modificando la altura del punto *P2* (lo que modifica también el parámetro *f*, de acuerdo con la ecuación (2), y recalculando luego la curva). Los botones mencionados reducen o aumentan esta altura en un cierto porcentaje.

**4.4.4 Cálculo de un área.** Este botón permite calcular el área de un pico sin alterar el formato de la curva. Una vez que la curva resulta satisfactoria para el analista (luego de utilizar cualquiera de los comandos 4.4.1, 4.4.2 y/o 4.4.3), se calcula el área del pico mediante este botón.

**4.5 Impresión.** El programa permite ir configurando una lista de impresión con los resultados del análisis de cada pico, el gráfico del espectro original o cualquiera de las presentaciones de pantalla obtenidas que pudieran interesar al analista.

**4.6 Modo de trabajo.** El espectro se analiza comenzando por el pico de mayor energía. Se obtiene la curva más adecuada, se envían los resultados a una lista de impresión y se descuenta el pico mediante el botón *eliminar*. De esta manera se avanza hasta completar el análisis de todos los picos.

**4.7 Funciones complementarias.** Algunos botones presentan funciones complementarias:

**4.7.1 Recalibración.** Permite recalibrar el espectro introduciendo numero de canal y radionucleido asociado o energía; la misma pantalla permite cargar una precalibración correspondiente a la cámara de interés.

**4.7.2 Identificación.** En la posición del cursor el programa identifica una lista de radionucleidos cercanos en energía, y al más cercano de ellos, y los muestra sobre una barra de herramientas ubicada en la parte superior del cuadro; se muestra también una ventana con el listado de energías y rendimientos correspondiente al radionucleido identificado como el más probable. Una aproximación a la conformación del multiplete es graficada sobre el cuadro mediante barras verticales proporcionales. Estas barras, así como la barra de herramientas permanecen visibles mientras se trabaja sobre el espectro, permitiendo identificar otros picos y solo desaparece al pulsar el botón ocultar posicionado sobre dicha barra.

**4.7.3 Información sobre emisores alfa.** Permite acceder a una pantalla donde seleccionando un radionucleido, se puede tener la información de energías y rendimientos, ordenada por cualquiera de estas dos categorías. Los valores de energía e intensidad fueron extraídos de la base de datos del programa RadDecay v3, de distribución gratuita, los que a su vez tienen origen en una publicación del DOE<sup>[12]</sup>.

**4.7.4 Superponer.** Permite acceder a un grupo de comandos para guardar en memoria la forma de un pico, superponer (convertido a una altura) en otra zona del mismo espectro o de otro, y mover el pico superpuesto.

**4.7.5 Fondo y límite de detección.** El programa permite visualizar el fondo, cuando la opción *descontar un fondo* ha sido afirmativa. Una opción de menú permite acceder a una pantalla destinada al cálculo de límites de detección, donde se consideran varias situaciones posibles.

## 5. RESULTADOS

La tabla 1 muestra una serie de resultados seleccionados al azar, correspondientes a espectros de un radionucleido monoenergético (<sup>210</sup>Po), obtenidos a partir de fuentes electropulidas y electrodepositadas (ver apéndice), y analizados por este método.

FWHM (can)	Contaje real	Contaje calculado	Diferencia (%)
4,63	26530	26930,9	1,51
4,52	26961	26968,5	0,03
4,11	26745	26700,6	-0,17
4,47	35069	35058	-0,03
4,78	28414	28387,6	-0,09
4,45	35145	35237,8	0,26
4,74	346021	34639,1	0,11

**Tabla 1.** Análisis de espectros de pico monoenergético de <sup>210</sup>Po.

La tabla 2 muestra una serie de resultados seleccionados al azar, correspondientes a espectros de diversos radionucleidos, obtenidos también a partir de fuentes electrodepositadas y electropulidas.

Radionucleido	Contaje real	Contaje calculado	Diferencia (%)
$^{241}\text{Am}$	48566	48366,7	-0,41
$^{239}\text{Pu}$	19564	19584,5	-0,1
$^{233}\text{U}$	36097	36040,9	-0,16
$^{243}\text{Am}$	9375	9335,8	-0,42
$^{243}\text{Am}$	2111	2106,8	-0,2
$^{241}\text{Am}$	60887	60898,5	0,02

**Tabla 2.** Análisis de varios espectros de pico único.

Algunos de los pares de radionucleidos que frecuentemente presentan solapamiento debido a su proximidad en energía son:  $^{241}\text{Am} / ^{243}\text{Am}$ ,  $^{242}\text{Pu} / ^{234}\text{U}$ ,  $^{228}\text{Th} / ^{232}\text{U}$ ,  $^{238}\text{Pu} / ^{228}\text{Th}$ ,  $^{234}\text{U} / ^{230}\text{Th}$ ,  $^{238}\text{U} / ^{232}\text{Th}$ . De ellos, el par  $^{241}\text{Am} / ^{243}\text{Am}$  es el que nunca se puede evitar por tratarse de isótopos del mismo elemento; además constituyen la relación analito / trazador y es un problema típico en espectrometría alfa debido a que la separación entre los picos es de solo 211 keV. Una evaluación de la respuesta de varios algoritmos en relación a dicho par <sup>[13]</sup>, muestra el interés que el problema despierta en la actualidad.

Para analizar la respuesta frente sistemas de dos picos, se utilizaron varios espectros obtenidos a partir de 3 fuentes electropulidas y electrodepositadas con soluciones patrón de  $^{241}\text{Am}$  y  $^{243}\text{Am}$ , en diferentes relaciones y en distintos detectores. La solución patrón de  $^{241}\text{Am}$  fue calibrada por centelleo líquido, mientras que la solución de  $^{243}\text{Am}$  lo fue por espectrometría alfa (con el agregado de  $^{241}\text{Am}$ ) a la distancia máxima que permite la cámara. La distancia al detector fue de aproximadamente 0,5 cm y el grado de superposición de 3-4% en relación al  $^{243}\text{Am}$ . Los resultados se resumen en la tabla 3, donde se aprecia una muy pequeña diferencia entre la relación de actividad obtenida por calibración y la que resultó de la obtención de las áreas por aplicación del algoritmo descrito.

$^{241}\text{Am} / ^{243}\text{Am}$ (real)	$^{241}\text{Am}$ (cuentas)	$^{243}\text{Am}$ (cuentas)	$^{241}\text{Am} / ^{243}\text{Am}$ (calculado)	Diferencia (%)
1,4135	39548,7	28269,2	1,399	-1,03
1,4135	18462,1	12828,4	1,4392	1,82
1,4135	37744,2	26623,3	1,4177	0,3
1,4135	59411,2	41936,4	1,4167	0,23
2,8762	53285,7	18408,3	2,8947	0,64
2,8762	135552,5	46500,6	2,9151	1,35
2,8762	65365,4	22738,2	2,8747	-0,05
5,0517	57418,2	11217	5,1189	1,3
5,0517	170079,5	33600,4	5,0608	0,2
5,0517	104361,8	20650,4	5,0537	0,04

**Tabla 3.** Análisis de varios espectros de  $^{241}\text{Am}$  y  $^{243}\text{Am}$ .

## 6. CONCLUSIONES

La metodología de análisis presentada en este trabajo para el análisis de espectros alfa es versátil, ya que se adapta con facilidad a diversos radionucleidos de análisis frecuente ( $^{234}\text{U}$ ,  $^{238}\text{U}$ ,  $^{239}\text{Pu}$ ,  $^{238}\text{Pu}$ ,  $^{242}\text{Pu}$ ,  $^{241}\text{Am}$ ,  $^{243}\text{Am}$ , etc), es relativamente simple y produce buenos resultados.

El programa desarrollado presenta una serie de funciones de utilidad para el analista, así como interactividad, variedad de recursos y rapidez.

## 7. APÉNDICE

**7.1 Electrodepositión y electropulido.** La determinación de emisores alfa requiere de la disolución de la muestra, si la matriz es sólida, la separación selectiva de los radionucleidos de la solución y finalmente la preparación de una fuente plana de capa muy delgada, lo que en el caso nuestro, se lleva a cabo por electrodeposición sobre un disco de acero inoxidable 316L. El método de electrodeposición utilizado, fue el desarrollado por Talvitie en 1972<sup>[14]</sup> y se lleva a cabo en viales de centelleo de plástico (figura 3), sobre discos de acero de 2 cm de diámetro y 1,6 cm de diámetro de depósito, con electropulido previo. El proceso se lleva a cabo en medio sulfato de amonio 1 M, a pH 2 y un volumen de aproximadamente 10 ml, con ánodo de Pt en espiral plano, con 2-3 mm de distancia entre electrodos y 1,2 A de corriente continua constante, durante 2 horas. El proceso de electropulido se realiza antes de electrodepositar y consiste en electrolizar 1,5 mL de una solución 45% de  $\text{H}_3\text{PO}_4$ , 35% de  $\text{H}_2\text{SO}_4$  y 20% de agua<sup>[15]</sup>, con corriente de 0,8 A invertida, en la misma celda de electrodeposición, durante 10 minutos. Luego el ánodo se lava hirviéndolo en una solución diluida de HCl, y la celda se desarma y se lava 10 a 15 veces con agua. El esquema del sistema es:

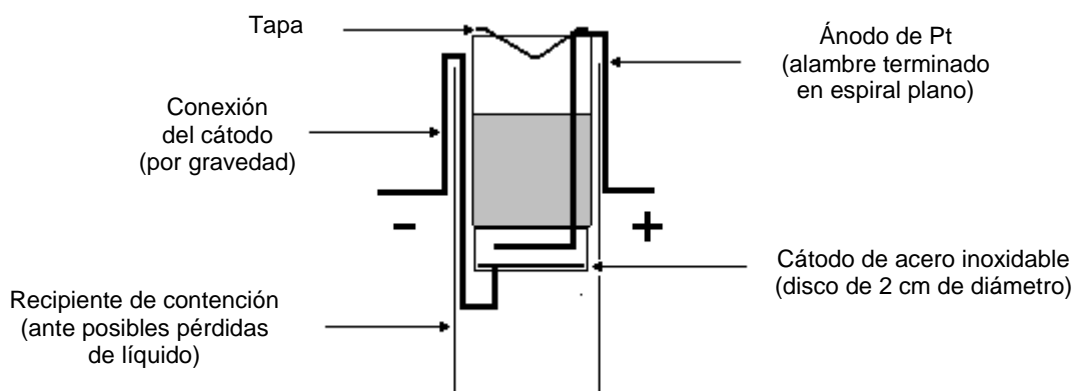


**Figura 3.** Esquema del sistema de electrodeposición

## **8. BIBLIOGRAFÍA**

1. Memoria Técnica ARN, 161, 2000.
2. Radioac. and Radiochem., 7, 1, 18, 1996.
3. IEEE Trans. Nucl. Sci., 39, 4, 958, 1992.
4. Nucl. Inst. and Meth. , A299, 272-275, 1990
5. Appl. Radiat. Isot., 38, 10, 831-837, 1987.
6. IEEE Trans. Nucl. Sci., 33, 1, 639, 1986.
7. Int. J. Appl. Radiat. Isot. , 35, 4, 279-283, 1984.
8. Nucl. Inst. and Meth. , 223, 356-359, 1984.
9. Nucl. Inst. and Meth., 185, 261-269, 1981.
10. Ortec, AlphaVision Software User's Manual, 1996.
11. Canberra, Genie 2000 Alpha Analyst User's Manual, 1998.
12. Kocher, Radiactive Decay Data Tables, Report DOE/TIC-11026.
13. Appl. Radiat. and Isot., 56, 57-63, 2002.
14. Anal. Chem., 44, 2, 280, 1972.
15. Anal. Chem., 49, 6, 842, 1977.

# Resultados de la participación de la ARN en el programa de garantía de calidad del EML- DOE Período 2002-2004

Equillor, H.E.; Serdeiro, N.H.; Fernández, J.A.; Gavini, R.M.;  
Grinman, A.D.R.; Lewis, E.C. y Palacios, M.A.



# **RESULTADOS DE LA PARTICIPACIÓN DE LA ARN EN EL PROGRAMA DE GARANTÍA DE CALIDAD DEL EML- DOE PERÍODO 2002-2004**

Equillor, H.E.; Serdeiro, N.H.; Fernández, J.A.; Gavini, R.M.; Grinman, A.D.R.; Lewis, E.C. y Palacios, M.A.

Autoridad Regulatoria Nuclear  
Argentina

## **RESUMEN**

En este informe se publican los resultados obtenidos por la Autoridad Regulatoria Nuclear (ARN) en mediciones de emisores alfa, beta y gamma, en cuatro tipos de matriz, en el marco del Programa de Evaluación de Calidad (Quality Assessment Pr ogram - QAP) organizado por el Laboratorio de Mediciones Ambientales (Environmental Measurements Laboratory - EML) de los Estados Unidos, correspondientes a los 5 ejercicios del período 2002-2004.

## **ABSTRACT**

In this report, the results corresponding to five consecutives exercises (period 2002-2004) obtained by the Autoridad Regulatoria Nuclear (ARN) in alpha, beta and gamma measurements, on four different matrixes, within the framework of Environmental Measurements Laboratory (EML) Quality Assessment Program (QAP) of the United States, are presented.

## **INTRODUCCIÓN**

Con el objetivo de mantener la calidad de las mediciones y de los análisis radioquímicos que se llevan a cabo rutinariamente, que son parte de los programas de monitoreo ambiental u ocupacional, la ARN participa en varios programas de intercomparación de resultados. Uno de ellos es el programa QAP organizado por el EML, que se realiza semestralmente. Publicaciones anteriores detallan los resultados obtenidos desde 1995, año en el que la ARN inició su participación, hasta 2001 [1-6].

## **DESCRIPCIÓN**

### **El Programa de Evaluación de Calidad del EML (QAP)**

El Environmental Measurements Laboratory [7], es una entidad gubernamental que hasta 2003 dependía del Department of Energy (DOE) de los EE. UU. y actualmente del Department of Homeland Security (DHS).

El programa QAP implica mediciones de emisores alfa, beta y gamma, y se aplica a cuatro tipos de matrices de tipo ambiental: agua, filtro, vegetal y suelo. Para cada intercalibración el EML envía un total de seis muestras, conteniendo una amplia variedad de radionucleidos en concentraciones de nivel ambiental. El número de análisis que son requeridos es aproximadamente de 52 y en la actualidad participan de este programa más de 150 laboratorios.

La ARN participa en los dos ejercicios anuales que organiza el EML, y hasta el momento ha participado en diecinueve ocasiones.

Este programa requiere la realización de mediciones de características diversas como espectrometría gamma, espectrometría alfa, centelleo líquido, detectores de ZnS, contador proporcional y fluorimetría para la determinación de masa de uranio.

Recientemente el EML ha anunciado la finalización del programa QAP [8] debido a los cambios introducidos en las misiones del organismo, por lo que el ejercicio número 60 es el último de la serie. En la Tabla 1 se detallan los tipos de muestra y los diferentes radionucleidos que se analizan, para cada matriz:

<b>Tipo de muestra</b>	<b>Cantidad de radionucleidos</b>	<b>Radionucleido</b>
<b>AGUA 1</b>	12	$^3\text{H}$ , $^{60}\text{Co}$ , $^{63}\text{Ni}$ , $^{90}\text{Sr}$ , $^{137}\text{Cs}$ , $^{234}\text{U}$ , $^{238}\text{U}$ , U, U ( $\mu\text{g}$ ), $^{238}\text{Pu}$ , $^{239}\text{Pu}$ , $^{241}\text{Am}$
<b>AGUA 2</b>	2	Alfa Total, Beta Total
<b>FILTRO 1</b>	13	$^{54}\text{Mn}$ , $^{57}\text{Co}$ , $^{60}\text{Co}$ , $^{90}\text{Sr}$ , $^{106}\text{Ru}$ , $^{137}\text{Cs}$ , $^{234}\text{U}$ , $^{238}\text{U}$ , U ( $\text{Bq}$ ), U ( $\mu\text{g}$ ), $^{238}\text{Pu}$ , $^{239}\text{Pu}$ , $^{241}\text{Am}$
<b>FILTRO 2</b>	2	Alfa Total, Beta Total
<b>VEGETAL</b>	8	$^{40}\text{K}$ , $^{60}\text{Co}$ , $^{90}\text{Sr}$ , $^{137}\text{Cs}$ , $^{238}\text{Pu}$ , $^{239}\text{Pu}$ , $^{241}\text{Am}$ , $^{244}\text{Cm}$
<b>SUELO</b>	14	$^{40}\text{K}$ , $^{90}\text{Sr}$ , $^{137}\text{Cs}$ , $^{212}\text{Pb}$ , $^{212}\text{Bi}$ , $^{214}\text{Pb}$ , $^{214}\text{Bi}$ , $^{228}\text{Ac}$ , $^{234}\text{U}$ , $^{238}\text{U}$ , U ( $\text{Bq}$ ), U ( $\mu\text{g}$ ), $^{239}\text{Pu}$ , $^{241}\text{Am}$

**Tabla 1.** Tipos de muestras y radionucleidos involucrados en el programa QAP.

#### Criterio de evaluación

De acuerdo a la metodología estadística adoptada por el EML [9], los resultados se clasifican en:

<b>Aceptados</b>	<b>Aceptados con reservas</b>	<b>Rechazados</b>
<b>Clase A</b>	<b>Clase W</b>	<b>Clase N</b>

## RESULTADOS

#### Resultados generales

En la Figura 1 y Figura 2 se muestra una comparación entre los resultados de la ARN y los obtenidos por todos los laboratorios en el período 2002-2004, exceptuando los dos últimos ejercicios de este período, dado que el EML no produjo el reporte que contiene el análisis estadístico correspondiente:

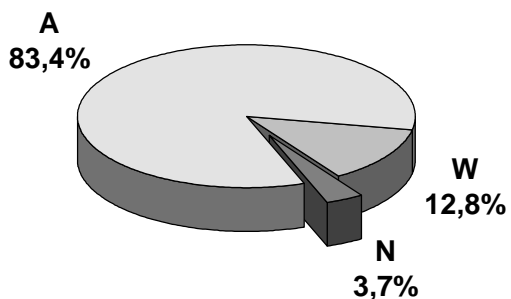


**Figura 1.** Promedio de los resultados de la ARN (periodo 2002-2004).

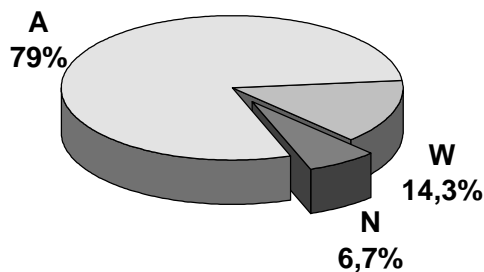


**Figura 2.** Promedio de los resultados de todos los laboratorios (periodo 2002-2003).

De la comparación surge en forma inmediata que los resultados de la ARN, a lo largo del período analizado, han merecido una calificación tipo A, un 5,6% mayor que la correspondiente al conjunto de los laboratorios participantes. Además el número de resultados clase N fue menor que el promedio del conjunto de los laboratorios, es decir que 180 de los 187 resultados informados (A + W), o sea el 96,3%, fueron aceptados. En la Tabla 2, se presentan los resultados generales de la ARN, basados en el análisis realizado por el EML [10-13]:

Año	QAP <sup>(*)</sup>	n <sup>(**)</sup>	Clase A		Clase W		Clase N	
			ARN %	Todos los laboratorios %	ARN %	Todos los laboratorios %	ARN %	Todos los laboratorios %
2002	56	40	85,0	79	12,5	14	2,5	7
2002	57	41	80,5	79	4,9	14	14,6	7
2003	58	40	85	79	15	15	0	6
2003	59	30	86,7	-- <sup>(a)</sup>	13,3	-- <sup>(a)</sup>	0	-- <sup>(a)</sup>
2004	60	36	80,6	-- <sup>(a)</sup>	19,4	-- <sup>(a)</sup>	0	-- <sup>(a)</sup>
<b>Promedio:</b>			83,4	79 <sup>(b)</sup>	12,8	14,3 <sup>(b)</sup>	3,7	6,7 <sup>(b)</sup>

**Total de análisis informados: 187**

**Tabla 2.** Resultados de la participación de la ARN, comparados con los resultados del conjunto de los laboratorios participantes.

(\*) Quality Assessment Program. Número dado por el EML a cada ejercicio de intercomparación.

(\*\*) Número de resultados informados por la ARN.

(a) Hasta la fecha (agosto/04), el EML no realizó su habitual reporte estadístico.

(b) Los promedios se obtuvieron considerando los 3 únicos datos disponibles.

Al observar individualmente los porcentajes de resultados clase A, se puede notar que en todos los ejercicios, los resultados informados por la ARN presentan valores mejores que los correspondientes al promedio del conjunto de los laboratorios participantes.

Puede destacarse también la estabilidad de los resultados, en las distintas categorías A, W y N. El número de resultados informados se mantuvo elevado en todo el período, y representan un alto porcentaje de los requeridos por el EML.

### **Resultados según el tipo de radionucleido emisor**

La Figura 3 muestra la distribución, en porcentaje, del número de datos informados según el tipo de emisor:

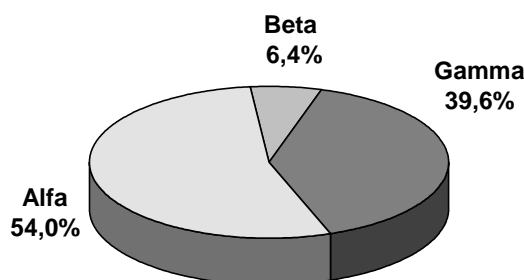


**Figura 3.** Número de datos informados por la ARN, en porcentaje, según el tipo de radionucleido emisor (período 2002-2004).

Los resultados clasificados según el tipo de emisor se ofrecen en la Tabla 3:

Emisor	n	Clase A		Clase W		Clase N	
		n <sub>A</sub>	n <sub>A</sub> %	n <sub>W</sub>	n <sub>W</sub> %	n <sub>N</sub>	n <sub>N</sub> %
<b>Alfa</b>	101	72	71,3	22	21,8	7	6,9
<b>Beta</b>	12	11	91,7	1	8,3	0	0
<b>Gamma</b>	74	73	98,6	1	1,4	0	0

**Tabla 3.** Distribución de los resultados de la ARN, de acuerdo con el tipo de radionucleido emisor.

n: número de resultados totales informados por la ARN.

n<sub>A</sub>%, n<sub>W</sub>%, n<sub>N</sub>%: porcentaje de resultados informados por la ARN con relación al número total de datos informados (n).

La diferencia en el número de datos informados n, es consecuencia de los distintos requerimientos del EML para cada una de las matrices.

## Resultados según el tipo de matriz

La Figura 4 muestra la distribución, en porcentaje, del número de datos informados según el tipo de matriz:

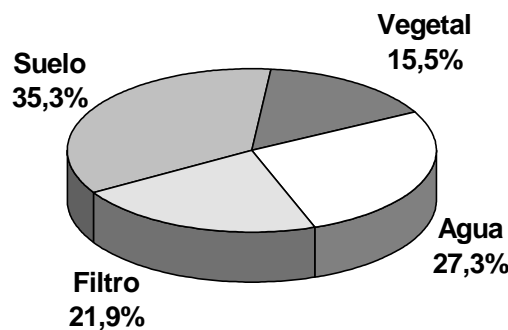


**Figura 4.** Número de datos informados por la ARN, en porcentaje, según el tipo de matriz (periodo 2002-2004).

En la Tabla 4 se presentan los datos distribuidos según el tipo de matriz:

Matriz	n	Clase A		Clase W		Clase N	
		n <sub>A</sub>	n <sub>A</sub> %	n <sub>W</sub>	n <sub>W</sub> %	n <sub>N</sub>	n <sub>N</sub> %
Filtro	41	34	82,9	3	7,3	4	9,8
Suelo	66	53	80,3	11	16,7	2	3
Vegetal	29	24	82,8	5	17,2	0	0
Agua	51	45	88,2	5	9,8	1	2,0

**Tabla 4.** Distribución de los resultados de la ARN, de acuerdo con el tipo de matriz y la calificación obtenida.

n: número de resultados totales informados por la ARN

n<sub>A</sub>%, n<sub>W</sub>%, n<sub>N</sub>%: porcentaje de resultados informados por la ARN con relación al número total de datos informados (n).

En este caso, se observa muy poca variación de los porcentajes de resultados clase A, W y N, para las distintas categorías de matriz.

## **CONCLUSIONES**

El promedio de resultados clase A en el período considerado (2000-2004) fue superior que el correspondiente al conjunto de los laboratorios participantes.

En el mismo período el promedio de resultados clase N fue inferior que el correspondiente al conjunto de los laboratorios participantes.

El promedio de resultados clase A+W, es decir los aceptados en general, fue superior que el correspondiente al conjunto de los laboratorios participantes.

El número de datos informados se mantuvo elevado durante todo el período.

## **BIBLIOGRAFÍA**

- [1] "Results of the ARN participation in the Quality Assessment Program of the EML - DOE during period 2000-2001", Publicación interna ARN PI 3/03, 2003.
- [2] "Resultados de la participación de la ARN en el programa de garantía de calidad del EML-DOE", Publicación interna ARN PI-1/02, 2002.
- [3] "Participación de la ARN en el programa de EML- USDOE para la evaluación de la calidad de las mediciones radioquímicas-período 1998-2000", V Regional Congress on Protection and Safety, IRPA, 2001.
- [4] "Resultados de la participación de la ARN en el programa de garantía de calidad del EML-DOE período 1995-1999", Publicación interna ARN PI-2/00, 2000.
- [5] "Participation of ARN-Argentina in the Quality Assessment Program, EML - USDOE since 1995 to 1999", NRC5, 5 International Conference on Nuclear and Radiochemistry, Switzerland, 2000.
- [6] "Participación de la ARN en el programa de garantía de calidad del EML - DOE", Jornadas sobre PR y SN, SAR, 2000.
- [7] <http://www.eml.doe.gov>.
- [8] <http://www.eml.doe.gov/qap/news>.
- [9] <http://www.eml.doe.gov/qap>.
- [10] <http://www.eml.doe.gov/qap/reports>.
- [11] QAP Report-EML617, Greenlaw, P.; Berne, A., 2002.
- [12] QAP Report-EML618, Greenlaw, P.; Berne, A., 2002.
- [13] QAP Report-EML621, Greenlaw, P.; Berne, A., 2003.

# Radiation-Induced Apoptosis of Neural Precursors Cell Cultures: Early Modulation of the Response Mediated by Reactive Oxygen and Nitrogen Species (ROS/RNS)

Gisone, P.A.; Dubner, D.L.; Robello, E.;  
Michelin, S.C. and Perez, M. del R.



## **Radiation-induced apoptosis of neural precursors cell cultures: early modulation of the response mediated by reactive oxygen and nitrogen species (ROS/RNS)**

Gisone, P.A.; Dubner, D.L.; Robello, E.; Michelin, S.C. and Perez, M. del R.

Autoridad Regulatoria Nuclear (ARN), Gerencia de Apoyo Científico, Laboratorio de Radiopatología, Avenida del Libertador 8250, (C1429BNP) Buenos Aires, Argentina

**Abstract.** Apoptosis, the typical mode of radiation-induced cell death in developing Central Nervous System (CNS), is closely related with the oxidative status. Enhanced radiation-induced generation of ROS/RNS has been observed after exposures to low radiation doses leading to cellular amplification of signal transduction and further molecular and cellular radiation-responses. Moreover Nitric oxide (NO) and hydroxil radical are implicated in domapinegeric neurotoxicity in different paradigms. This study is an attempt to address the participation of radiation-induced free radicals production, the contribution of endogenous NO generation, and the excitotoxic pathway, in the radiation-induced apoptosis of neural cortical precursors. Cortical cells obtained from at 17 gestational day (gd) were irradiated with doses from 0,2 Gy to 2 Gy at a dose-rate of 0,3 Gy/m. A significant decrease of Luminol-dependent Chemiluminescence was evident 30 m after irradiation reaching basal levels at 120 m follow for a tendency to increasing values Incubations with Superoxide Dismutase (SOD) decreased significantly the chemiluminiscence in irradiated samples. NO content estimated by measuring the stable products  $\text{NO}_2^-$  and  $\text{NO}_3^-$  released to the culture medium in the same period, has shown a time-dependent accumulation from 1 h post-irradiation. The apoptosis, determined 24 h post-irradiation by flow citometry, morphology and DNA fragmentation, revealed a dose-effect relationship with significant differences from 0,4 Gy. The samples pre-treated with 10 mM of N-acetyl ctyeine (NAC) a precursor of intracellular GSH synthesis, shown a significant decrease of the apoptosis. Apoptosis was significantly increased in irradiated cells after inhibition of nitric oxide synthase (NOS) byL-NAME. We conclude that ROS/RNS play a pivotal role in the early signaling pathway leading to a radiation-induced cell death.

### **1. Introduccion**

Even under very low doses of radiation, the developing brain is ones of the most radiosensitives organs in view of the amounts of structural abnormalities which can be induced in this tissue [1]

Developmental radiation-induced abnormalities of the cerebral cortex of fetuses are expressed in different ways, depending on the dose and on the gestation day of exposure [2].

An increased prevalence of Severe Mental Retardation (SMR) has been epidemiological evidenced in children who were prenatally exposed to the atomic bombing of Hiroshima and Nagasaki.[3].

The incidence of microcephaly in the Hiroshima and Nagasaki cohort was higher among atomic bomb survivors who were exposed at 8-10 weeks of gestation [4].

In order to supplement the knowledge of radiation-induced perturbations of brain development specifically in regards to potential mechanisms at the cellular levels, different animals models have been employed [5].

The animal studies have shown that prenatal irradiation results in microcephaly [6,7,8] impairment in neurotransmitters contents [9], behavioural deficits in adult life [11,12] and significant decreases in cortical thickness [12] .

The embrionic day 13 in mice and 15 to 17 days in rats corresponds to the highly radiosensitivity stage in humans. In these developmental periods, doses of 15 cGy are able to decelerate neuronal migration associated with a changing pattern expression of neural cell adhesion molecules [13].

Rats exposed to 1 Gy of X rays on day 15 showed microcephaly and impaired postnatal development of dendritic spines[8] This high susceptibility of the developing brain might be related with the rate of membrane lipid peroxidation, the development and modulation of

NMDA receptor sites, the intracellular  $\text{Ca}^{2+}$  influx mechanism, the expression of apoptotic and antiapoptotic genes, and the activation of caspases. [14].

The responses of cells to radiation are most likely initiated by the radiation-induced free radicals production. In fact, enhanced cellular generation of ROS/RNS has been observed after exposures to low radiation doses production and could lead to cellular amplification of signal transduction and further molecular and cellular radiation-responses [15].

Nitric Oxide (NO) and hydroxil radicals (OH) are implicated in dopaminergic neurotoxicity in different neurotoxic paradigms. [16].

In the last years growing evidence of NO as a neuroprotector is accumulating in the literature [17]. Since the effects of NO are modulated by both direct and indirect interactions that can be dependent of its content and of cell type specificity, pro-apoptotic and antiapoptotic effects has been described [18]. Low concentrations of NO can inhibit the apoptotic pathway through cGMP-dependent mechanisms, and caspases inhibition. In contrast, NO may have pro-apoptotic effects via mitochondria, DNA damage and inhibition of proteasome [18]. We have recently communicated that ionizing radiation induces an early increase of nNOS activity that correlates with a further augmentation in NO steady-state concentration playing an antioxidant role in irradiated developing rat brain.[19].

A number of studies have confirmed that radiation induced cell death in developing brain follows the apoptotic pathway [20,21] predominantly triggered by double strand breaks in the DNA.

In a similar model of irradiated neural precursor cells in vitro, we have shown that the radiation-induced programmed cell death is a caspase-3 dependent event [22].

The increased proteolytic activities of caspases might be responsible of a burst of ROS production as it has been proposed. [23].

This study is an attempt to address the participation of radiation-induced free radicals production and its behaviour, as well as the contribution of NO endogenous generation, in modulating the apoptotic response, in an in vitro model of neural cortical precursor cells exposes to Gamma radiation.

## 2. Material and methods

### 2.1-Cortical cell culture

Wistar female rats were housed with males overnight and pregnant dams, identified by sperm positive vaginal smears, were considered at gestational day ( gd ) 0.

Primary cell cultures were prepared according to the method of micromass described by Flint et al [24] with some modifications. Living fetuses were removed at the 17<sup>th</sup> gd and the brain was dissected out under sterile conditions. The meninges were removed and the cortical plate was collected in  $\text{Ca}^{2+}/\text{Mg}^{2+}$  free Hank's balanced salt solution (HBSS) containing 0.25% trypsin and 10ug/ml DNase. The tissue was digested for 15min and then mechanically dissociated by flushing through glass pipettes. The large clumps were allowed to descend to the bottom and the supernatant was centrifuged at 500xg for 5min. The pellet was redispersed in Dulbecco's modified Eagle's medium ( DMEM ) supplemented with 10% foetal bovine serum ( FBS ) and 50ug/ml gentamine and then transferred into petri dishes or 24-well plates at a density of  $10^6$  cells /ml.

Cultures were kept at 37°C in a humidified atmosphere of 95% air and 5%  $\text{CO}_2$ .

### 2.2 Irradiation and drug treatments

The irradiation were carried out with a  $^{60}\text{Co}$  teletherapy unit (Picker C4M60; Atomic Energy Commission/CAE). Doses from 0.2 to 2.0 Gy were given at a dose-rate of 0.3Gy/min. The exposure commenced 2h after plating in order to let cell attachment. Control samples were sham irradiated. The cells were then incubated and harvested at different time-points for different assays.

The various drugs were added to the culture medium and gently mixed. The cultures were incubated in the aforementioned conditions for the times indicated in the figures.

### **2.3 Immunocytochemical studies**

Nestin was determined on days 2 post-irradiation (pi). Cells were fixed overnight at 4°C on cover slips in 4% paraformaldehyde buffered in 50 mM sodium borate at pH 9.5, blocked with 5 % fetal serum in PBS, and exposed for 60 minutes at 37°C to the anti-nestin monoclonal antibody at 1/25 dilution (Chemicon International Inc. (Cat MAB353). Secondary antibody staining was performed by exposure to goat anti mouse IgG FITC at 1/10 dilution for 30 min a 37°C, (Boehringer Mannheim Biochemical). Samples stained only with goat anti mouse IgG FITC in the same conditions were used as negative controls.

For the determination of glial fibrillary acidic protein (GFAP) the cells were fixed in precooled methanol for 10 min at -20 0C. The cells were covered with the specific monoclonal antibody (clone G-A-5) (Boehringer Mannheim Biochemical) for 30 min at room temperature. Secondary antibody staining was performed by exposure to goat anti mouse IgG FITC at 1/10 dilution for 30 min at 37 °C (Boehringer Mannheim Biochemical). Samples exposed only with goat anti mouse IgG FITC in the same conditions were used as negative controls.

### **2-4 Morphological features**

Apoptotic cells were identified using conventional morphological criterio after staining with May Grunwald-Giemsa according to standard procedure.

In order to discriminate between cells in the process of apoptosis, living and dead (either necrotic or apoptotic) cells, a mixture of three fluorescent dyes, according to Piñero et al [25] was used. Briefly, 500ul of cells suspension ( $3 \times 10^6$  cells/ml) were incubated with 10ul of the fluorescent mix prepared in PBS ph 8, containing 2ug/ml of Hoescht 33342 (H), 15ug/ml of fluorescein diacetate ( FDA ), and 5ug/ml of propidium iodide (PI ). After 5 minute-incubation and once washed, samples were dropped onto slide and observed by a fluorescence microscopy (Carl Zeiss™ MC 80 DX).

### **2-5 DNA fragmentation in agarose gels**

Cortical cells (  $5 \times 10^6$  ) were lysed in a buffer containing 1% sodium dodecyl sulfate, 100mM NaCl, 20mM Tris-HCl ( ph 8 ) and 20mM EDTA for 30min in an ice- cold bath and centrifuged at 27000xg for 15min at 4°C. The soluble DNA recovered in the supernatant was incubated with 100ug/ml Proteinase K for 3h at 56°C and extracted with an equal volume of phenol/chloroform/isoamyl alcohol (25:24:1). The nucleic acids were precipitated with 2.5vol of ice-cold ethanol in the presence of 0.3M ammonium acetate (final concentration). DNA pellet was resuspended in 10ul of TE buffer and incubated with 3ul of 200ug/ml DNase-free RNase at 56°C for 1h.

Electrophoresis was carried out in TAE buffer (ph8.3) after loading equal concentration of DNA (10ug) onto wells of 1.8% agarosa gels added with 0.2ug/ml ethidium bromide.

DNA fragments were visualized and photographed on a UV transilluminator.

### **2-6 Analysis of apoptosis rate by flow cytometry**

The assay was performed as described by Darzynkiewicz et al [26] with minor modifications. Briefly,  $1 \times 10^6$  cells were collected from dishes and fixed in 70% ethanol at 4°C for 2h. After centrifuging, cells were washed and resuspended in PBS containing 50ug/ml RNase and 40ug/ml propidium iodide (PI). After 30min at room temperature, the apoptosis rate was analyzed using a Becton Dickinson® FACStar Plus flow cytometer. Apoptotic cells were identified in a DNA histogram as a sub-G1 hypodiploid population.

### **2-7 Measurement of NO production**

To ascertain the NO generation, nitrite/nitrate levels were measured in the culture supernatant. Nitrate was reduced according to Verdon et al. [27] , before assaying the resultant nitrite using the Griess reaction

## **2-8 Measurement of intracellular ROS production**

### **a) Chemiluminescence measurement**

Luminol-dependent chemiluminescence was measured in a Packard 1500 Tri-CARB® Liquid Scintillation Analyzer in the single photon counting mode.

Stock solution of Luminol (2mM) was prepared by dissolving in 0.1M bicarbonate and was stored in the dark at 4°C.

The reaction mixture included 1x 10<sup>6</sup> cells, 250ul of luminol stock solution and bicarbonate 0.1M (final concentration 25mM, pH 8.5) in a 5ml total volume of PBS.

### **b) Fluorescent assays**

Two oxidation – sensitive fluorescent dyes 2',7' Dichlorodihydrofluorescein diacetate ( H<sub>2</sub>DCFDA ) and dihydroethidium ( DHE ) were employed . H<sub>2</sub>DCFDA was reported to be preferential for hydrogen peroxide and DHE was used as an indicator of superoxide anion.

For the determination of hydrogen peroxide cells were washed in PBS and then H<sub>2</sub>DCFDA was added to a final concentration of 10µM for 30 min at 37°C.The cells were analysed by FACS with excitation at 488 and emission at 530nm.

For determination of superoxide anion cells were washed in PBS and stained with DHE 5µM at 37°C for 30min.The cells were examined by FACS with excitation at 488 and emission at 610nm

## **2-9 Statistical**

All data are represented as means +/- SEM. Statistical analysis was performed using the Student t-test

## **3. Results**

### **3-1 Immunocytochemical studies**

Cell cultured from the embryonic rat forebrain showed positive staining (90%) for nestin, an intermediate filament present in the cytoplasm of pluripotential central nervous system progenitor cells, and negativity for GFAP a glial fibrillary acidic protein present in astrocytes. This confirmed that cells cultured on 17 GD were neural precursors.

### **3-2 Apoptosis**

In this study, at first, we characterized the apoptotic response of the system.

The morphological changes observed in irradiated samples were those typical of apoptotic death, and included chromatin condensation with nuclear shrinkage and fragmentation.

Conventional agarose gel electrophoresis showed the characteristic DNA ladder pattern of 200 bp owing to internucleosomal fragmentation.

Apoptosis quantitation was assessed by flow cytometric measurement of DNA content after fixation and PI staining and by fluorescence microscopy. In this case, and after staining cells suspensions with three fluorescent dyes, apoptotic cells exhibited a green cytoplasm and blue spotted nuclear bodies.

The apoptotic response to radiation injury revealed a dose-effect relationship, showing a significant difference starting from 0,4 Gy (Fig. 1).

Figure 2 shows the time-course of apoptotic death up to 20 hours after sham or irradiation procedure. Even though the spontaneous rate increased progressively in control samples during the studied period, the irradiated cells showed a significant higher rate for a 2 Gy dose since 4 hours pi.

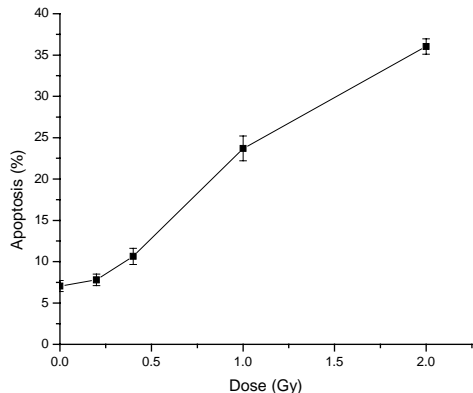


FIG.1. *Radiation induced apoptosis. Dose-effect relationship*

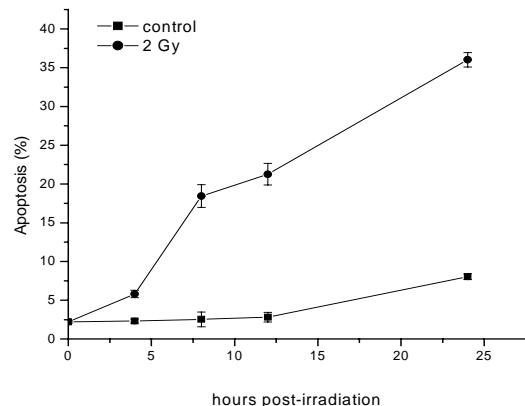


FIG.2. *Time course of radiation induced apoptosis in neural precursors irradiated with 2Gy*

The effect of pretreatment with N-acetyl cysteine (NAC) a precursor of intracellular GSH synthesis on radiation induced apoptosis was evaluated. The treatment with 10mM NAC from 24h before irradiation up to 24h pi, blocked apoptosis in the irradiated samples. Inversely incubation of the cells with 0.1mM BSO from 24h pi resulted in a significant increase in the apoptosis rate. No significant changes were observed in the control cells treated with either of the two drugs (Fig 3).

When the cultured cells were incubated in the presence of  $\text{NO}_2$ -nitro-L-arginine methyl ester ( L-NAME ), an inhibitor of NOS, a significant increase of the apoptosis rate could be detected. (Fig 4).

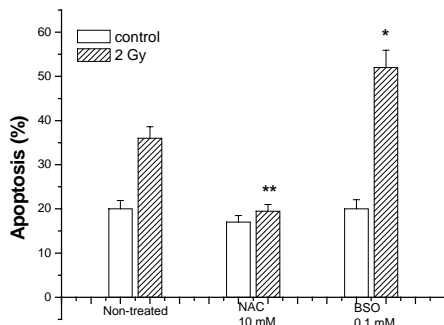


FIG.3. *Effect of NAC and BSO on radiation induced apoptosis*  
Significant differences from 2Gy: \*  $p < 0.01$ , \*\*  $p < 0.001$

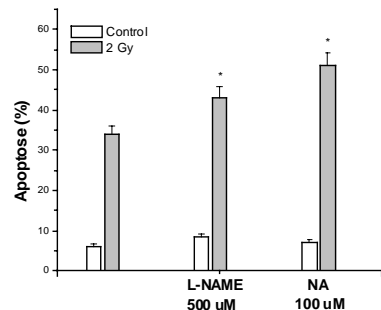


FIG.4. *Effect of L-NAME 0.5mM and NA 0.1mM on radiation induced apoptosis. The drugs were added 2h prior to irradiation up to 24h pi*  
Significant differences from 2Gy: \*  $p < 0.01$

### 3-3 NO production.

We then examined NO content, estimated by measuring the stable oxidation products  $\text{NO}_2^-$  and  $\text{NO}_3^-$ , released to the culture medium. Exposure of cells to gamma radiation stimulated NO production, from 1h pi , and thereafter, a time-dependent accumulation was observed through the early phase of the response studied ( Fig 5 ).

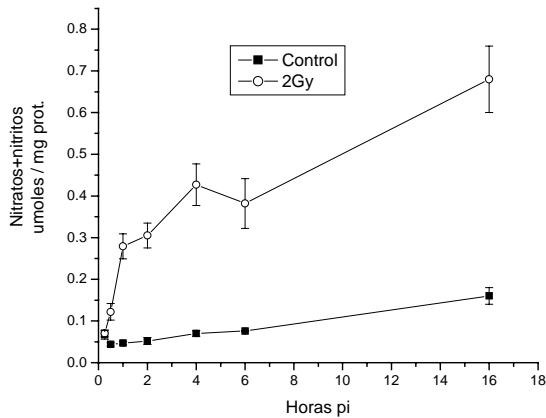


FIG.5. *Time course of NO production*  
Significant differences from control from 1h  
pi

### 3-4 ROS production

The intracellular ROS production measured by chemiluminescence showed a significant decrease in the irradiated samples up to h post-irradiation and then tended to normalize compared to control cells ( Fig 6 ).

When precursor cortical cells were incubated in the presence of L-NAME, the initial decrease observed in the irradiated samples disappeared and no changes with respect to control values were detected up to 4hpi where gradually increased to about three-fold by 6h pi ( Fig 6 ).

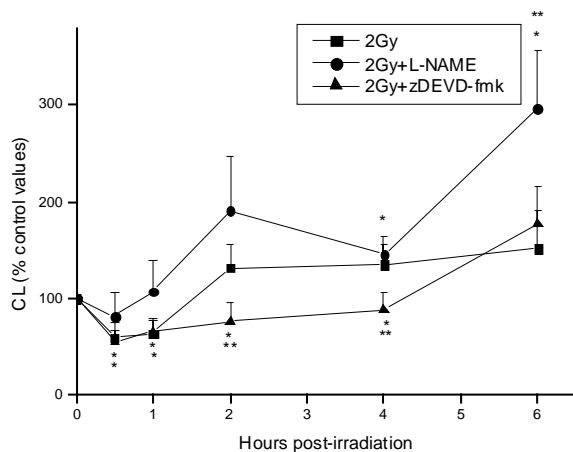
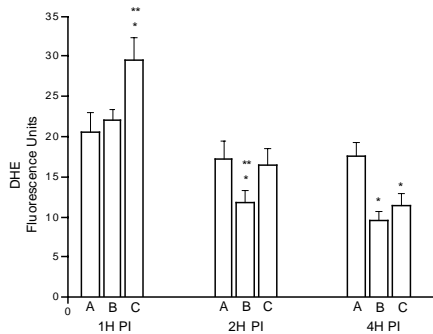


FIG.6. *Effect of radiation on intracellular ROS-RNS production detected by chemiluminescence.*  
Data are expressed as mean percentages of change from matched controls, taken as 100%  
Significant difference from control: \* $p<0.05$   
Significant difference from 2Gy: \*\* $p<0.01$

Examining the formation of superoxide anion by DHE revealed that the irradiated samples showed lower levels than the control ones since 2h pi whereas the presence of L-NAME significantly enhanced the superoxide anion levels up to 2h pi. These changes suggest that the early generation of NO could be scavenging the superoxide anion resulting in peroxynitrite production.( Fig 7 ).

When it was examined the time dependency of hydrogen peroxide levels by DCF staining it was found that the irradiated cells had lower levels than control ones during the first two hours pi and the inhibition of NO production did not change the pattern. By 4h pi, the addition of L-NAME resulted in a small but detectable increase (Fig. 8). These results suggest that in the early phase, the superoxide anion is not being converted to hydrogen peroxide by superoxide dismutase (SOD).



**FIG.7.** Time course of DHE fluorescence intensity following irradiation.  
**A:**Control, **B:**2Gy, **C:**2Gy+0.5mM L-NAME  
Significant difference from control: \* $p<0.05$   
Significant difference from 2Gy: \*\* $p<0.05$

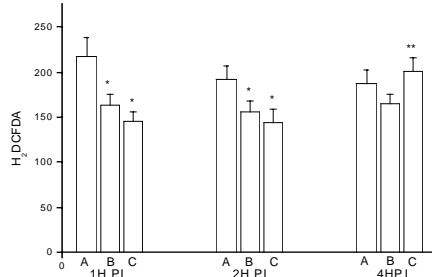


**FIG.8.** Time course of H<sub>2</sub>DCFDA fluorescence intensity following irradiation.  
**A:**Control, **B:**2Gy, **C:**2Gy+0.5mM L-NAME  
Significant difference from control: \* $p<0.05$   
Significant difference from 2Gy: \*\* $p<0.05$

Taken together these results indicate that NO and superoxide anion are the main species playing a role in the oxidative status of precursor neural cells in the firsts hours following irradiation. As it has been reported that caspase activation during the apoptotic process may lie on a pathway leading to generation of ROS [23] the effect of zDEVD-fmk a caspase inhibitor was tested..

Interestingly, zDEVD-fmk prevented the increase of reactive species induced by radiation since 2h pi (Fig. 6).

#### 4. Discussion

The effects of ionising radiation on cellular response systems are mediated through the interaction of radicals and reactive oxygen and nitrogen species. In this study, our goal was to investigate the relationship between oxidative stress, and endogenous NO production in the radiation induced early signalling related with programmed cell death in a cortical precursor cell cultures model, irradiated with Gamma radiation.

Within the complex network of cell signals elicited by ionising radiation the cell pathway controlling cell survival has a key role.

Our present results revealed that following 2 Gy of Gamma irradiation, the augmentation of the apoptotic fraction was already present at 4 h reaching the maximum at 24 h pi. This pattern could be related to the fact that as it has been reported, Gamma radiation is able to induce an early increased level of p53 protein and a down-regulation of IGF-I levels in cells cultures from developing brain as well an in vivo models which could lead to cell death by apoptosis. [29,30]

Moreover, we have previously shown in an in vivo model of prenatal irradiation of developing brain an early augmentation in nNOS activity that correlates with a further increase in NO steady-state concentration with antioxidant effects [19].

NO is a free radical and, hence, has a relative short half-life due to its reactivity with other intracellular constituents [31]. Likewise, NO is able to react and scavenge highly reactive oxygen species i.e, superoxide anion ( $O_2^-$ ) and Hydroxyl radicals ( $OH^-$ ) and converts them into

non radicals such nitrites and nitrates [32]. In physiological systems such nitrate is the major NO-derived metabolite. [33].

We observed in this in vitro model a significant increase of Nitrite/Nitrate concentration that was evident from 30 min p.i. to 6 h pi and whose time- dependent accumulation might result from their stability in vitro systems [34]. Since this finding is the indirect evidence of the augmentation of NO production and that on the other hand, the oxidative status assessed by QL showed significant decreased levels up to 60 min after irradiation, our results suggest that NO could have in this in vitro model, a neuroprotective role early after irradiation.

A transient generation of reactive ROS/RNS within few minutes after irradiation has been demonstrated in several systems [35]. While it is reasonable to assume that, these reactive species are generated from the primary ionizations events and according to several reports the hydroxyl radical would be the major component [36], secondary ROS products are also generated in latest time-points as a consequence of extranuclear amplification mechanisms, particularly superoxide anion and hydrogen peroxide [37].

Incubations with L-NAME and SOD allowed to demonstrate the increased production of the  $O_2^-$  performed by dihydroethidium, a fluorescent dye sensitive to superoxide anion, up to 2 h pi .in the irradiated sample. Then, it is possible to conclude that during the early phase of the response, the radiation-induced generation of endogenous NO is responsible of the scavenger effect on the  $O_2^-$ .

Similarly, incubation with L-NAME was able to modify the apoptotic response in the irradiated samples by increasing significantly the apoptotic levels 24 h post-irradiation.

It has been described that low at moderates levels of NO can increase  $O_2^-$  and  $H_2O_2$  production by inhibiting mitochondrial respiration, whereas at high level it inhibits  $H_2O_2$  production by scavenging the precursor superoxides [38]. In our experiments incubation with L-NAME seems do not modify the low level of  $H_2O_2$  found at early times in the irradiated sample related with its control ones. The difference between the increase of  $O_2^-$  and the decrease of  $H_2O_2$  might reflect the activity of peroxidases such as glutathion peroxidase.

In a previous work we have demonstrated a dose-dependent radiation induced activation of caspase-3 detectable by 2 h pi. and showing a peak at 4 h coinciding with the beginning of the apoptosis [22].

In this sense , the later increase of ROS is coincident with the augmentation of the Caspase.-3 activity . The efficacy of caspase inhibitor zDEVD-fmk to reduce the free radicals production in our experiment suggest the possibility that this secondary burst of ROS production would be directly dependent of the caspase-3 activation. These results are consisting with those communicated by Chen et al. [39]. Likewise it has been described a two-step process for cyt c release during radiation-induced apoptosis and a link between ROS production and mitochondrial cyt c depletion. This fact could explain the coincidence observed between the start of the apoptotic process and the late ROS burst.

GSH is the most abundant thiol in cells that can protect them from oxidative stress damage by scavenging peroxides in the cytosol and mitochondria [40]. The oxidative stress could lead to GSH consumption, which is also a major oxidant signal for apoptosis . Using incubations with NAC 24 h prior irradiation we have shown a significant decreased level of apoptosis at 24 h postirradiation , suggesting again that ROS are playing a relevant role in modulating the early signaling system that lead to programmed cell death. Although DCF has a high affinity for  $H_2O_2$  the exact nature of the ROS depicted by DCF in our experiment will need further confirmation. Nevertheless it is possible to assume that  $H_2O_2$  is the mean component in the late ROS burst, considering the potential intracellular GSH depletion and the inhibitory effect of NO on catalase activity. [38]

In conclusion, in vitro irradiation of neural precursor cells allowed us to demonstrate that, consisting with previous results obtained in an in vivo model, there is an early radiation-induced increased generation of NO exerting neuroprotector properties. In addition we found that ROS/RNS are able to modulate the apoptotic response and, at least in part, caspase-3 is responsible to the late ROS burst.

## 5. References

- [1] Hays, S.R., Xuelin, L., Kimler, B.F., *Is there adaptative response to radiation in the developing brain of the fetal rat?* Radiat Res 136: 293-296 (1993)
- [2] Dimberg, Y., Tottmar, O., Aspberg, A., et al. *Effects of low-dose X-irradiation on mouse-brain aggregation cultures.* Int J of Radiat Biol 66 : 793-800.(1992)
- [3] Radiation Protection. Commision of the European Communities Report EUR 8067 *Effects of prenatal irradiation with special emphasis on late effects.* (1984)
- [4] International Commission on Radiological Protection. ICRP *Developmental Effects of Irradiation on the brain of the embryo and Fetus*, . edited for Pergamon Press.Oxford and New York. (1986)
- [5] Kimler,B.F.,. *Prenatal irradiation : a major concern for the developing brain.* Int J Radiat Biol 73 (4) : 323-434. (1998);
- [6] Reyners ,H., Gianfelici de Reyners, E., Poortmans, F., et al. *Brain atrophy after foetal exposure to very low doses of ionizing radiation.* Int J Radiat Biol 62: 619-26 (1992)
- [7] Konermann, G.,. *Postnatal brain maturation damage induced by prenatal irradiation : modes o effects manifestation and dose-response relations.* In Low Doses radiation: Biological Bases of Risk assessment, edited by Baverstock KF and Stather JW (London: Taylor & Francis): 364-376. (1989)
- [8] Ferrer, I., Soriano, E., Martí, E., Laforet, E., Reyners, H., Gianfelici de Reyners, E., *Naturally occurring postnatal cell death in the cerebral cortex of the micrencephalic rat induced by prenatal X-irradiation.* Neuroscience Research.; 12: 446-451. (1991)
- [9] Guelman, L.R., Zieher, L.M., Rios, H., Mayo, J., and Dopico, A.M., *Motor abnormalities and changes in noradrenaline content and the cytoarchitecture of developing cerebellum following X-irradiation at birth.* Molecular and Chemical Neuropathology; 20: 45-57. (1993)
- [10] Sienkiewicz, Z.J., Haylock, R.G., and Saunders RD. *Prenatal irradiation and spatial memory in mice: investigation of dose- response relationship.* Int J Radiat Biol; 65: 611-618. (1994)
- [11] Sienkiewicz, Z.J., Haylock, R.G., and Saunders, R.D., *Differential learning impairments produced by prenatal exposure to ionizing radiation in mice.* Int J Radiat Biol; 75: 121-127. (1999)
- [12] Takanori, M., Yoshihiro, F., Yoshiaki, T., and Masahiro, I., *A quantitative study of the effects of prenatal X-irradiation on the development of cerebral cortex in rats.* Neuroscience Research; 23: 241-247. (1995)
- [13] Fushiki, S., Matsushita, K., Yoshioka, H., and Schull, W.J., *In utero exposure to low-doses of ionizing radiation decelerates neuronal migration in the developing rat brain.* Int J Radiat Biol; 70: 53-60. (1996)
- [14] Mishra, O.P., Fritz, K.I., Delivoria-Papadopoulos, M., *NMDA receptor and neuronal hypoxic brain injury.* Ment Retard Dev D R; 7: 249-253. (2001)
- [15] Schmidt-Ullrich, R.K., Dent, P., Grant, S., Mikkelsen, R.B., Valerie K. *Signal transduction an cellular radiation responses.* Radiat Res 153: 245-257. (2000)
- [16] Mohanakumar, K.P., Thomas, B., Sharma, S.M., et al . *Nitric oxide an antioxidant and neuroprotector .* Ann NY Acad Sci. 962 : 389-401.(2002)
- [17] Rauhala, P., Khaldi, A., Mohanakumar, K.P., Chiueh, C.C., *Apparent role of hydroxyl radicals in oxidative brain injury induced by sodium nitroprusside.* Free Radic Biol Med 24 (7/8) 1065-1073. (1998)
- [18] Kim, P.K.M., Zamora, R., Petrosko, P., Billiar, T.R., *The regulatory role of nitric oxide in apoptosis.* International Immunopharmacology; 1: 1421-1441. (2001)
- [19] Gisone, P., Boveris, A.D, Dubner, D., Perez, M.R., Robello, E., Puntauro, S., *Early neuroprotective effect of nitric oxide in developing rat brain irradiated in utero.* Neurotoxicology 182: 1-9.(2002)
- [20] Ferrer, I., Serrano, T., Alcántara, S., Tortosa, A., and Graus, F., *X-ray induced cell death in the developing hippocampal complex involves neurons and requires protein synthesis.* Journal of Neuropathology and Experimental Neurology; 52: 370-378. (1993)

- [21] Borovistkaya, A.E., Evtushenko, V.I., Sabol, S.L., *Gamma-irradiation-induced cell death in the fetal rat brain possesses molecular characteristics of apoptosis and is associated with specific messenger RNA elevations.* Mol Brain Research; 35: 19-30. (1996)
- [22] Michelin, S., Perez, M.R., Dubner, D., et al . *Increased activity and involvement of caspase-3 in radiation-induced apoptosis in neural cells precursors from developing rat brain.* Neurotoxicology (in press)
- [23] Lievre, V., Becuwe, P., Bianchi, A., et al . *Free radical production and changes in superoxide dismutases associated with hypoxia/reoxygenation-induced apoptosis of embryonic rat forebrain neurons in culture.* Free radical Biology & Medicine.; 29: 1291-1301. (2000)
- [24] Flint, O.P., *A micromass culture method for rat embryonic neural cells.* J.Cell. Sci., 61:247-262, (1983)
- [25] Piñero, J., López-Baena, M., Ortiz, T., Cortez, F., *Apoptotic and necrotic cell death are both induced by electroporation in HL60 human promyeloid leukaemia cell.* Apoptosis 2: 214-220, (1998)
- [26] Darzynkiewicz, Z., Juan, G., Li, X., Gorczyca, W., Murakami, T., Traganos, F., *Cytometry in cell necrobiology: analysis of apoptosis and accidental cell death 8 necrosis.* Cytometry 27:1-20, (1997).
- [27] Verdon, C..P., Burton, B., Prior, R.,. *Sample pretreatment with nitrate reductase and glucose-6-phosphate dehydrogenase quantitatively reduces nitrate while avoiding interference by NADP<sup>+</sup> when the Griess reaction is used to assay for nitrite.* Annal..Biochem., 224:502-8, (1995)
- [28] Satoh, T., Numakawa, T., Abiru, Y., Yamagata, T., Ishikawa, Y., Enokido, Y., Hatanaka, H. *Production of reactive oxygen species and release of L-glutamate during superoxide anion-induced cell death of cerebellar granule neurons.* J.Neurochem., 70:316-324, (1998) .
- [29] Bolaris, S., Bozas, E., Benekou, A., Philippidis, H., and Stylianopoulou, F.,: *In utero radiation-induced apoptosis and p53 expression in the developing rat brain.* Int J Radiat Biol; 77 (1) : 71-81. (2001)
- [30] Benekou, A., Bolaris, S., Kazanis, E., Bozas, E., Philippidis, H., and Stylianopoulou, F.,. *In utero radiation-induced changes in growth factor levels in the developing brain.* Int J Radiat Biol; 77 (1) : 83-93. (2001)
- [31] Stewart, V.C., and Healles, S.J.R.,. *Nitric oxide-induced mitochondrial dysfunction : implications for neurodegeneration.* Free Radical Biology & Medicine. 34 : 287-303. (2003)
- [32] Chiueh, C.C., *Neuroprotective properties of Nitric Oxide.* Annals NY Academy of Sciences, 890 :301-311. (1999)
- [33] Grisham, M.B., Johnson, G.G., Lancaster, J.R., *Quantitation of nitrate and nitrite in extracellular fluids.* Methods Enzymology; 268: 237-246. (1996)
- [34] Moshage, H., *NO determination: Much Ado about NO thing?* Clinical Chemistry 43: 553-556. (1997).
- [35] Schmidt-Ullrich, R.K., Dent, P., Grant, S., et al *Signal transduction and cellular radiation responses.* Rad Res, 153: 245-257. (2000)
- [36] Leach, J.K., Van Tuyle, G., Lin, P.S., et al . *Ionizing radiation-induced, mitochondria-dependent generation of reactive oxygen/nitrogen.* Cancer Res 61 : 3894-3901.(2001)
- [37] Narayanan,P., Goodwin, E., and Lehnert, B., . *Alpha particles initiate biological production of superoxide anions and hydrogen peroxide.* Can Res. 57 : 3963-3971 (1997)
- [38] Brown, G.C., and Borutait, V., *Nitric Oxide, Mitochondria, and cell death.* IUBMB; 52:189-95. (2001)
- [39] Chen, Q., Chai, Y.C., Mazumder, S., et al . *The late increase in intracellular free radical oxygen species during apoptosis is assosciated with cytochrome c release, caspase activation and mitochondrial dysfunction.*; Cell death differentiation 10: 323-334. (2003)
- [40] Boehringer,D.W.,*Bcl-2 and glutathione: alterations in cellular redox state that regulate apopotosis sensitivity .* Free Radic Biol Med . 27:945-950. (1999)

# The ARN Critical Dosimetry System

Gregori, B.N.; Papadópolos, S.; Cruzate, J.A.;  
Equillor, H.E. and Kunst, J.J.



# THE ARN CRITICAL DOSIMETRY SYSTEM

Gregori, B.N.; Papadópolos, S.; Cruzate, J.A.; Equillor, H.E. and Kunst, J.J.

Autoridad Regulatoria Nuclear  
Argentina  
bgregori@cae.arn.gov.ar

## Abstract

The ARN critical dosimetry system is shown in this work. It includes personal and area dosemeters, and the information of typical spectra. The spectra of the critical facilities in our country are characterised by measurements with our Bonner Sphere System (BSS) or by computational methods in order to evaluate the dose in each case with the actual spectrum. The personal and area dosemeters are able to evaluate the gamma and neutron contributions. The detectors used are thermoluminescents, (TLD)  $^{7}\text{Li}:\text{Mg},\text{Ti}$  for gamma and threshold detectors (Indium and sulphur pellets) and activation detectors Au (bare and Cd cover) for neutron. The Gamma-ray spectrometry is made with GeHp and MCA (Canberra) calibrated with  $^{133}\text{Ba}$  and  $^{137}\text{Cs}$  sources. The Beta-ray counting is made with a Geiger Muller (LND)(8%) with an electronic counter prototype developed in Argentina. The system is calibrated with the tioacetamida-technique carried out in our chemistry laboratory. The TLD are calibrated in Argentine SSDL with  $^{60}\text{Co}$  source, free in air. The calibration curve has been extended up to 10Gy. The neutron fluence distribution is obtained considering the thermal region as a Maxwellian distribution with a modal energy of 0.0253 eV and the intermediate region with a 1/E spectrum from 0.5 eV to E=200 keV. The basic data are the measured activities in the gold foils. The fast neutron fluence is calculated considering the mean cross section for the selected spectrum over the energy range. The basic data are the measured activities in indium foil and sulphur pellets with threshold energy of 1.7MeV y 2.5MeV respectively. The neutron kerma dose, the recoil charged particle dose and the contribution of the  $^{1}\text{H}(\text{n}, \gamma)^{2}\text{H}$  dose component, are calculated applying the dose conversion factors published in TRS211. The area dosimeter gives the gamma incident radiation kerma, and the personal dosimeter, the gamma total dose. This system has participated at the International Intercomparison of Criticality Accident Dosimetry Systems at Silene Reactor in 2002, showing a good performance.

## 1. Introduction

Critical accident dosimetry is required to screen and provide a rapid personnel dose assessment following a criticality accident. For this requirement specific techniques are used to determine both neutron and gamma contributions of the acute radiation dose to the body.

In order to evaluate the dose in a critical accident the Physical Dosimetric Group (PDG) of Nuclear Regulatory Authority has elaborated a procedure to attend the situation based on international recommendations and its own experience. PDG has developed a critical dosimetric system, (SDC), personal and area dosemeters, and is still working in the neutron spectrum facility characterisation using the Multisphere Spectrometric System (MSS).

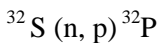
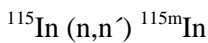
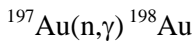
In this framework the performance of the system was evaluated in the International Intercomparison of Criticality Accident Dosimetry Systems at Silene in Valduc (France). The objectives were to test and evaluate the SDC under realistic conditions in order to establish the dose-assessment performance for different quality radiation fields (different neutron spectra and neutron to gamma dose ratios).

## 2. Dosimetry System

The SDC ( personal and area dosemeters ) has gamma and neutron detectors.  
The gamma-ray dosimeter is based on TLD,  $^{7}\text{Li}:\text{Mg},\text{Ti}$  (TLD-700, Bicron).

The neutron dosimeter is based on activation detectors: gold foil (bare and Cd covered), and threshold indium foil and sulphur pellet.

The reactions considered are:



The main characteristics of the activation detectors used are showed in the Table 1:

**Table 1:** Components of Activation Detectors

COMPONENTS OF ACTIVATION DETECTORS			
Material detector	Mass (g)	Isotopes to be measure	Energy (MeV)
Gold (bare)	0.05	$^{198}\text{Au}$	$(\gamma) 0.412$
Gold (Cd)	0.05		
Indium	0.2	$^{115m}\text{In}$	$(\gamma) 0.336$
Sulphur	1.08	$^{32}\text{P}$	$(\beta) 1.7$

The foils have a thickness of 0.02 mm and a diameter of 12 mm, meanwhile the pellets dimension is 0,04 mm and 16mm respectively.

### 3. Measurements procedures

The gamma-ray spectrometry is made with a GeHp and a MCA (Canberra). The system is calibrated with  $^{133}\text{Ba}$  and  $^{137}\text{Cs}$  sources.

The beta ray counting is performed with a Geiger Muller (LND) with an 8% efficiency. It works with an electronic counter and associated software (NuclearLab) [1]. The system is calibrated with the tioacetamida technique, improved in Argentine [2].

The gamma-ray dosimeters are processed in a TLD reader, Bicron-Harshaw 3500QS. The detectors are calibrated in the Argentine Secondary Standard Dosimetry Laboratory with a  $^{60}\text{Co}$  source, free in air. The calibration curve has been extended up to 10Gy.

### 4. Evaluation procedure

In order to obtain the neutron fluence distribution, the following assumptions were made:

- For thermal and intermediate-energy fluences assessment, a Maxwellian distribution has been chosen: with a modal energy of 0.0253 eV for thermal, with a  $1/E$  spectrum for the intermediate-energy region from 0.5 eV ( $E_{\text{Cd}}$ ) to  $E_2$  (200 keV),.

The measured activities in the gold foils, bare ( $A_{\text{Au}}$ ) and under cadmium ( $A_{\text{AuCd}}$ ), are converted into incident fluence as shown below [3]:

Thermal fluence:

$$\phi_{th} = \frac{1.13}{\lambda N \sigma_0} [A_{Au} - A_{AuCd}] \quad (1)$$

Intermediate fluence:

$$\phi_{int} = \Phi_{epi} \ln(E_2 / E_{Cd}) \quad (2)$$

$$\Phi_{epi} = \frac{A_{AuCd}}{\lambda N RI} \quad (3)$$

Where,  $\lambda$  is the decay constant for  $^{198}\text{Au}$ ;  $N$  is the number of Au atoms;  $\sigma_0$  is the cross-section of gold at 2200 m/s; RI is the resonance integral from  $E_{Cd}$  to  $E_2$ .

- For fast neutron fluence distribution it is necessary to make several assumptions or to measure previously the critical facility characteristic spectrum. The spectra of several Argentine critical facilities have been measured with the MSS [4].

The basic data is obtained from indium foil and sulphur pellets with threshold energy of 1.7 and 2.5MeV respectively.

The following expression is used to calculate the fast neutron fluence

$$\phi_{E > E_{act(i)}} = \frac{A_{(i)}}{\lambda N \langle \sigma \rangle_{i(E > E_{act(i)})}} \quad (4)$$

Where i means indium or sulphur reactions;  $A(i)$  is the activity,  $E_{act(i)}$  is a  $i$ - threshold energy and  $\langle \sigma \rangle_{i(E > E_{act(i)})}$  is the mean cross section of  $i$  for the selected spectrum till  $E_{act(i)}$ .

The theoretical calculation of the apparent cross section,  $\langle \sigma \rangle_{i(E > E_{act(i)})}$  for a given neutron reaction, is obtained solving the following expression:

$$\langle \sigma \rangle_{i(E > E_{act(i)})} = \frac{\int_{E_{min}}^{E_{max}} \phi(E) \sigma(E) dE}{\int_{E_{min}}^{E_{max}} \phi(E) dE} \quad (5)$$

Where  $\phi(E)$  is the differential fluence of the particular spectrum selected and the neutron energy  $E$  ranges between energy points of interest.

The total neutron fluence is calculated considering the apparent cross section of the reaction  $i$  for the selected spectrum over all the energy range.

#### 4. Dose assessment

The gamma dose is calculated as:

$$D_\gamma = L(nC) . S(nC/Gy) . S_k \quad (6)$$

Where  $L$  (nC) is the net TLD reading;  $S$  (nC/Gy) is the  $^{60}\text{Co}$  calibration factor in free air and

$S_k$  is the individual sensitivity factor.

The net TLD readings have been also corrected for fast neutron influence [3]. The personal dosimeter gives the gamma total dose ( $K\gamma$ , backscatter component and  $^1H(n, \gamma)^2H$ ), corrected by the tissue energy-mass absorption coefficient ratio.

The area dosimeter gives the gamma incident radiation kerma,  $K\gamma$ .

The thermal and intermediate neutron dose is calculated as follow [3]:

$$\begin{aligned} \text{Thermal neutron dose, } & D_{th} = 5,8 \cdot 10^{-13} \phi_{th} \\ \text{Intermediate neutron dose, } & D_{int} = 1,18 \cdot 10^{-12} \phi_{int} \\ & = 1,55 \cdot 10^{-11} \Phi_{epi} \end{aligned} \quad (7)$$

Where  $\phi_{th}$  is the total neutron fluence,  $\phi_{int}$  is the total intermediate fluence and  $\Phi_{epi}$  is the fluence per unit lethargy, assumed to be constant over this energy region.

In order to calculate the neutron kerma dose, the recoil charged particle dose and the  $^1H(n, \gamma)^2H$  dose components in all the energy range, the dose conversion factors are obtained from the selected spectrum. The dosimetric quantities are calculated by:

$$D = \frac{\int d_k(E) \phi(E) dE}{\int \phi(E) dE} \quad (8)$$

Where  $d_k$  is a fluence to dose conversion factor [3] and  $\phi(E)$  the total fluence .

## 5. Intercomparison

The performance of the system was evaluated in the International Intercomparison of Criticality Accident Dosimetry Systems in the Silene Reactor (Valduc, France) in 2002.

During the exercise, the participants determined with their dosimeters, for each pulse, both gamma and neutron components of the dose, giving a first data. These evaluation results were informed to the organisers to compare with those given by the other participants.

The Silene staff was in charge of positioning the participants dosimeters. The area dosimeters were located in free air, and the personal dosimeters were on an anthropomorphic phantom. Both were located on 4m arc from the reactor at 1.2m height

The experience consist of three independent irradiations, two were free evolutions with bare and lead shield reactor configurations respectively and another one was a steady evolution with a lead shield reactor configuration.

After the irradiation, the dosimeters were stored until the rate exposition was low enough to manipulate them according with the international radiology protection recommendations

The SDC results were obtained in 24 hours. The data request were not only dose quantities but also reaction rates per atoms.

The gamma-ray spectrometry and beta measurements were made in Valduc with our equipment, but the TLD were processed with a Harshaw Bicron 3500QS that belongs to Canada group . The TLD used for gamma calibration were carried from Argentina.

In order to evaluate the total neutron dose, the Silene spectrum reactor was selected from published data [5]. The assessment was made considering the mean spectrum resulting from experimental spectra determined by National Physical Laboratory (NPL), Fontenay-aux-Roses (ISPN) and Harwell (AEA Technology). The specific neutron reactions analysed were those related to the criticality detectors used at measurements. The reference measurements were made under free air condition. However, the neutron

measurements are expressed, not only in terms of neutron kerma ( $K_n$ ) appropriate to free air conditions, but also in terms of the dose recoil charged particle and the  $^1H(n,\gamma) ^2H$  component of the dose appropriate to dosimeters exposed on the front of the phantom. Because of that, the calculation of the apparent values of these quantities was made applying formula (8).

The components thermal and intermediate of the dose were evaluated applying equation [7].

The table 2 shows the dosimetric results to the reference data ratio [6] for each pulse and reactor configuration.

**Table 2:** Performance of the ARN Critical Dosimetric System in the International Intercomparison of Criticality Accident Dosimetry Systems in Silene Reactor

	Quantities	Bare - Free evolution	Lead - Steady state	Lead - Free evolution
		ARN / reference	ARN / reference	ARN / reference
Area Dosemeter	neutron kerma	1,16	1,01	1,02
	neutron recoil dose	1,17	1,01	1,03
	neutron $^1H(n,\gamma) ^2H$	0,85	0,78	0,82
	incident $\gamma$ dose	0,80	1,66	1,57
Personal Dosemeter	neutron kerma	1,30	1,03	1,08
	neutron recoil dose	1,30	1,01	1,08
	neutron $^1H(n,\gamma) ^2H$	0,94	0,81	0,86
	total $\gamma$ dose	0,84	1,06	1,00

Same methods have been used in measurement, calculations and conversion factor to evaluate area and personal dosimeters.

For the lead shielded configurations, there is good agreement between the neutron kerma and neutron recoil dose values to the reference values , better than 10%, for both area and personal dosimeter.

For the bare configuration, the neutron kerma and neutron recoil dose measured by the area dosimeter agrees with the reference better than 20%., meanwhile the personal dosimeter over measured the neutron kerma and the neutron recoil dose, with no further explanation yet.

In the case of lead reactor configurations, the incident gamma dose is over evaluated. The published results [7] show that the ratio of the mean value of the laboratories to the reference are  $1,73 \pm 0,4(1\sigma)$ in steady state and  $1,57 \pm 0,46(1\sigma)$ in free evolution, and the Argentine data are included in those ranges. These results show the difficulties of measuring the gamma-ray dose in mixed fields with lead shield configurations.

There is a good agreement in the measurement of total gamma-ray dose (better than 20%).

The thermal and intermediate contributions to the total neutron dose were less than 12%.

## 6. Conclusions

The DCS showed a good performance in the intercomparison not only about the evaluation results but also in the capability of giving them in a short time. The dose given at the Valduc meeting was about 5% higher than the final reported results.

The DCS response is strongly dependent of the spectrum selected, variation between the facility spectra obtained by different method influenced both the cross section and the dose calculation.

As the Silene spectrum is fission one, the best detector to evaluate the neutron dose is based on the Indium reaction.

The DCS assessment method can be applied even though one of the activation measurements (indium or sulphur reactions) failed because it is a redundant methodology.

In this exercise, as the thermal and intermediate dose components do not contribute significantly, the performance in terms of the dose has not been analysed.

Performance criteria for criticality accident dosimetry systems recommended for doses greater than 250mGy [5] that the neutron and gamma components of dose uncertainties should be less than  $\pm 25\%$  each.

If it assume that the true dose is given by the reference dose ( $\pm 10\%$ ) then the data evaluated satisfy the criteria except in the case of lead configuration - incident gamma kerma and of bare configuration-personal neutron dose.

## 7. Acknowledgments

We want to thanks the help giving by the Silene Staff to solve the equipment problems and to Dr, Louise Prud'Homme-Lalonde (Canada) that lets us used their TLD reader.

## 8. Bibliography

- 1- NuclearLab . *Counter NLA-003*. Technical Report.. Argentina (2002).
- 2- Equillor, H; Papadópolos, S; Gregori, B., *Activity determination of  $^{32}\text{P}$  in sulphur critical dosimeters by liquid centelleo*. IRPA , Lima- Perú (2002).
- 3- International Atomic Energy Agency. *Dosimetry for Critical Accident*. Technical Reports Series No. 211, Vienna, 1982.
- 4- Gregori, B., Papadópolos, S., Cruzate J.A., Kunst, J.J., *Multisphere Neutron Spectrometric System With Thermoluminescent Detectors: Sensitive Improvement*. Rad. Prot. Dos. Vol 101, Nos 1-4, pp133-136 (2002).
- 5- Medioni, R., Delafield H.J., *An International Intercomparison of Criticality Accident Dosimetry Systems at the Silene Reactor*, Report HPS/TR/H/3(95), Valduc, Dijon, France, 7-18 June 1993.
- 6- Asselineau, B., Trompier, F., Texier, C., Itié, C., Medioni, R., Tikunov, D., Muller, H., Pelcot, G., *Reference Dosimetry Measurements For The International Intercomparison Of Criticality Accident Dosimetry*, Ninth Neutron Dosimetry Symposium. The Netherlands. 2003.
- 7- Medioni, R., Asselineau, B., Verrey,B., Trompier F., Itie, C., Texier, C., Muller H., Pelcot, G., Clairand, I., Jacquet X., and. Pochat, J.L., *Criticality Accident Dosimetry Systems. An International Intercomparison At The Silene Reactor*, Ninth Neutron Dosimetry Symposium. The Netherlands. 2003.

# Conceptual Analysis of the Fuel Management Strategy for the RA-3 Research Reactor at 10 MW

Lerner, A.M.; Madariaga, M.R. and Waldman, R.M.



# **CONCEPTUAL ANALYSIS OF THE FUEL MANAGEMENT STRATEGY FOR THE RA-3 RESEARCH REACTOR AT 10 MW**

Lerner, AM.; Madariaga, M.R. and Waldman, R.M.

Nuclear Regulatory Authority  
Argentina

## **ABSTRACT**

The Argentine Research Reactor RA-3 was designed to produce radioisotopes and it operates with LEU ( $U_3O_8$ ) fuel since 1990. Its initial power was 5 MW and it has recently been upgraded to 10 MW. The National Atomic Energy Commission (CNEA) is both its owner and operator.

At the beginning of this year, the Nuclear Regulatory Authority extended its operation license to an authorised power of 10 MW after a series of modifications and tests carried out by the installation during 2002 and 2003.

As a consequence of this power increase, the installation introduced some non-systematic modifications in its fuel management strategy with the purpose of preserving the operation period in 20 days approximately. The main change was to load 2 fuel elements per cycle in some cycles (instead of 1 as it used to be at 5 MW).

The purpose of this work is to perform a conceptual analysis of possible fuel management strategies for the RA-3 reactor, that could provide quantitative elements for a safety assessment, as well as to evaluate the fuel management flexibility at 10 MW in compliance with standards in force.

It is concluded that operation at 10 MW with a 2 FE/cycle strategy leads to a significant excess reactivity at the beginning of cycle, but still in compliance with the margins established by the standards of application.

## **1. Introduction**

The Argentine Research Reactor RA-3 was designed to produce radioisotopes and it operates with LEU ( $U_3O_8$ ) fuel since 1990. Its initial power was 5 MW and it has recently been upgraded to 10 MW. The National Atomic Energy Commission (CNEA) is both its owner and operator.

At the beginning of this year, the Nuclear Regulatory Authority (ARN) extended its operation license to an authorised power of 10 MW after a series of modifications and tests carried out by the installation during 2002 and 2003.

As a consequence of this power increase, the installation introduced some non-systematic modifications in its fuel management strategy with the purpose of preserving the operation period in 20 days approximately. The main change was to load 2 fuel elements per cycle in some cycles (instead of 1 as it used to be at 5 MW).

The purpose of this work is to perform a conceptual analysis of possible fuel management strategies for the RA-3 reactor, that could provide quantitative elements for a safety assessment, as well as to evaluate the fuel management flexibility at 10 MW in compliance with standards in force.

The installation has already submitted documents [1] showing that the reactor can operate at 10 MW, with, for example, a 1 FE/cycle strategy, similar to that used at 5 MW. In other words, it is already demonstrated that the reactor is operable at 10 MW. We are here only interested in analysing the limitations that this upgraded power may impose on the fuel management, and particularly the feasibility of changing to a permanent 2 FE/cycle strategy.

As concerns the core safety, the two interesting items related to fuel management are: compliance with reactivity safety margins and limitation of the power peaking factor (PPF smaller than 3.5 for the present configuration with 25 FE).

According to the corresponding thermal-hydraulic analysis [2], the improvements carried out in the cooling circuit are such that the power upgrade from 5 to 10 MW does not require a modification of the maximum power peaking factor (PPF) allowed. Therefore, if no increase of the actual core PPF occurs, the safety margin that guarantees the correct fuel element cooling will not decrease. The actual PPF value can change as a consequence of a change in the burnup distribution, or because the control rods will be more inserted due to the increase of the beginning of cycle (BOC) reactivity.

In several opportunities the RA-3 core was loaded with fuel elements containing more uranium mass than the standard, be the case of a  $U_3Si_2$  FE or 2 standard fresh FE in the same cycle. In every case the PPF was always smaller than 3.1 with an average value of 2.8. This shows that there is an adequate margin to the maximum value allowable of 3.5.

On the contrary, a new fuel strategy with a permanent loading of 2 FE/cycle, will undoubtedly lead to an increase of the BOC reactivity. Moreover, even without a change in the fuel strategy, the power upgrade from 5 to 10 MW implies a certain BOC reactivity increase. It is because of this fact that this paper mainly concentrates on the analysis of the compliance with reactivity safety margins.

## 2. Calculation model

The model chosen in order to carry out the conceptual analysis of different fuel management strategies is simple, and enables to achieve some general conclusions quite easily. It consists of a 5x5 grid without control rods. Except its central position, in which an irradiation box has been located, all the other positions are filled with standard fuel elements (SFE) of the  $U_3O_8$  type, giving a total of 24 FE. The fuel region is surrounded by a first annulus of graphite blocks and by a second outer annulus of a water reflector. The dimensions are those of the corresponding RA-3 reactor regions. A simplified graph is shown in Figure 1 as well as the refuelling chains used.

For the description of the FE in the reactor model, an explicit frame model was used.

For the 5 MW case, a usual cross section (XS) library generated with WIMS for all the involved materials was used [3]. This library is routinely used in the ARN for the RA-3 reactor calculations at that power. For the 10 MW case, only the XS for fuel and frames have been recalculated.

Based on this model the following working plan was proposed:

- a) Generate (macro)  $XS = f(Bu)$  with equilibrium Xe for 5 and 10 MW (**WIMS**)
- b) Prepare a simple reactor model with 24 FE and central irradiation box (**CITVAP**)
- c) Obtain equilibrium core for the standard previous conditions:  $P=5\text{MW}$ ,  $T=20\text{ days}$ , 1 FE/cycle. The end of cycle reactivity  $\rho_{EOC}$  thus obtained will be used as a reference value.
- d) Obtain new equilibrium cores changing 5 to 10 MW; 1 to 2 FE/cycle and matching  $\rho_{EOC}$  to the reference value previously obtained.

- e) Comparing  $\rho_{BOC}$  (c and d) obtain  $\Delta\rho_{BOC}$  due to the different effects.
- f) Using e extrapolate new values of  $\rho_{BOC}$  and analyse compliance with standards in force.

### **3. Effects on reactivity**

We will estimate the reactivity changes (BOC without xenon) due to the three effects described in what follows. We will consequently estimate the shut down margin decrease produced according to the results.

#### **3.1. Xenon effect**

Comparing theoretically the equilibrium BOC cores when the reactor is operating at 5 MW and 10 MW, with the same fuel shuffling strategy, particularly 1 FE/cycle, it may be concluded that:

The cycle length changes from a value of  $T_5$  to a new value  $T_{10}$ .

If no changes were produced due to xenon poisoning, it would result that  $T_{10} = 1/2 T_5$ . Thus, the FE would achieve exactly the same discharge burnup and burnup distribution in both cores would be the same. In that situation, the maximum reactivity value (BOC, cold without Xe) would be the same for both cases, 5 and 10 MW.

As Xe is not saturated at 5 MW, the reactivity loss due to Xe undergoes a certain increase (at 10 MW as compare with 5 MW).

If a fixed reference value for reactivity is considered at the EOC, the cycle length results somewhat smaller,  $T_{10} < 1/2 T_5$ . Therefore the average BOC core burnup is smaller and thus the maximum reactivity (cold without Xe) is increased.

#### **3.2. Modified fuel strategy (1 → 2 FE/cycle)**

A systematic strategy change from 1 FE/cycle to 2 FE/cycle preserving the strategy type (out → in or in → out, represented with the symbols OI o IO) enables, on one hand, to increase the cycle length significantly re-establishing a value  $T_{10} \approx T_5$ . Thus the average core burnup difference between BOC and EOC increases, therefore increasing the reactivity change during the cycle.

Again, as the EOC reactivity value is fixed, the maximum excess reactivity also increases.

#### **3.3. Modified fuel shuffling (OI → IO)**

We here refer to the effect produced when inverting the trajectory sense of the FE in the core (OI → IO). This effect is not too important but has been also analysed.

When the fresh FE are loaded into the core in its central region (IO), the BOC reactivity undergoes an increase as compared with the equivalent OI strategy.

### **4. Calculations and results**

Using the program CITVAP, the equilibrium state was found for the core described, operating at 5 MW, with a cycle length fixed in 20 days, corresponding to an average

actual cycle length. For such equilibrium condition the BOC and EOC reactivity values were calculated. Some graphite blocks surrounding the fuel region were eliminated in order to achieve a not so high EOC reactivity for the hot, non-Xe state ( $\rho_{EOC}$ ).

Although the value obtained  $\rho_{EOC} = 2052.6$  pcm is not the actual EOC reactivity (near to 1000 pcm), this value is useful as a reference to define the comparison criterion with other cycles. Independently of the fuel management strategy and/or the power at which the reactor is operating, the core should always provide the same EOC reactivity reserve in order not to penalise the irradiation capacity of the installation. Therefore, it will be considered an imposed condition to have  $\rho_{EOC} = 2052.6$  pcm in the new cycles with modified power or fuel strategy.

Several strategies were then analysed, varying the number of FE discharged per cycle, the type of strategy and the power, adjusting the cycle length in order to obtain  $\rho_{EOC} = 2052.6$  pcm for every case.

Two basic variations were considered as concerns the number of FE discharged per cycle:

- 1 FE/cycle
- 2 FE/cycle

and two different types of strategy for each case:

- From the outer region to the inner one (**OI**)
- From the inner region to the outer one (**IO**)

Table 1 shows the general results obtained with CITVAP for the BOC and the EOC reactivities in different situations.

The Xe reactivity worth for all the analysed situations was approximately 2830 pcm at 5MW, and some 3250 pcm at 10 MW.

The BOC reactivity increase for the hot, non-Xe state due to each of the analysed changes is shown in Table 2. As a consequence of the fact that the temperature effect is essentially the same for 5 and 10 MW, the previous results also correspond to the BOC reactivity increase for the cold non-Xe state.

It is noticed that an increase from **5 to 10 MW**, and almost independently of the fuel management strategy, produces a BOC reactivity increase of some **330 pcm**.

If **2 FE** are discharged per cycle instead of **1**, the reactivity increases in about **650 pcm**, while a modification in the type of strategy from OI to IO produces an increment of at least **150 pcm** for each fresh FE loaded per cycle.

The actual fuel management strategy used in the reactor is not completely systematic, so that it is not possible to describe it clearly as belonging to the OI or the IO type, so that the values here shown should be considered only as a trend.

## 5. Estimation of the new shut down margins

Table 3 shows the excess reactivity, the reactivity worth of the safety rods, the shut down margin (SM) and the reactivity safety factor (RSF) for different situations. The corresponding values for 5 MW are representative of a typical core and were obtained as a conservative average of several actual configurations with greater excess reactivity, having smaller burnup values than the equilibrium ones. These values correspond to a cold non-Xe core with 6 mini-plates of approximately 1 g U<sub>235</sub> each, loaded at the central irradiation box.

The new operation margins for 10 MW were estimated by adding to the typical values for 5 MW, an increment of 330 pcm due to the Xe effect plus another 650 pcm due to

the change of fuel management strategy from 1 FE/cycle to 2 FE/cycle when corresponds.

As it may be noticed, for both the 1 FE/cycle and 2 FE/cycle fuel strategies, the margins established by the Argentinean Standards are by far fulfilled [4]. Even taking into account the approximations in the conceptual model used, it may be concluded that the operation at 10 MW does not impose a restriction on the type of fuel management strategy, at least for a 2 FE/cycle strategy.

Nevertheless, as it may be seen in Table 3, the condition of subcriticality with two control rods only (CR1+CR4), results preserved with difficulty. For the case of 1 FE/cycle, the shut down margin with only two rods  $SM_{(CR1 + CR4)}$  is only 170 pcm. For a 2 FE/cycle strategy, and in the most reactive condition with CR1 and CR2 inserted, the core is super-critic with a reactivity  $\rho_{CR1+CR4} = + 480$  pcm. It should be noticed that this reactivity is almost equal to the reactivity provided by the 6 mini-plates for  $^{99}\text{Mo}$  production.

The preceding values show that if a permanent 2 FE/cycle strategy is used at 10 MW, it is very probable that under certain circumstances, the pair CR1+CR4 could result insufficient to maintain the BOC core in a subcritical state. In such case, the first start up should be carried out decreasing the excess reactivity, for instance, withdrawing some graphite blocks of the reflector.

Another choice could be to replace (permanently) the pair of control rods defined as Safety and Compensating Rods (at present CR1 and CR4) by some other pair with greater reactivity worth.

For instance, the pair (CR2,CR4) is frequently more absorbing than the pair (CR1,CR4) being its reactivity worth between 200 and 900 pcm greater according to the burnup distribution. The drawback of using this pair (CR2,CR4) would be that during the first operation day with CR2 inserted, while the Xe is established, it will affect the neutron flux at the central irradiation box in a greater amount than CR1.

The pair (CR1,CR3) could also be chosen, being the one having the greatest reactivity worth for almost every core configuration. Such pair would result in an addition of approximately 1000 pcm or more to the shut down margin. The drawback of using this pair is that the flux perturbation on the central irradiation box would occur during the whole cycle. Symmetry would also be broken, although it is not a strict symmetry due the asymmetric flux distribution. Nevertheless, this could be solved moving the rods symmetrically.

## 6 Conclusions

It is concluded that the operation at 10 MW with both types of fuel management strategies, 1 FE/cycle and 2 FE/cycle, is completely compatible with the Argentinean Standards in force [1].

It is probable that the condition fixed by the reactor logic (CR2 and CR3 withdrawn while rising power), could not always be fulfilled for the BOC, cold, non-Xe core when loading two fresh FE per cycle. Although this is not an original regulatory requirement, it has been added by the installation into the mandatory documentation of the RA-3 reactor.

In view of the results obtained it would be convenient for the installation to define a long-term fuel strategy, loading 1 or 2 FE/cycle. If the second option were chosen, the installation should evaluate the actions to be followed in order to guarantee subcriticality during start up with the above mentioned two control rods withdrawn.

## **7 References**

- [1] Technical Report CNEA-CAB 047-023/02, "Simulation of a fuel management for the RA-3 reactor at 10 MW". O. Serra
- [2] CNEA.C.RCN.ITE.153, "Thermal-hydraulic analysis of the RA-3 reactor for its operation at 5 and 10 MW, with a configuration with 25 FE".
- [3] IT-571/2000. "New model for the follow up of the RA-3 reactor operation having a central irradiation device". A. M. Lerner - M. Madariaga. ARN.
- [4] Standard AR 4.2.2 and Regulatory Guide GR 4. ARN.

## 8. Tables

Power (MW)	Cycle length (days)	Nº FE / cycle	Strategy type	$\rho(\text{BOC})$ hot with Xe (pcm)	$\rho(\text{BOC})$ hot without Xe (pcm)	$\rho(\text{EOC})$ (pcm)
5	20	1	OI	2716.0	5562.8	<b>2052.6</b>
5	38.65	2	OI	3315.7	6149.7	2056.2
5	23.12	1	IO	2880.4	5715.8	2042.7
5	44.30	2	IO	3628.8	6442.6	2054.2
10	9.59	1	OI	2654.3	5911.5	2052.5
10	18.54	2	OI	3202.6	6460.1	2055.6
10	11.10	1	IO	2813.2	6062.5	2039.6
10	21.25	2	IO	3509.1	6750.8	2054.6

**Table 1.** BOC reactivity for the hot, with and without Xe core, and EOC reactivity for the 5 and 10 MW and two different fuel management strategies.

Cause of $\Delta\rho_{\text{BOC}}$ (cold, no Xe): →			
POWER	Refuelling strategy	$\Delta\rho_{\text{BOC}}$ (pcm)	
5 → 10 MW (Xe increase)	1 FE/cycle	OI	348.7
		IO	346.7
	2 FE/cycle	OI	310.4
		IO	308.2
5 MW	1 → 2 FE/cycle	OI	586.9
		IO	726.8
	1 FE/cycle	OI → IO	153.0
	2 FE/cycle		292.9
10 MW	1 → 2 FE/cycle	OI	548.6
		IO	688.3
	1 FE/cycle	OI → IO	151.0
	2 FE/cycle		290.7

**Table 2.** BOC reactivity increase for the cold, non-Xe core.

Parameter	Range established by standards	5 MW (6 minipl. IN)	10 MW (6 minipl. IN) <sup>(2)</sup>	
		1 FE / Cycle <sup>(1)</sup>	1 FE / Cycle	2 FE / Cycle
Excess reactivity (pcm )	No limit	6200	6530	7180
Reactivity worth of the safety rod bank (pcm)	No limit	16000	16000	16000
SM <sub>4 SE</sub> (pcm)	≥3000	9800	9470	8820
SM <sub>(4 – 1)SE</sub> (pcm)	≥1000	4800	4470	3820
SM <sub>(CR1 + CR4)</sub> (pcm)	≥0	500	170	CR1 + CR4 <b>do not</b> make the reactor subcritical (cold, non Xe)
RSF	≥1.5	2.58	2.45	2.23

**Table 3. Estimated BOC, cold, non-Xe reactivity values for the operation at 10 MW and safety reactivity margins.**

(1) Typical values, taken from the analysis of historical values for 5 MW.

(2) Estimated values on the basis of <sup>(1)</sup> and corrected with the variations shown in Table 2.

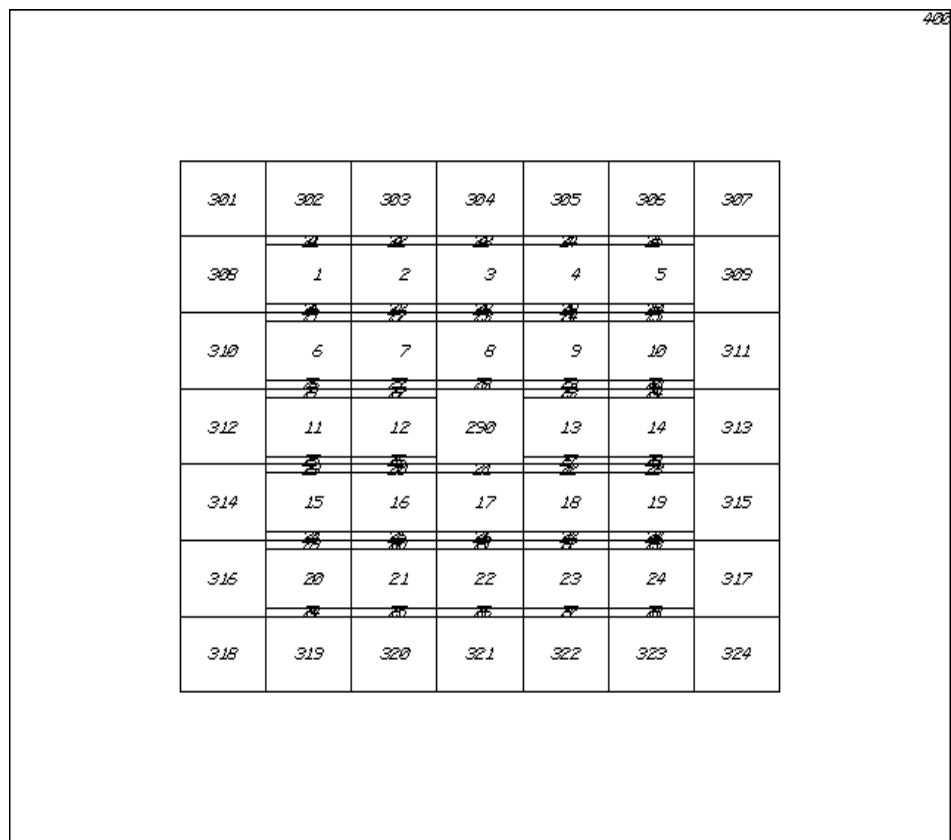


**Figure 1. Schematic cross section of the core according to the proposed model.**

**Unique refuelling chain for 1 LEU FE/cycle**

FRESH → 1 → 5 → 24 → 20 → 2 → ... → 13 → 17 → 12 → 8

**Two refuelling chains for 2 LEU FE/cycle**

FRESH → 1 → 24 → 2 → ... → 13 → 12

FRESH → 5 → 20 → 10 → ... → 17 → 8

**OBS. : 21 SFE + 4 CFE  $\cong$  24 SFE**



# Código de evaluación de dosis debida a la descarga de efluentes líquidos de la Central Nuclear Embalse

López, F.O.; Boutet, L.I.; Bruno, H.A. y Gavini, R.M.



# CÓDIGO DE EVALUACIÓN DE DOSIS DEBIDA A LA DESCARGA DE EFLUENTES LÍQUIDOS DE LA CENTRAL NUCLEAR EMBALSE

López, F.O.; Boutet, L.I.; Bruno, H.A. y Gavini, R.M.

Autoridad Regulatoria Nuclear  
Argentina

## RESUMEN

Se presenta una nueva metodología para efectuar la evaluación del impacto radiológico a la población, debido a las descargas al medio ambiente de efluentes líquidos de la Central Nuclear Embalse (CNE), ubicada en la Provincia de Córdoba de la República Argentina.

Para llevar a cabo la evaluación de dosis se desarrolló un código, denominado EDDELIQ, en éste el cálculo de la concentración de los radionucleidos en el agua del lago Embalse se realiza mediante un modelo físico sencillo del tipo de mezcla completa. El modelo físico planteado es resuelto numéricamente mediante un método de Runge Kutta de segundo orden.

## ABSTRACT

A new methodology is presented to assess the evaluation of the radiological impact to the population, due to the discharges to the environment of liquids effluents of Central Nuclear Embalse (CNE), located in the Province of Cordoba of the República Argentina.

In order to carry out the dose evaluation, a code denominated EDDELIQ was developed, in this code the calculation of the radionucleidos concentration in the water lake is made by means of a simple physical model of the type of complete mixture. The raised physical model is solved numerically by means of Runge Kutta method of second order.

## INTRODUCCIÓN

La hidrosfera constituye una vía importante por la cual los materiales radiactivos emitidos por una central nuclear pueden dispersarse en el medio ambiente y, por lo tanto llegar al hombre.

La Central Nuclear Embalse (CNE) opera comercialmente desde el 20 de enero de 1984. Se encuentra situada a 110 kilómetros al sudoeste de la Ciudad de Córdoba. Sus instalaciones se hallan en la costa sur del Embalse del Río Tercero, en la península de Almafuerte a 665 metros por sobre el nivel del mar. La CNE pertenece al tipo de centrales nucleares conocidas como PHWR, subgrupo "tubos de presión", esto es, sus canales de combustible se encuentran presurizados con agua pesada, y emplea como combustible en sus 380 canales, uranio natural (0,72% de uranio 235).

En este trabajo se presenta un código de evaluación de dosis debido a las descargas líquidas (EDDELIQ) que la Central Nuclear Embalse vierte, en condiciones normales de operación, en aguas del lago Embalse de Río Tercero, que es la fuente principal de agua potable de la población circundante.

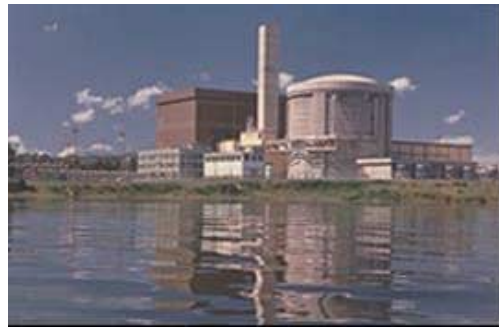


**Figura 1.** Central Nuclear Embalse

En el código desarrollado, el cálculo de las concentraciones en agua del lago de los radionucleidos descargados por la central se realiza mediante la resolución de un modelo físico del tipo mezcla completa sencillo, que predice la variación temporal de dichas concentraciones [1-2]. El modelo propuesto es resuelto numéricamente mediante el método de Euler modificado, que es uno de los métodos de Ruge Kutta de segundo orden más utilizados [3,4].

A partir de los valores calculados de las concentraciones en el agua del lago de los distintos radionucleidos descargados, y sobre la base de las recomendaciones realizadas por el Organismo Internacional de Energía Atómica (OIEA) [1], se calculan las concentraciones de los mismos en las distintas matrices que se deben tener en cuenta en la evaluación de dosis. Estas matrices son peces, sólidos en suspensión, sedimentos del fondo del lago y sedimentos de la orilla.

La estimación de dosis se realiza a partir de las siguientes vías de exposición:

- **Irradiación externa:** Inmersión en el lago y sedimentos de la orilla
- **Irradiación interna:** Ingestión de agua de bebida e ingestión de pescados

El código EDDELIQ la evaluación se efectúa para dos grupos etarios, adultos y niños menores de un año.

## CÁLCULO DE LA CONCENTRACIÓN DE ACTIVIDAD EN EL AGUA DEL LAGO

### Modelo Físico Desarrollado

El modelo desarrollado es del tipo mezcla completa, que simula un estanque de ciclo cerrado en el que se produce una mezcla completa en todo el “volumen efectivo” que representa la parte activa; no se consideran en él las derivaciones no efectivas. Se supone que los efluentes de la central se mezclan instantánea y completamente con todo el volumen de agua [1,2].

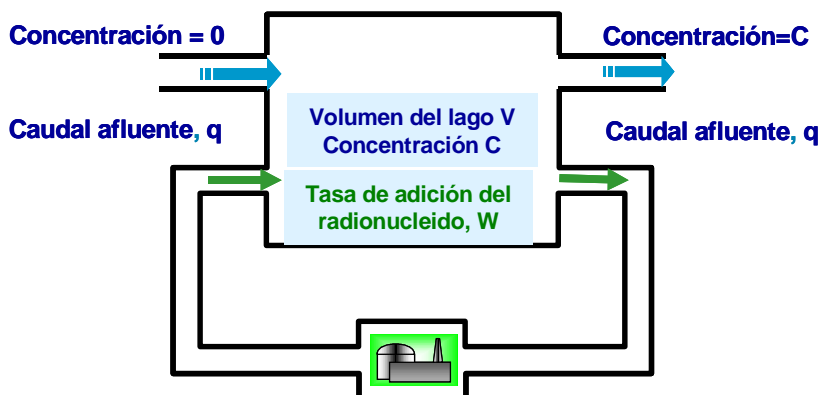


**Figura 2.** Esquema del modelo de mezcla completa

En este modelo son de importancia dos parámetros. El primero es la constante de tiempo correspondiente al barrido del estanque por la corriente de aportación y la del efluente. Se define como  $V/q$ , donde  $V$  es el volumen efectivo del estanque y  $q$  es el caudal efluente (igual al caudal de aportación, sin tener en cuenta la evaporación). El segundo es la constante de tiempo correspondiente a la desintegración de los radionucleidos.

Los parámetros de entrada necesarios son:

- el volumen efectivo,  $V$  ( $\text{m}^3$ )
- el caudal de desagüe,  $q$  ( $\text{m}^3 \text{ s}^{-1}$ )
- la tasa de adición de radionucleidos,  $W$  ( $\text{Bq s}^{-1}$ )
- la constante de desintegración radiactiva,  $\lambda$ .( $\text{s}^{-1}$ )

Como resultado de todo lo expuesto la concentración del radionucleido C puede obtenerse a partir de la siguiente ecuación:

$$V \cdot \frac{dC}{dt} = -(q \cdot C) + W - \lambda \cdot (C \cdot V) \quad (1)$$

El modelo propuesto es resuelto numéricamente mediante el método de Euler modificado. Los detalles de esta resolución numérica del modelo propuesto pueden observarse en la referencia [2], para el caso del estudio de la variación temporal de la concentración de tritio en aguas de lago.

A continuación se presenta la validación de los resultados obtenidos mediante el modelo frente a los valores de concentración de actividad de tritio determinados en el monitoreo ambiental, que lleva a cabo en forma rutinaria la Autoridad Regulatoria Nuclear, en los alrededores de la Central Nuclear Embalse, en el período comprendido entre los años 1997 y 2003.

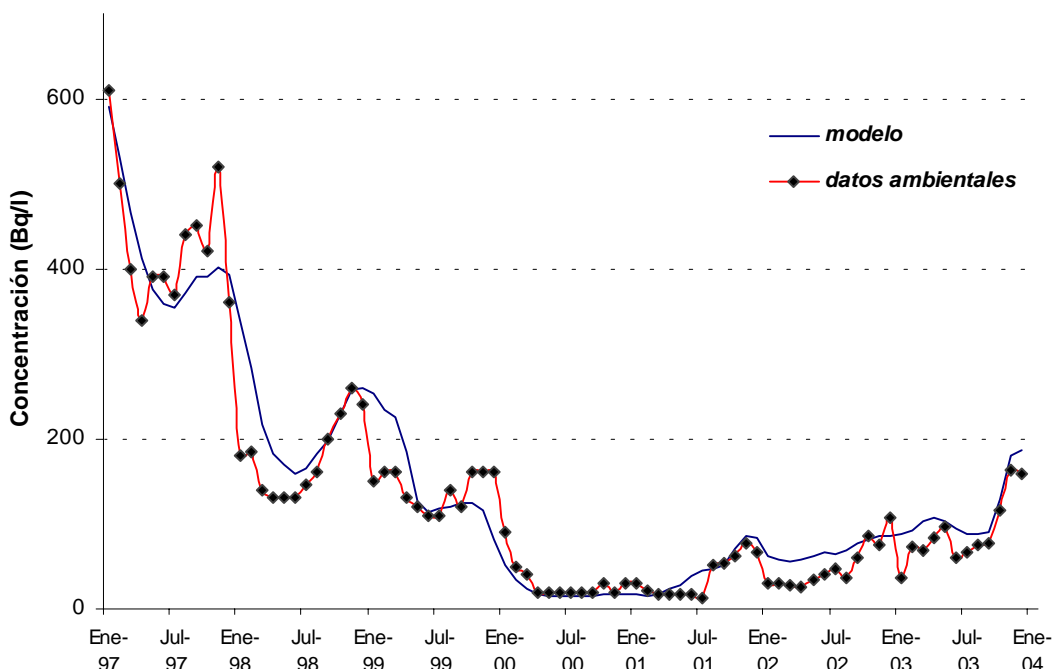


**Figura 3.** Comparación de los resultados obtenidos, para la concentración de actividad de tritio en agua del lago, mediante el modelo físico resuelto numéricamente y los datos ambientales en el período enero de 1997 a diciembre de 2003.

## CORRECCIÓN POR SEDIMENTACIÓN

Cuando los sedimentos interactúan con los radionucleidos disueltos en el agua, la concentración de estos puede disminuir a medida que sean adsorvidos por las partículas de sedimentos. En consecuencia, la concentración de radionucleidos en sólidos en suspensión, en los sedimentos del fondo, en los sedimentos los bancos formados en el cuerpo de agua y en los sedimentos de la orilla, puede verse incrementada.

La relación entre la cantidad de radionucleido adsorbido por las partículas de sedimento con respecto a la cantidad disuelta en el agua es expresado mediante el coeficiente de distribución  $K_d$  ( $\text{L kg}^{-1}$ ). Este coeficiente es definido para cada radionucleido mediante la siguiente expresión:

$$K_d = \frac{\text{Concentración del radionucleido adsorbido en los sedimentos (Bq kg}^{-1}\text{)}}{\text{Concentración del radionucleido disuelto en el agua (Bq L}^{-1}\text{)}} \quad (2)$$

### Concentración de radionucleidos en el agua filtrada

La concentración de un radionucleido en el agua filtrada ( $\text{Bq m}^{-3}$ ) puede ser calculada a partir de la siguiente expresión:

$$C_{A,S} = \frac{C_{A,tot}}{1 + 0,001 K_d S} \quad (3)$$

donde  $C_{A,tot}$  ( $\text{Bq m}^{-3}$ ) es la concentración del radionucleido en el agua sin filtrar, calculada mediante el modelo resuelto anteriormente y  $S$  es la concentración de sólidos en suspensión, generalmente expresado en  $\text{kg m}^{-3}$  ó  $\text{g L}^{-1}$ . El 0,001 es un factor de corrección de unidades.

### Concentración de radionucleidos en sólidos en suspensión

La concentración de radionucleidos adsorbidos en sólidos en suspensión ( $\text{Bq kg}^{-1}$ ) puede ser obtenida mediante la siguiente expresión [1]:

$$C_{S,A} = \frac{0,001 K_d C_{A,tot}}{1 + 0,001 K_d S} = 0,001 K_d C_{A,S} \quad (4)$$

### Concentración de radionucleidos en sedimentos del fondo

Los sedimentos del fondo pueden contener radionucleidos provenientes del depósito de sólidos en suspensión, en los cuales los radionucleidos están adsorvidos, y de la adsorción directa de radionucleidos disueltos en el agua. Los valores de  $K_d$  asociados con los sedimentos de fondo son mucho menores que los correspondientes a los sólidos en suspensión [1]. En este trabajo se asume que los coeficientes correspondientes a los sedimentos del fondo son un décimo de los que corresponden a los sólidos en suspensión [1]. La concentración de radionucleidos en sedimentos del fondo, expresada en  $\text{Bq kg}^{-1}$ , puede calcularse a través de la siguiente expresión:

$$C_{S,F} = \frac{0,1 \cdot 0,001 K_d C_{A,tot}}{1 + 0,001 K_d S} \frac{1 - \exp(-\lambda_i T_e)}{\lambda_i T_e} = 0,1 C_{S,A} \frac{1 - \exp(-\lambda_i T_e)}{\lambda_i T_e} \quad (5)$$

donde  $T_e$  es el tiempo efectivo de acumulación de sedimentos en el fondo (s). Se considera para este período de acumulación  $T_e$  un valor de  $3,15 \cdot 10^7$  s (1 año) [1].

### **Concentración de radionucleidos en sedimentos de la orilla**

La concentración de actividad de un radionucleido adsorbida en los sedimentos de la orilla ( $\text{Bq m}^{-2}$ ), se obtiene mediante la siguiente expresión:

$$C_{S,O} = \frac{0,1\ 0,001\ K_d\ 60\ C_{A,tot}}{1+0,001K_d S} \frac{1-\exp(-\lambda_i T_e)}{\lambda_i T_e} = 60\ C_{S,F} \quad (6)$$

donde  $T_e$  es el tiempo efectivo de acumulación (s). Al igual que en el caso de la acumulación en los sedimentos de fondo, en este caso se considera un tiempo de acumulación de  $3,15\ 10^7$  s (1 año). El factor 60 ( $\text{kg m}^{-2}$ ) representa la densidad superficial de la capa superior (5 cm) de los sedimentos de la orilla [1].

### **Concentración de radionucleidos en los peces**

Los radionucleidos descargados en el medio acuático son también asimilados por los organismos vivos. Algunos de estos radionucleidos pueden llegar al hombre a través de la cadena de alimentación del medio acuático.

En el código EDDELIQ, el modelo que describe el transporte de radionucleidos desde la descarga líquida a los peces es expresado de la siguiente forma:

$$C_P = C_{A,S} B_P 0,001 \quad (7)$$

donde:  $C_P$ , es la concentración del radionucleido en los pescados ( $\text{Bq kg}^{-1}$ ),  $C_{A,S}$  es la concentración del radionucleido disuelto en el agua filtrada ( $\text{Bq m}^{-3}$ ) y  $B_P$  es el factor de bioconcentración ( $\text{L kg}^{-1}$ ). Este factor relaciona, en condiciones de equilibrio, la concentración del radionucleido en los peces y la concentración del mismo radionucleido disuelta en agua.

$$B_P = \frac{\text{Concentración del radionucleido } i \text{ en los peces } (\text{Bq kg}^{-1})}{\text{Concentración del radionucleido } i \text{ disuelto en el agua } (\text{Bq L}^{-1})} \quad (8)$$

## **MODELO DE ESTIMACIÓN DE DOSIS DEBIDA A LA DESCARGA DE EFLUENTES LÍQUIDOS**

El cálculo de dosis debido a la descarga de efluentes líquidos va a estar referido al denominado grupo crítico. Se asume que este grupo representa a aquellos miembros del público más expuesto a la fuente sujeta a control. Los miembros de este grupo crítico presentan una razonable homogeneidad con respecto a todos aquellos factores que influyen de manera importante en la dosis recibida.

El cálculo de dosis a los integrantes del grupo crítico se realiza a partir de los datos de concentración en agua del lago, en sólidos en suspensión, en sedimentos de fondo, en sedimentos de la orilla y en los pescados.

Las vías de exposición externa consideradas son:

- Sedimentos de la orilla del lago
- Inmersión en el agua del lago

En el caso de irradiación interna las vías consideradas son las siguientes:

- Ingestión de agua
- Ingestión de pescados

Se realiza la estimación de dosis para dos grupos etarios, adultos y niños menores de un año. Los factores de conversión de dosis utilizados en este código fueron establecidos por la Autoridad Regulatoria Nuclear en base a distintas recomendaciones del OIEA [1].

### Cálculo de dosis externa

En el cálculo de la dosis anual externa se consideran dos componentes, una debida a los sedimentos de la orilla y la que corresponde a la inmersión en agua del lago.

#### **Cálculo de la dosis externa debida a los sedimentos de la orilla**

La dosis anual efectiva debida a la exposición externa de los sedimentos de la orilla del lago,  $E_{SO}$  ( $\text{Sv a}^{-1}$ ), puede obtenerse mediante la siguiente expresión:

$$E_{SO} = C_{SO} F_{i,ext} F_O \quad (9)$$

donde  $C_{SO}$  es la concentración de actividad del radionucleido por unidad de superficie de los sedimentos de la orilla ( $\text{Bq m}^{-2}$ ), calculada mediante la ecuación (6).  $F_{i,ext}$  es el factor de conversión de dosis por irradiación externa, este factor es expresado en  $\text{Sv m}^2 \text{Bq}^{-1} \text{a}^{-1}$ . Finalmente,  $F_O$  es el factor de ocupación, que depende del grupo etario sobre el cual se esté realizando la evaluación de dosis.

#### **Cálculo de la dosis externa debido a la inmersión en aguas del lago**

La dosis por irradiación externa por inmersión en el agua del lago,  $E_{inm,A}$  ( $\text{Sv a}^{-1}$ ), se compone de tres aportes:

- actividad disuelta en el agua
- actividad adsorbida en los sólidos en suspensión
- actividad adsorbida en los sedimentos del fondo

La componente de dosis efectiva anual que depende de la irradiación externa debida a la actividad disuelta en agua se puede obtener a partir de la siguiente expresión:

$$E_{inm,A,A} = C_{A,S} F_{inm,A} F_O \quad (10)$$

donde  $E_{inm,A,A}$  es la componente de dosis efectiva que corresponde a los radionucleidos disueltos en el agua ( $\text{Sv a}^{-1}$ ).  $C_{A,S}$  ( $\text{Bq m}^{-3}$ ) es la concentración del radionucleido en el agua filtrada (ecuación (3)).  $F_{inm,A}$  es el factor de conversión de dosis debido a la inmersión en el agua ( $\text{Sv m}^3 \text{Bq}^{-1} \text{a}^{-1}$ ). Por último  $F_O$  es el factor de ocupación.

Por otro lado, la componente de dosis externa debida a la concentración actividad presente en los sólidos en suspensión se puede estimar de la siguiente manera:

$$E_{inm,A,SS} = S C_{S,A} F_{inm,A} F_O \quad (11)$$

donde  $S$  es la concentración de sólidos en suspensión ( $\text{kg m}^{-3}$ ) y  $C_{S,A}$  es la concentración en actividad del radionucleido adsorbida en los sólidos en suspensión. Esta concentración, expresada en  $\text{Bq kg}^{-1}$ , es calculada mediante la ecuación (4).

Por último, la componente de dosis debido a los radionucleidos adsorbidos en los sedimentos del fondo, puede calcularse mediante la siguiente expresión:

$$E_{inm,A,SE} = 60 C_{S,F} F_{i,ext} F_O \quad (12)$$

donde el factor 60 ( $\text{kg m}^{-2}$ ) representa la densidad superficial de la capa superior (5 cm) de los sedimentos del fondo,  $C_{S,F}$  ( $\text{Bq kg}^{-1}$ ) es la concentración de actividad del radionucleido adsorbido en estos sedimentos.  $F_{i,\text{ext}}$  ( $\text{Sv m}^2 \text{Bq}^{-1} \text{a}^{-1}$ ) es el factor de conversión de dosis por irradiación externa, debida al depósito en el fondo.

En consecuencia, la dosis por irradiación externa por inmersión en aguas del lago total, puede obtenerse sumando todos los aportes:

$$E_{inm,A} = E_{inm,A,A} + E_{inm,A,SS} + E_{inm,A,SF} \quad (13)$$

### **Cálculo de dosis interna**

#### **Cálculo de dosis interna debida a la ingestión de agua**

La estimación de la dosis interna, debida a la ingestión de agua, tanto para adultos como para niños, se obtiene a partir de la siguiente expresión:

$$E_{int,A} = C_{A,S} F_{ing} F_C \quad (14)$$

donde  $E_{int,A}$  es la componente de dosis interna debido a la ingestión de agua ( $\text{Sv a}^{-1}$ ),  $C_{A,S}$  es la concentración de actividad del radionucleido disuelto en el agua filtrada ( $\text{Bq m}^{-3}$ ), esta concentración es obtenida a partir de la ecuación (3).  $F_{ing}$  es el factor de conversión de dosis por ingestión, este factor depende, obviamente de cada radionucleido estudiado, y del grupo etario.  $F_C$  es el factor de consumo.

#### **Cálculo de dosis interna debida a la ingestión de pescados**

El cálculo del componente de la dosis interna debido a la ingestión de pescados, se efectúa de la siguiente manera:

$$E_{int,P} = C_P F_{ing} F_C \quad (15)$$

donde  $C_P$  ( $\text{Bq kg}^{-1}$ ) es la concentración de actividad en pescados, esta concentración es obtenida a partir de la ecuación (7).

## **CONCLUSIONES**

La estimación de dosis que pueden recibir los individuos del público como consecuencia de las descargas de una central nuclear en operación normal puede ser un proceso complejo. En determinadas condiciones, cuando las dosis esperadas son muy bajas (muy alejadas del nivel de referencia) y, fundamentalmente, cuando se disponen de pocos parámetros y datos de la zona, es posible hacer simplificaciones y supuestos conservadores en la evaluación. A medida que se posee mayor información sobre el sitio que se analiza (datos meteorológicos, características específicas del medio acuático al que se vierte el efluente), con el fin de optimizar la evaluación, los modelos utilizados deben ser lo más realistas posibles ya que suposiciones conservadoras pueden viciar las decisiones basadas en dicha optimización.

En esta dirección se puede concluir que el código desarrollado, al calcular la concentración de cada radionucleido en el agua del lago mediante un modelo físico resuelto en forma numérica a través de un método desarrollado específicamente para este caso, y al tener en cuenta los nuevos criterios de protección radiológica, garantiza que toda la evaluación del impacto radioológico a la población, debida a las descargas líquidas de la Central Nuclear Embalse, sea mucho más precisa que la obtenida a partir de otros métodos más generales.

## **REFERENCIAS**

- 1 - International Atomic Energy Agency, Generic Models for Use in Assessing the Impact of Discharges of Radioactive Substances to the Environment. Safety Reports Series Nº19, Viena, 2001
- 2 - Análisis del Comportamiento Temporal de la Concentración de Tritio en el Lago Embalse Río Tercero, Fabio López y Héctor Bruno,. Autoridad Regulatoria Nuclear ARN-PI-29/98, 1998.
- 3 - Análisis Numérico. Burden, R.L.; Faires, J.D. Grupo Editorial Iberoamérica, México, 1985
- 4 - Solución Numérica de Ecuaciones Diferenciales, Tomo 1, Ecuaciones Diferenciales Ordinarias, Marshall, G., Editorial Reverté. Argentina. 1985.
- 5 - National Council on Radiation Protection and Measurements, Screening Models for Releases of Radionucleides to Atmosphere, Surface Water, and Ground. NCRP Report Nº 123. I, 1996.

# Passive Method for the Equilibrium Factor Determination between $^{222}\text{Rn}$ Gas and its Short Period Progeny

López, F.O. and Canoba, A.C.



**PASSIVE METHOD FOR THE EQUILIBRIUM FACTOR DETERMINATION  
BETWEEN  $^{222}\text{Rn}$  GAS AND ITS SHORT PERIOD PROGENY**  
**López, F.O. and Canoba, A.C.**  
**Autoridad Regulatoria Nuclear, Argentina**

**Abstract**

$^{222}\text{Rn}$  is the most important source of natural radiation, being responsible for approximately half of the dose to man taking into consideration the totality of the natural sources.  $^{222}\text{Rn}$  gas decays in a series of radionuclides of short half life that are radioactive isotopes of lead, polonium and bismuth. These short period radionuclides are highly reactive alpha emitters that can attach to dust particles of the environment thus remaining in suspension.  $^{222}\text{Rn}$  gas and its progeny are inhaled with the subsequent emission of the alpha particles to the bronchial epithelium. Only a small fraction of  $^{222}\text{Rn}$  decays inside the respiratory system, the greater part of the dose is derived from the inhalation of the short lived progeny.  $^{222}\text{Rn}$  gas and its progeny concentration are related by an equilibrium factor  $F$ . This factor is the ratio between the equilibrium equivalent concentration of  $^{222}\text{Rn}$  with its progeny EEC and the concentration of  $^{222}\text{Rn}$  gas. Due to the radiological importance of  $^{222}\text{Rn}$  gas and its progeny of short period it is extremely necessary to count with an adequate methodology for the determination of its concentration in the different atmospheres in which human activity is developed. In this work a method was developed to determine the concentration of  $^{222}\text{Rn}$  gas and the equilibrium factor between the concentration of the gas and its descendants, by means of a single device that has two Makrofol passive tracks detectors. This device is completely passive and integrated, conditions that make it very appropriate to be used in any atmospheres in which human activity is developed, for example in houses, schools, places of work, underground mines, etc.

**1. Introduction**

$^{222}\text{Rn}$  is the most important source of natural radiation, being responsible for approximately half of the dose to man taking into consideration the totality of the natural sources [1].

$^{222}\text{Rn}$  gas decays in a series of radionuclides of short half life that are radioactive isotopes of lead, polonium and bismuth. These short period radionuclides are highly reactive alpha emitters that can attach to dust particles of the environment thus remaining in suspension.  $^{222}\text{Rn}$  gas and its progeny are inhaled with the subsequent emission of the alpha particles to the bronchial epithelium. Only a small fraction of  $^{222}\text{Rn}$  decays inside the respiratory system, the greater part of the dose is derived from the inhalation of the short lived progeny.  $^{222}\text{Rn}$  gas and its progeny concentration are related by an equilibrium factor  $F$ . This factor is the ratio between the equilibrium equivalent concentration of  $^{222}\text{Rn}$  with its progeny EEC and the concentration of  $^{222}\text{Rn}$  gas.

In order to estimate in a precise way the value of the equilibrium factor  $F$ , it is fundamental to rely on a suitable methodology that allows its determination in all kinds of environments, and as a consequence of this, a better determination of the dose due to  $^{222}\text{Rn}$  gas and its short period progeny will be achieved. Equilibrium factor values may be obtained by means of diverse methodologies [2-13].

It is necessary to remember that  $^{222}\text{Rn}$  gas concentration and its progeny changes rapidly with time. Therefore, to achieve a suitable determination of the equilibrium factor it is indispensable to have a time integrated method.

In general, to perform this type of time integrated determinations, nuclear track detectors are used [12-20].

These types of detectors are widely used in the environmental monitoring of ionizing radiations, under diverse conditions. They are the most efficient passive detectors that can be used for the determination of certain levels of time integrated concentrations. For the measurement of  $^{222}\text{Rn}$  gas and its short period progeny the solid nuclear track detectors most used are: CR-39 [13], Kodak LR-115 Type II [14-17], Kodak CN-85 [12], Terradex [18] and Makrofol [19-22].

In this work, the implementation of a reliable and adequate method for routine determinations of  $^{222}\text{Rn}$  gas concentration and equilibrium factor by means of only one device is proposed. This method is time integrated and completely passive.

## 2. Theory

In this work, the proposed method uses two passive nuclear track detectors placed in a cup like device. The detector used is Makrofol type E (300  $\mu\text{m}$  of thickness), a polycarbonate widely used in the detection of alpha radiation [19-22].

One of these detectors (shielded detector) is placed in the device, as is shown in FIG. 1, at the bottom of a chamber that possesses a filter that only allows  $^{222}\text{Rn}$  gas to enter. The other one (unshielded detector), is exposed without filter, therefore it is in contact with both the gas and its short period progeny from the air.

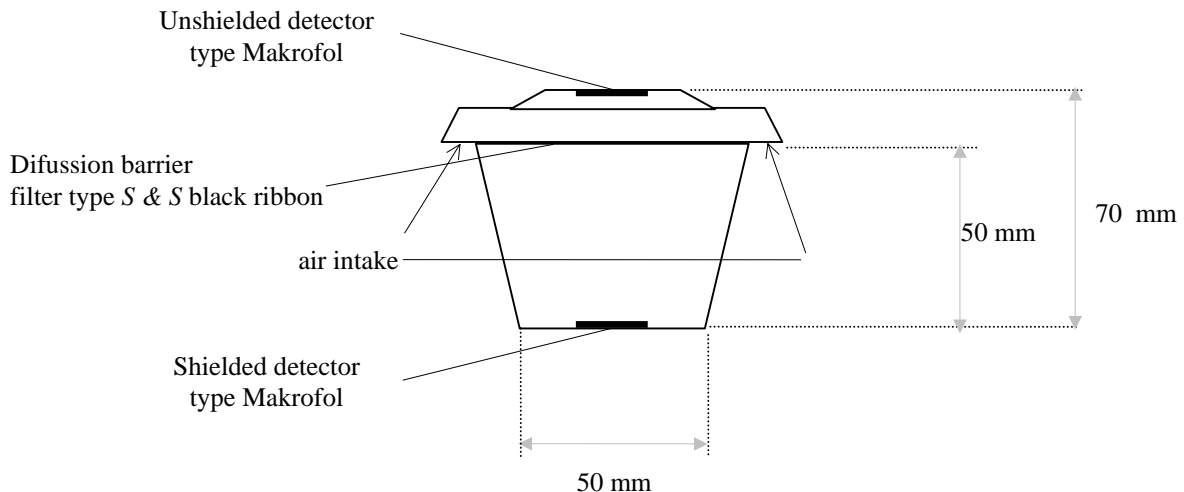


*FIG. 1. Scheme of the device presented in this work.*

In the case of the detector without filter (unshielded detector), the surface density of tracks  $D_1$ , due to  $^{222}\text{Rn}$  gas and its daughters, can be expressed by the following form [23]:

$$D_1 = K_{Rn} E_{Rn} \quad (1),$$

Where  $K_{Rn}$  is the sensibility coefficient of the detector to  $^{222}\text{Rn}$  (tracks  $\text{cm}^{-2} \text{Bq}^{-1} \text{m}^3 \text{day}^{-1}$ ) and  $E_{Rn}$  ( $\text{Bq m}^{-3} \text{day}$ ) is the product between the  $^{222}\text{Rn}$  gas concentration to which the detector was exposed  $C_{Rn}$  ( $\text{Bq m}^{-3}$ ) and the time of exposure  $t_e$  (day).

$$E_{Rn} = C_{Rn} t_e \quad (2),$$

The relationship between the  $K_{Rn}$  coefficient and the equilibrium factor  $F$  can be expressed by [12]:

$$K_{Rn} = a \exp(bF) \quad (3)$$

If equation (3) is replaced in equation (1), the following expression is obtained:

$$D_1 = a \exp(bF) E_{Rn} \quad (4)$$

On the other hand, in the case of the detector with filter (shielded detector), the surface density of tracks  $D_2$ , due to  $^{222}\text{Rn}$  gas, may be expressed by means of the following equation:

$$D_2 = d E_{\text{Rn}} \quad (5),$$

Where  $d$  is the sensibility coefficient of the detector (tracks  $\text{cm}^{-2} \text{Bq}^{-1} \text{m}^3 \text{day}^{-1}$ ), this coefficient obviously does not depend on the equilibrium factor.

Then, if the ratio between equation (4) and (5) is realized, it is possible to obtain the equilibrium factor  $F$  as:

$$F = \frac{1}{b} \ln \left( \frac{d}{a} \frac{D_1}{D_2} \right) \quad (6),$$

Where  $a$ ,  $b$  and  $d$  are constants, characteristic to the detectors.

This work proposes to determine, in an experimental way, the values of the constants  $a$ ,  $b$  and  $d$  for the described device. For this purpose, a series of experiments were made in a reference chamber at different equilibrium factor conditions.

### 3. Material and methods

The surface area of both Makrofol detectors was  $4 \text{ cm}^2$ . As may be observed in FIG. 1, one of the detectors was placed inside the device at a distance of 50 mm from the filter. In this detector, only the tracks belonging to  $^{222}\text{Rn}$  gas in the air were registered. The other detector was placed in the interior part of the lid of the monitor. In this case, both, the tracks produced by the alpha decay of  $^{222}\text{Rn}$  gas and its progeny were registered. The filter paper used was S&S black band.

For the determination of the constants  $a$ ,  $b$  and  $d$ , of equation (6), a series of experiments were performed in the reference chamber of our laboratory. The calibration chamber is a one cubic meter acrylic chamber that contains uranium ore as the  $^{222}\text{Rn}$  source. Temperature, humidity,  $^{222}\text{Rn}$  concentration and  $^{222}\text{Rn}$  progeny are controlled and monitored continuously.  $^{222}\text{Rn}$  concentration is measured using two kind of devices: activated charcoal detectors [24] and a continuous monitor Model Sun Nuclear 1027 [25]. Radon progeny is measured using a continuous monitor Model Thomson & Nielsen TN-WL-02 [26].

In each experiment, sets of ten devices were exposed inside the chamber described previously at a certain condition of equilibrium. The concentrations of  $^{222}\text{Rn}$  as well as its progeny, were produced under controlled environmental conditions. The values of  $F$  studied ranged between 0,05 and 0,80. The  $^{222}\text{Rn}$  gas concentration varied from 10 to  $990 \text{ Bq m}^{-3}$ . The  $^{222}\text{Rn}$  progeny concentration varied from 4 to  $340 \text{ Bq m}^{-3}$  and was established for each experiment. The different equilibrium conditions were obtained either by the movement of the air mass or by varying the particle concentration. This was obtained by means of introducing or not cigarette smoke within the chamber. The particle concentration varied from  $200 \text{ particles.cm}^{-3}$  to  $1,2 \cdot 10^6 \text{ particles.cm}^{-3}$ . The different equilibrium conditions were maintained for several days (between 30 and 120 days according to each experiment) by a continuous strict control of  $^{222}\text{Rn}$  concentration and  $^{222}\text{Rn}$  progeny so as to assure an accurate  $F$  value for each period of exposure. It is important to remember that the measurements methods used as reference ones were a combination of continuous and time integrated methods. In the case of the continuous methods (Sun Nuclear and TN WL-02 for  $^{222}\text{Rn}$  gas and  $^{222}\text{Rn}$  progeny assessment respectively), the values were recorded per hour and the mean values were calculated for the period of exposure chose. In the case of a time integrated method (activated charcoal for  $^{222}\text{Rn}$  gas assessment) the values were recorded weekly, the monitors were replace, and then, the mean values were calculated for the period of exposure desired. The fact to count with  $F$  values per hour in a continuous

way allowed us to maintain  $F$  within the values desired for each experiment. As soon as it was detected that  $F$  value began to separate from the value chose, control mechanisms were started to take place, either air ventilation or aerosols injection to the chamber environment, according to each case.

Once the time of exposure finished, both Makrofol detectors were treated by two processes to enlarge the tracks. Firstly: a conventional pre-etching: a solution of 0,5N KOH is used at the unirradiated backside of the detector whereas a solution of 6,5N KOH:C<sub>2</sub>H<sub>5</sub>OH 1:1 is used at the irradiated side of the detector, during 3 hours and 45 minutes at 37 °C. Secondly, with the same etching solutions, and electrochemical etching using an electrical field of 33 Kv.cm<sup>-1</sup> is applied for 1 hour and 45 minutes and is followed with a 20 minutes of etching without electric field [19-21]. The surface density of tracks, of each detectors, was determined with the help of a microfilm viewer.

During the time of exposure, in each of the experiments, the temperature and the relative humidity were kept constant. The values of these parameters were 22 °C and 45 % respectively. It is important to say that the presence of water has a negligible effect on the sensitivity of the Makrofol detectors [27-28], that is the reason why the proposed method may be applied to measurements in all range of humidity.

The sensibility coefficient value of the detector that was exposed with filter, d, was determined from the values of <sup>222</sup>Rn gas concentration  $C_{Rn}$ , the time of exposure  $t_e$  and the surface density of tracks  $D_2$ , by means of equation (5).

$K_{Rn}$ 's values were obtained for every experiment from the surface tracks density measured in the detector exposed without filter  $D_1$ , <sup>222</sup>Rn gas concentration  $C_{Rn}$  and the time of exposure  $t_e$ , according to equation (1).

On the other hand, the equilibrium factor  $F$  was calculated in each case as the ratio between the <sup>222</sup>Rn daughters concentration  $EEC$  and the <sup>222</sup>Rn gas concentration  $C_{Rn}$ , using the reference methods described previously. Then, from the  $K_{Rn}$  values obtained in each experiment and the equilibrium factors  $F$  calculated in each case, the constants a and b were determined, by means of equation (3).

Finally, so as to show an application of the method, the developed device was used to measure both, <sup>222</sup>Rn gas concentration and equilibrium factor  $F$ , in several cities of Argentina. Then, the corresponding effective equivalent doses were estimated.

#### 4. Results

FIG. 2 shows the values of the surface track density registered in the detector that was exposed with filter  $D_2$  for every value of  $E_{Rn}$ . Thus, from the linear regression, the following is obtained:  
 $d = 0,0237 \pm 0,0005$  tracks cm<sup>-2</sup> Bq<sup>-1</sup> m<sup>3</sup> day<sup>-1</sup>, with a correlation coefficient equal to 0,999.

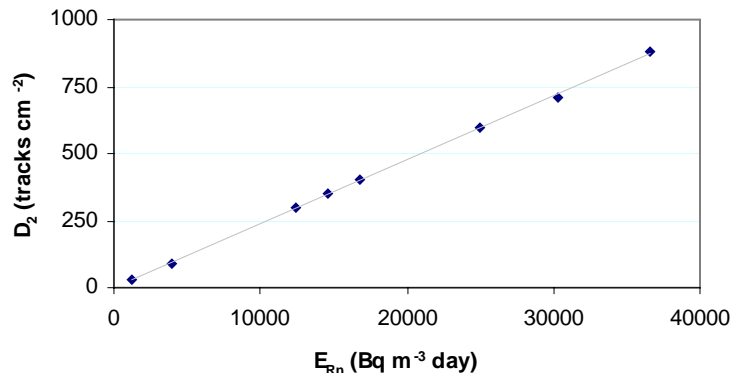


FIG. 2. linear regression between the values of the superficial density of tracks obtained in the detector exposed with filter ( $D_2$ ) and the product between  $^{222}\text{Rn}$  concentration and the time of exposure ( $E_{\text{Rn}}$ ).

On the other hand, in each experiment, the  $K_{\text{Rn}}$  values and the  $F$  values were determined. In FIG. 3, it is presented the relationship  $K_{\text{Rn}}$  vs  $F$ .

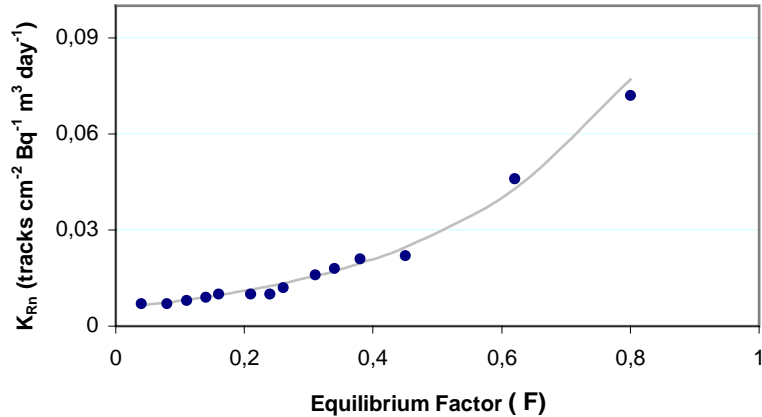


FIG. 3. Regression curve between  $K_{\text{Rn}}$ 's values and those of the equilibrium factor ( $F$ ) obtained in every experience.

The equation that describes the curve presented in FIG. 3 is of the form:

$$y = a \exp(bx)$$

On the base of the empirical data obtained by means of the regression study, we find that the  $a$  and  $b$  coefficients values are the following:

$$a = 0,0054 \pm 0,0006 \text{ tracks cm}^{-2} \text{ Bq}^{-1} \text{ m}^3 \text{ day}^{-1}$$

$$b = 3,3 \pm 0,2 \text{ (without units), with a correlation coefficient equal to 0,98.}$$

Then, from the values determined for the constants  $a$ ,  $b$  and  $d$ , and by means of the surface nuclear track density on both Makrofol detectors,  $F$  may be calculated as following:

$$F = \frac{1}{b} \ln \left( \frac{d}{a} \frac{D_1}{D_2} \right) \quad (6)$$

A summary of all the parameters measured in each experiment is shown in Table I.

EEC (Bq m <sup>-3</sup> )	C <sub>Rn</sub> (Bq m <sup>-3</sup> )	F	t <sub>e</sub> (days)	E <sub>Rn</sub> (Bq m <sup>-3</sup> day)	K <sub>Rn</sub> (tracks cm <sup>-2</sup> Bq <sup>-1</sup> m <sup>3</sup> day <sup>-1</sup> )
39,6	990	0,04	37	36630	0,007
62,4	781	0,08	32	24992	0,007
104	947	0,11	32	30304	0,008
76,0	543	0,14	31	16833	0,009
69,8	436	0,16	39	17004	0,010
68,3	325	0,21	45	14625	0,010
87,8	366	0,24	34	12444	0,010
32,5	125	0,26	36	4500	0,012
3,7	11,8	0,31	117	1381	0,016

42,4	125	0,34	29	3625	0,018
338	890	0,38	28	24920	0,021
65,3	145	0,45	27	3915	0,024
7,7	12,4	0,62	108	1339	0,046
8,2	10,3	0,80	120	1236	0,072

Table I. Summary of all the parameters measured in each experiment is shown for each condition of equilibrium

### **Measurements in Argentina**

As a complement of the  $^{222}\text{Rn}$  monitoring program that is carry out since 1980, (more than 2300 dwellings analysed) [29], during 2001 the equilibrium factor  $F$  and  $^{222}\text{Rn}$  gas were measured in several dwellings of cities of our country by means of the detector developed above during an exposure time of three months. The measurements were carry out in Buenos Aires, Córdoba, Malargüe, Bariloche, San Rafael, Neuquén and Río Turbio. These cities are representative of the different geological zones of our country. The dwellings measured were constructed mainly with concrete and bricks (construction materials more common in Argentina).

From  $F$  and  $C_{Rn}$  values the consequent effective doses  $H_g$  were calculated for each case, by means of the following equation [30]:

$$H_g = C_{Rn} (d_0 + d_1 F) \quad (7),$$

where  $d_0$  and  $d_1$  are the conversion factors of the equivalent effective dose corresponding to  $^{222}\text{Rn}$  gas and to its progeny respectively. The values recommended for these conversion factors are [13]:  $d_0 = 0,33 \mu\text{Sv.y}^{-1}$  per  $\text{Bq.m}^{-3}$  and  $d_1 = 80 \mu\text{Sv.y}^{-1}$  per  $\text{Bq.m}^{-3}$ .

$^{222}\text{Rn}$  gas values in our country are low mainly because dwellings here are well ventilated and due to the geological characteristic of the majority of the ground that is sedimentary land.

It is important to emphasize that, before this, so as to assess the equivalent effective dose, usually a multiplication of the  $^{222}\text{Rn}$  concentration by a dose equivalent conversion factor was used ( $25 \mu\text{Sv.y}^{-1} \cdot \text{Bq}^{-3}\text{m}^3$ ) [1], but these data do not take into account the concentrations of the  $^{222}\text{Rn}$  daughters in air. Therefore, the  $F$  factor is introduced to include these measurements and finally, equivalent effective dose values are assessed in a more precise way.

A summary of the results is shown in Table II.

Table II  $^{222}\text{Rn}$  in air and equilibrium factor ( $F$ ) measurements in dwellings of Argentina with the consequently effective doses ( $H_g$ )

City	$C_{Rn}$ ( $\text{Bq m}^{-3}$ )			$F$			$H_g$ ( $\text{mSv y}^{-1}$ )			n
	Average	Max.	Min.	Average	Max.	Min.	Average	Max.	Min.	
Buenos Aires	19,7	61,0	7,0	0,33	0,70	0,10	0,49	1,37	0,10	36
Malargüe	51,6	69,0	28,0	0,30	0,46	0,18	1,27	2,45	0,71	6
Córdoba	62,0	77,0	49,0	0,34	0,44	0,25	1,71	2,18	1,26	7
Bariloche	34,0	81,0	9,0	0,34	0,63	0,10	0,84	2,07	0,10	10
San Rafael	42,2	60,6	27,0	0,33	0,57	0,10	1,09	2,41	0,33	18
Neuquén	33,6	59,3	24,4	0,25	0,50	0,10	0,67	2,01	0,22	8
Río Turbio	24,3	36,2	17,3	0,47	0,80	0,18	0,88	1,17	0,53	6

### **5. Conclusions**

A suitable and reliable method of  $^{222}\text{Rn}$  gas concentration and equilibrium factor determinations has been implemented for routine measurements by means of only one device. This method is fundamental for a more precise estimation of the population dose due to  $^{222}\text{Rn}$  and its short period progeny.

The developed method is extremely adequate to achieve measurements in all kinds of environments. Besides, due to the fact that  $^{222}\text{Rn}$  gas and its progeny concentrations change rapidly with time, it is fundamental, in order to obtain a good determination, that the method must be a time integrated one.

On the base of the results observed in FIG. 3, it is possible to assure that the response of this detector is ideal for different equilibrium conditions between  $^{222}\text{Rn}$  and its progeny. It is necessary to indicate that the values of the equilibrium factor studied changed from levels near to zero (environments in which the ventilation levels are important), up to levels near to one (outdoor determinations).

## 6. References

- [1] UNSCEAR, United Nations Scientific Committee On The Effects Of Atomic Radiation, (1993).
- [2] Cliff, K. D., Wrixon A. D., Green, B. M. R. and Miles, J. C., Health Phys., 45 (1983) 323.
- [3] George, A. C., Knutson, E. O. and Franklin, H., Health Phys., 45 (1983) 413
- [4] Breslin, A. J. and George, A. C., HASL-220. Health ans Safety Laboratory U.S.A.E.C., New York, (1969).
- [5] Stranden, E. and Bertaig, L., Health Phys., 42 (1982) 479.
- [6] Strong, J.C., Laidlaw, A. J. and O'Riordan, M. C., NRPB R-39, Report, (1975).
- [7] Kotrappa, P and Mayya, Y. S., Healrh Phys., 31(1976) 380.
- [8] Snish, J.O. and Ehdwall, H.Proceeding of N. E: A. Meeting on Personal Dosimetry and Area Monitoring Suitable for Radon and Daugther Products. Elliot Lake, Canada, (1976) 191.
- [9] Chruscielewski, W., Domanski, T. and Orzechowski, W., Health Phys. 45 (1983) 421.
- [10] Domanski, T., Chruscielewski, W. and Dobrzynska, K., Health Phys., 36 (1979) 448.
- [11] Frank, A.L. and Benton, E. V., Nucl. Tract. Detectors, 1 (1977) 149.
- [12] Domanski, T., Chruscielewski, W. and Zórawski, A., Radiat. Prot. Dosim., 8 (1984) 231.
- [13] Farid, S. M., Rad. Prot. Dosim. 50 (1993) 57.
- [14] Planinic, J. and Vukovic, B., J. of Radioanal. and Nucl. Chem., Lettrs 175 (5) (1993) 333.
- [15] Faj, Z. and Planinic, J., Radiat. Prot. Dosim., 35 (1991) 265.
- [16] Azam, A., Naqvi, A.H. and Srivastava; D.S., Nucl. Geophys. 9 (1995) 653.
- [17] Mayya, Y. S., Eappen, K.P. and Nambi, K.S.B., Radiat. Prot. Dosim., 77 (1998) 177.
- [18] Alter, H. W. and Fleischer, R.L., Health Phys., 40 (1981) 693.
- [19] Urban, M., Nuclear Tracks, 12 (1986) 685.
- [20] Al-Najjar, S.A.R., Oliveira, A. and Priesch; E., Radiat. Prot. Dosim., 27 (1989) 5.
- [21] Dörschel, B. and Priesch; E., Radiat. Prot. Dosim., 54 (1994) 41.
- [22] Priesch; E., Burgkardt, B. and Sauer, D., Nucl. Tracks. Radiat. Meas., 19 (1991) 211.
- [23] Domanski, T., Wojda, A., Chruscielewski, W. and Zórawski, A., Nucl. Tracks, 9 (1984) 1.
- [24] Canoba, A.C., López, F.O. and Oliveira, A.A., J. Radioanal. Nucl. Chem. 240 (1999) 237.
- [25] W. E. Simon and M. B. Schell, International Symposium On Radon and Radon Reduction Technology, Atlanta, GA (United States), (1990), 3.11.
- [26] 4<sup>th</sup> Annual Fall Conference of the American Association of Radon Scientists and Technologists, radon-the nations's n° 1 environmental threat. Camp Hill, PA.US., 4-6 Oct. (1990)
- [27] H. A. Khan, Nucl. Instr. and Meth., 173, (1980), 55.
- [28] K. Becker, Radiation Res., 36, (1968), 107.
- [29] A. C. Canoba, M. I. Arnaud, F. O. López and A. A. Oliveira, Indoor radon measurements in Argentina, 10<sup>th</sup> International Congress of the International Radiation Protection Association-IRPA, Hiroshima, Japón, 14-19 may, (2000).
- [30] J. Planinic and Z. Faj, Nucl. Instr. and Meth., A292, (1990), 176.



# 1994 – 2004, Ten Years of Total Safeguards Application

Saavedra, A.D. and Maceiras, E.



# **1994 – 2004, TEN YEARS OF TOTAL SAFEGUARDS APPLICATION**

Saavedra, A.D. and Maceiras, E.

Nuclear Regulatory Authority  
Argentina

## **ABSTRACT**

In March 1994, the Quadripartite Agreement was signed between the Republic of Argentina, the Federative Republic of Brazil, the Brazilian-Argentine Agency for Accounting and Control of Nuclear Materials (ABACC), and the International Atomic Energy Agency (IAEA) for the application of Safeguards. In Argentina a new period was initiated in the nuclear material control process which has contributed to show to the international community that the nuclear activities are developed with peaceful purposes and in the framework of submitted declarations.

The implementation of the Quadripartite Agreement provisions has had during these ten years several stages. The initial one has represented a very big effort due to the great quantity of data to be processed and to the need of designing and implementing a new approach of the State System of Accounting for and Control of Nuclear Materials (SSAC), which has involved a great effort from the National Authority and the facilities operators. After the IAEA an ABACC verification and consolidation of the initial report, it was necessary to implement and put into operation new procedures for handling systems of accounting information, inspections, design information, etc. Nowadays, the Nuclear Regulatory Authority is in a period where the routine application of the procedures of the Quadripartite Agreement shows the knowledge and the experience achieved.

This work shows a brief review from the Quadripartite Agreement signature and the main features of its application in Argentina and in the region. It also explains the operation of the State System of Accounting for and Control and the Safeguards Inspections System and their big relations with the regional system applied by ABACC.

Besides, the evolution of the main parameters of the SSAC for this period is presented, as well as the development and the situation of the negotiations of the facility attachments.

Finally, the conclusions drawn by the agencies and the forecasts and tendencies towards to the future application of more integrated Safeguards approaches are showed.

## **INTRODUCTION**

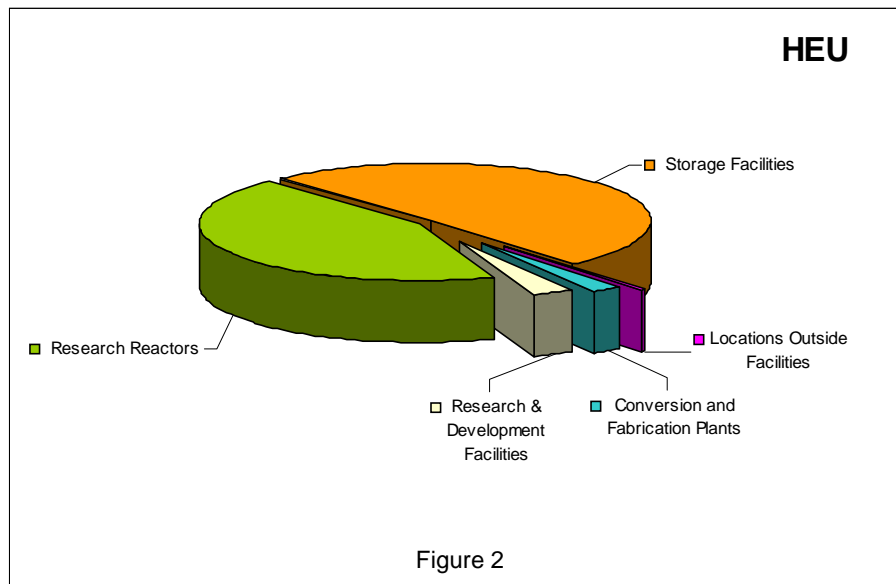
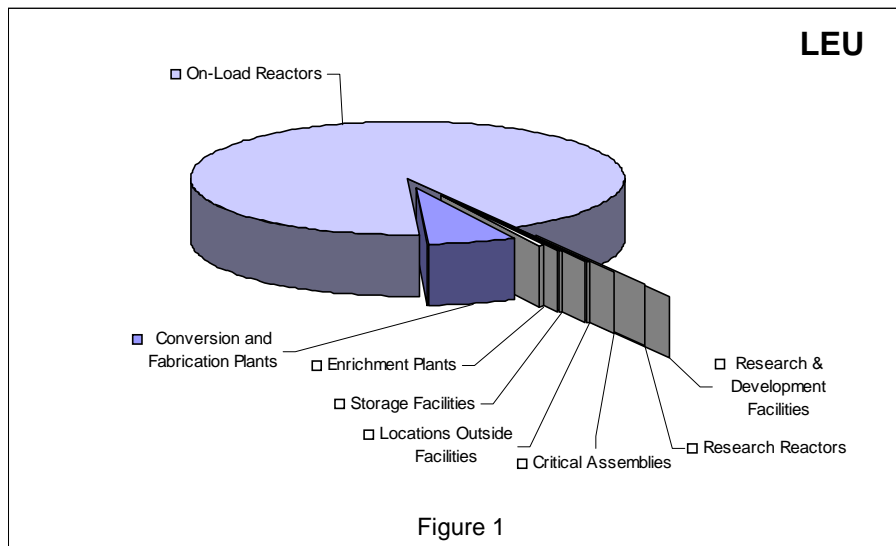
Since the beginning of nuclear activities in Argentina a national regulatory system had been established, developed and enforced, concerning aspects of radiological protection, nuclear safety, physical protection and, in particular, nuclear non-proliferation. This activity was carried out for the National Commission of Atomic Energy (CNEA) since the first times to 1995, when was created a nuclear regulatory body. Since that moment the Nuclear Regulatory Authority (ARN) have been responsible for the regulatory matter.

In the framework of the national nuclear policy of non-proliferation, the Safeguard Department had established a State System of Accounting for and Control of Nuclear Material (SSAC) as part of Regulatory Standard which is applicable to all nuclear materials and other materials, equipment and information of nuclear interest. It is aimed at ensuring that such elements are not intended for an unauthorized use, and that the international agreements are fully respected.

In Argentina, natural and LEU fuel cycle for electrical power production comprises: mining and milling; one facility for UO<sub>2</sub> powder production; one nuclear fuel fabrication plant for CANDU

and Atucha I types; two Nuclear Power Plants, Embalse and Atucha I, and one under construction; one heavy water production plant; one special alloy plant that supply structural components for fuel elements; and a gaseous diffusion enrichment uranium plant and a UF6 production plant, both non operative. There are also storage, research and development laboratories and research reactors where is processed LEU and HEU. The total significant quantities in Argentina are more than 330 for LEU and less than 1 for HEU.

The Figures N° 1 and N° 2 show the nuclear material distribution for each facility types.



## **AGREEMENTS IN FORCE**

- Bilateral Agreement: "Agreement between the Republic of Argentine and the Federative Republic of Brazil for the Exclusively Peaceful Use of Nuclear Energy". In force since 1991.
- Quadripartite Agreement: "Agreement between the Argentine Republic, the Federative Republic of Brazil, Brazilian-Argentine Agency for Nuclear Material Accountancy and Control and the International Atomic Energy Agency for the Application of Safeguards". In force since 1994.

At the end of 1980s, by means of presidential joint declarations and reciprocal visits to their most sensitive nuclear facilities, Argentina and Brazil reaffirmed their decision to provide mutual transparency to their nuclear programs. This process led to establishment of the Common Systems of Accounting for and Control of Nuclear Materials (SCCC). The first bilateral action was to make the SSACs of both countries compatible and to exchange initial and subsequent declarations of all nuclear materials in all nuclear activities in each country.

The second step was the conduction of the first reciprocal inspections to the SSAC's reporting systems. Simultaneously, political and technical authorities continued consultations, and in 1991 they signed the Bilateral Agreement on the Exclusively Peaceful Uses of Nuclear Energy. This agreement established the general basis of the SCCC as a comprehensive bilateral safeguards system and created the regional administrator "Brazilian-Argentine Agency for Nuclear Material Accountancy and Control" (ABACC) as an independent regional body to apply the SCCC.

At the end of same year both countries and ABACC signed with the IAEA a comprehensive safeguards agreement based on the SCCC and on INFIRC/153 model. The application in both countries of a total safeguard system began when the Quadripartite Agreement entered in force in March of 1994.

Otherwise Argentina has another bilateral agreements in force with United State of America and Canada on the basis of treaties of cooperation on nuclear activities.

## **TOTAL SAFEGUARDS IMPLEMENTATION**

In Argentina during the first months of 1994 the Safeguard Department worked with the facilities operators to collect, process and summarize an enormous quantity of data to prepare the Initial Report of nuclear material inventories. Likewise, in order to establish the Initial point of Total Safeguards and verify the quantities of nuclear material the Safeguards Department performed during this time national inspections in every areas where nuclear material were present. These activities represented a very big effort for all parties and the first version of Initial Report was sent to the agencies according with the time established for the Quadripartite Agreement. Also during 1994 the agencies performed the inspections for verification of the initial inventory and the consolidation of the Initial Report.

The implementation of the Quadripartite Agreement provisions represented for the ARN the need of designing a new approach on the SSAC. It was necessary to develop and implement new procedures and goals for handling design information, accounting information and perform the inspections.

The first step on this process was to establish the MBAs according with the Quadripartite Agreement definitions and taking into account the nuclear activities performed. At present there are 43 facilities which represent 44 MBAs. The different types of facilities are shown in Figure N° 3.

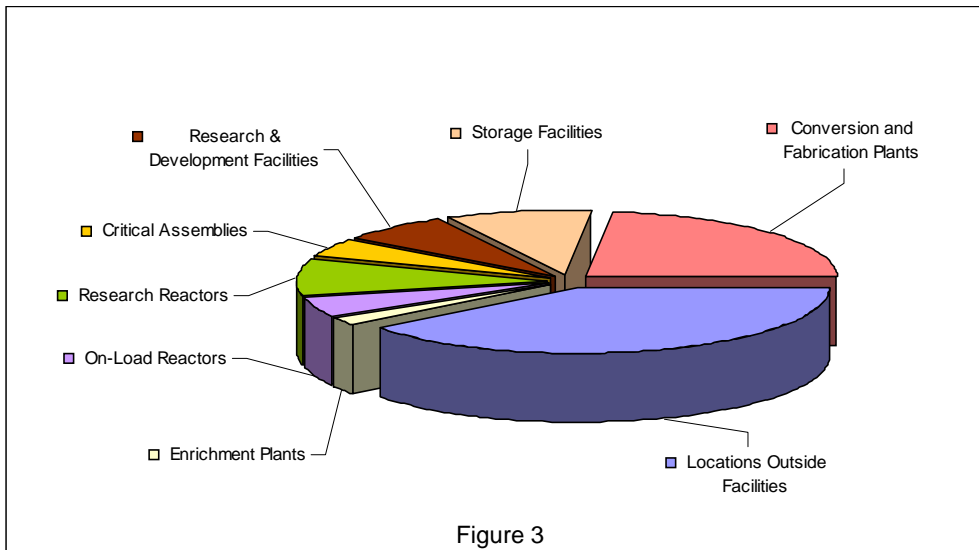


Figure 3

At every time, the ARN Safeguards Staff in cooperation with the facility operators analyzed and designed the accounting and measurement systems for each MBA. All this information was transcribed into the DIQ's formats according to the Subsidiary Arrangements of the Quadripartite Agreement.

During these ten years the design information for each MBA was updated taking into account changes in the designs, processes or purposes and the comments made by the agencies. New MBAs were incorporated when necessary. Therefore the ARN performs periodically examinations and inspections of information designs, at least once a year for the greatest facilities.

The accountancy of the nuclear material is up to now one of the principles of the SSAC. The ARN standardized the formats of each MBA's records (General Ledgers, Transfer Documents) in order to make the auditing faster and to emphasize the source documents evaluations. The General Ledgers were opened on 01/04/94 with an initial inventory according to the Initial Report.

Moreover the ARN implemented at headquarters a centralized accounting system as an important part of the SSAC. The facility operators have to send the accounting reports to ARN in a correspondent time and format. Since 1996 an electronic database (SCMN) allows to record this data and make some checking before sending the information to the agencies. In particular for each MBA the SMCN system checks the report consistence with the provision of Code 10, DIQ and FFAA information and the coherence between the MBR-PIL and ICRs. Otherwise allows making monthly a matching of domestic transfers between MBAs in order to avoid discrepancies.

The Agreement requires that the reports were sent to IAEA through ABACC in the format according with Code 10. In the first time the file was sent to ABACC on paper and then on diskette by diplomatic mailbag. An e-mail system between ABACC and ARN was agreed and implemented two years ago, with encrypted and electronic signature and an appropriated level of security.

The other basic principle of the SSAC is the National Inspections System. ARN Safeguards Staff performs an annual plan of inspection in order to fulfill its own standards and to verify with a reasonable certain degree that nuclear material is used in the declared purpose. The

inspections could be routinely for timeliness goal or transfer verification, for annual inventory verification, for design verification or to cover any special situation. Also Safeguards Staff oversees, coordinates and follows the inspections performed by ABACC and IAEA.

The inspection frequency associated to typical activities is shown in the next Table.

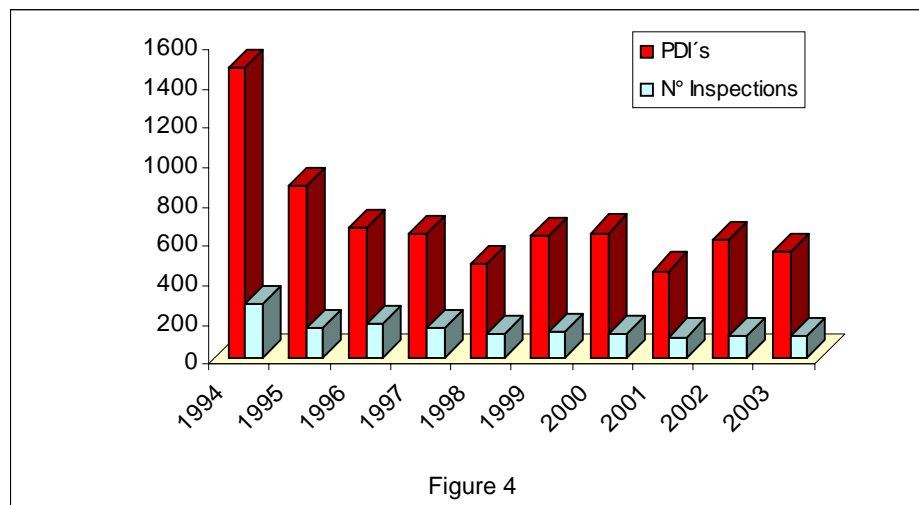
Type of facility	National inspections frequency
Power Reactors	At least 4 inspection a year (including PIV)
Conversion and Fuel fabrication Plants	Up to 4 inspection a year (including PIV)
Research Reactors	1 inspection a year (PIV)
Storage Facilities	1 inspection a year (PIV)
Research and Development Facilities	At least 1 inspection a year (PIV)
Enrichment plant	Up to 4 inspection a year (including PIV)
Critical Assemblies	1 inspection in a period of 14 months (PIV)
Locations outside Facilities	1 inspection in a period of 14 months (PIV)

The application of new Safeguards techniques was initiated with the Program 93+2 implementation tending to the strengthening the effectiveness and improving the efficiency of the Safeguards Systems.

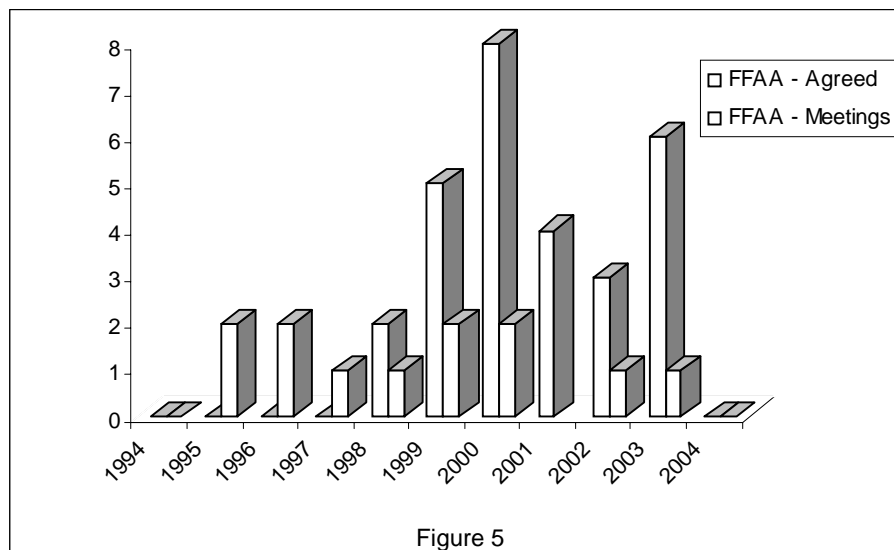
In this framework, the Nuclear Regulatory Authority in Argentina is implementing environmental sampling techniques as part of SSAC and this may offer the possibility of sharing the lab capability with the agencies.

## MAIN PARAMETERS EVOLUTION

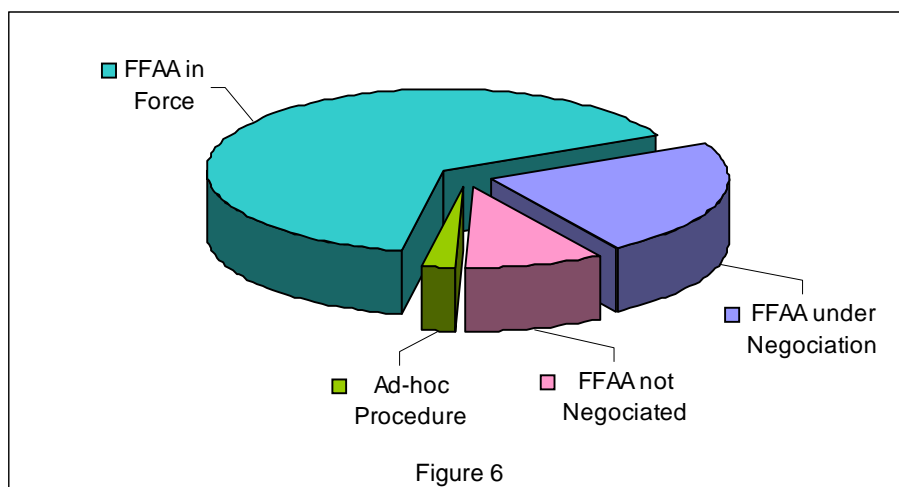
During these ten years have been performed a great number of inspections due to Initial Report Verification at the beginnings. Then, the inspection effort decreased in person day inspection and inspections quantities. Although, it remains high due to a lot of activities carried out in different types of facilities, like design verification, new approaches implementation, etc. The Figure N° 4 shows the inspection effort evolution.



In Argentina the negotiation of Facilities Attachments with both agencies began in 1995. Up to the present time 13 meetings were carried out, 28 FFAA are in force, 10 are near conclusion and the rest are going to be negotiated in as near future. The codes which have required a careful analysis from all parties were those in connection with the nuclear loss reporting, the unannounced inspections (both issues are not closed yet), the periodic re-verification of design information, the taking of the baseline for swipe samples, the activities and efforts of inspections. The Figure N° 5 shows the evolution of FFAA on these 10 years.



The current status of FFAA of the 43 facilities is shown in Figure N° 6.



On the other hand the Agreement foresees two forums for a quadripartite discussion of matters arising of the implementation on both countries of the regimen of total safeguards: the Liaison Committee (LC) for policy matters and the Technical Subcommittee of LC for technical issues. During the 10 meetings of the LC and the 13 meetings of the LSC were analyzed some issues related with aspects of the FFAA, accounting issues, the use of new technologies and the review of the safeguards approach for some facilities. In particular the currently safeguard

approach for Embalse NPP was analyzed and designed for a specific Working Group in the frame of LSC.

The ARN understands that the SSAC is supported on an experienced team of safeguard inspectors independent of facility operators, on NDA and C/S expertise, and on an independent DA capability. So during these ten years there was a permanent training of the staff of safeguard, with the participation on Regional and International Training Courses and on international Meetings related with the non-proliferation issues.

Otherwise the ARN performs a permanent research and development program, sometimes in cooperation with ABACC, OIEA and DOE. During these ten years some Actions Sheets related with some technical aspects of the implementation of safeguard had been conclude with DOE and the Agency.

Besides, the ARN has performed some training courses focusing different topics for facility operators and permanent training for its Safeguards Staff. Sometimes the courses where organized in cooperation with ABACC and IAEA.

The Imports and Exports of Nuclear Materials are informed to and can be verified by both agencies following the provision of the Bilateral and Quadripartite Agreements. Imports of yellow cake (before the starting point of safeguards) are also notified in accordance to the provisions set forth in the Quadripartite Agreement. In order to improve the transparency of the system, Argentina voluntary agreed to report to IAEA the national production of yellow cake on an annual basis.

## **AGENCIES REPORTS AND INSPECTIONS RESULTS**

The conclusions reach for both agencies respect of each material balance area and the results of its inspection are sent to the Nuclear Regulatory Authority periodically.

In this 10 years the conclusions of the inspection results and safeguards evaluation for each material balance area have been satisfactory and shown the fulfillment of the agreements clauses.

Some particular case like Atucha NPP where the safeguards approach was completed last year have been published in the IAEA Safeguards Implementation Report until this was closed.

## **FORECASTS AND CONCLUSIONS**

The fulfillment of the clauses of the two agreements in force along these years shows the sternness, the reliability and the credibility of National Safeguards System.

During these ten years the incorporation of new electronic technologies to the processing of accounting information had allowed to increase the coherence, decrease the number of errors and improve the fulfillment of the periods for each consignment.

The ARN Safeguards Staff and the facility operators achieved a big experience on accounting for and control of the nuclear material systems. Based on this experience, it is under analyze the implementation of a software, at operator level, for the accounting for and control of stock, with validation and authentication functions, compatible with the SCMN centralized safeguards data base. It is also being explored the possibility of a remote interrogation of that software in order to make easier safeguards reports and records auditing.

It is being reviewed the possible application of remote monitoring to the periodic confirmation of the non-operative state of same facilities shutdown, on order to reduce verification effort.

The successful application of the SCCC for this ten years and the atmosphere of cooperation between the countries, ABACC and the IAEA regarding international safeguards, confirm the effective contribution to the nuclear non-proliferation regime.

Otherwise in the Program 93+2 some measures has been identified to enhance international safeguard effectiveness and efficiency. In particular ARN has worked during these 10 years in order to increase the cooperation between the SSAC with ABACC and IAEA.

At this juncture where the international community is trying to identify objectives, States factors or elements related to the strengthening of safeguards and their integration at State levels, Argentina understands that it is essential to increase the cooperation with the agencies and the transparency of the SSAC.

Finally, the ARN has began to analyze the measures that could be adopted tending to integrate the traditional safeguards measures to the ones stated in the Additional Protocol.

## REFERENCES

- 1) Nuclear Regulatory Authority Annual Reports, 1995-2003.
- 2) Agreement between the Argentine Republic, the Federative Republic of Brazil, Brazilian-Argentine Agency for Nuclear Material Accountancy and Control and the International Atomic Energy Agency for the Application of Safeguards. March, 1994.
- 3) Agreement between the Republic of Argentina and the Federative Republic of Brazil for the Exclusively Peaceful Use of Nuclear Energy. July, 1991.
- 4) National Safeguards Standard: "Warranties of non-diversion of nuclear material, material, equipment and information of nuclear interest". June, 1995

# Retrospective Biological Dosimetry by FISH and Alternative Techniques

Nasazzi, N.B.; Mühlmann, M. and Otero, D.



# RETROSPECTIVE BIOLOGICAL DOSIMETRY BY FISH AND ALTERNATIVE TECHNIQUES

Nasazzi, N.B.<sup>1</sup>; Mühlmann, M.<sup>2,3</sup> and Otero, D.<sup>2</sup>

<sup>1</sup> Autoridad Regulatoria Nuclear, Avda. del Libertador 8250, CPA C1429BNP, Buenos Aires, Argentina

E-mail: nnasazzi@cae.arn.gov.ar

<sup>2</sup> Comisión Nacional de Energía Atómica – Centro Atómico Constituyentes, Avda. Gral. Paz 1499 CPA 1650, Buenos Aires, Argentina

<sup>3</sup> Consejo Nacional de Investigaciones Científicas y Técnicas, Avda. Rivadavia 1917, CPA 1033, Buenos Aires, Argentina

**Abstract:** Cytogenetical dosimetry based on the stable chromosome aberrations frequency was one of the major challenges until ten years ago, when G or R banding were the only inexpensive but extremely time consuming tools available. Since the development of the pioneer molecular cytogenetic techniques, Fluorescence in situ Hybridization (FISH), much work has been done. Even though FISH is an easy to score technique, it is very expensive. Curiously, now the circle appears to close by using FISH to get multicolor banded chromosomes, which reminds, to some extent, to the classical banding techniques allowing us to recognize more subtle chromosomal abnormalities (inversions and deletions). Those, very well known by cytogeneticists through G or R banding, are still undetectable by means of Whole Chromosome Painting (WCP) a traditional FISH technique. In this work we present some alternatives to perform retrospective dosimetry according to different scenarios, explored extensively by our group. Possibly, these alternatives will be useful in countries with different biological dosimetry laboratory infrastructures, different budgets and different personnel capabilities in banding techniques.

## Introduction

Chromosome aberration frequency measured in peripheral lymphocytes of persons exposed to ionizing radiation has been used since 1960s for dose assessment. Suspected overexposure is usually evaluated by the frequency of dicentrics and centric rings using an appropriate in vitro calibration curve, according to the radiation quality. However, these chromosome aberrations are unstable with time after exposure and dose reconstruction may encounter uncertainties when the time between the exposure and the analysis is considerable or even unknown.

If those called stable chromosome aberrations (translocations and inversions) certainly persist with time after exposure then, they may be used in retrospective dosimetry for evaluating acute past overexposures and, moreover, to show the accumulation of cytogenetical information which correlates with dose received under fractionated, chronic or occupational exposure conditions. Nowadays, the stability of translocations and inversions is practically accepted [1] [2].

All type of stable chromosome aberrations may be detected using G-banding, an inexpensive simple and rapid staining technique although it is a time consuming method for aberration scoring and requires a highly trained personnel.

For ten years, the combined application of conventional cytogenetics and molecular biology have been allowing the identification, through Fluorescence in situ Hybridization (FISH) technique, of some structural chromosome aberrations

The most promising alternative is the so called "chromosome painting", a method based on painting only some chromosome pairs with specific whole chromosome DNA probes (WCP) and then extrapolating the observed translocation frequencies to the full genome [3].

However, this method is *unable to recognize inversions and deletions*.

In general, FISH is expensive and it is not easily available yet for the majority of the laboratories, but allows a faster aberration scoring than banding techniques and appears as a promissory tool in biodosimetry, particularly when it is necessary to assess low doses and, consequently, to score a large number of metaphases, i.e. radiation workers exposed within dose limits.

Anyway, assessing doses retrospectively is a must for a biological dosimetry laboratory and it should be faced in some way.

In this work we propose different alternative techniques in order to perform retrospective dosimetry in three possible laboratory scenarios each one with some particular handicap.

- (1) A conventional cytogenetics laboratory with neither FISH equipment nor supplies but with very well trained personnel in conventional banding techniques.
- (2) A complete FISH laboratory infrastructure (including fluorescence microscope) but not enough budgets to acquire commercial DNA probes and with personnel untrained in banding techniques.
- (3) A complete laboratory (see below, in FISH equipments) but without fluoresce microscope or trained personnel in banding techniques.

## **Materials and Methods**

### *Cultures*

We use a modified micromethod [4]. Briefly, whole heparinized blood cultures for in vivo or in vitro studies were set up, using phytohemagglutinin P (PHA P, 60 g/ml) as a mitogen. Stimulated lymphocytes were grown in 10 ml RPMI 1640 medium enriched with 15% of fetal calf serum, supplemented with 2mM L-glutamine and 20 µM 5-bromo-deoxyuridine. The incubation time was 48 h at 37 °C. Colchicine was added in a concentration of 0.4 g/ml 2 h before harvesting. After hypotonic treatment with KCl (0.075 M) for 10 min at 37°C, the lymphocytes were fixed by three changes in methanol - acetic acid (3:1), air dried and stored at 60 °C overnight.

### *Aging and storage*

Slide aging is necessary for G banding; in our experience, at least two weeks..

FISH does not require previous aging but it is possible to use slides stored at -20°C several months later.

G banding is storable at 0°C and FISH slides at -20°C for several months.

### *FISH Equipment*

Starting with a full conventional dosimetry laboratory, the minimum requirement is:

-Fluorescent microscope + filters

### *Probe development equipment*

-Micro dissection device + Inverted microscope  
-Thermo circler  
-Electrophoresis cube  
-Puller

## Performing retrospective biological dosimetry

### Scenario 1

Let us consider three approaches depending on cytogeneticists expertise.

- (a) To build an in vitro dose response relationship scoring translocations, inversions or both on the whole G or R banded karyotype with at least 350 bands according to the *International System for human Cytogenetic Nomenclature (ISCN)* [5].

For special studies the same slides, conveniently stored, can be used later for scoring small deletions, insertions or complex arrangements. For these analyses it is convenient increase the band number to 500 bands (FIG.1) shortening time and increasing colchicine (or colcemid) concentration. Obviously, Premature Chromosome Condensation (PCC) technique allows 800 bands, but it is out of the scope of this work and our experience.

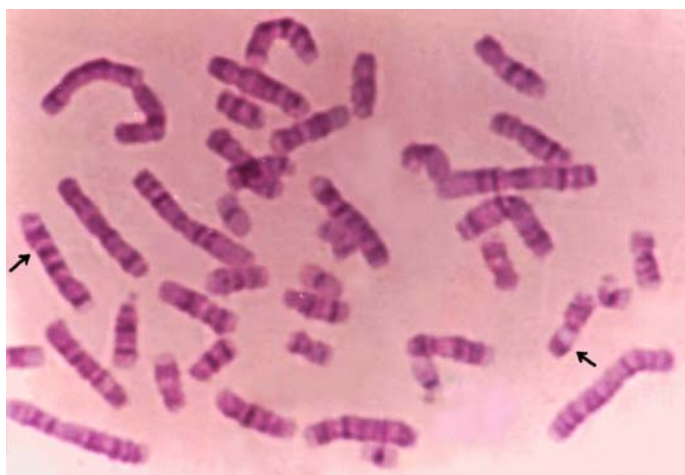


FIG. 1. G banded metaphase, 500 bands (ISCN).  
Arrows show a reciprocal translocation t7 q34::9q12

- (b) As a second approach we have proposed a less time consuming method mimicking FISH by scoring translocations using only three pairs of chromosomes and extrapolating to the whole karyotype.

In this scenario it is very easily to score inversions too. If scoring includes inversions, it is necessary a *corrected extrapolation formula* [6].

$$F_G = F_p / 2.05 \times f_p \times (1-f_p) \times (f_p)^2$$

where

$F_G$  is the full genome translocation and inversion frequency

$F_p$  is the translocation and inversion frequency detected by G banding

$f_p$  is the fraction of genome (number of pairs of chromosomes) used in the analysis

The above mentioned approaches are possible only for very well trained cytogenetists.

(c) Software support for “not so well trained” cytogeneticists.

We have developed software which helps to observe more bands and to detect inversions and small deletions, e.g. as biomarkers of past exposure to densely ionizing radiation [7].

Based on the fact that the human eye can distinguish 50 of 256 possible gray tones and unable to separate 5 very close tones we have developed software to “see” more bands than G banding images offers to the naked eye, pseudocoloring those tones.

Briefly, the binary transformed microscope image has 256 gray tones. In order to assign pseudo-colors to gray tones a particular algorithm was built relating the cubic matrix  $(256)^3$  with the maximum number of tones. Due to the fact that it is impossible to establish a bi-univocal relationship between gray tones and colors, the software automatically associates a color range from a discrimination level. It is noted that “light” pseudo-colored bands correspond to “dark” G bands

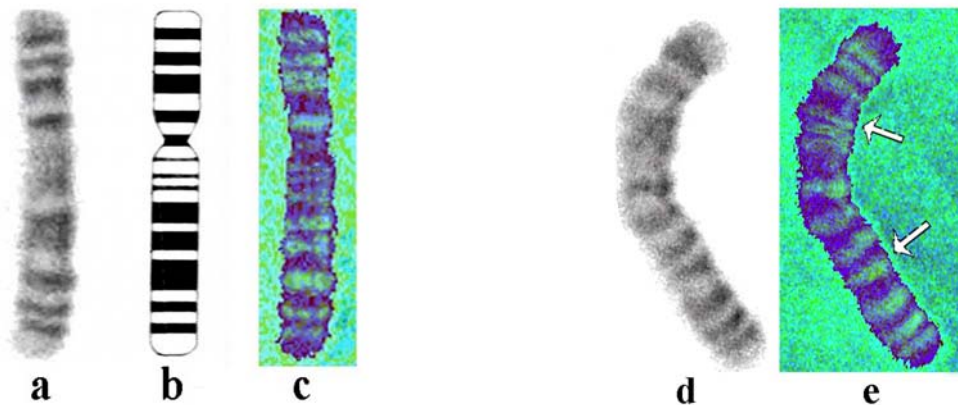


*FIG 2. Human chromosome 2. (a) G banded chromosome (19 bands), (b) Ideogram (27 bands), (c) pseudo-colored chromosome (24 bands), (d) and (e) G banded and pseudo-colored chromosome with inversion. Arrows show break points: inv 2p1 :: 2q23.*

**Scenario 2**

In this special case we propose to perform ISH (In situ Hybridization) using DNA probes which result, after an enzymatic process, in brown staining detectable by conventional light microscope. So fluorescent microscope is not required.

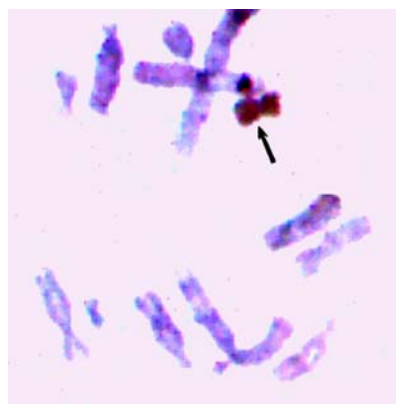


*FIG. 3. ISH. Arrow shows human chromosome 11*

This method is not so impressive but results substantially cheaper than FISH, particularly if probes are synthesized by micro dissection (*see later, Scenario 3*).

### **Scenario 3**

FISH applications reach different fields: basic genetic research in man and *other species*, medical diagnosis and prognosis related to constitutive and somatic cell genetics and, of course, retrospective dosimetry.

Performing FISH in general or particularly “Chromosome Painting” with commercial DNA direct probes is easier than the traditional indirect method but, apart from their cost, commercial DNA probes are storable usually up to six months. Up to now, in our country as in Latin America, FISH is performed using commercial DNA probes.

In a joint effort between CONICET, CNEA and ARN, Argentina has concluded the project to set up the Synthesis of chromosome probes by Micro dissection stained with Fluorescent dyes (*SMF*). It is suitable for any species lowering costs to about one sixth of the equivalent commercial probes.

It is remarkable that *SMF* not only *lowers* costs but also expands the possibilities of working with other species besides man. At the same time improves the traditional Chromosome Painting staining by using different fluorescent dyes and increases sensitivities developing probes for only parts (arms or less) of chromosomes.

The general *SMF* protocol, the cost analysis comparing with commercial probes and the minimum requirement for technology transfer and implementation of this technique in Latin American countries have been presented [7].

We show in the present work some additional images of human and other species *SMF* probes. (FIG. 4,5).

#### *Human SMF*

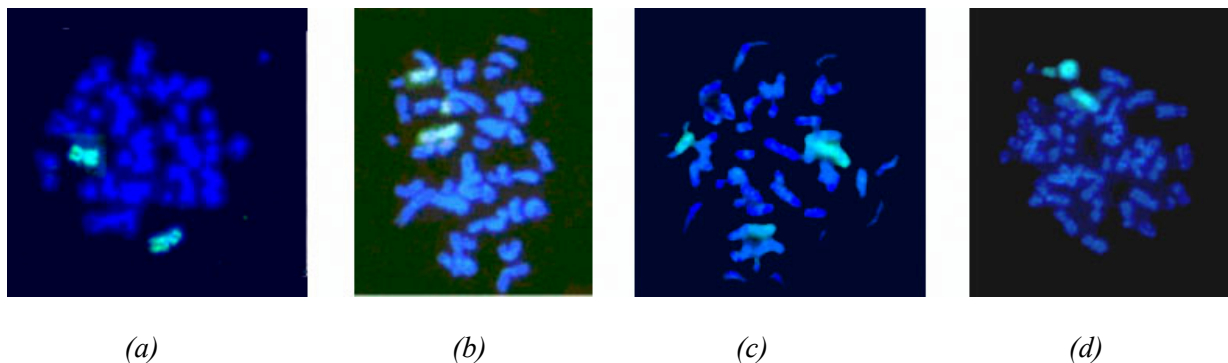


FIG.4. (a) WCP with *SMF* chromosome 3 (green). (b) reciprocal translocation. (c) deletion. (d) ring.

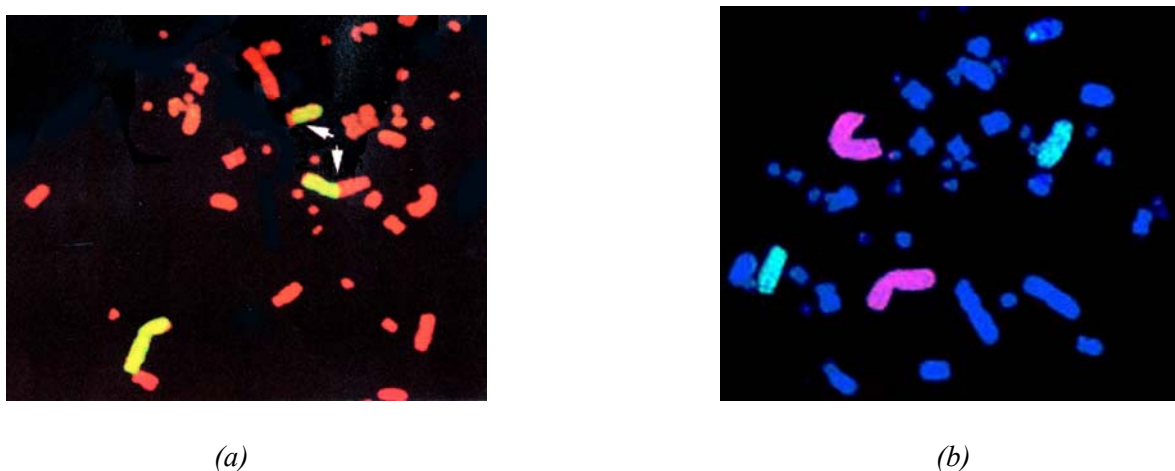


(a)

(b)

*FIG.5. (a) both human X chromosomes (yellow) show insertions and translocations induced *in vitro* after 7 Gy of gamma rays. [8]. (b) Complex arrangement between chromosome 2 (red) and chromosome 3 (green).*

#### *Other species SMF*



(a)

(b)

*FIG. 6. Turtle *Trachemys scripta*. (a) WCP Reciprocal translocation chromosome 1.[9]. (b) WCP 1 green, 3 red.*

#### **Conclusions**

As can be seen in the present work, retrospective dosimetry is a matter of choice. It depends on where every laboratory has its strong point: the facilities and budgets or training in cytogenetics. Not always the expensive alternatives give better results.

## References

1. Natarajan, A.T., Santos, S.J., Darroudi, F. et al, *<sup>137</sup>Cesium-induced chromosome aberrations analyzed by fluorescence in situ hybridization: eight years follow up of the Goiania accident victims.* Mut. Res., 400: 299-312 (1998).
2. Nasazzi, N., Di Giorgio, M., Taja, M.R. *Retrospective dosimetry using chromosome painting,* Proceedings IRPA X International Congress, Vol. 1: 223-228 (2000).
3. Lucas, J.N., Awa, A., Straume, T., et al, *Rapid translocation frequency analysis in humans decades after exposure to ionising radiation.* Int. J. Radiat Biol., 62: 53-63 (1992).
4. IAEA, *Cytogenetics analysis for radiation dose assessment,* Technical Report Series N<sup>a</sup> 404 (2001).
5. Mitelman, F., *An International System for Human Cytogenetic Nomenclature (ISCN),* Cytogenetics and Cell Genetics, 5: 210-219 (1995).
6. Nasazzi, N., Di Giorgio, M., Ferraro, M., et al, *Evaluación de la dosis integrada por dosimetría citogenética en trabajadores de Centrales Nucleares,* Proceedings IRPA II Regional Gongress, Vol.II: 126-200 (1993).
7. Prakash Hande, M., Azizova, V., Geard, R., et al, *Past Exposure to Densely Ionizing Radiation Leaves a Unique Permanent Signature in the Genome,* A. J. Hum. Genet., 72: 1162-1170 (2003)
8. Nasazzi, N., Marañón, D., Mühlmann, M. *Detección por FISH de anomalías cromosómicas. El estado del arte en la Argentina,* Proceedings IRPA VI Regional Congress (2003).
9. Mühlmann, M. *Molecular cytogenetics in metaphase and interphase cells for cancer and genetic research, diagnosis and prognosis. Application in tissue sections and cell suspensions.* Genetics and Molecular Research 1 (2): 117-127 (2002).
10. Ulsh, B.; Mühlmann-Díaz, M.C.; Whicker, F.; Hinton, J.; Congdon, J. and Bedford, J. *Chromosome translocation in turtles: a biomarker in a sentinel animal for ecological dosimetry* Rad. Res. 153: 752-759 (2000).



# La protección radiológica del paciente: marco conceptual, nuevas recomendaciones a nivel internacional

Gisone, P.A. y Perez, M. del R.



# **LA PROTECCIÓN RADIOLÓGICA DEL PACIENTE: MARCO CONCEPTUAL, NUEVAS RECOMENDACIONES A NIVEL INTERNACIONAL**

Gisone, P.A. y Perez, M. del R.

Autoridad Regulatoria Nuclear  
Argentina

## **1. La protección radiológica del paciente: marco conceptual**

La población incluida en el concepto de “exposiciones médicas” está conformada por:

- 1) Pacientes sometidos a prácticas diagnósticas
- 2) Pacientes sometidos a irradiaciones terapéuticas
- 3) Individuos sanos bajo vigilancia médico-laboral de rutina
- 4) Sujetos incluidos en programas de “screening” poblacional
- 5) Personas involucradas en procedimientos de carácter médico-legal
- 6) Voluntarios incluidos en programas de investigación biomédica
- 7) Personas que aceptan voluntariamente participar en el cuidado de pacientes sometidos a exposiciones médicas fuera de todo vínculo laboral (familiares o amigos)

Las irradiaciones médicas constituyen la contribución mas importante a las exposiciones humanas a radiación ionizante de carácter artificial. Las estadísticas mundiales indican una tendencia creciente en el número anual de prácticas así como en la cantidad de instalaciones y recursos humanos destinados a tales fines. Esto explica la preocupación creciente de las sociedades científicas y los organismos reguladores por los aspectos vinculados a la protección radiológica del paciente [1–8].

Con el objeto de proteger al hombre contra los efectos nocivos de las radiaciones ionizantes (RI) sin que esto conspire contra los beneficios asociados a su aplicación en los distintos ámbitos, la radioprotección se funda sobre tres principios básicos: la justificación, la optimización y la limitación de las dosis [9]. La protección radiológica del paciente se sustenta en los dos primeros principios.

## **2.- La justificación de las prácticas médicas: ¿un nuevo paradigma?**

En toda nueva práctica médica de carácter diagnóstico o terapéutico hay una etapa de justificación genérica del procedimiento por parte de las asociaciones profesionales en coordinación con autoridades competentes. Una vez reconocida como práctica de rutina, se impone la justificación de cada caso individual por parte del médico solicitante y de los especialistas que van a efectuar dicho procedimiento.

La justificación de una práctica diagnóstica se sustenta en la consideración de que la información esperada a partir de la misma contribuirá a confirmar un diagnóstico u orientar la estrategia terapéutica. El beneficio esperado debe ser superior al que aportaría otra técnica alternativa que involucre menores dosis o que no implique exposición a RI.

Para las prácticas de naturaleza terapéutica la justificación está implícita en la convicción del médico radioterapeuta o especialista en medicina nuclear de que la misma constituye el tratamiento indicado para la patología que presenta el paciente, tomando en consideración toda la información aportada por el médico que la solicitó.

La directiva EURATOM 97/43 [10] recomendó la elaboración de criterios de indicación para prácticas de carácter diagnóstico con el objeto de garantizar que tales exámenes sean solicitados sólo cuando estén debidamente justificados. Un ejemplo de implementación práctica de estas recomendaciones es la publicación por parte de la Comisión Europea de la “Guía para la correcta solicitud de pruebas de diagnóstico por imagen” [11]. Esta guía clasifica las indicaciones de los exámenes de diagnóstico por imágenes en función de los síntomas y/o signos que caracterizan las distintas situaciones clínicas. Los exámenes se categorizan de acuerdo al rango de dosis efectiva asociada a los mismos (cuadro 1). Asimismo la guía incorpora un doble sistema de categorización del nivel de indicación que tiene cada práctica en base a la experiencia clínica y a la demostración de la evidencia de su utilidad a la luz de trabajos científicos reconocidos (cuadro 2). Este sistema responde al criterio de la medicina “basada en la evidencia” aplicado en la actualidad en otros ámbitos asistenciales.

**Cuadro 1.** Categorización de las prácticas diagnósticas de acuerdo al rango de dosis efectiva asociada (valores medios para adultos)

Clase	Rango de dosis efectiva (mSv)	Ejemplos
0	0	Ultrasonido, resonancia magnética
I	< 1	Rx de tórax, extremidades, articulaciones, pelvis, cráneo, columna dorsal
II	1 – 5	Urograma excretor, mamografía, abdomen simple, seriada gastroduodenal, Rx de columna lumbar, tomografía computada de cabeza y cuello, centellograma tiroideo y óseo, renograma, ventilación/perfusión
III	5 – 10	Tomografía computada de tórax, abdomen y pelvis, colon por enema, estudios de dinámica cardíaca por medicina nuclear
IV	> 10	Ciertas exploraciones de medicina nuclear

**Cuadro 2.** Categorización del nivel de indicación de las prácticas diagnósticas

Experiencia clínica	Tipo de validación internacional
<ul style="list-style-type: none"> <li>• Examen indicado</li> <li>• Examen especializado prescripto luego de discusión con el especialista en diagnóstico por imágenes</li> <li>• No indicado en primera intención</li> <li>• No indicado habitualmente</li> </ul> <p>No indicado</p>	<p><b>A:</b> ensayos randomizados, meta-análisis, estudios sistemáticos</p> <p><b>B:</b> trabajos experimentales u observaciones confiables</p> <p><b>C:</b> otros elementos probatorios fundados en opinión de expertos y avalados por autoridades en la materia. Se incluyen en esta categoría las indicaciones para las que los datos científicos son contradictorios</p>

### 3. La optimización de las prácticas médicas

Una vez justificado el procedimiento, se deberán crear las condiciones que permitan optimizar la relación entre la dosis absorbida a nivel del paciente y la calidad de la imagen que garantice de cumplimiento del propósito diagnóstico. En el caso de las prácticas terapéuticas la optimización implica alcanzar una dosis que garantice un óptimo control de la patología con la máxima

protección de los tejidos sanos vecinos. No corresponde la aplicación de límites de dosis en pacientes sometidos a prácticas diagnósticas o irradiaciones terapéuticas. Sólo se recomiendan restricciones de dosis en el caso de los voluntarios incluidos en programas de investigación y acompañantes de pacientes.

Estos objetivos sólo pueden ser alcanzados en el marco de la ejecución de programas de garantía de calidad. Estos deberían incluir la redacción de procedimientos escritos que protocolicen conductas frente a las distintas situaciones posibles, como etapa previa a la acreditación de los Servicios de Diagnóstico por Imágenes, Radioterapia y Medicina Nuclear. Deben considerarse en forma particular las exposiciones médicas pediátricas y la protección de la mujer gestante.

#### **4. Niveles de referencia diagnósticos (NRD)**

La noción de NRD fue introducida por la Comisión Internacional de Protección Radiológica (ICRP) [3] e incluida en la Directiva EURATOM 97/43. En el año 2001 el Comité 3 del ICRP se abocó a la preparación de un documento específico sobre este tema [12].

Se trata de un concepto de aplicación específica en el ámbito de la exposiciones médicas referido a niveles de dosis en radiodiagnóstico determinados en base a mediciones y/o cálculos (o niveles de actividad administrada en medicina nuclear obtenidos mediante encuestas) correspondientes a exámenes “tipo” realizados en pacientes o fantomas de características “standard”, en un dado país o región.

Los NRD son indicadores de la calidad de equipos y procedimientos, no se aplican a casos individuales, no constituyen límites ni son “dosis óptimas”. Su valor numérico no surge de un valor promedio sino que se establece mediante un método estadístico tomando en consideración el percentil 75 de la distribución de dosis medidas (o de las actividades administradas). Esto significa que en un 25% de los casos las dosis (o actividades) se sitúan por encima del NRD [13]. Identificando y eliminando las causas, la curva gaussiana se desplazará hacia la izquierda con la consecuente disminución del valor de NRD. Aquí reside el rasgo “dinámico” del concepto de NRD: partir del conocimiento de una realidad local para intentar modificarla teniendo a la reducción progresiva de las dosis hasta alcanzar un valor óptimo. No debe olvidarse que la noción de NRD es indisociable de la de “calidad informativa de la imagen”. Es asimismo un concepto evolutivo que deberá actualizarse acorde al desarrollo de la tecnología disponible en cada país y/o región.

#### **5. La Propuesta**

Se propone generar un plan de acción de Protección Radiológica del Paciente sustentado en la búsqueda de acuerdos y convergencias con autoridades sanitarias, sociedades científicas y asociaciones profesionales. La modalidad propuesta para la ejecución de este plan de acción es la constitución de grupos de trabajo interdisciplinarios para abocarse a algunas tareas básicas:

- análisis conjunto de recomendaciones y directivas internacionales a partir de documentos-base y adecuación de dichas recomendaciones a las condiciones nacionales;
- elaboración de guías orientativas sobre indicaciones para la solicitud de exámenes en pacientes adultos y pediátricos;
- promoción de acciones tendientes a la implementación de sistemas de calidad en las exposiciones médicas;
- discusión de procedimientos para pacientes adultos y pediátricos que contribuyan a la optimización de las dosis;

- determinación de niveles de referencia diagnósticos (NRD);
- promoción de actividades de formación de recursos humanos tendientes a introducir la noción de la cultura de la radioprotección desde el pre-grado;
- promoción de la formación teórico-práctica de los especialistas, su re-entrenamiento y actualización;
- aprovechamiento de herramientas informáticas para la difusión de la cultura de la seguridad (páginas WEB; enlaces a sitios de interés (internacionales, regionales y nacionales) que permitan acceder a bibliotecas virtuales, documentos, guías, materiales educativos, etc.

## **6. Perspectivas futuras**

El uso racional de las técnicas de diagnóstico por imágenes contribuirá a la supresión de exámenes “inútiles” constituyendo así una medida simple y eficaz de radioprotección. La jerarquización del principio de justificación parece plantear un cambio de paradigma en el enfoque actual de la protección radiológica del paciente. En este contexto adquiere una nueva relevancia la figura del médico que prescribe una dada práctica quien, junto al especialista en diagnóstico por imágenes, radioterapia o medicina nuclear, será co-responsable de la aplicación del principio de justificación.

En lo concerniente a la optimización de las dosis como a la implementación de los NRD la convocatoria se extiende más allá de los médicos y radioproteccionistas. La figura del especialista en física médica está llamada a jugar un rol relevante en la coordinación de las acciones así como la del técnico especializado para la ejecución de las mismas.

La ejecución de un plan de acción conjunto para la Protección Radiológica del Paciente en el ámbito nacional posibilitaría la optimización de recursos humanos y materiales.

## **7. Bibliografía de referencia**

- [1] ICRP Publication 34: *Protection of the patient in diagnostic radiology* Annals of the ICRP Vol 9/2 (1983).
- [2] ICRP Publication 52: *Protection of the patient in nuclear medicine* Annals of the ICRP Vol 17/4 (1988).
- [3] ICRP Publication 73: *Radiological Protection and Safety in Medicine* Annals of the ICRP Vol 26/2 (1996).
- [4] Documents of the NRPB Vol 10 “*Guidelines on Patient Dose to promote the optimization of protection for diagnostic medical exposures*” (1999).
- [5] ICRP Publication 84: *Pregnancy and Medical Radiation* Annals of the ICRP Vol30/1 (2000).
- [6] Proceedings of the International Conference on the *Radiological Protection of Patients in Diagnostic and Interventional Radiology, Nuclear Medicine and Radiotherapy*, Málaga, Spain (2001).
- [7] IAEA Safety Standards Series N°-RS-G-1.5 *Radiological Protection for Medical Exposure to Ionizing Radiation* (2002).
- [8] Dossier: *La radioprotection des patients* Contrôle (Revue de l'Autorité de Sûreté Nucléaire) N° 148 (2002).

[9] ICRP Publication 60: *Recommendations of the International Commission on Radiological Protection* Vol 21/ 1-3 (1991) .

[10] Directiva EURATOM 97/43 del Consejo sobre protección de la salud en relación con exposiciones médicas (1997).

[11] Guía de Protección Radiológica N° 118 de la Comunidad Europea “Indicaciones para la correcta solicitud de pruebas de diagnóstico por imagen” (2000).

[12] Documento del Comité 3 del ICRP “*Diagnostic reference levels in medical imaging*” Draft en [www.icrp.org](http://www.icrp.org) (2001).

[13] Beauvais-March H, Valero M., Biau A. y Bourguignon M. *Niveaux de référence diagnostiques: spécificités de la démarche française en radiologie* Radioprotection Vol 38 (2): 187-200 (2003).



# Apoptosis of Neural Precursor Cells Following Gamma Irradiation is Early Modulated by Free Radicals

Robello, E.; Dubner, D.L.; Michelin, S.C.; Perez M. del R.;  
Puntarulo, S. and Gisone, P.A.



# **Apoptosis of Neural Precursor Cells Following Gamma Irradiation Is Early Modulated by Free Radicals**

**E. Robello<sup>1</sup>, D. Dubner<sup>2</sup>, S. Michelin<sup>2</sup>, M.R. Pérez<sup>2</sup>,  
S. Puntarulo<sup>1</sup> and P. Gisone<sup>2</sup>**

*<sup>1</sup>Physical Chemistry Department, School of Pharmacy and Biochemistry,  
University of Buenos Aires, Buenos Aires, Argentina. <sup>2</sup>Nuclear Regulatory  
Authority (ARN) Scientific Support, Radiopathology Lab; Buenos Aires, Argentina*

## **Summary**

Radiation-induced nitric oxide (NO) generation in cortical precursor cultures was highly increased within 1 h post-irradiation (pi) and free radical production was observed after 2 h pi. However, when NO production was inhibited by L-NAME, not only a higher radiation-induced luminol-dependent chemiluminiscence (CL) but also an enhanced radiation-induced apoptosis (at 24 h pi) was observed. Moreover, if SOD was added to L-NAME treated cells, a decline in CL occurred within 2 h pi. Inhibition of caspase-3 activity produced a decrease in CL after 2 h pi. These data indicated that NO could act as an antioxidant and neuroprotective factor in an early period immediately after irradiation *in vitro*; besides, it is suggested that caspase-3 activity is closely related to a late free radical generation.

## **Introduction**

The developing brain is highly sensitive to ionizing radiation, even under very low doses. An increased prevalence of severe mental retardation has been epidemiological evidenced in children who were prenatally exposed to the atomic bombing of Hiroshima and Nagasaki (1). Cell Responses to radiation are most likely initiated by radiation-induced free radical production. Moreover, apoptosis, the typical mode of radiation-induced cell death in developing central nervous system, is closely related to the oxidative status (2). NO has been shown to have both

neuroprotector and neurotoxic roles, depending on its concentration, the studied cell-type, and the oxidative-reductive cell status (3). In a previous work we have showed a dose-dependent radiation induced activation of caspase-3 detectable at 2 h pi with a maximum at 4 h pi, which was concurrent with the beginning of the apoptosis (4). This study was performed to address the participation of radiation-induced radical production in modulating the apoptotic response in an *in vitro* model of neural cortical precursor cells exposed to Gamma radiation.

## Materials and Methods

Wistar female rats were mated overnight and the pregnant ones, identified by sperm positive vaginal smears, were considered at gestational day (gd) 0. Primary cell cultures were prepared according to Flint (5). The cultures were irradiated at a dose rate of 0.3 Gy/min with a  $^{60}\text{Co}$  teletherapy unit with 2 Gy dose. Apoptotic cell fractions were analyzed by flow cytometer according to Darzynkiewicz et al. (6), and where indicated, 500  $\mu\text{M}$  L-NAME was added to the media 1 h before irradiation.  $\text{NO}_2^-$  plus  $\text{NO}_3^-$  release to the culture medium was determined according to Verdon et al. (7) and  $\text{NO}_2^-$  content was measured by the Griess reaction. Cells ( $1 \times 10^6$ ) resuspended in PBS were supplemented with 100  $\mu\text{M}$  of luminol and chemiluminiscence (CL) was measured in a Packard 1500 Tri-CARB® liquid scintillation analyzer.

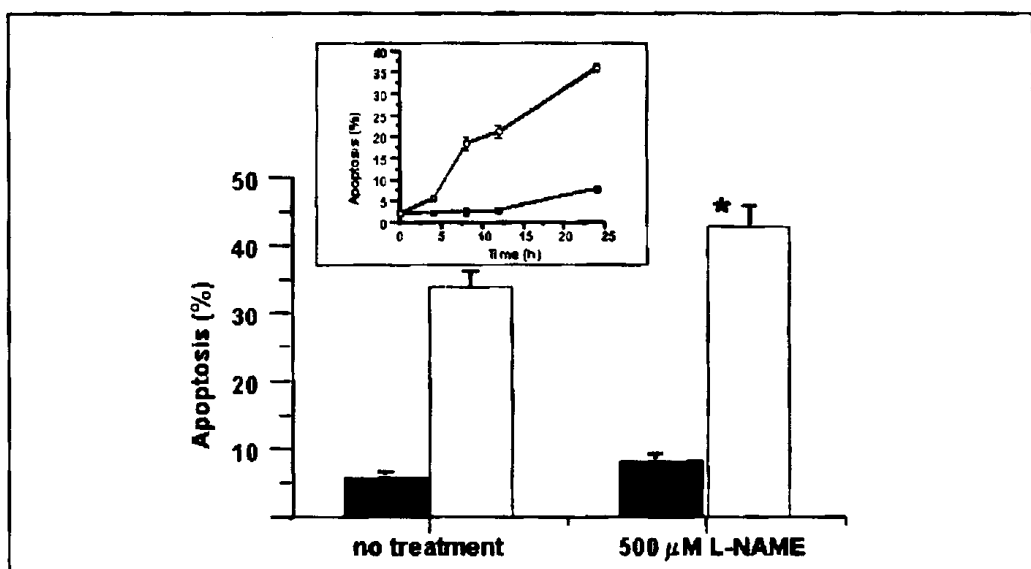


**Fig. 1:** Effect L-NAME on the content of radiation-induced apoptotic cells 24 h after irradiation. Control (■), irradiated cells (□). Inset: Time course of apoptotic process. Control (■), irradiated sample (○). Data are means  $\pm$  SE.

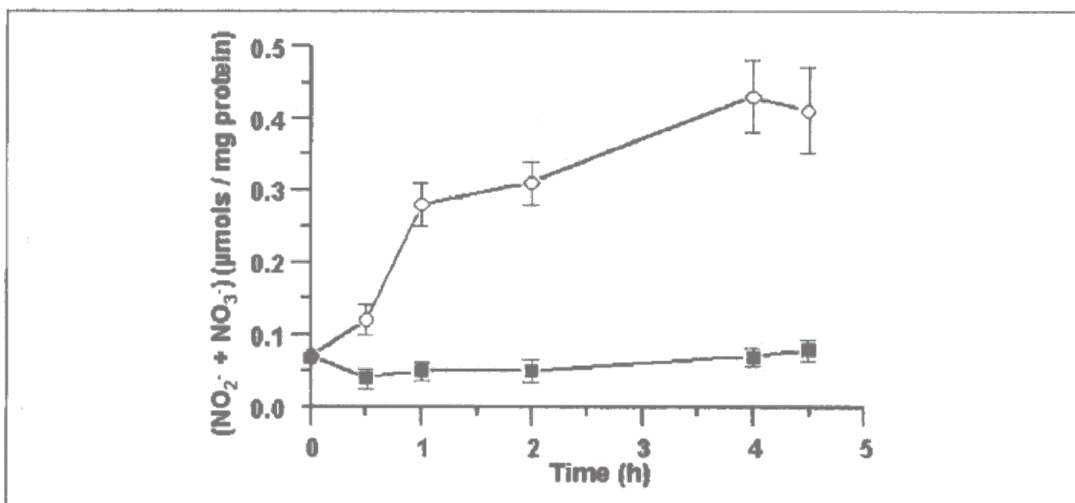


Fig. 2: Time course for  $\text{NO}_2^-$  and  $\text{NO}_3^-$  accumulation in the culture media. Control (■), irradiated cells (○). Data are means  $\pm$  SE.

## Results

Inhibition of NO production by L-NAME significantly increased the apoptotic fraction in irradiated samples treated at 24 h pi (Fig. 1). The apoptotic response to radiation injury revealed a time-dependence mode, showing a significant difference from control cells after irradiation with 2 Gy (Fig. 1, inset). The content of NO content stable products,  $\text{NO}_2^-$  and  $\text{NO}_3^-$ , has showed a time-dependent accumulation within 1 h pi with 2 Gy (Fig. 2). Luminol-dependent CL of the culture cells exposed to 2

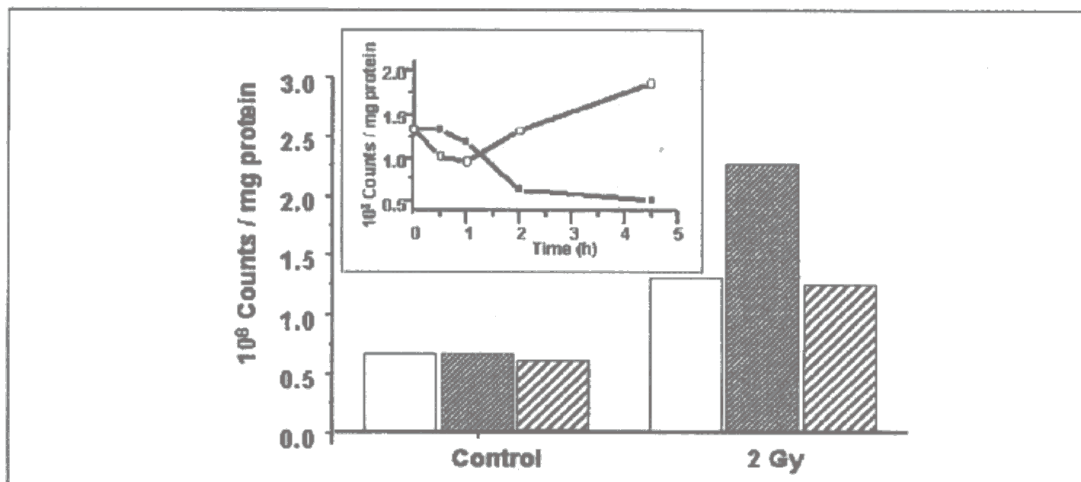


Fig. 3: Effect of inhibitors on luminol-dependent CL. Cells not supplemented (□), cells supplemented with 500  $\mu\text{M}$  L-NAME (▨), and cells supplemented with 500  $\mu\text{M}$  L-NAME and 50 U/ml SOD (▨). Shown data correspond to a representative experiment. Inset: Time course of luminol-induced CL in control (■) and radiation exposed cells (2 Gy) (○).

Gy radiation was significantly increased as compared to control cells (Fig. 3, inset). L-NAME supplementation to irradiated cells induced an increase in CL (Fig. 3). When SOD was added to L-NAME treated cells irradiated with 2 Gy, the L-NAME effect was inhibited (Fig. 3). A caspase inhibitor (zDEVD-fmk) was tested on cellular CL. The addition of zDEVD-fmk to the reaction medium prevented the increase of reactive species generation by radiation 2 h pi (data not shown).

## Conclusions

Our results showed that NO release follows a time-dependent accumulation pattern. This fact is consistent with previous results from experiments performed employing *in utero* irradiated fetus (8). Moreover, the study in the presence of the inhibitors suggested that NO could be acting in an early period immediately after irradiation as an anti-oxidant *in vitro*. Addition of SOD significantly decreased the CL in irradiated samples treated with L-NAME. Thus, O<sub>2</sub><sup>-</sup> seems to be one of the radiation-induced species that is produced in these cells. Since apoptosis was significantly increased in irradiated cells after incubation with L-NAME, NO could be acting as a neuroprotective factor in this system. The data presented here suggest that after *in vitro* irradiation of neural precursor cells there is an early radiation-induced increase in the generation of NO, exerting neuroprotector effects. Free radical generation seems to be able to modulate the apoptotic response and, at least in part, caspase-3 appears to be responsible for the late free radical burst.

## References

1. STREFFER C, PATRICK G, Effects of prenatal irradiation with special emphasis on late effects, EULEP symposium, 29 July 1982, Bordeaux (France), EUR-8067, Report, Bruselas, Luxemburgo, Commission of the European Communities, 1984.
2. INTERNATIONAL COMMISSION OF RADIATION PROTECTION, Developmental effects of irradiation on the brain of the embryo and fetus, Annals of the ICRP, 16 (4), Publication 49, Pergamon Press. Oxford, UK, 1986.
3. JOSH MS, PONTHIER JL, LANCASTER JR, JACK R, Cellular antioxidant and pro-oxidant actions of nitric oxide. Free. Radic. Biol. Med., 27, 1357-1366, 1999.
4. MICHELIN S, PÉREZ MR, DUBNER D, GISONE P, Increased activity and involvement of caspase-3 in radiation-induced apoptosis in neural cells precursors from developing brain. Neurotoxicology, In press.
5. FLINT O, A micromass culture method for rat embryonic neural cells. J. Cell. Sci., 61, 247-62, 1983.
6. DARZYNKIEWICZ Z, JUAN G, LI X, GORCZYCA W, MURAKAMI T

- AND TRAGANOS F, Cytometry in cell necrobiology: analysis of apoptosis and accidental cell death 8 necrosis. *Cytometry*, 27, 1-20, 1997.
7. VERDON CP, BURTON B, PRIOR R, Sample pretreatment with nitrate reductase and glucose-6-phosphate dehydrogenase quantitatively reduces nitrate while avoiding interference by NADP<sup>+</sup> when the Griess reaction is used to assay for nitrite. *Anal. Biochem.*, 224, 502-8, 1995.
  8. GISONE P, BOVERIS AD, DUBNER D, PÉREZ MR, ROBELLO E, PUNTARULO S, Early neuroprotective effect of nitric oxide in developing brain irradiated in utero. *Neurotoxicology*, 182, 1-9, 2002.



# NDA Measurements for Isotopic Homogeneity of UO<sub>2</sub> Powder from Mechanical Blending and Results Comparison between Gamma and Mass Spectrometry

Rojas, C.A.; Rojo, M. and Cristallini, O.



**NDA MEASUREMENTS FOR ISOTOPIC HOMOGENEITY OF UO<sub>2</sub>  
POWDER FROM MECHANICAL BLENDING AND RESULTS  
COMPARISON BETWEEN GAMMA AND MASS SPECTROMETRY**

Rojas, C.A. y Rojo, M.  
Nuclear Regulatory Authority

Cristallini, O.  
Brazilian-Argentine Agency for Accounting and Control of Nuclear Materials  
Argentina

**ABSTRACT**

Eight batches of 0.95% UO<sub>2</sub> powder, obtained by mechanical blending of 3.5% and 0.711 % UO<sub>2</sub> powders, were sampled. From each batch, samples at the top and the bottom from four drums were taken.

Each sample was analysed using different measurement systems, two with NaI(Tl) detectors and another two with HPGe detectors. The Mini Multichannel Analyser (MMCA), model GBS 166, and the calculation codes NaIGEM and MEGAU-EM for peak area analysis and enrichment determination were used. For all cases the WinSPEC acquisition code was used.

From the statistical analysis of the measurement results it arises that it is possible to determine the homogeneity grade of UO<sub>2</sub> powder samples with a lower error than 0.5% for both types of detectors. The performance of the HPGe measurement system is only slightly more precise than the NaI system.

**1. INTRODUCTION**

The production of UO<sub>2</sub> powders of specific enrichment from mechanical blending requires a very strict control of the blending homogeneity. It is important an appropriate sampling from each production batch, followed by the analysis of each sample to determine their isotopic composition.

The commonly used method for isotopic analysis is the mass spectrometry. This technique, fully proven, assures very exact and precise results, but it is associated to very high costs and long analysis times. Besides, the homogeneity control of the UO<sub>2</sub> powder mixtures, require sampling and isotopic analysis of a big number of drums, with an error lower than 0,5% in a short time, mainly at the process starting point.

The gamma spectrometry technique for measuring enrichment, fully used in nuclear safeguards, requires less expensive equipment than the mass spectrometry technique and the equipment required is very easy to be operated and maintained. Gamma spectrometry technique, properly implemented, can offer very precise results with relatively short measurement times. This enrichment measurement method, although intrusive as it requires sampling, is still a Non Destructive Assay (NDA) method.

### **3. PROCEDURE**

#### **3.1 Measurement Systems**

Four different measurement systems were used, two with scintillation and two with semiconductor detectors. In all cases for spectral analysis it was used a portable Mini Multichannel Analyser, MMCA-166 GBS Elektronik, which includes an amplifier and a high voltage polarisation source (HV).

The scintillation detectors consist of a 2"x1" NaI mono crystal activated with Tl, coupled to the photomultiplier tube and preamplifier with an external shielding and collimator.

The semiconductor detectors are constituted by a HPGe mono crystal (LEGGe), provided with an external shielding and a collimator, coupled to a preamplifier with field effect transistor (FET), mounted on a cryostat cooled with liquid N<sub>2</sub>. The technical features in both systems are given in chart 1.

In all the cases the WinSPEC program was used for data acquisition and the NaIGEM and MGAU-EM programs were used for enrichment measurement of the samples with quasi-infinite thickness for the NaI and HPGe detectors.

The CBNM-295-023 patron was used ( $2,9492 \pm 0.0021\%$  U-235) to obtain the calibration spectra for the four measurement systems.

**CHART 1: Characteristic of the detection systems**

System	Detector	Size	shielding Pb	Collimator Pb	Cd	Resolution 186keV	Net area	
			cm	cm	mm	canales	cps/%U <sup>235</sup>	
NaI-1	NaI	2"x1"	1	4 x 1,5	1	29	19.3	289
NaI-2	NaI	2"x1"	1	2.9 x 2	1	31	19.6	93
GeHP-1	LEGGe GL2015R	2000 mm <sup>2</sup> x 15 mm	1	3 x 1,5	1	8	0.716	72
GeHP-2	GL0515R	500 mm <sup>2</sup> x 15 mm	1	2.5 x 0.7	1	8.6	0.770	39

#### **3.2 SAMPLING**

For each measurement system, 64 UO<sub>2</sub> powder samples from eight production batches, of approximately 200 g each, were measured. For each batch eight samples from four drums were taken. The samples were collected at the top and at the bottom of the drums, what stands for two samples from each drum.

Each sample was taken in an Al container of 6 cm diameter and 3 cm height, with uniform bottom thickness of  $1,15 \pm 0.01$  mm. The sample mass, for the recipient size and the selected geometry were adapted to fulfill, for all the measurement systems, the quasi-infinite geometry condition required for the enrichment determination for NaIGEM and MGAU-EM codes.

## **4. RESULTS**

The enrichment measurement results for all the samples, analyzed with different gamma spectrometry systems, are shown in chart 2, each line corresponds at a batch where it can be seen mean values, standard deviations and bias, for each measurement system. The last three columns correspond to the average of the mean values and its associated standard and bias deviation for the four systems for each batch.

In Figure 1 it is shown an statistical graph for all the measurements systems with its associated error, mean value and limits for  $\sigma = 0.5\%$  for all the samples taken.

In figure 2, it is shown an statistical graphic, only for batch 1, for the 4 measurement systems, their associated error, mean value and limits for  $\sigma = 0.5\%$

From figures 3 to 6, it can be seen the statistical graphics of all the measurements for each system and for the considered batches with their associated error, mean value and limits for  $\sigma = 0.5\%$

## **5. ANALYSIS OF THE RESULTS**

The mean values obtained with HPGe-1, HPGe-2 and NaI-2 systems don't differ from the reference value. Meanwhile, with the NaI-1 system there is a difference between the obtained mean value ( $MV = 0.951$ ) and the reference value ( $RV = 0.955$ ). The reason for this is that in the case of the NaI-1 system with a  $40 \times 15\text{mm}$  collimator, the quasi-infinite thickness condition was not fulfil, for the dimensions of the sample recipient.

Sources of significant statistical errors were not detected with any of the measurement systems.

In respect to the measurement systems performance it can be seen that in systems 1 a less dispersion (more precision) is shown than from systems 2. In these last ones an inferior bias (higher exactitude) is shown. In all cases, however, the standard deviation and the bias are inferior to 0,5% (Figure 7).

## **6. CONCLUSION**

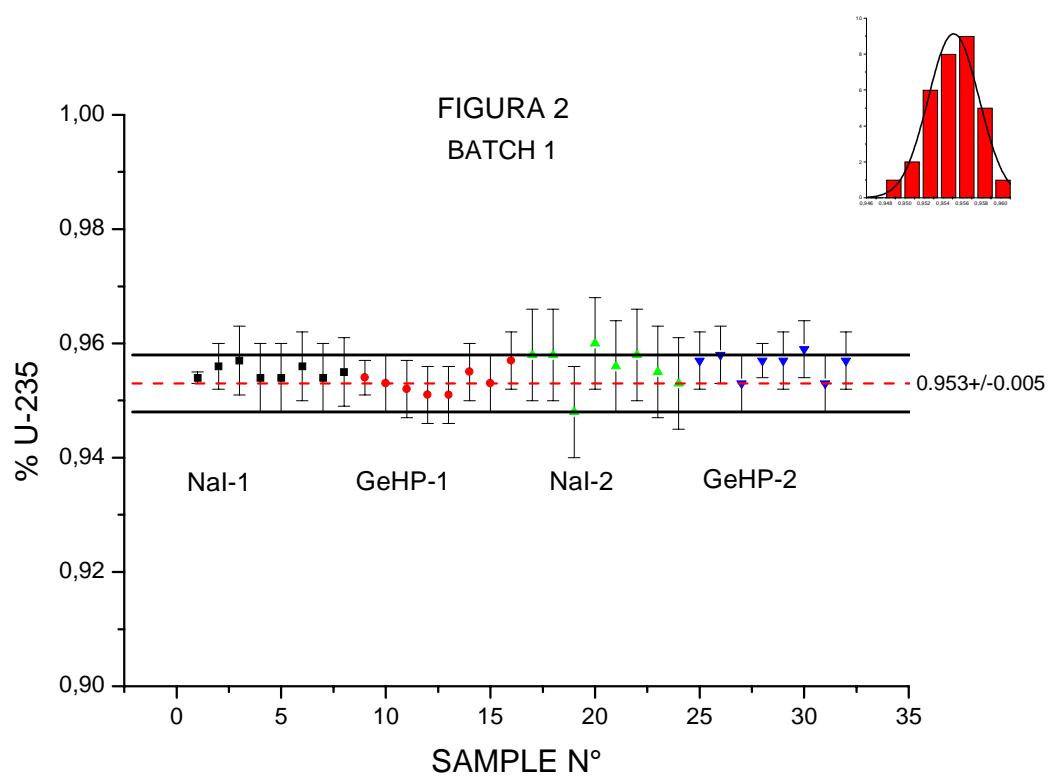
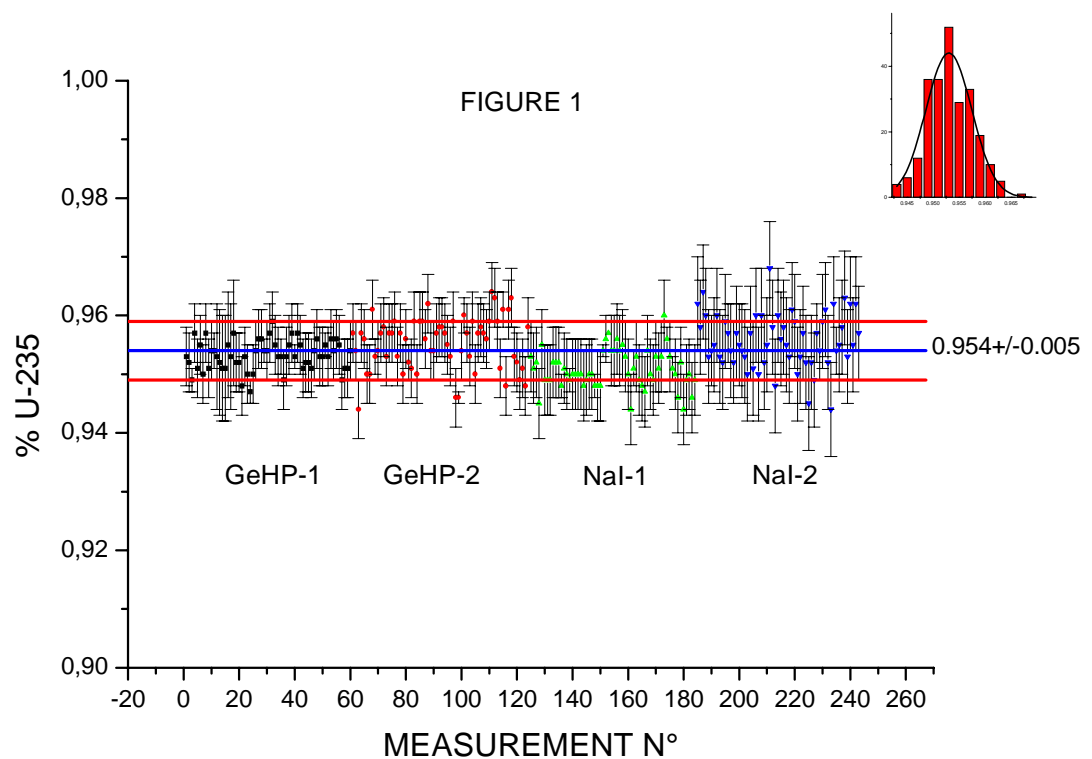
The obtained results show the viability of the gamma spectrometry method for enrichment measurement to be used in the control of homogeneity of a mechanical blending of UO<sub>2</sub> powder, as well as, the similar performance between the NaI(Tl) systems with the NaIGEM code, and the HPGe systems with the MGAU-EM code.

## **8. ACKNOWLEDGMENT**

We want to offer our acknowledgment to Lic. Adolfo Esteban for his worthy suggestions and corrections.

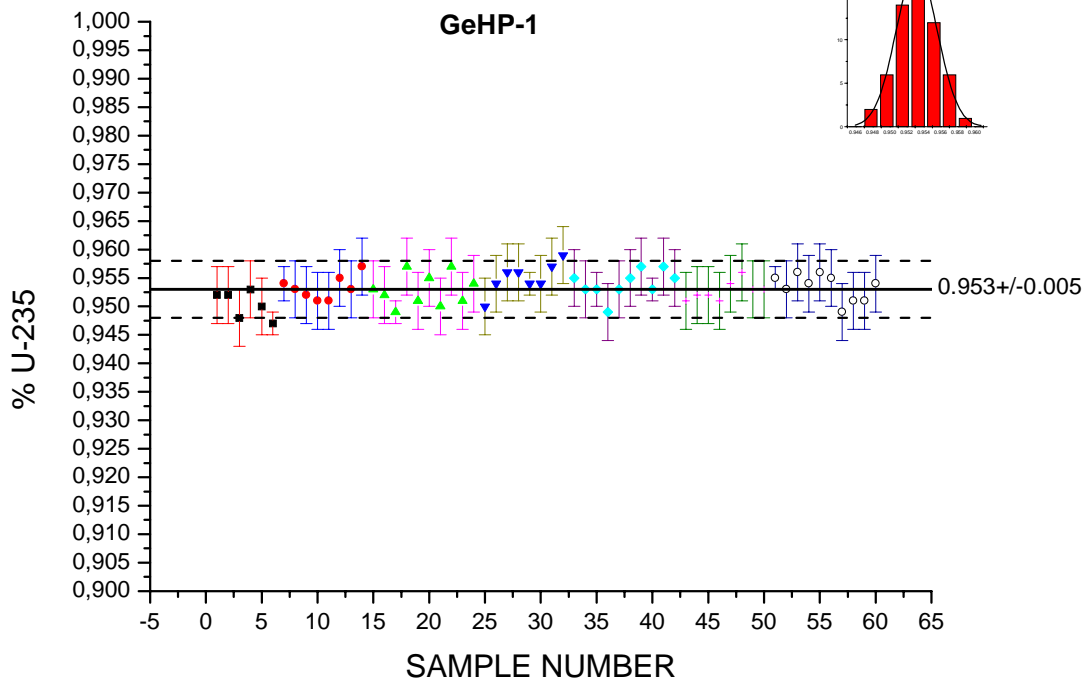
## **8. BIBLIOGRAPHY**

- ❖ J. Morel et al. Results from Uranium Enrichment Measurement exercise. *Final Report*, Note technique LPRI/98/23, DAMRI, 1998
- ❖ Aigner,H, Khun E, Deron S, Results of the Analysis of the Inter comparison Samples of the Natural Dioxide SR-1, IAEA/RL/69, August 1980.
- ❖ Matussek P, Gamma-Spectroscopic Measurements of the U-235 Isotope Abundance in a UF<sub>6</sub> Sample. KfK 4784 October 1990, Page. 3, Fig 1.



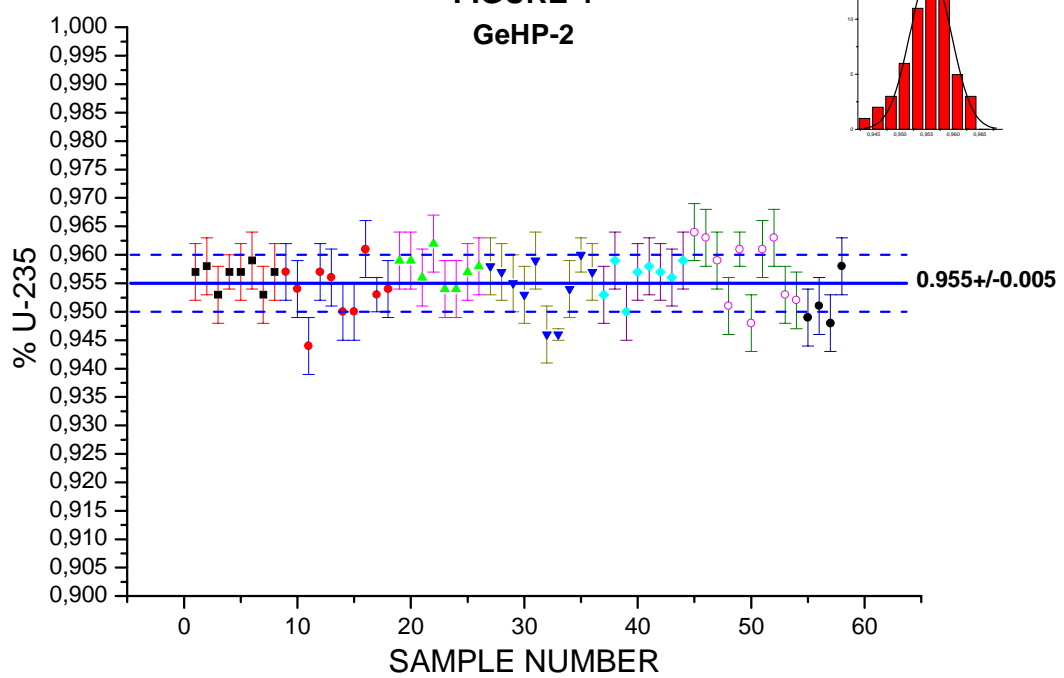
**FIGURE 3**

**GeHP-1**



**FIGURE 4**

**GeHP-2**



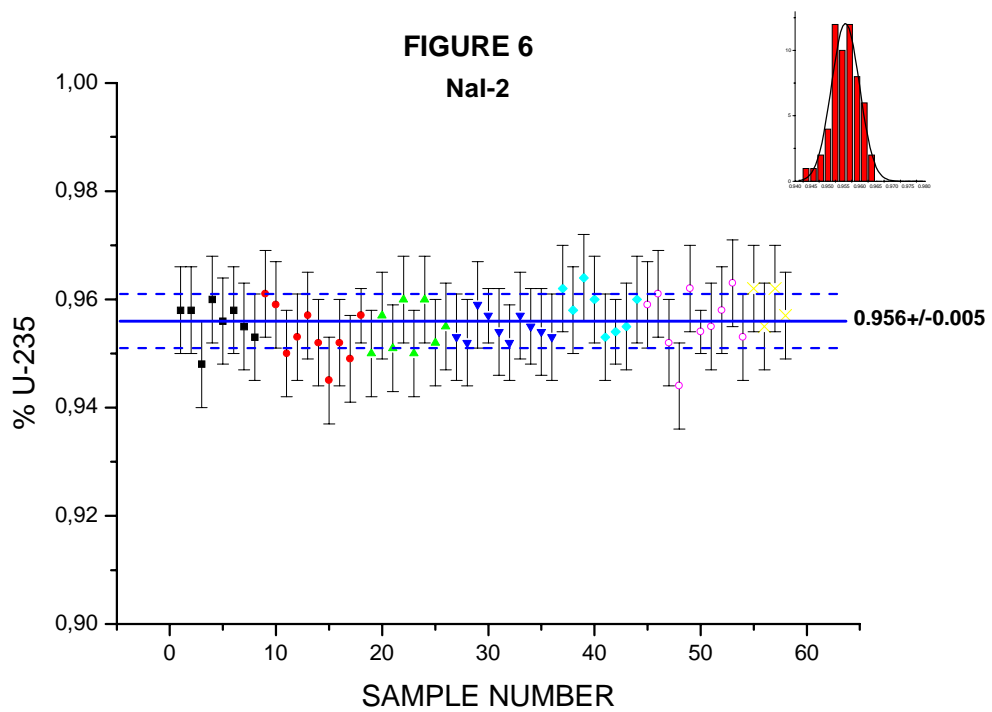
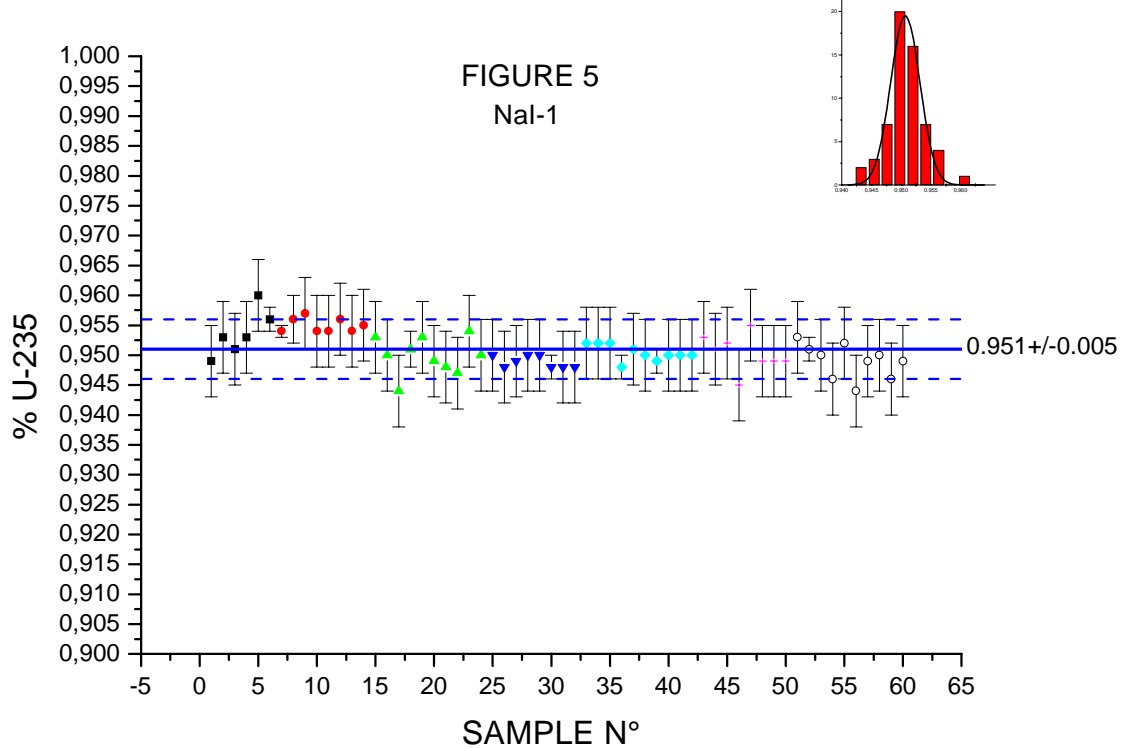


FIGURE 7

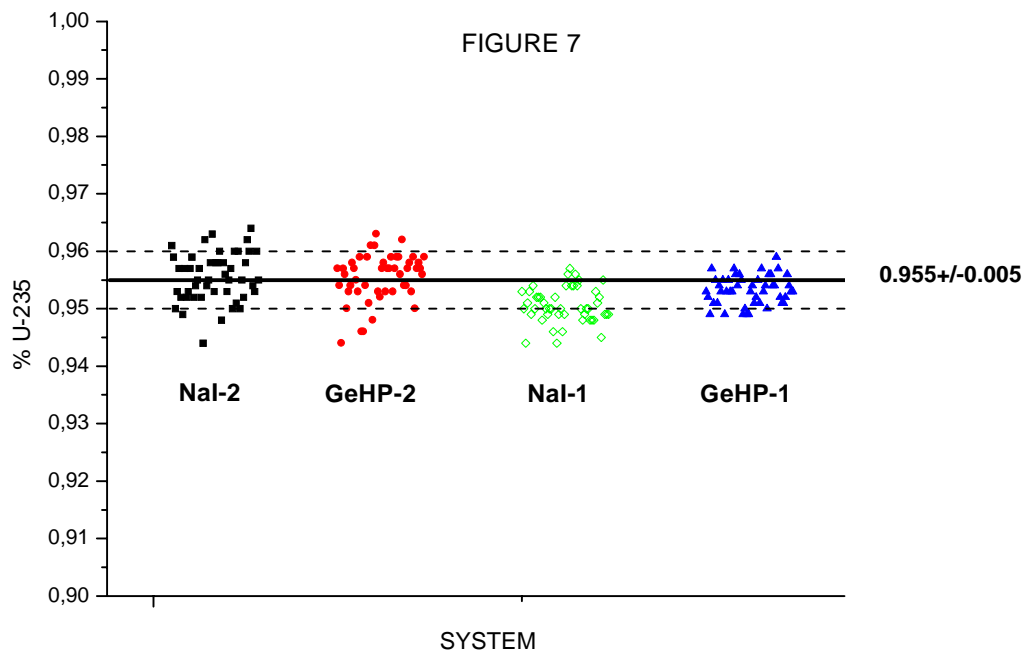


CHART 2

BATCH	E	E ± σE		σE	Bias	E ± σE		σE	Bias	E ± σE		σE	Bias	E ± σE		σE	Bias			
UO2	% U235	% U235		%	%	% U235		%	%	% U235		%	%	% U235		%	%			
	Ref. Value	NalGEM 1				MGAU-EM 1				NalGEM 2				MGAU-EM 2				Mean Values		
BATCH 1	0,955	0,954	± 0,004	0,4	-0,1	0,950	± 0,002	0,4	-0,5					0,953	± 0,004	0,4	-0,2	0,952	± 0,002	-0,3
BATCH 2	0,955	0,955	± 0,001	0,13	0,00	0,953	± 0,002	0,2	-0,2	0,956	± 0,004	0,4	0,1	0,956	± 0,002	0,2	0,14	0,955	± 0,001	0,01
BATCH 3	0,955	0,950	± 0,003	0,31	-0,5	0,953	± 0,003	0,3	-0,2	0,954	± 0,005	0,49	-0,2	0,954	± 0,005	0,5	-0,1	0,952	± 0,003	-0,3
BATCH 4	0,955	0,949	± 0,001	0,1	-0,6	0,955	± 0,003	0,3	0,0	0,954	± 0,004	0,4	-0,1	0,957	± 0,003	0,3	0,2	0,954	± 0,002	-0,1
BATCH 5	0,955	0,950	± 0,001	0,1	-0,5	0,954	± 0,002	0,2	-0,1	0,955	± 0,002	0,2	0,0	0,955	± 0,005	0,5	-0,1	0,953	± 0,001	-0,2
BATCH 6	0,955	0,950	± 0,003	0,3	-0,5	0,953	± 0,002	0,2	-0,2	0,958	± 0,004	0,4	0,3	0,956	± 0,003	0,3	0,1	0,954	± 0,001	-0,1
BATCH 7	0,955	0,949	± 0,003	0,3	-0,6	0,953	± 0,002	0,2	-0,2	0,956	± 0,006	0,6	0,1	0,958	± 0,006	0,6	0,3	0,954	± 0,003	-0,1
BATCH 8	0,955	0,949	± 0,001	0,1	-0,6	0,954	± 0,003	0,3	-0,1	0,959	± 0,004	0,4	0,4	0,952	± 0,005	0,5	-0,4	0,955	± 0,002	0,0

# Dosimetría interna en medicina nuclear: dosis absorbida en el feto por la administración de radiofármacos a la madre

Rojo, A.M. y Michelin, S.C.



# **DOSIMETRÍA INTERNA EN MEDICINA NUCLEAR: DOSIS ABSORBIDA EN EL FETO POR LA ADMINISTRACIÓN DE RADIOFÁRMACOS A LA MADRE**

Rojo, A.M. y Michelin, S.C.

Autoridad Regulatoria Nuclear  
Argentina

## **INTRODUCCIÓN**

Las fuentes de radiaciones ionizantes (RI) pueden ser de origen natural o artificial (producidas por el hombre). Las primeras contribuyen con el 85,5% de la dosis recibida mientras que los usos médicos de las radiaciones ionizantes con fines diagnósticos y terapéuticos representan el 14%. El resto se divide entre los productos de antiguos ensayos nucleares atmosféricos y productos de la energía nuclear. Entre las aplicaciones médicas, la administración de radiofármacos a la mujer en momentos previos y durante la gestación implica que también el embrión o feto estará expuesto a una dosis determinada.

Este documento resume conceptos básicos sobre radiaciones ionizantes, las magnitudes y unidades dosimétricas utilizadas y las dosis recibidas por el embrión o feto debido a la utilización de  $^{99m}\text{Tc}$ ,  $^{131}\text{I}$ ,  $^{201}\text{TI}$  y  $^{67}\text{Ga}$  en las prácticas médicas más frecuentes con fines diagnósticos y terapéuticos.

### **Conceptos básicos sobre radiaciones ionizantes**

El término radiación describe un proceso por el cual la energía producida en una reacción atómica es liberada y transferida a distancia. Las radiaciones se clasifican en ionizantes y no ionizantes dependiendo de su energía para producir iones a partir de los átomos con los que interactúan. En este trabajo solo nos referiremos a las RI. Las RI pueden ser: a) radiación electromagnética (rayos x y gamma), b) partículas, (protones, neutrones, partículas alfa, (compuestas por 2 neutrones y 2 protones) y partículas beta, (electrones o positrones).

Los rayos x se originan en un proceso que involucra cambios en los niveles orbitales de los electrones alrededor del núcleo mientras que la radiación gamma se emite desde el núcleo del átomo radiactivo durante su decaimiento hacia átomos más estables. Este decaimiento puede ir acompañado además por la emisión de rayos x y partículas.

En cuanto a la capacidad de penetración en los tejidos, puede ir desde micrones a varias decenas de centímetros dependiendo del tipo de radiación y de su energía. Para una energía dada, la radiación electromagnética, constituida por fotones, tiene una penetración muy superior a la de las partículas.

Los fotones actúan produciendo la liberación de electrones de los átomos con los que interactúan, los cuales a su vez, inducen la ionización de otros átomos.

Los protones, partículas alfa y beta son partículas eléctricamente cargadas y causan ionización directamente. Los neutrones, eléctricamente neutros, causan ionización indirectamente a partir de los protones liberados por su colisión con los núcleos. El número de ionizaciones debido a partículas alfa y protones son cientos de veces más numerosos que las debidas a electrones.

## RADIACIÓN NATURAL Y ARTIFICIAL

La radiación natural está compuesta por radionucleidos que forman parte de la corteza terrestre y por partículas de alta energía y fotones integrantes de la radiación cósmica. Esta radiación llega a la tierra siendo absorbida mayoritariamente en las capas superiores de la atmósfera, induciendo, a su vez, radiación cósmica secundaria, que es recibida por el hombre. Por otra parte, partículas cargadas de alta energía así como aproximadamente 2000 radionucleidos, pueden ser producidas artificialmente por el hombre, en ciclotrones, aceleradores lineales o reactores.

Los tiempos de semidesintegración física ( $T_{1/2}$  físico) de los radionucleidos (tiempo que tarda en decaer su actividad a la mitad) pueden ser de fracciones de segundos a millones de años. Los utilizados en medicina tienen  $T_{1/2}$  físico de pocas horas (empleados para diagnóstico), varios días y hasta años (empleados para terapia).

## FUENTES DE RADIACIÓN IONIZANTE

Aproximadamente el 86% de la dosis recibida por la población mundial, es debida a la radiación de fondo lo cual representa una dosis efectiva de 2,4 mSv/año. En la figura 1 se esquematiza la contribución de cada una de las fuentes. Se debe tener en cuenta que los niveles de radiación varían ampliamente dependiendo de la altitud y la abundancia de isótopos en rocas y suelo. El 14% restante, (0,4 mSv/año) es producido por el hombre, siendo un 10% debido a Rx y 4% por procedimientos de medicina nuclear. Estos porcentajes son considerablemente más altos en los países más avanzados debido al amplio empleo de estas técnicas.

En la figura 1 se detallan las contribuciones a la radiación natural de fondo

### Radiación Natural de Fondo (mSv/y)



Figura 1

## EFFECTOS DE LA RI

Los efectos de las radiaciones ionizantes son el resultado de complejas reacciones iniciadas por el proceso de ionización. El daño depende del nivel de exposición, para medias o altas dosis existe una pérdida de la función debido a la muerte celular. Los efectos a altas dosis son bien conocidos en radioterapia. Además de la muerte celular deseada, los efectos secundarios incluyen cambios en la piel (eritema, ulceración y necrosis), aplasia medular y edemas. Estos aparecen evidentes luego de horas o días y aumenta su severidad con el aumento de la dosis. Estos efectos se denominan, efectos determinísticos.

La probabilidad de una exposición accidental a altas dosis en el lugar de trabajo es un evento poco frecuente y puede ocurrir solamente con fuentes intensas tales como aparatos analíticos de rayos x, o fuentes selladas de radionucleidos para radioterapia y usos industriales.

Las bajas dosis pueden causar efectos que aparecerán solamente luego de un largo período. Estos efectos son denominados, efectos estocásticos y son causados por mutaciones en las células las cuales no han sido reparadas. En estos casos, la dosis absorbida no es importante para la severidad del efecto pero sí para la probabilidad de ocurrencia. Ejemplos de efectos estocásticos son la transformación neoplásica y efectos hereditarios para los cuales no existe umbral de dosis. A mayor dosis la probabilidad del efecto aumenta y podría disminuir a mayores dosis donde la muerte celular se hace evidente.

## MAGNITUDES Y UNIDADES DOSIMÉTRICAS

A continuación se definen las magnitudes y unidades dosimétricas utilizadas en protección radiológica, así como el concepto de actividad.

### Dosis absorbida, D

Con el término dosis, se define el cociente entre  $d\bar{\epsilon}$  y  $dm$ , donde  $d\bar{\epsilon}$  es la energía media impartida por la radiación ionizante a una masa  $dm$  de materia.

$$D = \frac{d\bar{\epsilon}}{dm} \quad \text{unidad: Joule.kg}^{-1}$$

A esta unidad se le da el nombre de gray, abreviado Gy.

### Dosis absorbida media en órgano, $D_T$

Con el propósito de la protección radiológica se ha definido esta magnitud como el cociente,

$$D_T = \frac{\varepsilon_T}{m_T} \quad \text{unidad: Joule.kg}^{-1} = \text{Gy}$$

Donde  $\varepsilon_T$  es la energía total impartida a un tejido u órgano de masa  $m_T$ .

### Dosis equivalente en un órgano o tejido, $H_T$

Los estudios radiobiológicos han indicado que iguales dosis de diferentes tipos de RI, no necesariamente presentan igual detrimiento biológico. En el caso particular de los neutrones, las diferentes energías producen efectos diferentes. Para ello se ha introducido el término  $w_R$  como factor de ponderación, dando por resultado la dosis equivalente. Esta se define como el producto de la dosis absorbida media en el órgano o tejido  $T$  por el factor de ponderación de la radiación

$$H_T = w_R \cdot D_{T,R} \quad \text{unidad: Joule.kg}^{-1} = \text{Sv}$$

Donde R representa el tipo de radiación.

La unidad de la magnitud dosis equivalente en órgano o tejido recibe el nombre de sievert (Sv). Para el caso de campos de radiación compuestos por diferentes tipos de partículas y energías, la expresión más general para la definición de la dosis equivalente en órgano  $H_T$  es,

$$H_T = \sum_R w_R D_{TR}$$

La dosis absorbida y dosis equivalente son numéricamente iguales para radiación beta, x y gamma, no siendo así para la radiación alfa, protones y neutrones.

En la tabla 1 se muestran los valores para los factores de ponderación de la radiación  $w_R$  según distintos tipos de radiaciones, los que han sido seleccionados por el Comité Internacional de Protección Radiológica (ICRP), para reflejar la eficacia biológica relativa (RBE) de las radiaciones en la producción de efectos estocásticos a bajas dosis.

**Tabla 1.** Factores de ponderación de la radiación,  $w_R$

Tipo de radiación	$w_R$
Fotones de todas las energías	1
Electrones y muones, todas las energías	1
Neutrones con energías,	
<10 keV	5
10 keV a 100 keV	10
>10 keV a 2 MeV	20
>2 MeV a 20 MeV	10
>20 MeV	5
Protones, salvo los de retroceso, de $E >2$ MeV	5
Partículas alfa, fragmentos de fisión y núcleos pesados	20

### Dosis efectiva, $E$

El riesgo de la ocurrencia de efectos de carácter estocásticos, no sólo depende del tipo de radiación considerado por medio del factor  $w_R$ , sino que distintos órganos y tejidos muestran diferentes radiosensibilidades para determinados efectos. La consideración de este comportamiento se introduce con otro factor de ponderación por órgano o tejido,  $w_T$ . Los órganos y tejidos para los cuales el ICRP asigna valores específicos del factor  $w_T$ , son los indicados en la tabla 2.

**Tabla 2.** Factores de ponderación de los tejidos,  $w_T$

Tejido u órgano	$w_T$
Gonadas	0,20
Médula ósea (roja)	0,12
Colon	0,12
Pulmón	0,12
Estómago	0,12
Vejiga	0,05
Mamas	0,05
Hígado	0,05
Esófago	0,05
Tiroide	0,05
Piel	0,01
Superficie ósea	0,01
Resto	0,05

El "Resto" está compuesto, a los efectos del cálculo, por los siguientes tejidos u órganos; glándulas suprarrenales, cerebro, intestino grueso superior, intestino delgado, riñón, músculo, páncreas, bazo, timo y útero.

Los valores de  $w_T$  se aplican a una población de referencia, con igual número de individuos de ambos sexos y para un amplio intervalo de edades.

La dosis efectiva se define por medio de una doble sumatoria, de los productos de la dosis absorbida media en órgano por los correspondientes factores de ponderación de radiación y de órgano,

$$E = \sum_T w_T \cdot H_T = \sum_T w_T \cdot \sum_R w_R \cdot D_{T,R} \quad \text{unidad: J.kg}^{-1}$$

Donde  $D_{T,R}$  indica la dosis absorbida media en el órgano o tejido  $T$  debida a la radiación del tipo  $R$ . La radiación incidente sobre el cuerpo puede ser producida por una fuente externa por un radionucleido incorporado al cuerpo. La dosis efectiva es de aplicación a trabajadores ocupacionalmente expuestos y al público, para ambos sexos.

## MAGNITUDES PARA DOSIMETRÍA INTERNA

Tras la incorporación al organismo de material radiactivo, hay un período de tiempo durante el cual y a tasa variable, este material esta irradiando los tejidos corporales vecinos. Su distribución espacial y temporal está regida por la vía de entrada, la forma fisicoquímica y el comportamiento metabólico del radionucleido y del compuesto transportador. La integral en el tiempo de la tasa de dosis equivalente se denomina dosis equivalente comprometida.

### Dosis equivalente comprometida en un órgano o tejido, $H_T(\tau)$

Es la dosis que recibirá un órgano o tejido luego de un tiempo  $\tau$ , debido a la incorporación de un radionucleido.

$$H_T(\tau) = \int_{t_0}^{t_0 + \tau} \dot{H}_T(t) dt \quad \text{unidad: J.kg}^{-1} = \text{Sv}$$

La integral corresponde a una sola incorporación al tiempo  $t_0$  y donde,  $\dot{H}_T$  es la tasa de dosis equivalente en un tejido u órgano  $T$ , al tiempo  $t$  y  $\tau$  es el período de tiempo sobre el cual se efectúa la integración.

Cuando se trata de dosis a trabajadores y  $\tau$  no está especificado, se toma igual 50 años y para el caso de público, se integra hasta la edad de 70 años.

Por extensión se define de la misma forma la dosis efectiva comprometida

### Dosis efectiva comprometida, $E(\tau)$

Se define como la sumatoria sobre los tejidos u órganos expuestos de los productos de la dosis equivalente comprometidas por el factor de peso  $w_T$ , para cada uno de ellos.

$$E(\tau) = \sum_T w_T \cdot H_T(\tau) \quad \text{unidad: J.kg}^{-1} = \text{Sv}$$

## CONCEPTO DE ACTIVIDAD

La actividad (A) de un radionucleido se define como el promedio de las transformaciones nucleares que ocurren en una cantidad de partículas en un tiempo dado.

$$A = \frac{dN}{dt} = \lambda N$$

donde  $\lambda$  es la vida media del isótopo

La actividad es medida en Becquerel (Bq), (1 Bq representa 1 desintegración por segundo). Debido a que esto es una cantidad muy pequeña se utiliza el kilo ( $10^3$ ), mega ( $10^6$ ) o giga ( $10^9$ ) Bq. En la tabla 3 se describen los factores de conversión entre las actuales y antiguas unidades para la actividad, dosis absorbida y dosis equivalente.

**Tabla 3**

Magnitud	actual	anterior	equivalencias	
Actividad	Becquerel (Bq)	Curie (Ci)	$1 \text{ Bq} = 2,7 \times 10^{-11} \text{ Ci}$	$1 \text{ Ci} = 3,7 \times 10^{10} \text{ Bq}$
Dosis absorbida	gray (Gy)	rad	$1 \text{ Gy} = 100 \text{ rad}$	$1 \text{ rad} = 0,01 \text{ Gy}$
Dosis equivalente	sievert (Sv)	rem	$1 \text{ Sv} = 100 \text{ rem}$	$1 \text{ rem} = 0,01 \text{ Sv}$

## APLICACIONES DIAGNÓSTICAS Y TERAPÉUTICAS DE LOS RADIOISÓTOPOS

El empleo de radioisótopos en medicina, permite tener información sobre el estado y funcionamiento de diferentes tejidos y órganos. Algunos de estos elementos se concentran naturalmente en órganos específicos, por ejemplo el yodo es captado, en sus diferentes isótopos, casi exclusivamente por la tiroides, mientras que el  $^{99m}\text{Tc}$  es captado por los huesos, el corazón, etc, dependiendo de la biocinética del compuesto al que está unido. El  $^{99m}\text{Tc}$  es usado en el 80% de los estudios diagnósticos por las características de sus emisiones y su T1/2 de 6 h, que contribuye a minimizar el riesgo para el paciente.

Los radioisótopos más usados en aplicaciones diagnósticas, además del  $^{99m}\text{Tc}$ , son el  $^{131}\text{I}$ , el  $^{67}\text{Ga}$  y el  $^{201}\text{Tl}$ . Dado que su empleo puede realizarse en un amplio rango de edades, su utilización en mujeres embarazadas o en edad fértil deberá estar debidamente justificada.

- Protección radiológica de mujeres en edad fértil**

Se considera que el riesgo de muerte prenatal, malformación o deterioro del desarrollo mental del futuro individuo, no presenta un incremento apreciable sobre la incidencia natural de esos factores debido a los procedimientos diagnósticos en medicina nuclear. Habitualmente no son urgentes y ante la presunción de embarazo el médico deberá evaluar la posibilidad de posponer la práctica. La ICRP84 recomienda que "los diagnósticos y procedimientos terapéuticos que causen exposición del abdomen de mujeres presuntamente embarazadas, deben ser evitados a menos que exista una indicación clínica impostergable que justifique dicha práctica", por ejemplo, en caso que el riesgo para la madre, si no se realiza dicho procedimiento, sea mayor que el riesgo de daño potencial para el feto (1).

Si la práctica diagnóstica esta debidamente justificada, se debe administrar a la paciente embarazada la mínima actividad necesaria para obtener un examen de calidad suficiente y se debe intentar reducir la dosis en útero mediante la hidratación materna y vaciado frecuentemente de la vejiga en caso que el elemento radiactivo sea eliminado por orina.

La mayoría de los procedimientos diagnósticos de medicina nuclear son realizados con radio-nucleidos de cortos períodos de semidesintegración que no causan dosis fetales elevadas. Cuando estos no atraviesan la placenta, la dosis fetal se debe a la irradiación originada por la radiactividad presente en los tejidos maternos.

Sin embargo existen algunos radionucleidos como los isótopos del yodo, que atraviesan la placenta y se concentran en órganos o tejidos específicos del feto, (según su edad gestacional), y por lo tanto presentan riesgos fetales significativos.

Es aconsejable que una mujer no quede embarazada hasta que la dosis efectiva comprometida en el feto que originarían los radiofármacos que permanezcan en su organismo sea menor a 1 mGy.

La interrupción del embarazo es una decisión individual condicionada por diversos factores que deben evaluar los progenitores y el cuerpo médico. Las dosis efectivas comprometidas en el feto menores que 100 mGy no deberían ser consideradas como una razón para interrumpirlo.

## **DOSIS EN FETO POR LA INCORPORACIÓN DE RADIONUCLEIDOS POR LA MADRE**

La evaluación de dosis en el feto por administración de radiofármacos a la mujer gestante es de interés dada la distinta radiosensibilidad del feto en los diferentes períodos gestacionales y por lo tanto merecen una consideración especial para cada etapa de la gestación.

En este documento, además de las características generales de los isótopos, se presentan diferentes tablas con las dosis recibidas por los fetos debido a los procedimientos más comunes en diagnósticos y tratamientos con radiofármacos.

Luego de la administración de un radiofármaco, su distribución entre los distintos órganos debe ser considerada teniendo en cuenta los modelos biocinéticos ya establecidos.

Como se expuso previamente, durante el desarrollo en útero, el efecto biológico sobre el feto será diferente según la etapa de desarrollo pues existen períodos de diferente sensibilidad dado por el grado de desarrollo de los diferentes órganos. Para efectos determinísticos, se divide el período de gestación en varias etapas. Etapa de preimplantación de 0 a 8 días post concepción, de 9 a 60 días correspondiendo a la organogénesis, de 61 a 104 período fetal temprano, de 105 a 175 fetal medio más de 175 días fetal tardío (2).

En algunas prácticas, y mientras sea posible, es aconsejable elegir el radiofármaco con T1/2 físico más corto como pueden ser los gases inertes. Por ejemplo el uso del  $^{133}\text{Xe}$ , para la fase de ventilación del examen del pulmón, determinará una menor dosis fetal que si se utilizara DTPA en aerosol marcado con  $^{99\text{m}}\text{Tc}$  el cual, además, será excretado por orina y mientras se encuentre en la vejiga materna contribuirá a la dosis fetal.

## RADIOFÁRMACOS

### TECNECIO 99m

#### 1. Características generales del $^{99m}\text{Tc}$ :

Período de Semidesintegración  
( $T_{1/2}$  físico) 6 horas

Emisión principal  
Radiación Gamma 141 keV (89%)

#### 2. Aspectos dosimétricos

**Modelo biocinético:** El modelo biocinético depende del fármaco al que esté unido el tecnecio y en cada caso puede encontrarse la descripción en la publicación 53 de la ICRP y su adendum 80 (3-4).

En la tabla 4 se especifican las dosis recibidas por el feto dependiendo del período de gestación en el momento de la administración para varias prácticas utilizando  $^{99m}\text{Tc}$  unido a diferentes transportadores (5).

En la tabla 4 se expresa la actividad administrada en MBq y en mCi, entre paréntesis. La dosis fetal se expresa en mGy y en rad, entre paréntesis.

**Tabla 4.** Dosis fetal debido a distintos procedimientos con  $^{99m}\text{Tc}$   
(el sombreado indica contribución materna y fetal a la dosis)

Radiofármaco	Actividad MBq (mCi)	Dosis Fetal			
		Temprana mGy (rad)	3 meses mGy (rad)	6 meses mGy (rad)	9 meses mGy (rad)
$^{99m}\text{Tc}$ Disofenina	350 (9,5)	$6,0 \times 10^0$ $(6,0 \times 10^{-1})$	$5,2 \times 10^0$ $(5,2 \times 10^{-1})$	$4,2 \times 10^0$ $(4,2 \times 10^{-1})$	$2,3 \times 10^0$ $(2,3 \times 10^{-1})$
$^{99m}\text{Tc}$ DMSA (Ac. Dimercaptosuccínico)	220 (6)	$1,1 \times 10^0$ $(1,1 \times 10^{-1})$	$1,0 \times 10^0$ $(1,0 \times 10^{-1})$	$8,8 \times 10^{-1}$ $(8,8 \times 10^{-2})$	$7,5 \times 10^{-1}$ $(7,5 \times 10^{-2})$
$^{99m}\text{Tc}$ DTPA imagen renal y filtración glomerular	750 (20)	$9,0 \times 10^0$ $(9,0 \times 10^{-1})$	$6,5 \times 10^0$ $(6,5 \times 10^{-1})$	$3,1 \times 10^0$ $(3,1 \times 10^{-1})$	$3,5 \times 10^0$ $(3,5 \times 10^{-1})$
imagen cerebral y perfusión renal	750 (20)	$9,0 \times 10^0$ $(9,0 \times 10^{-1})$	$6,5 \times 10^0$ $(6,5 \times 10^{-1})$	$3,1 \times 10^0$ $(3,1 \times 10^{-1})$	$3,5 \times 10^0$ $(3,5 \times 10^{-1})$
1 <sup>er</sup> paso	350 (9,5)	$4,2 \times 10^0$ $(4,2 \times 10^{-1})$	$3,0 \times 10^0$ $(3,0 \times 10^{-1})$	$1,4 \times 10^0$ $(1,4 \times 10^{-1})$	$1,6 \times 10^0$ $(1,6 \times 10^{-1})$
reflujo gástrico	10 (0,27)	$1,2 \times 10^{-1}$ $(1,2 \times 10^{-2})$	$8,7 \times 10^{-2}$ $(8,7 \times 10^{-3})$	$4,1 \times 10^{-2}$ $(4,1 \times 10^{-3})$	$4,7 \times 10^{-2}$ $(4,7 \times 10^{-3})$
hipertensión	800 (22)	$9,6 \times 10^0$ $(9,6 \times 10^{-1})$	$7,0 \times 10^0$ $(7,0 \times 10^{-1})$	$3,3 \times 10^0$ $(3,3 \times 10^{-1})$	$3,8 \times 10^0$ $(3,8 \times 10^{-1})$
determinación del residuo de orina	350 (9,5)	$4,2 \times 10^0$ $(4,2 \times 10^{-1})$	$3,0 \times 10^0$ $(3,0 \times 10^{-1})$	$1,4 \times 10^0$ $(1,4 \times 10^{-1})$	$1,6 \times 10^0$ $(1,6 \times 10^{-1})$
$^{99m}\text{Tc}$ DTPA Aerosol (Dietilentriaminopentaacético)	40 (1,1)	$2,3 \times 10^{-1}$ $(2,3 \times 10^{-2})$	$1,7 \times 10^{-1}$ $(1,7 \times 10^{-2})$	$9,2 \times 10^{-2}$ $(9,2 \times 10^{-3})$	$1,2 \times 10^{-1}$ $(1,2 \times 10^{-2})$
$^{99m}\text{Tc}$ Glucoheptano imagen renal	750 (20)	$9,0 \times 10^0$ $(9,0 \times 10^{-1})$	$8,2 \times 10^0$ $(8,2 \times 10^{-1})$	$4,0 \times 10^0$ $(4,0 \times 10^{-1})$	$3,4 \times 10^0$ $(3,4 \times 10^{-1})$
imagen cerebral	750 (20)	$9,0 \times 10^0$ $(9,0 \times 10^{-1})$	$8,2 \times 10^0$ $(8,2 \times 10^{-1})$	$4,0 \times 10^0$ $(4,0 \times 10^{-1})$	$3,4 \times 10^0$ $(3,4 \times 10^{-1})$
$^{99m}\text{Tc}$ HDP	750 (20)	$3,9 \times 10^0$ $(3,9 \times 10^{-1})$	$4,10 \times 10^0$ $(4,0 \times 10^{-1})$	$2,3 \times 10^0$ $(2,3 \times 10^{-1})$	$1,9 \times 10^0$ $(1,9 \times 10^{-1})$

<sup>99m</sup> Tc NAPO diesteroisomero de hexametilpropilenoamina-oxina	750 (20)	$6,5 \times 10^0$ ( $6,5 \times 10^{-1}$ )	$5,0 \times 10^0$ ( $5,0 \times 10^{-1}$ )	$3,6 \times 10^0$ ( $3,6 \times 10^{-1}$ )	$2,7 \times 10^0$ ( $2,7 \times 10^{-1}$ )
<sup>99m</sup> Tc Albumina en macroagregados	200 (5,5)	$1,0 \times 10^0$ ( $1,0 \times 10^{-1}$ )	$6,0 \times 10^{-1}$ ( $6,0 \times 10^{-2}$ )	$5,2 \times 10^{-1}$ ( $5,2 \times 10^{-2}$ )	$4,4 \times 10^{-1}$ ( $4,4 \times 10^{-2}$ )
<sup>99m</sup> Tc MAA perfusión de arteria hepática imagen pulmonar venografía isotópica	150 (4)	$4,2 \times 10^{-1}$ ( $4,2 \times 10^{-2}$ )	$6,0 \times 10^{-1}$ ( $6,0 \times 10^{-2}$ )	$7,5 \times 10^{-1}$ ( $7,5 \times 10^{-2}$ )	$6,0 \times 10^{-1}$ ( $6,0 \times 10^{-2}$ )
	200 (5,5)	$5,6 \times 10^{-1}$ ( $5,6 \times 10^{-2}$ )	$8,0 \times 10^{-1}$ ( $8,0 \times 10^{-2}$ )	$1,0 \times 10^0$ ( $1,0 \times 10^{-1}$ )	$8,0 \times 10^{-1}$ ( $8,0 \times 10^{-2}$ )
	220 (6)	$6,2 \times 10^{-1}$ ( $6,2 \times 10^{-2}$ )	$8,8 \times 10^{-1}$ ( $8,8 \times 10^{-2}$ )	$1,1 \times 10^0$ ( $1,1 \times 10^{-1}$ )	$8,0 \times 10^{-1}$ ( $8,0 \times 10^{-2}$ )
<sup>99m</sup> Tc MAG3	750 (20)	$1,4 \times 10^1$ ( $1,4 \times 10^0$ )	$1,0 \times 10^1$ ( $1,0 \times 10^0$ )	$4,1 \times 10^0$ ( $4,1 \times 10^{-1}$ )	$3,9 \times 10^0$ ( $3,9 \times 10^{-1}$ )
<sup>99m</sup> Tc MDP (Metilendifosfonato)	750 (20)	$4,6 \times 10^0$ ( $4,6 \times 10^{-1}$ )	$4,0 \times 10^0$ ( $4,0 \times 10^{-1}$ )	$2,0 \times 10^0$ ( $2,0 \times 10^{-1}$ )	$1,8 \times 10^0$ ( $1,8 \times 10^{-1}$ )
<sup>99m</sup> Tc MIBI- (Metoxi isobutiril-isonitrilo) reposo	1100 (30)	$1,7 \times 10^1$ ( $1,7 \times 10^0$ )	$1,3 \times 10^1$ ( $1,3 \times 10^0$ )	$9,2 \times 10^0$ ( $9,2 \times 10^{-1}$ )	$5,9 \times 10^0$ ( $5,9 \times 10^{-1}$ )
<sup>99m</sup> Tc MIBI-stress	1100 (30)	$1,3 \times 10^1$ ( $1,3 \times 10^0$ )	$1,0 \times 10^1$ ( $1,0 \times 10^0$ )	$7,6 \times 10^0$ ( $7,6 \times 10^{-1}$ )	$4,8 \times 10^0$ ( $4,8 \times 10^{-1}$ )
<sup>99m</sup> Tc Pertecnectato imagen cerebral	1100 (30)	$1,2 \times 10^1$ ( $1,2 \times 10^0$ )	$2,4 \times 10^1$ ( $2,4 \times 10^0$ )	$1,5 \times 10^1$ ( $1,5 \times 10^0$ )	$1,0 \times 10^1$ ( $1,0 \times 10^0$ )
imagen tiroida	400 (11)	$4 \times 10^0$ ( $4,4 \times 10^{-1}$ )	$8,8 \times 10^0$ ( $8,8 \times 10^{-1}$ )	$5,6 \times 10^0$ ( $5,6 \times 10^{-1}$ )	$3,7 \times 10^0$ ( $3,7 \times 10^{-1}$ )
imagen de glándulas salivales	200 (5,5)	$2,2 \times 10^0$ ( $2,2 \times 10^{-1}$ )	$4,4 \times 10^0$ ( $4,4 \times 10^{-1}$ )	$2,8 \times 10^0$ ( $2,8 \times 10^{-1}$ )	$1,9 \times 10^0$ ( $1,9 \times 10^{-1}$ )
localización placentaria	110 (3)	$1,1 \times 10^0$ ( $1,1 \times 10^{-1}$ )	$2,4 \times 10^0$ ( $2,4 \times 10^{-1}$ )	$1,5 \times 10^0$ ( $1,5 \times 10^{-1}$ )	$1,0 \times 10^0$ ( $1,0 \times 10^{-1}$ )
pool sanguíneo	1100 (30)	$1,1 \times 10^1$ ( $1,1 \times 10^0$ )	$2,4 \times 10^1$ ( $2,4 \times 10^0$ )	$1,4 \times 10^1$ ( $1,4 \times 10^0$ )	$1,0 \times 10^0$ ( $1,0 \times 10^0$ )
detección de bypass cardiovascular	550 (15)	$6,0 \times 10^0$ ( $6,0 \times 10^{-1}$ )	$1,2 \times 10^1$ ( $1,2 \times 10^0$ )	$7,7 \times 10^0$ ( $7,7 \times 10^{-1}$ )	$5,1 \times 10^0$ ( $5,1 \times 10^{-1}$ )
1 <sup>er</sup> paso	550 (15)	$6,0 \times 10^0$ ( $6,0 \times 10^{-1}$ )	$1,2 \times 10^1$ ( $1,2 \times 10^0$ )	$7,7 \times 10^0$ ( $7,7 \times 10^{-1}$ )	$5,1 \times 10^0$ ( $5,1 \times 10^{-1}$ )
<sup>99m</sup> Tc PYP imagen ósea	550 (15)	$3,3 \times 10^0$ ( $3,3 \times 10^{-1}$ )	$3,6 \times 10^0$ ( $3,6 \times 10^{-1}$ )	$2,0 \times 10^0$ ( $2,0 \times 10^{-1}$ )	$1,6 \times 10^0$ ( $1,6 \times 10^{-1}$ )
	700 (19)	$4,2 \times 10^0$ $4,2 \times 10^0$	$4,6 \times 10^0$ $4,6 \times 10^0$	$2,5 \times 10^0$ $2,5 \times 10^0$	$2,0 \times 10^0$ $2,0 \times 10^0$
imagen de pool sanguíneo	700 (19)	$4,2 \times 10^0$ $4,2 \times 10^0$	$4,6 \times 10^0$ $4,6 \times 10^0$	$2,5 \times 10^0$ $2,5 \times 10^0$	$2,0 \times 10^0$ $2,0 \times 10^0$
<sup>99m</sup> Tc RBC – marcado in vitro	930 (25)	$6,3 \times 10^0$ ( $6,3 \times 10^{-1}$ )	$4,4 \times 10^0$ ( $4,4 \times 10^{-1}$ )	$3,2 \times 10^0$ ( $3,2 \times 10^{-1}$ )	$2,6 \times 10^0$ ( $2,6 \times 10^{-1}$ )
<sup>99m</sup> Tc RBC – in vivo en reposo en ejercicio	550 (15)	$3,5 \times 10^0$ ( $3,5 \times 10^{-1}$ )	$2,4 \times 10^0$ ( $2,4 \times 10^{-1}$ )	$1,8 \times 10^0$ ( $1,8 \times 10^{-1}$ )	$1,5 \times 10^0$ ( $1,5 \times 10^{-1}$ )
	930 (25)	$6,0 \times 10^0$ ( $6,0 \times 10^{-1}$ )	$4,0 \times 10^0$ ( $4,0 \times 10^{-1}$ )	$3,1 \times 10^0$ ( $3,1 \times 10^{-1}$ )	$2,5 \times 10^0$ ( $2,5 \times 10^{-1}$ )
<sup>99m</sup> Tc Sulfuro Coloide normal imagen de hígado-bazo imagen de médula aspiración pulmonar	300 (8)	$5,4 \times 10^{-1}$ ( $5,4 \times 10^{-2}$ )	$6,3 \times 10^{-1}$ ( $6,3 \times 10^{-2}$ )	$9,6 \times 10^{-1}$ ( $9,6 \times 10^{-2}$ )	$1,1 \times 10^0$ ( $1,1 \times 10^{-1}$ )
	450 (12)	$8,1 \times 10^{-1}$ ( $8,1 \times 10^{-2}$ )	$9,5 \times 10^{-1}$ ( $9,5 \times 10^{-2}$ )	$1,4 \times 10^0$ ( $1,4 \times 10^{-1}$ )	$1,7 \times 10^0$ ( $1,7 \times 10^{-1}$ )
	20 (0,5)	$3,6 \times 10^{-2}$ ( $3,6 \times 10^{-3}$ )	$4,2 \times 10^{-2}$ ( $4,2 \times 10^{-3}$ )	$6,4 \times 10^{-2}$ ( $6,4 \times 10^{-3}$ )	$7,4 \times 10^{-2}$ ( $7,4 \times 10^{-3}$ )
	200 (5,5)	$7,6 \times 10^{-1}$ ( $7,6 \times 10^{-2}$ )	$5,6 \times 10^{-1}$ ( $5,6 \times 10^{-2}$ )	$5,8 \times 10^{-1}$ ( $5,8 \times 10^{-2}$ )	$5,6 \times 10^{-1}$ ( $5,6 \times 10^{-2}$ )

## YODO 131

### 1.- Características generales del $^{131}\text{I}$

Es uno de los radiofármacos más utilizados con fines diagnósticos y/o terapéuticos en la patología tiroidea. A continuación se presentan algunas características físicas y aspectos dosimétricos en el feto según la edad gestacional.

Período de Semidesintegración  
( $T_{1/2}$  físico) 8,04 días

Emisión principal  
Radiación Gamma 364 keV  
Beta 606 keV (energía máxima)

### 2. Aspectos dosimétricos

**Modelo biocinético:** El modelo biocinético es particular del compuesto que esté unido al yodo y en cada caso puede encontrarse la descripción en la publicación 53 de la ICRP y su addendum 80 (3-4).

El período de eliminación biológica del yodo ( $\text{INa}$ ) de la tiroides en el hombre de referencia se ha fijado en 80 días, mientras que para niños de 15, 10, 5 y 1 año, los tiempos son de 65, 50, 40 y 30 días.

Luego de la incorporación, el yodo se fija en la glándula tiroides y considera uniformemente distribuido en el resto del cuerpo. Las simplificaciones del modelo tienen una influencia poco significativa en el cálculo de dosis a los otros órganos especialmente en el caso del  $^{131}\text{I}$  que determina que la dosis en tiroides contribuya en un 95% a la dosis efectiva.

En la tabla 5 se especifican las dosis recibidas por el feto dependiendo del período de gestación en el momento de la administración para varias prácticas utilizando diferentes transportadores unidos a  $^{131}\text{I}$  (5).

**Tabla 5.** Dosis fetal debido a distintos procedimientos  
(el sombreado indica contribución materna y fetal a la dosis)

Radiofármaco	Actividad MBq (mCi)	Dosis Fetal			
		Temprana mGy (rad)	3 meses mGy (rad)	6 meses mGy (rad)	9 meses mGy (rad)
$^{131}\text{I}$ Hipurato					
	función renal	1,3 (0,035)	$8,3 \times 10^{-2}$ $(8,3 \times 10^{-3})$	$6,5 \times 10^{-2}$ $(6,5 \times 10^{-3})$	$2,5 \times 10^{-2}$ $(2,5 \times 10^{-3})$
	imagen renal	1,3 (0,035)	$8,3 \times 10^{-2}$ $(8,3 \times 10^{-3})$	$6,5 \times 10^{-2}$ $(6,5 \times 10^{-3})$	$2,5 \times 10^{-2}$ $(2,5 \times 10^{-3})$
$^{131}\text{I}$ HAS	0,5 (0,013)	$2,6 \times 10^{-1}$ $(2,6 \times 10^{-2})$	$9,0 \times 10^{-2}$ $(9,0 \times 10^{-3})$	$8,0 \times 10^{-2}$ $(8,0 \times 10^{-3})$	$6,5 \times 10^{-2}$ $(6,5 \times 10^{-3})$
$^{131}\text{I}$ MAA	55 (1,5)	$3,7 \times 10^0$ $(3,7 \times 10^{-1})$	$2,3 \times 10^0$ $(2,3 \times 10^{-1})$	$2,2 \times 10^0$ $(2,2 \times 10^{-1})$	$2,3 \times 10^0$ $(2,3 \times 10^{-1})$
$^{131}\text{I}$ MIBG (meta iodobencilguanidina)	20 (0,5)	$2,2 \times 10^0$ $(2,2 \times 10^{-1})$	$1,1 \times 10^0$ $(1,1 \times 10^{-1})$	$7,6 \times 10^{-1}$ $(7,6 \times 10^{-2})$	$7,0 \times 10^{-1}$ $(7,0 \times 10^{-2})$
$^{131}\text{I}$ Nal (Diagnóstico)					
	captación tiroidea	0,55 (0,015)	$4,0 \times 10^{-2}$ $(4,0 \times 10^{-3})$	$3,7 \times 10^{-2}$ $(3,7 \times 10^{-3})$	$1,3 \times 10^{-1}$ $(1,3 \times 10^{-2})$
	Centellograma	4 (0,11)	$2,9 \times 10^{-1}$ $(2,9 \times 10^{-2})$	$2,7 \times 10^{-1}$ $(2,7 \times 10^{-2})$	$9,2 \times 10^{-1}$ $(9,2 \times 10^{-2})$

localización de metástasis extra tiroideas	40 (1,1)	$2,9 \times 10^0$ ( $2,9 \times 10^{-1}$ )	$2,7 \times 10^0$ ( $2,7 \times 10^{-1}$ )	$9,2 \times 10^0$ ( $9,2 \times 10^{-1}$ )	$1,1 \times 10^1$ ( $1,1 \times 10^0$ )
$^{131}\text{I}$ Nal (Terapéutico)					
Hipertiroidismo	350 (9,5)	$2,5 \times 10^1$ ( $2,5 \times 10^0$ )	$2,3 \times 10^1$ ( $2,3 \times 10^0$ )	$8,1 \times 10^1$ ( $8,1 \times 10^0$ )	$9,5 \times 10^1$ ( $9,5 \times 10^0$ )
ablaclación de tejido normal tiroideo	1900 (50)	$1,4 \times 10^2$ ( $1,4 \times 10^1$ )	$1,3 \times 10^2$ ( $1,3 \times 10^1$ )	$4,4 \times 10^2$ ( $4,4 \times 10^1$ )	$5,1 \times 10^2$ ( $5,1 \times 10^1$ )

- Casos especiales: embarazo posterior a la administración del yodo**

Si bien se recomienda a las pacientes que no queden embarazadas luego del tratamiento con yodo, esto puede ocurrir. En este caso, el yodo que aún se está eliminando, es el que va a irradiar al embrión. Las dosis resultantes en el embrión en función de las semanas transcurridas desde la administración del yodo hasta el momento de la concepción se presentan en la tabla 6.

**Tabla 6**

a) pacientes hipertiroideas

Dosis absorbida por el feto en casos de hipertiroidismo (mGy/MBq)

% Max Uptake	Semanas transcurridas desde la administración hasta la concepción							
	1	2	3	4	5	6	7	8
5%	4,1E-04	1,9E-04	8,7E-05	4,0E-05	1,9E-05	8,7E-06	4,0E-06	1,9E-06
10%	8,3E-04	3,8E-04	1,7E-04	8,0E-05	3,7E-05	1,7E-05	7,8E-06	3,6E-06
15%	1,3E-03	5,8E-04	2,6E-04	1,2E-04	5,5E-05	2,5E-05	1,1E-05	5,2E-06
20%	1,7E-03	7,8E-04	3,5E-04	1,6E-04	7,2E-05	3,3E-05	1,5E-05	6,7E-06
25%	2,2E-03	9,8E-04	4,4E-04	2,0E-04	8,8E-05	4,0E-05	1,8E-05	8,0E-06
30%	2,7E-03	1,2E-03	5,3E-04	2,3E-04	1,0E-04	4,6E-05	2,0E-05	9,1E-06
35%	3,2E-03	1,4E-03	6,1E-04	2,7E-04	1,2E-04	5,2E-05	2,3E-05	1,0E-05
40%	3,7E-03	1,6E-03	7,0E-04	3,0E-04	1,3E-04	5,7E-05	2,4E-05	1,1E-05
45%	4,3E-03	1,8E-03	7,9E-04	3,3E-04	1,4E-04	6,0E-05	2,6E-05	1,1E-05
50%	4,8E-03	2,0E-03	8,5E-04	3,6E-04	1,5E-04	6,3E-05	2,6E-05	1,1E-05
55%	5,4E-03	2,2E-03	9,2E-04	3,8E-04	1,6E-04	6,4E-05	2,7E-05	1,1E-05
60%	6,0E-03	2,4E-03	9,8E-04	4,0E-04	1,6E-04	6,4E-05	2,6E-05	1,0E-05
65%	6,7E-03	2,6E-03	1,0E-03	4,0E-04	1,6E-04	6,2E-05	2,5E-05	9,7E-06
70%	7,3E-03	2,8E-03	1,1E-03	4,1E-04	1,5E-04	5,9E-05	2,2E-05	8,6E-06
75%	7,9E-03	2,9E-03	1,1E-03	4,0E-04	1,5E-04	5,4E-05	2,0E-05	7,2E-06
80%	8,5E-03	3,0E-03	1,1E-03	3,7E-04	1,3E-04	4,6E-05	1,6E-05	5,7E-06
85%	9,1E-03	3,0E-03	1,0E-03	3,4E-04	1,1E-04	3,8E-05	1,3E-05	4,2E-06
90%	9,6E-03	3,0E-03	9,2E-04	2,9E-04	8,9E-05	2,8E-05	8,6E-06	2,7E-06
95%	9,8E-03	2,8E-03	7,9E-04	2,2E-04	6,3E-05	1,8E-05	5,1E-06	1,4E-06
100%	9,8E-03	2,4E-03	6,1E-04	1,5E-04	3,8E-05	9,3E-06	2,3E-06	5,8E-07

b) pacientes eutiroideas

Dosis absorbida por el feto en casos de eutiroidismo (mGy/MBq)

% Max Uptake	Semanas transcurridas desde la administración hasta la concepción							
	1	2	3	4	5	6	7	8
5%	3,1E-04	1,5E-04	7,7E-05	3,8E-05	1,9E-05	9,5E-06	4,7E-06	2,4E-06
15%	8,8E-04	4,4E-04	2,2E-04	1,1E-04	5,6E-05	2,8E-05	1,4E-05	7,2E-06
25%	1,4E-03	7,1E-04	3,6E-04	1,8E-04	9,2E-05	4,7E-05	2,4E-05	1,2E-05

El radioyodo atraviesa la barrera placentaria por lo que la administración de dosis terapéuticas puede causar problemas significativos para el feto, especialmente un hipotiroidismo permanente.

Si inadvertidamente se produce la administración de yodo a la mujer embarazada es importante calcular la dosis fetal para evaluar los riesgos potenciales.

## TALIO 201

### 1. Características generales:

Período de Semidesintegración  
( $T_{1/2}$  físico) 3,04 días

Emisión principal  
Radiación Gamma 71 keV

### 2. Aspectos dosimétricos

#### Modelo biocinético

La descripción del modelo biocinético puede encontrarse en la publicación 53 de la ICRP y su addendum 80 (3-4).

En la tabla 7 se especifican las dosis recibidas por el feto dependiendo del período de gestación en el momento de la administración para varias prácticas utilizando  $^{201}\text{TI}$  (5).

**Tabla 7.** Dosis fetal estimadas para varias prácticas de medicina nuclear

Radiofármaco	Actividad MBq (mCi)	Dosis Fetal			
		Temprana mGy (rad)	3 meses mGy (rad)	6 meses mGy (rad)	
$^{201}\text{TI}$ Cloruro imagen planar	150 (4)	$1,5 \times 10^1$ ( $1,5 \times 10^0$ )	$8,7 \times 10^0$ ( $8,7 \times 10^{-1}$ )	$7,0 \times 10^0$ ( $7,0 \times 10^{-1}$ )	$4,0 \times 10^0$ ( $4,0 \times 10^{-1}$ )
imágenes con SPECT	110 (3)	$1,1 \times 10^1$ ( $1,1 \times 10^0$ )	$6,4 \times 10^0$ ( $6,4 \times 10^{-1}$ )	$5,2 \times 10^0$ ( $5,2 \times 10^{-1}$ )	$3,0 \times 10^0$ ( $3,0 \times 10^{-1}$ )
perfusión miocárdica	55 (1,5)	$5,3 \times 10^0$ ( $5,3 \times 10^{-1}$ )	$3,2 \times 10^0$ ( $3,2 \times 10^{-1}$ )	$2,6 \times 10^0$ ( $2,6 \times 10^{-1}$ )	$1,5 \times 10^0$ ( $1,5 \times 10^{-1}$ )
imagen tiroidea	80	$7,8 \times 10^0$	$4,6 \times 10^0$	$3,8 \times 10^0$	$2,2 \times 10^0$

## GALIO 67

### 1. Características generales:

Período de Semidesintegración  
( $T_{1/2}$  físico) 3,26 días

Emisión principal  
Radiación gamma 93,31 keV

### 2. Aspectos dosimétricos

#### Modelo biocinético:

La descripción del modelo biocinético puede encontrarse en la publicación 53 de la ICRP y su addendum 80 (3-4).

En la tabla 8 se especifican las dosis recibidas por el feto dependiendo del período de gestación en el momento de la administración para varias prácticas utilizando  $^{67}\text{Ga}$  (5).

**Tabla 8.** Dosis fetal debido a distintos procedimientos  
(el sombreado indica contribución materna y fetal a la dosis)

Radiofármaco	Actividad MBq (mCi)	Dosis Fetal			
		Temprana mGy (rad)	3 meses mGy (rad)	6 meses mGy (rad)	9 meses mGy (rad)
$^{67}\text{Ga}$ Citrato	190 (5)	$1,8 \times 10^1$ ( $1,8 \times 10^0$ )	$3,8 \times 10^1$ ( $3,8 \times 10^0$ )	$3,4 \times 10^1$ ( $3,4 \times 10^0$ )	$2,5 \times 10^1$ ( $2,5 \times 10^0$ )

### AGRADECIMIENTOS

A la doctora Ana María Fadel, jefa del Servicio de Medicina Nuclear del Hospital General de Agudos, Carlos G. Durand, por su colaboración en la lectura crítica de este manuscrito.

### BIBLIOGRAFÍA

- 1) International Commission on Radiological Protection. "Pregnancy and Medical Radiation". ICRP Publication 84. Annals of the ICRP 30(1). Pergamon Press, Oxford (2000).
- 2) Steenvoorde, P.; Pauwels, E.K.J.; Harding, L.K.; Bourguignon, M.; Mariere, B.; Broerse, J.J. Diagnostic Nuclear Medicine and Risk for the Fetus. European Journal of Nuclear Medicine, 25 (2):193-199, 1998.
- 3) International Commission on Radiological Protection, Oxford, 1987, Radiation Dose to Patients from Radiopharmaceuticals, Publication 53.
- 4) International Commission on Radiological Protection, Oxford, 1998, Radiation Dose to Patients from Radiopharmaceuticals, Publication 80, Addendum to ICRP 53.
- 5) Russell, J.R. et ál. Radiation Absorbed Dose to the Embryo/Fetus from Radiopharmaceuticals. Health Physics 73(5):756-769, 1997.

# Procedimiento para la determinación de emisores alfas en muestras de orina y heces

Serdeiro, N.H.



# **PROCEDIMIENTO PARA LA DETERMINACIÓN DE EMISORES ALFAS EN MUESTRAS DE ORINA Y HECES**

Serdeiro, N.H.

Autoridad Regulatoria Nuclear  
Argentina

## **1. OBJETIVO**

Establecer el procedimiento para la identificación y cuantificación de radionucleidos emisores alfa en muestras de orina y heces. Los emisores alfa a determinar son: uranio, torio, americio, curio y plutonio.

## **2. CAMPO DE APLICACIÓN**

Este procedimiento se aplica a todos los laboratorios de los países participantes del Proyecto ARCAL LXXVIII que efectúan determinaciones de radionucleidos emisores alfa en muestras biológicas para evaluaciones dosimétricas.

## **3. REFERENCIAS NORMATIVAS**

- 3.1 Manual de Técnicas de Laboratorio, ARN, Julio 2002
- 3.2 Elaboración de Procedimientos, IRD 5.0-01, 20/03/2003
- 3.3 ISO 12790-1: Radiation Protection-Performance Criteria for Radiobioassay
- 3.4 Scientific Report SCK.CEN-BLG-935 - OMINEX Work Package 3, "Uncertainty on bioassay measurements", April 2003
- 3.5 EURACHEM/CITAC Guide CG4, "Quantifying Uncertainty in Analytical Measurement", 2000
- 3.6 Health Physics Society, ANSI 13.30, 1996, "Performance Criteria for Radiobioassay"

## **4. SIGLAS Y ABREVIATURAS**

ARCAL - Acuerdo Regional de Cooperación para la Promoción de la Ciencia y Tecnología Nucleares en América Latina y El Caribe

ARN - Autoridad Regulatoria Nuclear

EA - Emisores Alfa

IRD - Instituto de Radioprotección y Dosimetría

ISO - International Organization for Standardization

PO - Procedimiento Operacional

## **5. DETERMINACIÓN DE EMISORES ALFA EN MUESTRAS DE ORINA Y HECES**

### **5.1 MUESTRAS DE ORINA**

#### **5.1.1 Introducción**

Este procedimiento describe un método para la separación, purificación y medición de uranio, torio, plutonio, americio y curio en muestras de orina. El método consiste en tomar un litro de muestra, cuando es factible, y coprecipitar los actínidos con CaHPO<sub>4</sub>. Luego se disuelve el precipitado en medio nítrico y se siembra en la columna Eichrom® UTEVA para separar y purificar uranio y torio selectivamente, del plutonio, americio y curio. La fracción conteniendo el uranio se electrodeposita y se mide por espectrometría alfa (Anexo I). Idem para la fracción conteniendo el torio.

La solución de siembra más lavados proveniente de la columna UTEVA, se siembra en la columna Eichrom® TRU para la separación y purificación del plutonio y americio-curio. La fracción conteniendo el plutonio se electrodeposita y se mide por espectrometría alfa (Anexo I). Idem para la fracción conteniendo el americio y curio.

#### **5.1.2 Equipamiento**

5.1.2.1 Sistema de espectrometría alfa: cámara de vacío con detector de ion implantado, pre-amplificador, amplificador, multicanal. El sistema es controlado por una computadora a través de un software, que permite el análisis de los datos, el almacenamiento de la información y la implementación de programas de trabajo

5.1.2.2 Plancha Calefactora

5.1.2.3 Centrífuga de pie, con capacidad para recipientes de 250 mL.

5.1.2.4 Recipientes de vidrio Pyrex™ de base redonda, de 250 mL, para ser usados en la centrífuga

5.1.2.5 Agitador magnético.

5.1.2.6 Balanza analítica

#### **5.1.3 Reactivos**

5.1.3.1 Soluciones calibradas de <sup>232</sup>U, <sup>242</sup>Pu, <sup>229</sup>Th, <sup>243</sup>Am, como trazadores

5.1.3.2 Solución de hidroxilamina NH<sub>2</sub>OH.HCl 0,7% (P/V) en HCl 0,2 M

5.1.3.3 Nitrito de sodio NaNO<sub>2</sub> (s) p.a.

5.1.3.4 Fosfato ácido de Calcio, CaHPO<sub>4</sub>, p.a.

5.1.3.5 Ácido nítrico, HNO<sub>3</sub> p.a.

5.1.3.6 Hidróxido de sodio, NaOH 10 M

5.1.3.7 Peróxido de Hidrógeno, 100 volúmenes p.a.

5.1.3.8 Resina de partición Eichrom® UTEVA (pre-packed column)

5.1.3.9 Solución de ácido nítrico, HNO<sub>3</sub> 3 M

5.1.3.10 Solución de nitrato de aluminio 1 M en HNO<sub>3</sub> 3 M

5.1.3.11 Solución de sulfamato ferroso 0,6 M

5.1.3.12 Ácido ascórbico, p.a.

5.1.3.13 Solución de ácido clorhídrico, HCl 9 M

5.1.3.14 Solución de ácido oxálico 0,05 M en HCl 5 M

5.1.3.15 Solución de ácido clorhídrico, HCl 0,01 M

#### **5.1.4. Procedimiento**

5.1.4.1 Medir 1 L de la muestra de orina y colocar en un vaso de precipitado.

5.1.4.2 Agregar una cantidad conveniente de solución calibrada de cada uno de los trazadores de <sup>232</sup>U, <sup>242</sup>Pu, <sup>229</sup>Th, <sup>243</sup>Am y homogeneizar. Es conveniente que la relación entre el trazador y el radionucleido a determinar sea 1.

5.1.4.3 Agregar 10 mL de HNO<sub>3</sub> (c) y calentar sobre plancha calefactora durante una hora a 80°C.

5.1.4.4 Agregar 200 mg de CaHPO<sub>4</sub> en agitación constante hasta disolución total.

5.1.4.5 Agregar NH<sub>4</sub>OH (c) gota a gota, con agitación continua, y precipitar hasta pH 10.

5.1.4.6 Dejar en digestión hasta el día siguiente.

5.1.4.7 Luego, sin mover el vaso de precipitado, hacer vacío (por efecto sifón) para retirar la mayor cantidad de líquido sobrenadante, hasta un volumen de aproximadamente 200 mL.

5.1.4.8 Trasvasar a un recipiente de centrífuga

5.1.4.9 Centrifugar durante 15 minutos a 1600 rpm.

5.1.4.10 Eliminar el sobrenadante.

5.1.4.11 Disolver el precipitado con 5 mL de HNO<sub>3</sub> (c), y trasvasar al vaso utilizado en 5.1.4.1, empleando una pipeta de transferencia descartable.

5.1.4.12 Lavar el recipiente de centrífuga con 2 porciones de 5 mL de HNO<sub>3</sub> (c) y trasvasar al vaso de precipitado

5.1.4.13 Mineralizar con pequeñas porciones de HNO<sub>3</sub> y H<sub>2</sub>O<sub>2</sub> de 100 volúmenes sobre plancha calefactora, hasta obtener un residuo totalmente blanco.

5.1.4.14 Hidrolizar a reflujo sobre plancha calefactora.

5.1.4.15 Llevar a casi sequedad y disolver el residuo en 15-20 ml de solución (HNO<sub>3</sub> 3 M + Al(NO<sub>3</sub>)<sub>3</sub> ) 1 M.

5.1.4.16 Agregar 2 ml de sulfamato ferroso (NH<sub>2</sub> SO<sub>3</sub> )<sub>2</sub>Fe 0,6 M.

5.1.4.17 Agregar 200 mg de ácido ascórbico p.a. Esperar 3-5 minutos.

5.1.4.18 Sembrar en la columna de resina de partición Eichrom® UTEVA, previamente acondicionada en medio nítrico 3 M.

5.1.4.19 Lavar con 5 ml de HNO<sub>3</sub> 3 M.

5.1.4.20 Recoger los líquidos de siembra y lavados, conteniendo Pu, Am y Cm, y reservar para su pasaje por la columna TRU. (Aregar agua bidestilada hasta obtener una solución HNO<sub>3</sub> 2 M).

5.1.4.21 Lavar la columna con 5 ml de HCl 9 M.

5.1.4.22 Eluir el Th de la columna UTEVA con 15 ml de ( HCl 5 M + ácido oxálico 0,05 M ) y reservar para la electrodeposición.

5.1.4.23 Eluir el U con 20 ml de HCl 0,01 M y reservar para la electrodeposición.

5.1.4.24 Llevar a sequedad y mineralizar con gotas de HNO<sub>3</sub> (c) y H<sub>2</sub>O<sub>2</sub> 100 vol. cada uno de los eluidos de los pasos 22 y 23.

5.1.4.25 Electrodepositar el uranio y el torio

5.1.4.26 Medir por espectrometría alfa (ANEXO I)

5.1.4.27 Sembrar en la columna TRU, acondicionada en HNO<sub>3</sub> 2 M, la solución proveniente del paso 20.

5.1.4.28 Lavar la columna con 5 mL de solución de NaNO<sub>2</sub> 0,1 M en HNO<sub>3</sub> 2 M, para oxidar el Pu<sup>3+</sup> a Pu<sup>4+</sup>. Descartar estas soluciones.

5.1.4.29 Eluir el Am con 3 mL de HCl 9 M y 20 mL de HCl 4 M, y reservar para la electrodeposición.

5.1.4.30 Lavar la columna con 4 mL de solución HCl 4M + HF 0,01M, para eliminar trazas de torio y descartar.

5.1.4.31 Eluir el Pu con 20 mL de solución de bioxalato de amonio 0,1 M y reservar para la electrodeposición.

5.1.4.32 Llevar a sequedad y mineralizar con gotas de HNO<sub>3</sub> (c) y H<sub>2</sub>O<sub>2</sub> 100 vol. cada uno de los eluidos de los pasos 29 y 31.

5.1.4.33 Electrodepositar el americio y el plutonio.

5.1.4.34 Medir por espectrometría alfa.

## 5.1.5. Cálculos

5.1.5.1 Cálculo de la concentración de actividad de uranio-238 en orina:

$$\text{Actividad}_{U - 238} (Bq / L) = \frac{\text{cuentas}(U - 238)}{\text{cuentas}(U - 232)} \times \frac{\text{Actividad}(U - 232)}{V_{\text{orina}}}$$

donde:

Actividad (U-232): actividad de trazador agregada a la muestra, en Bq.

Cuentas (U-238): cuentas de U-238 presentes en la muestra, obtenidas del espectro.

Cuentas (U-232): cuentas de U-232 obtenidas del espectro.

$V_{orina}$ : volumen de muestra de orina, en L.

- 5.1.5.2 Para calcular la actividad de U-234 y U-235 en orina, la fórmula es la misma pero se reemplaza U-238 por U-234 y por U-235 respectivamente.

Cálculo de la concentración de actividad de plutonio 238 en orina:

$$Actividad_{Pu-238}(Bq/L) = \frac{cuentas(Pu-238)}{cuentas(Pu-242)} \times \frac{Actividad(Pu-242)}{V_{orina}}$$

donde:

Actividad (Pu-242): actividad de trazador agregada a la muestra, en Bq.

Cuentas (Pu-238): cuentas de Pu-238 presentes en la muestra, obtenidas del espectro.

Cuentas (Pu-242): cuentas de Pu-242 obtenidas del espectro.

$V_{orina}$ : volumen de muestra de orina, en L.

- 5.1.5.3 Para calcular la actividad de plutonio-239 en orina, la fórmula es la misma pero se reemplaza Pu-238 por Pu-239.

5.1.5.4 Cálculo de la concentración de actividad de americio 241 en orina:

$$Actividad_{Am-241}(Bq/L) = \frac{cuentas(Am-241)}{cuentas(Am-243)} \times \frac{Actividad(Am-243)}{V_{orina}}$$

donde:

Actividad (Am-243): actividad de trazador agregada a la muestra, en Bq.

Cuentas (Am-241): cuentas de Am-241 presentes en la muestra, obtenidas del espectro.

Cuentas (Am-243): cuentas de Am-243 obtenidas del espectro.

$V_{orina}$ : volumen de muestra de orina, en L.

- 5.1.5.5 La misma fórmula se aplica para el cálculo de curio-244, pero reemplazando Am-241 por Cm-244.

5.1.5.6 Cálculo de la concentración de actividad de torio-232 en orina:

$$Actividad_{Th-232}(Bq/L) = \frac{cuentas(Th-232)}{cuentas(Th-229)} \times \frac{Actividad(Th-229)}{V_{orina}}$$

donde:

Actividad (Th-229): actividad de trazador agregada a la muestra, en Bq.

Cuentas (Th-232): cuentas de Th-232 presentes en la muestra, obtenidas del espectro.

Cuentas (Th-229): cuentas de Th-229 obtenidas del espectro.

$V_{\text{orina}}$ : volumen de muestra de orina, en L.

- 5.1.5.7 La actividad de torio-230 y de torio-228 se calculan en forma similar, reemplazando Th-232 por Th-230 y Th-228 respectivamente.

### 5.1.6. Rendimiento químico

El rendimiento químico de cada actínido se calcula aplicando la siguiente fórmula con el trazador correspondiente:

$$RQ = \frac{\text{cuentas(trazador)}}{\text{actividad(trazador)} \times E_f} \times 100$$

donde:

$E_f$  : eficiencia del detector

RQ: rendimiento químico

### 5.1.7 Actividad mínima detectable

Para 1 litro de orina, empleando un detector de eficiencia 0,40 cpm / dpm, un rendimiento químico de 60%, un tiempo de medición de 1000 minutos y para un fondo de 2,5 cuentas por día, la actividad mínima detectable es 0,63 mBq/L, para un nivel de confianza del 95%.

Para un tiempo de medición de la muestra igual al tiempo de medición del fondo, la fórmula a aplicar es la siguiente:

$$AMD(Bq/L) = \frac{3 + 4,65 \times \sqrt{c_f}}{t \times E_f \times RQ \times V_{\text{orina}}}$$

donde:

$c_f$ : cuentas correspondientes al fondo

$t$ : tiempo de medición (en segundos)

$E_f$ : eficiencia del detector

RQ: rendimiento químico

$V_{\text{orina}}$ : volumen de orina (en L)

NOTA: se debe tener en cuenta la contribución de las cuentas provenientes del trazador, a las cuentas en la zona de interés.

## 5.2 MUESTRAS DE HECES

### 5.2.1 Introducción

Este procedimiento describe un método para la separación, purificación y medición de uranio, torio, plutonio, americio y curio en muestras de heces. El método consiste en calcinar la muestra completa, empleando una rampa de temperatura adecuada, disolver las cenizas en medio nítrico y mineralizar hasta obtener un residuo totalmente blanco.

Luego se disuelve el residuo en medio nítrico y se siembra en la columna Eichrom® UTEVA para separar y purificar uranio y torio selectivamente, del plutonio, americio y curio. La fracción conteniendo el uranio se electrodeposita y se mide por espectrometría alfa (Anexo I). Idem para la fracción conteniendo el torio.

La solución de siembra más lavados proveniente de la columna UTEVA, se siembra en la columna Eichrom® TRU para la separación y purificación del plutonio y americio-curio. La fracción conteniendo el plutonio se electrodeposita y se mide por espectrometría alfa. Idem para la fracción conteniendo el americio y curio.

### **5.2.2. Equipamiento**

- 5.2.2.1 Sistema de espectrometría alfa
- 5.2.2.2 Plancha Calefactora
- 5.2.2.3 Materiales para electrodeposición
- 5.2.2.4 Horno de muflado, con rampa de temperatura programable
- 5.2.2.5 Agitador magnético
- 5.2.2.6 Balanza analítica

### **5.2.3. Reactivos**

- 5.2.3.1 Soluciones calibradas de  $^{232}\text{U}$ ,  $^{242}\text{Pu}$ ,  $^{229}\text{Th}$ ,  $^{243}\text{Am}$ , como trazadores
- 5.2.3.2 Solución de hidroxilamina  $\text{NH}_2\text{OH} \cdot \text{HCl}$  0,7% (P/V) en  $\text{HCl}$  0,2 M
- 5.2.3.3 Nitrito de sodio  $\text{NaNO}_2$  (s) p.a.
- 5.2.3.4 Fosfato ácido de Calcio,  $\text{CaHPO}_4$ , p.a.
- 5.2.3.5 Ácido nítrico,  $\text{HNO}_3$  p.a.
- 5.2.3.6 Hidróxido de sodio,  $\text{NaOH}$  10 M
- 5.2.3.7 Peróxido de Hidrógeno, 100 volúmenes p.a.
- 5.2.3.8 Resina de partición Eichrom® UTEVA (pre-packed column)
- 5.2.3.9 Solución de ácido nítrico,  $\text{HNO}_3$  3 M
- 5.2.3.10 Solución de nitrato de aluminio 1 M en  $\text{HNO}_3$  3 M
- 5.2.3.11 Solución de sulfamato ferroso 0,6 M
- 5.2.3.12 Ácido ascórbico, p.a.
- 5.2.3.13 Solución de ácido clorhídrico,  $\text{HCl}$  9 M
- 5.2.3.14 Solución de ácido oxálico 0,05 M en  $\text{HCl}$  5 M
- 5.2.3.15 Solución de ácido clorhídrico,  $\text{HCl}$  0,01 M

#### **5.2.4. Procedimiento**

- 5.2.4.1 Colocar la muestra pesada en una cápsula de porcelana y cubrir con papel aluminio perforado.
- 5.2.4.2 Calcinar en mufla, a 100 °C durante 6 horas y luego incrementar la temperatura a razón de 50°C hasta llegar a 550 °C con períodos de aproximadamente 4 horas. Dejar a 600°C durante 48 horas.
- 5.2.4.3 Retomar cuidadosamente el residuo con HNO<sub>3</sub> (50%).
- 5.2.4.4 Agregar una cantidad conveniente de solución calibrada de cada uno de los trazadores de <sup>232</sup>U, <sup>242</sup>Pu, <sup>229</sup>Th, <sup>243</sup>Am y homogeneizar.
- 5.2.4.5 Trasvasar cuantitativamente a un vaso de precipitado y mineralizar con sucesivos agregados de HNO<sub>3</sub> (c) y H<sub>2</sub>O<sub>2</sub> de 100 volúmenes sobre plancha calefactora, hasta obtener un residuo totalmente blanco.
- 5.2.4.6 De ser necesario transferir a un vaso de Teflon de base grafitada y calentar sobre plancha calefactora. Llevar a sequedad y agregar HNO<sub>3</sub> (c) y HF (c). Repetir hasta total eliminación de sílice. La aplicación de este paso depende de la composición de la matriz ya que no siempre el residuo obtenido en el paso anterior es soluble en HNO<sub>3</sub> 3M.
- 5.2.4.7 Llevar a sequedad y eliminar el HF con HNO<sub>3</sub>. Disolver el residuo en 15-20 ml de solución HNO<sub>3</sub> 3 M + Al(NO<sub>3</sub>)<sub>3</sub> 1 M.
- 5.2.4.8 Agregar 2 ml de sulfamato ferroso (NH<sub>2</sub> SO<sub>3</sub> )<sub>2</sub>Fe 0,6 M.
- 5.2.4.9 Agregar 200 mg de ácido ascórbico p.a. Esperar 3-5 minutos.
- 5.2.4.10 Sembrar en la columna de resina de partición Eichrom® UTEVA, previamente acondicionada en medio nítrico 3 M.
- 5.2.4.11 Lavar con 5 ml de HNO<sub>3</sub> 3 M.
- 5.2.4.12 Recoger los líquidos de siembra y lavados, conteniendo Pu, Am y Cm, y reservar para su pasaje por la columna TRU. (Agregar agua bidestilada hasta obtener una solución HNO<sub>3</sub> 2M).
- 5.2.4.13 Lavar la columna con 5 ml de HCl 9 M.
- 5.2.4.14 Eluir el Th de la columna UTEVA con 15 ml de (HCl 5 M + ácido oxálico 0,05 M) y reservar para la electrodeposición.
- 5.2.4.15 Eluir el U con 20 ml de HCl 0,01 M y reservar para la electrodeposición.
- 5.2.4.16 Llevar a sequedad y mineralizar con gotas de HNO<sub>3</sub> (c) y H<sub>2</sub>O<sub>2</sub> 100 vol. cada uno de los eluidos de los pasos 14 y 15.
- 5.2.4.17 Electrodepositar el uranio y el torio.
- 5.2.4.18 Medir por espectrometría alfa.
- 5.2.4.19 Sembrar en la columna TRU®, acondicionada en HNO<sub>3</sub> 2 M, la solución proveniente del paso 12.
- 5.2.4.20 Lavar la columna con 5 mL de solución de NaNO<sub>2</sub> 0,1 M en HNO<sub>3</sub> 2 M, para oxidar el Pu<sup>3+</sup> a Pu<sup>4+</sup>. Descartar estas soluciones.

5.2.4.21 Eluir el Am con 3 mL de HCl 9 M y 20 mL de HCl 4 M, y reservar para la electrodeposición.

5.2.4.22 Lavar la columna con 4 mL de solución HCl 4 M + HF 0,01 M, para eliminar trazas de torio y descartar.

5.2.4.23 Eluir el Pu con 20 mL de solución de bioxalato de amonio 0,1 M y reservar para la electrodeposición.

5.2.4.24 Llevar a sequedad y mineralizar con gotas de HNO<sub>3</sub> (c) y H<sub>2</sub>O<sub>2</sub> 100 vol. cada uno de los eluidos de los pasos 21 y 23.

5.2.4.25 Electrodepositar el americio y el plutonio.

5.2.4.26 Medir por espectrometría alfa.

## 5.2.5 Cálculos

Las cuentas correspondientes al área de cada pico se calculan con el software asociado al sistema de medición.

5.2.5.1 Cálculo de la concentración de actividad de uranio total en heces:

$$\text{Actividad}_{U-238} (\text{Bq/Kg}) = \frac{\text{cuentas}(U - 238)}{\text{cuentas}(U - 232)} \times \frac{\text{Actividad}(U - 232)}{M_{\text{heces}}}$$

donde:

Actividad (U-232): actividad de trazador agregada a la muestra, en Bq.

Cuentas (U-238): cuentas de U-238 presentes en la muestra, obtenidas del espectro.

Cuentas (U-232): cuentas de U-232 obtenidas del espectro.

M<sub>heces</sub>: masa de heces, en kg.

5.2.5.2 Para calcular la actividad de U-234 y U-235 en orina, la fórmula es la misma pero se reemplaza U-238 por U-234 y por U-235 respectivamente.

5.2.5.3 Cálculo de la concentración de actividad de plutonio-238 en heces:

$$\text{Actividad}_{Pu} (\text{Bq/Kg}) = \frac{\text{cuentas}(Pu - 238)}{\text{cuentas}(Pu - 242)} \times \frac{\text{Actividad}(Pu - 242)}{M_{\text{heces}}}$$

donde:

Actividad (Pu-242): actividad de trazador agregada a la muestra, en Bq.

Cuentas (Pu-238): cuentas de Pu-238 presentes en la muestra, obtenidas del espectro.

Cuentas (Pu-242): cuentas de Pu-242 obtenidas del espectro.

M<sub>heces</sub>: masa de heces, en kg.

5.2.5.4 Para calcular la actividad de plutonio-239 en heces, la fórmula es la misma pero se debe reemplazar Pu-238 por Pu-239.

5.2.5.5 Cálculo de la concentración de actividad de americio-241 en heces:

$$Actividad_{Am} (Bq / Kg) = \frac{cuentas(Am - 241)}{cuentas(Am - 243)} \times \frac{Actividad(Am - 243)}{M_{heces}}$$

donde:

Actividad (Am-243): actividad de trazador agregada a la muestra, en Bq.

Cuentas (Am-241): cuentas de Am-241 presentes en la muestra, obtenidas del espectro.

Cuentas (Am-243): cuentas de Am-243 obtenidas del espectro.

M <sub>heces</sub>: masa de heces, en kg.

5.2.5.6 La misma fórmula se aplica para el cálculo de curio-244, pero reemplazando Am-241 por Cm-244.

5.2.5.7 Cálculo de la concentración de actividad de torio-232 en heces:

$$Actividad_{Th} (Bq / Kg) = \frac{cuentas(Th - 232)}{cuentas(Th - 229)} \times \frac{Actividad(Th - 229)}{M_{heces}}$$

donde:

Actividad (Th-229): actividad de trazador agregada a la muestra, en Bq.

Cuentas (Th-232): cuentas de Th-232 presentes en la muestra, obtenidas del espectro.

Cuentas (Th-229): cuentas de Th-229 obtenidas del espectro.

M <sub>heces</sub>: masa de heces, en kg.

5.2.5.8 La actividad de torio-230 y de torio-228 se calculan en forma similar, reemplazando Th-232 por Th-230 y Th-228.

### 5.2.6. Rendimiento químico

El rendimiento químico de cada actínido se calcula aplicando la siguiente fórmula con el trazador correspondiente:

$$RQ = \frac{cuentas(trazador)}{actividad(trazador) \times E_f} \times 100$$

donde:

E<sub>f</sub> : eficiencia del detector

RQ: rendimiento químico

### **5.2.7. Actividad mínima detectable**

Para 300 g de heces, empleando un detector de eficiencia 0,40 cpm / dpm, un rendimiento químico de 60%, un tiempo de medición de 1000 minutos y para un fondo de 2,5 cuentas por día, la actividad mínima detectable es 2 mBq/kg, para un nivel de confianza del 95%.

Para un tiempo de medición de la muestra igual al tiempo de medición del fondo, se aplica la siguiente fórmula:

$$AMD(Bq/Kg) = \frac{3 + 4,65 \times \sqrt{c_F}}{t \times Ef \times RQ \times M_{heces}}$$

donde:

c<sub>F</sub>: cuentas correspondientes al fondo

t: tiempo de medición (en segundos)

E<sub>f</sub>: eficiencia del detector

RQ: rendimiento químico

M<sub>heces</sub>: masa de heces (en kg)

NOTA: se debe tener en cuenta la contribución de las cuentas provenientes del trazador, a las cuentas en la zona de interés.

## **5.3. ELECTRODEPOSICIÓN**

### **5.3.1. Materiales**

5.3.1.1 Fuente de tensión regulable a corriente constante

5.3.1.2 Celdas para electrodeposición de actínidos

5.3.1.3 Ánodos de platino

5.3.1.4 Discos de acero inoxidable 304L de 2 cm de diámetro con una de sus caras pulida “a espejo”.

### **5.3.2 Reactivos**

5.3.2.1 Indicador Azul de Timol, solución 0,04%: disolver 0,1 g de la sal en 21 mL de NaOH 0,01 M y agregar 230 mL de agua destilada

5.3.2.2 Ácido oxálico 0,5 M: disolver 6,3 g de ácido oxálico dihidrato p.a. y llevar a 100 mL con agua destilada

5.3.2.3 Ácido sulfúrico, H<sub>2</sub>SO<sub>4</sub> p.a.

5.3.2.4 Hidróxido de amonio, NH<sub>4</sub>OH p.a.

5.3.2.5 Papel indicador de pH de 0-7

5.3.2.6 Solución de ácidos fosfórico y sulfúrico (3 + 1): solución para electropulido

### **5.3.3. Procedimiento**

- 5.3.3.1 Evaporar en presencia de  $\text{HNO}_3$  la solución conteniendo los actínidos.
- 5.3.3.2 Disolver el residuo en 0,5 mL de  $\text{H}_2\text{SO}_4$  (c) y calentar. Agregar gotas de  $\text{H}_2\text{O}_2$  100 volúmenes p.a. para eliminar nitratos y calentar hasta humos blancos y dejar enfriar. Agregar 4 mL de  $\text{H}_2\text{O}$  destilada.
- 5.3.3.3 Agregar 0,1 mL de ácido oxálico 0,5 M para complejear el  $\text{Fe}^{3+}$ , eventualmente presente, y 1 gota del indicador azul de Timol. Llevar a pH 2,5 con  $\text{NH}_4\text{OH}$ , es decir, hasta el viraje del indicador del rosa al amarillo.
- 5.3.3.4 Transferir la solución a la celda de electrodeposición. Enjuagar 2 veces el vaso de precipitado con 2 mL de  $\text{H}_2\text{O}$  destilada y transferir a la celda.
- 5.3.3.5 Ajustar el flujo de corriente a 1,2 A. Electrodepositar durante 2 hs. Nota: Regular el volumen con agregado de más cantidad de  $\text{H}_2\text{O}$  destilada.
- 5.3.3.6 Despues de 2 hs agregar 1 mL de  $\text{NH}_4\text{OH}$  a la celda para neutralizar y así evitar la disolución del depósito en medio ácido; interrumpir inmediatamente la corriente.
- 5.3.3.7 Desarmar la celda y enjuagar con abundante  $\text{H}_2\text{O}$  destilada. Retirar el disco de acero inoxidable y continuar enjuagando. Nota: La manipulación del disco debe hacerse con pinzas para evitar cualquier contacto con grasa.
- 5.3.3.8 Colocar el disco en un vidrio de reloj y dejarlo debajo de una lámpara infrarroja hasta que llegue a sequedad.
- 5.3.3.9 La muestra se encuentra en condiciones de ser medida por espectrometría alfa.

### **5.3.4. Electropulido de los discos de acero inoxidable**

Para lograr depósitos adecuados que conduzcan a espectros bien resueltos, donde los picos sean muy finos, es conveniente el electropulido “a espejo” de los discos de acero inoxidable con una mezcla de ácido fosfórico y ácido sulfúrico (3 + 1).

- 5.3.4.1 Transferir la 5 mL de la mezcla de ácidos fosfórico y sulfúrico (3+1) a la celda de electrodeposición.
- 5.3.4.2 Conectar el polo negativo al electrodo de platino y el polo positivo al disco de acero (conexión inversa a la electrodeposición).
- 5.3.4.3 Ajustar el flujo de corriente a 1,2 A y electropulir durante 5 minutos.
- 5.3.4.4 Interrumpir la corriente y enjuagar con abundante agua destilada.
- 5.3.4.5 El disco pulido está en condiciones de ser electrodepositado.

## **5.4. INCERTIDUMBRE**

Empleando la fórmula para el cálculo de la actividad y la ley de propagación de errores, la incertidumbre relativa en la concentración de actividad se expresa como:

$$\frac{\sigma_{A_A}}{A_A} = \sqrt{\left( \frac{\sigma_{A_T}}{A_T} \right)^2 + \left( \frac{\sigma_{C_T}}{C_T} \right)^2 + \left( \frac{\sigma_{C_A}}{C_A} \right)^2 + \left( \frac{\sigma_{V_{orina}}}{V_{orina}} \right)^2}$$

donde:

$A_A$ : concentración de actividad del radionucleido a determinar (U-234, U-235, U-238, Pu-238, Pu-239, Am-241, Cm-244, Th-228, Th-230, Th-232)

$A_T$ : actividad agregada de trazador

$C_T$ : cuentas del trazador

$C_A$ : cuentas del radionucleido a determinar

$V_{orina}$ : volumen de orina

$\sigma_{AT}$ : incertidumbre asociada a la actividad del trazador

$\sigma_{CT}$ : incertidumbre asociada a las cuentas del trazador

$\sigma_{CA}$ : incertidumbre asociada a las cuentas del radionucleido a determinar

$\sigma_{V_{orina}}$ : incertidumbre asociada al volumen de orina

En el caso de heces, se reemplaza  $V_{orina}$  por  $M_{heces}$ .

## 6. REGISTROS

### 6.1 MUESTRAS

Las muestras se registran en una base de datos donde se detalla el tipo de muestra, la procedencia, el solicitante del análisis, la fecha de toma de muestra, la fecha de ingreso al laboratorio, los resultados de la determinación, los espectros asociados a la medición y la fecha de informe de resultados. Cualquier otro dato que aporte información debe ser registrado.

### 6.2. SOLUCIONES DE REFERENCIA

Se lleva un registro de todas las soluciones de referencia empleadas, indicando proveedor, fecha de compra, fecha de calibración, fecha de validez, cantidad.

### 6.3. EQUIPAMIENTO

Se lleva un registro periódico de la calibración de los detectores y de los fondos, indicando las fechas y las novedades. Los períodos de calibración y fondos se establecen en función de las necesidades de medición. Es conveniente trazar gráficos de control de los mismos.

## 7. REFERENCIAS

- 7.1 A. Yamato, Journal of Radioanalytical Chemistry, Vol. 75, Nros. 1-2 (1982) 265.
- 7.2 S. Ballestra, R. Fukai, Talanta. Vol 30. No1.(1983) 45-48.
- 7.3 N.A. Talvite. Anal. Chem, (1972) 44, 280.

## **8. ANEXOS**

**ANEXO I: PO-EA-01-AN 01:** Instructivo para medición por espectrometría alfa

**ANEXO II: PO-EA-01-AN 02:** Diagrama de las celdas de electrodeposición

## **ANEXO I** **INSTRUCTIVO PARA MEDICIÓN POR ESPECTROMETRÍA ALFA**

### **1. OBJETIVO**

Describir instrucciones para la identificación y medición de radionucleidos emisores alfa presentes en una fuente alfa.

### **2. CAMPO DE APLICACIÓN**

Se aplica a todos los laboratorios que efectúan mediciones por espectrometría alfa.

### **3. REFERENCIA**

- 3.1. Manual de Técnicas de Laboratorio, Autoridad Regulatoria Nuclear, Julio 2002
- 3.2. Manual del sistema de espectrometría alfa y del software asociado

### **4. DESCRIPCIÓN**

#### **4.1. EQUIPAMIENTO**

- 4.1.1 Sistema de espectrometría alfa.
- 4.1.2 Fuente alfa de actividad conocida (“patrón alfa”).
- 4.1.3 Fuente alfa de tres picos

#### **4.2 IDENTIFICACIÓN DE RADIONUCLEIDOS EMISORES ALFA**

- 4.2.1 Calibrar en energía el sistema de espectrometría alfa, con la geometría que se empleará en las mediciones
- 4.2.2 Medir el fondo, con la misma geometría, como mínimo durante un día.
- 4.2.3 Medir la fuente de radionucleidos emisores alfa desconocidos, durante el tiempo necesario para colectar suficiente número de cuentas, de manera tal que sea posible la identificación de picos en el espectro.
- 4.2.4 Archivar el espectro obtenido.
- 4.2.5 Cuando el tiempo de medición del fondo es igual al de la muestra, descontar el espectro de fondo, empleando el software asociado, o bien descontando las cuentas correspondientes a la zona de interés del espectro. Cuando los tiempos no son iguales, se descuentan las cpm correspondientes a la zona de interés.
- 4.2.6 Identificar los picos del espectro en función de la energía, empleando una tabla de radionucleidos alfa, o bien mediante la base de datos incorporada al software.

- 4.2.7 Si para un mismo pico corresponden 2 o más radionucleidos, que no sean isótopos entre sí, se aplica la separación química de dichos elementos según los procedimientos radioquímicos correspondientes.

### **4.3. EFICIENCIA DEL DETECTOR**

- 4.3.1 Colocar la fuente alfa de actividad conocida “patrón alfa” en la cámara, con la geometría empleada para la medición.
- 4.3.2 Medir durante el tiempo necesario para colectar suficiente número de cuentas.
- 4.3.3 Archivar el espectro obtenido.
- 4.3.4 Descontar del pico las cuentas correspondientes al fondo.
- 4.3.5 Empleando el software asociado al sistema de espectrometría alfa, determinar las cuentas por segundo del pico del emisor alfa patrón en el espectro.
- 4.3.6 Determinar la eficiencia del detector empleando la siguiente expresión:

$$Ef(cps/Bq) = \frac{C_p}{t \cdot \epsilon \cdot A_p}$$

donde:

$C_p$ : cuentas correspondientes al pico del emisor alfa patrón

$t$ : tiempo de medición (segundos)

$A_p$ : actividad del radionucleido patrón (Bq)

$\epsilon$ : emisividad del pico

### **4.4 MEDICIÓN DE LA ACTIVIDAD DE UN RADIONUCLEIDO EMISOR ALFA**

- 4.4.1 Colocar la fuente del radionucleido emisor alfa de actividad desconocida en la cámara, con la geometría empleada para la medición de fondo y eficiencia.
- 4.4.2 Medir durante el mismo tiempo de medición de fondo.
- 4.4.3 Calcular la actividad del radionucleido en la fuente empleando la siguiente expresión:

$$A(Bq) = \frac{C}{t \cdot Ef}$$

donde:

$C$ : cuentas del radionucleido emisor alfa cuya actividad se quiere determinar

$t$ : tiempo de medición (segundos)

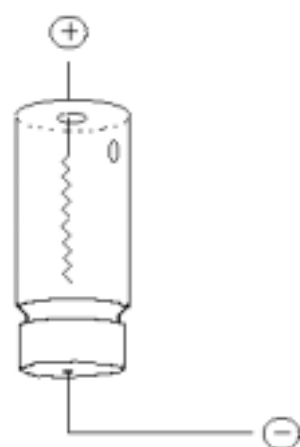
$Ef$ : eficiencia del detector (cps/Bq)

#### **4.5 CONTROL DE CALIDAD**

Todo programa de control de calidad para los sistemas de espectrometría alfa debe incluir:

1. Mediciones de fondo rutinarias.
2. Calibración en eficiencia rutinarias.
3. Calibración en energía rutinarias.
4. Gráficos de control de los parámetros anteriores.
5. Participación en programas de intercomparación con laboratorios extranjeros que involucran la medición de un considerable número de emisores alfa.
6. Registros de cada una de las calibraciones.

**ANEXO II**  
**DIAGRAMA DE LAS CELDAS DE ELECTRODEPOSICIÓN**



Primer ejercicio de intercomparación  
para la Argentina organizado por la ARN  
para la determinación de uranio  
en muestras de agua y orina

Serdeiro, N.H. y Equillor, H.E.



# **PRIMER EJERCICIO DE INTERCOMPARACIÓN PARA LA ARGENTINA ORGANIZADO POR LA ARN PARA LA DETERMINACIÓN DE URANIO EN MUESTRAS DE AGUA Y ORINA**

Serdeiro, N.H. y Equillor, H.E.

Autoridad Regulatoria Nuclear  
Argentina

Un ejercicio de intercomparación organizado por la Autoridad Regulatoria Nuclear fue llevado a cabo durante el año 2000 para la determinación de uranio en muestras de agua y orina. El objetivo de este ejercicio de intercomparación fue comparar los valores de uranio que los distintos laboratorios informan sobre una misma muestra, y promover la identificación de incertidumbres vinculadas con el proceso de obtención del resultado. Participaron 6 laboratorios que usualmente realizan este tipo de análisis. En este trabajo se presentan los valores informados por cada laboratorio, así como una evaluación del desempeño de cada uno de ellos.

## **1. INTRODUCCIÓN**

En el ámbito de la protección radiológica, tanto en lo ocupacional como ambiental, la confiabilidad en los resultados del análisis de cualquier radionucleido es de importancia crucial. Esto se debe a que el cálculo de dosis y las decisiones a tomar, dependen de la certeza de los resultados de medición.

La confiabilidad de las mediciones llevadas a cabo por los laboratorios puede ser puesta de relieve por medio de ejercicios de intercomparación y la participación continua en estos ejercicios debería llevar a una mejora en las técnicas radioquímicas y/o de medición, y consecuentemente en la confiabilidad de los resultados. En una publicación reciente<sup>[1]</sup>, donde se exponen los resultados de la participación de la ARN, en los ejercicios de intercomparación QAP (Quality Assessment Program) organizados por el EML (Environmental Measurements Laboratory), se muestra gráficamente el mejoramiento progresivo evidenciado por el conjunto de los laboratorios participantes (aproximadamente 150), durante el período 1995-2001. El ejercicio de intercomparación organizado por la ARN durante el año 2000 apunta a cubrir esta necesidad.

## **2. LAS MUESTRAS**

Para cada uno de los laboratorios participantes, se prepararon dos muestras conteniendo uranio, una de agua y la otra de orina. El tiempo de análisis aproximado fue de 30 días. La participación fue anónima, y cada laboratorio tuvo asignado un número de código, que fue puesto en conocimiento de cada uno de los participantes en forma individual en el momento en que se dieron a conocer los resultados de la intercomparación.

Las muestras tuvieron las siguientes características:

**AGUA:** Volumen: 200 mL  
Contenido de uranio natural: entre 10 y 100 µg / L  
Medio: HNO<sub>3</sub> 1 M

**ORINA:** Volumen: 200 mL  
Contenido de uranio natural: entre 5 y 50 µg / L  
Medio: HNO<sub>3</sub> 0,2 M

**ORINA BLANCO:** Esta muestra no contenía agregado de uranio y fue entregada para ser utilizada como blanco.

La muestra de agua fue preparada a partir de agua destilada acidificada con ácido nítrico y contaminada, por pesada, con una solución patrón de U natural.

La muestra de orina fue preparada a partir de orina blanco, de personal no expuesto y acidificada con ácido nítrico. Una alícuota se reservó para ser usada como blanco y el resto de la orina fue contaminada con la misma solución patrón de U natural.

La solución de U natural fue preparada gravimétricamente por dilución de una solución patrón de la empresa Analytics Inc., la cual mantiene trazabilidad con el NIST (National Institute of Standards and Technology). La dilución fue chequeada por espectrometría alfa.

### **3. CRONOGRAMA**

Ambas muestras fueron enviadas el 6 de noviembre de 2000 y la fecha límite para informar los resultados fue el 7 de diciembre de 2000.

### **4. LABORATORIOS PARTICIPANTES**

#### ***Comisión Nacional de Energía Atómica***

U.A. Química - Grupo Servicios Analíticos  
Laboratorio de análisis especiales  
Método: Espectrometría de absorción molecular con Br-PADAP

#### ***Comisión Nacional de Energía Atómica***

U.Protección Radiológica y salvaguardias  
Laboratorio Dosimetría personal y de Área  
Método: Espectrometría alfa / Fluorimetría directa

#### ***Comisión Nacional de Energía Atómica***

U.A. Geología  
Laboratorio Geoquímica  
Método: Fluorescencia láser

#### ***Dioxitek S.A.***

Laboratorio Químico -ICP-MS  
Método: ICP-MS

#### ***Facultad de Ciencias Aplicadas a la Industria (U.N.C.)***

Laboratorio Radiológico  
Método: Fluorimetría con UA3 de Scintrex

#### ***Autoridad Regulatoria Nuclear***

Gerencia de Apoyo Científico  
Laboratorio de Análisis Radioquímicos  
Método: Fluorimetría directa

### **5. RESULTADOS Y EVALUACIÓN**

#### ***5.1 Muestra de agua***

El criterio de evaluación adoptado ha sido el de la ISO guide 43<sup>[2]</sup>, que establece criterios estadísticos de performance para intercomparaciones entre laboratorios. Este criterio es utilizado también por otras instituciones<sup>[3-6]</sup>. Para la evaluación de los resultados se toma en cuenta el valor de Z que se define como:

$$Z = \frac{VI - VR}{\sigma}$$

siendo:

VR: valor de referencia, establecido por la ARN

VI: valor informado por el laboratorio correspondiente

$\sigma$ : la desviación estándar de los valores informados, exceptuando valores extremos

El resultado se considera *aceptado* si  $|Z| \leq 2$ , y en ese caso lo llamaremos "A". Si  $2 < |Z| \leq 3$ , el resultado se considera *questionable*, lo que denotaremos con una "C". Para  $|Z| > 3$ , el resultado es *no aceptable* o fuera de control, y lo llamaremos "N".

La desviación estándar ( $\sigma$ ) calculada fue: 0,743 (excluyendo al laboratorio 5, cuyo  $|Z|$  fue mayor que 10, por lo que fue descartado). Los límites de aceptabilidad ( $L = Z \cdot \sigma + VR$ ) resultaron:

$$33,41 \leq A \leq 36,39$$

$$32,67 < C \leq 33,41 \quad y \quad 36,39 < C \leq 37,13$$

$$32,67 > N > 37,13$$

La tabla 1 muestra los valores informados por cada uno de los laboratorios sobre la muestra de agua y los correspondientes valores de Z, mientras que las figuras 1 y 2 permiten apreciar esos valores con sus errores así como también el Z:

Muestra: AGUA

Valor de referencia (VR): 34,9  $\mu\text{g} / \text{L}$

Error (1 sigma): 1,7  $\mu\text{g} / \text{L}$

Código del laboratorio	Valor informado (VI)	Error informado	Z	Evaluación
1	35,1	2,5	0,27	A
2	34	3	-1,21	A
3	34	4	-1,21	A
4	33,0	0,3	-2,56	C
5	27	3	-10,63	N
6	34	4	-1,21	A

**Tabla 1.** Valores de uranio informados

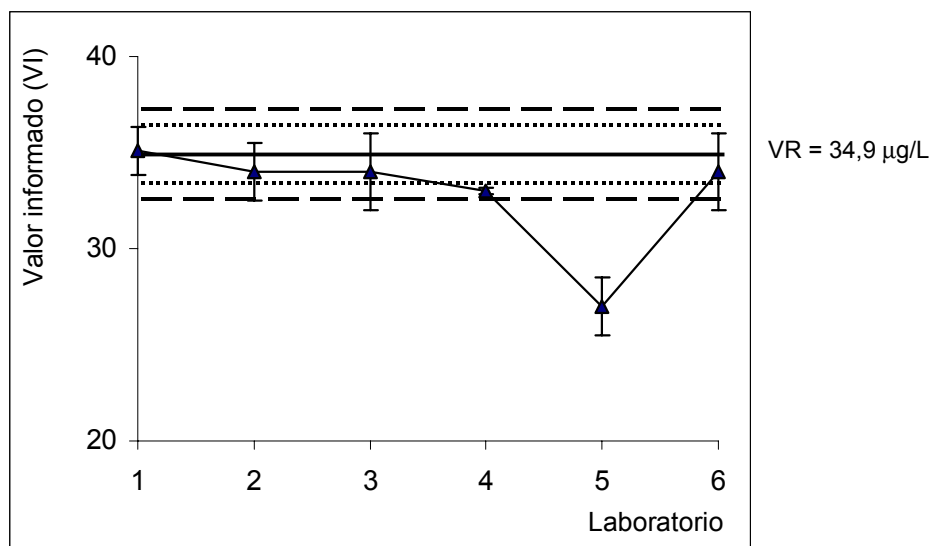


**Figura 1.** Valores informados para la muestra de agua

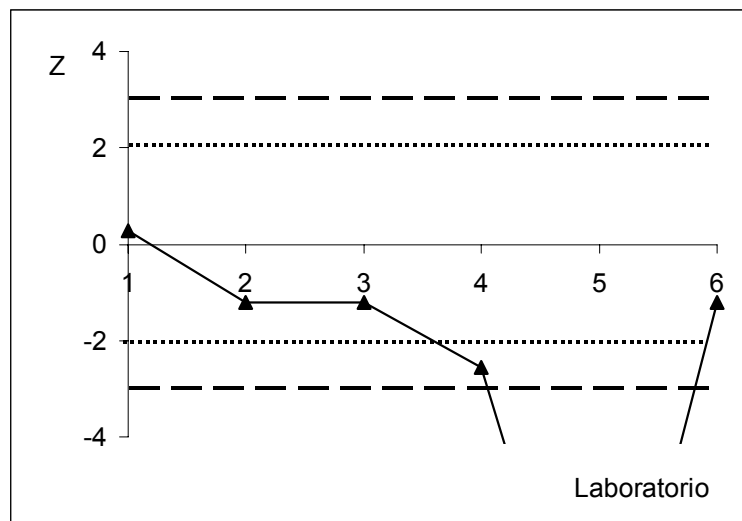


**Figura 2.** Valores de Z para la muestra de agua y límites de aceptabilidad

### 5.2 Muestra de orina

Para la evaluación de los resultados se ha tomado en cuenta el desvío relativo, como una medida de cuan cercano se encuentra el valor informado al valor esperado o de referencia y se define como:

$$D = \frac{VI - VR}{VR}$$

siendo:

VR: valor de referencia, establecido por la ARN

VI: valor informado por el laboratorio correspondiente

De acuerdo a la norma ISO 12790-1<sup>[7]</sup>, que establece criterios estadísticos de performance para radiobioensayo (mediciones in vivo e in vitro) orientados a la radioprotección, el valor de  $D$  deberá estar comprendido entre -0,25 y 0,50. Otras publicaciones de relevancia<sup>[8-10]</sup> asumen

también este criterio. Las categorías de “A” (aceptado) y “N” (no aceptado) permitirán visualizar en forma inmediata si el valor informado se encuentra dentro de dichos límites o por el contrario, los supera. Los límites de aceptabilidad ( $L = D \cdot VR + VR$ ) resultaron:

$$18,08 \leq A \leq 36,15$$

$$18,08 > N > 36,15$$

La tabla 2 muestra los valores informados por cada uno de los laboratorios sobre la muestra de orina, mientras que las figuras 3 y 4 permiten apreciar esos valores con sus errores así como también el D:

Muestra: ORINA

Valor de referencia ( VR ): 24,1  $\mu\text{g} / \text{L}$

Error (1 sigma): 1,2  $\mu\text{g} / \text{L}$

Código del laboratorio	Valor informado ( VI )	Error informado	D	Evaluación
1	21,5	4,4	-0,108	A
2	23	3	-0,045	A
3	27	3	0,12	A
4	25,7	0,2	0,066	A

**Tabla 2.** Valores de uranio informados

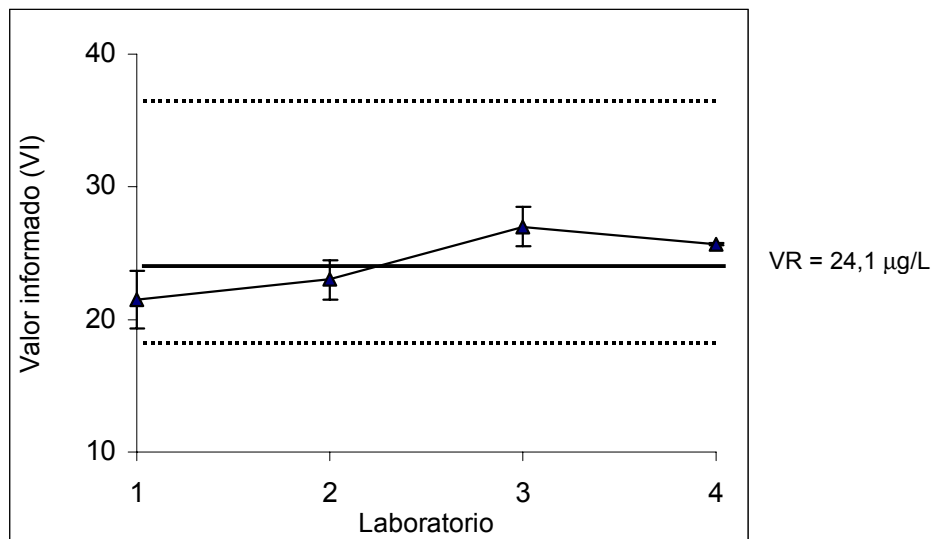


**Figura 3.** Valores informados para la muestra de orina

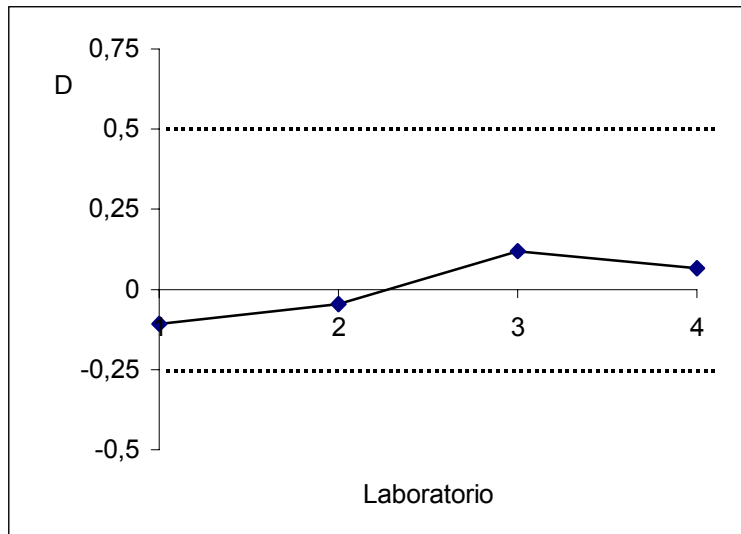


**Figura 4.** Valores de D para la muestra de orina y límites de aceptabilidad

## 6. CONCLUSIONES

En el caso de la muestra de agua, la mayoría de los resultados recibidos se ubicaron dentro de los límites de aceptación adoptados, que siguen criterios incluidos en la norma internacional ISO/IEC. Uno de los resultados cayó dentro de la segunda categoría, es decir la denominada *cuestionable*, y uno fue claramente *no aceptable*.

En el caso de la muestra de orina, todos los resultados recibidos se ubicaron dentro de los límites de aceptación adoptados, que siguen criterios incluidos en la norma internacional ISO/FDIS para muestras biológicas.

## 7. BIBLIOGRAFÍA

1. ARN PI-3/03, Equillor H., Serdeiro N., etc., "Results of the ARN participation in the Quality Assessment Program of the EML-DOE during period 2000-2001", 2003.
2. ISO/IEC guide 43, "Proficiency testing by interlaboratory comparisons", 1997.
3. IAEA-384, "Report on the intercomparison run", 2000.
4. IAEA-381, "Report on the intercomparison run", 1999.
5. Quasimeme Lab., "Assessment rules for the evaluation of the Q.L.", 1999.
6. CAN-P-43, "Proficiency testing by interlaboratory comparisons", 2001.
7. International Standard ISO/FDIS 12790-1, "Radiation Protection-Performance criteria for radiobioassay".
8. Regulatory Standards S-106 (E), "Technical and quality assurance standards for dosimeter services in Canada", 1998.
9. DOE-STD-1112-98, "The Department of Energy laboratory accreditation program for radiobioassay", 1998.
10. ORPGUIDE, Safety Guide RS-Guide-1.2, "Assessment of occupational exposure due to intake of radionuclides", IAEA, 1999.

# A Rapid Method for Determination of Uranium, Americium, Plutonium and Thorium in Soils Samples

Serdeiro, N.H. and Marabini, S.



# A Rapid Method for Determination of Uranium, Americium, Plutonium and Thorium in Soils Samples

Serdeiro, N.H<sup>1</sup> and Marabini, S.<sup>2</sup>

<sup>1</sup>Autoridad Regulatoria Nuclear, Av. Del Libertador 8250, C.P.1429, Buenos Aires, Argentina  
E-mail: nserdeir@cae.arn.gov.ar

<sup>2</sup>Comisión Nacional de Energía Atómica, Av. Del Libertador 8250, C.P.1429, Buenos Aires,  
Argentina

**Abstract.** A simple and fast method for actinides determinations in soils samples is described. Uranium, plutonium, americium and thorium are separated using UTEVA and TRU Eichrom® Resins. The sample is traced with uranium 232, plutonium 242 and americium 243, and then is digested with a mixture of nitric, hydrofluoric and perchloric acids in a sealed bomb with Teflon® at 150°C during 4 hours. The solution is transferred into a Teflon® beaker with graphite base and evaporated to near dryness. Nitric acid is added several times in order to eliminate the hydrofluoric acid and then is evaporated to dryness to eliminate perchloric acid. The residue is dissolved in nitric acid and aluminum nitrate solution. Then ferrous sulfamate and ascorbic acid are added. The sample solution is passed through the UTEVA® Resin column. The loading and rinsing effluent is reserved for the subsequent americium and plutonium separation. The UTEVA® Resin column is rinsed several times in order to eliminate polonium, since <sup>210</sup>Po interfere in the uranium measurement by alpha spectrometry. Thorium and neptunium are eluted with hydrochloric and oxalic acids. The uranium is eluted with diluted hydrochloric acid. The reserved solution for the americium and plutonium separation is passed through the TRU® Resin column. The americium is eluted from TRU® with hydrochloric acid and the plutonium is eluted with ammonium bioxalate. The actinides are electrodeposited on stainless steel disc and measured by alpha spectrometry. Several standard samples were analyzed and their results are presented.

## 1. Introduction

For identification and quantification alpha emitters radionuclides it is necessary to separate and purify from each other in order to obtain highly accurate results. A rapid and reliable determination is a desirable and necessary option in most of the radiochemical analysis.

Current techniques for sample dissolution and for actinides separation and purification, include leaching with strong acids, microwave digestion, precipitation, solvent extraction, ion exchange and extraction chromatography. In the following method, a proper combination of some of these techniques, allows to obtain a very good separation of U, Th, Pu y Am into four spectroscopically distinct groups. The total dissolution of soil samples is necessary to improve the U quantification. The elimination of some steps, like precipitation and solvent extractions, permits an important reduction of the time required for the analysis. Using only two extraction chromatography columns, Eichrom® UTEVA and TRU [1,2], permits a significant reduction of acids volumes and their concentration.

## 2. Procedure

Pre-packed UTEVA and TRU Eichrom® Resin columns were used for all tests. Reference soils (QAP and IAEA) and tracer solutions of uranium-232, plutonium-242 and americium-243 were used in the testing procedures.

The used recipient for sample dissolution was a sealed bomb with Teflon®. This is an appropriate hermetic recipient sealed of Teflon with an O'Ring® of Viton®.

The following method was developed through a series of experiences that included:

- Different techniques for soil samples dissolution
- Different sizes of soil samples.
- Tests with and without calcium oxalate precipitation in the sample preparation
- Different techniques to resolve the problem of interference of polonium-210 with uranium-232 tracer.

## **2.1. Sample preparation**

A 0.5g of soil sample was placed in the recipient of Teflon®. Uranium-232, plutonium-242 and americium-243 were added as tracers. Then, 8 ml of HNO<sub>3</sub>(c), 12 ml of HF(c) and 2 ml of HClO<sub>4</sub> (c) were added to the sample. The recipient was hermetically closed and the sample was digested at 150°C for about 5 hours.

The obtained solution was transferred to a Teflon® baker with graphite base and was evaporated to near dryness. The residue was dissolved in 5 ml of HF(c) and evaporated to near dryness again. The last step was repeated until no evidence of Si was in the sample. 10 ml of HNO<sub>3</sub>(c) were added and evaporated to dryness in order to eliminate the HF. The residue was dissolved in the minimum necessary amount of (3M HNO<sub>3</sub> + 1M Al(NO<sub>3</sub>)<sub>3</sub>). Usually, 13-15 ml are necessary for total dissolution.

3 ml of ferrous sulfamate 0.6M and 200 mg of ascorbic acid were added to the sample solution. It was allowed to stand for 5 minutes prior to load onto columns.

## **2.2. Actinides separation and purification**

The soil solution was passed through the UTEVA column. The resin was rinsed with 20 ml of 3 M HNO<sub>3</sub>. The loading and washing solutions were collected and reserved to pass through the TRU column. This solution is named “second loading” and contains Pu, Am and small traces of Th. It is important do not let it stand more than 3 hours until TRU loading.

The medium was changed passing through the UTEVA column 5 ml of 9M HCl. Th was eluted with 20 ml of (5M HCl + oxalic acid 0.05 M) and saved for the subsequent electrodeposition. Finally, U was eluted using 20 ml of 0.01M HCl and reserved for polonium elimination and electrodeposition.

The second loading solution was passed through the TRU column.

In order to oxidize the possible Pu<sup>3+</sup> to Pu<sup>4+</sup>, 5 ml of (3 M HNO<sub>3</sub> + 0.1 M NaNO<sub>2</sub>) was passed through the TRU resin. Am was eluted using 3 ml of 9M HCl and 20 ml of 4 M HCl, and this eluate was reserved for the subsequent electrodeposition.

To eliminate possible contamination with small traces of Th, the TRU resin was rinsed with 8 ml of (4 M HCl + 0.01 M HF).

Pu was eluted with 20 ml of ammonium bioxalate 0.1 M and reserved for electrodeposition.

## **2.3. Polonium removal**

It was observed that small traces of polonium are eluted with uranium, even though the first rinse with 3M HNO<sub>3</sub>. Since alpha particle energies of <sup>210</sup>Po and <sup>232</sup>U are similar, and impossible to resolve spectroscopically, the remaining polonium must be removed previous to electrodeposition.

The uranium eluate was evaporated to dryness and dissolved in HCl (c); 0.5 g of hydrazine dichlorhydrate was added and let it stand for 10 minutes, to reduce Po<sup>4+</sup>. The solution was evaporated to dryness and was maintained at 250°C for about 4 hours in order to remove the PoCl<sub>2</sub>. To assure the total elimination of polonium and the hydrazine decomposition, the residue was subjected to 500°C in a furnace for 8 hours. Uranium was dissolved in HNO<sub>3</sub> (c) and prepared for electrodeposition.

The procedure chart of this method is shown in figure 1.

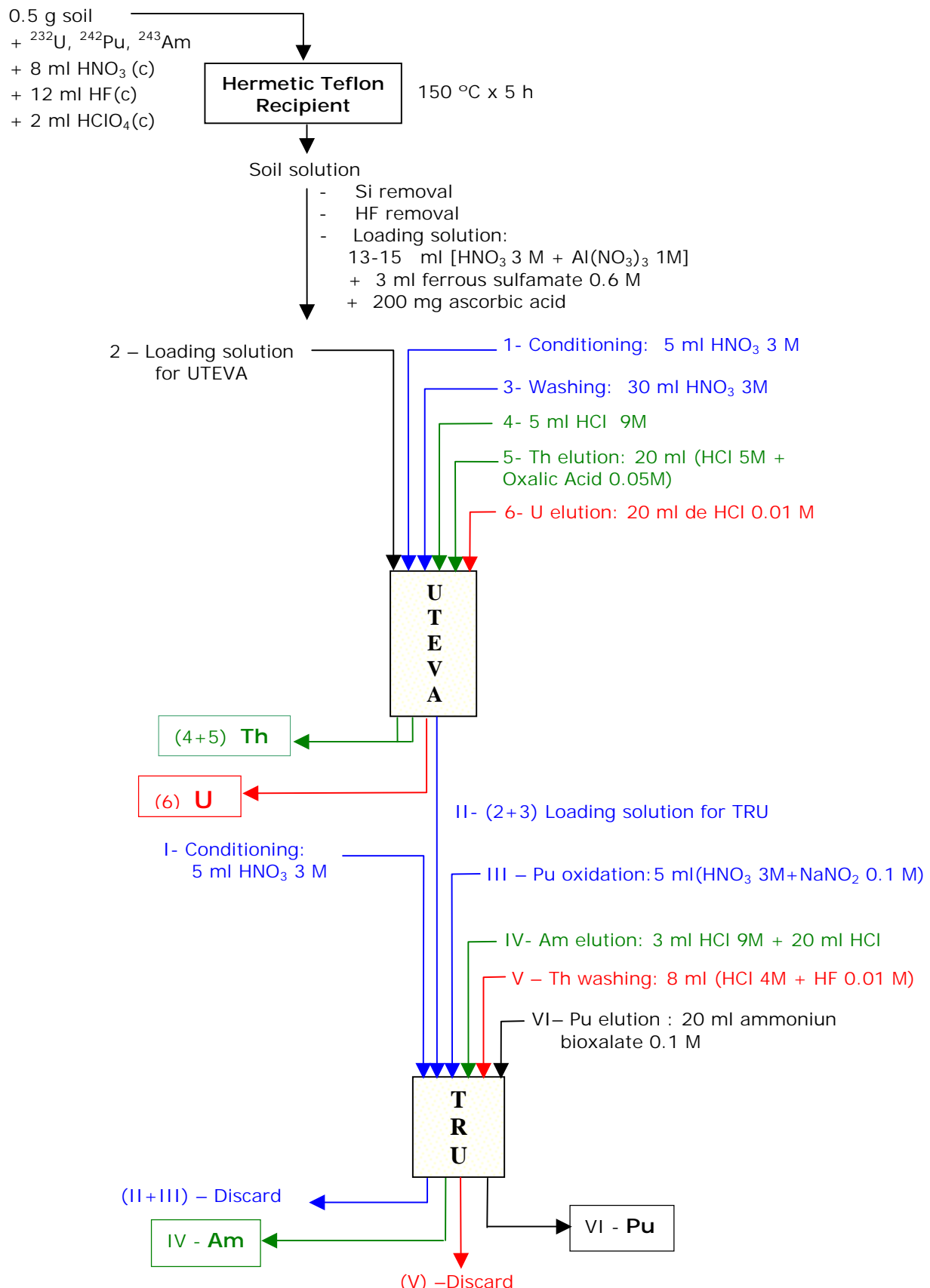


FIG. 1. Procedure chart

## 2.4. Electrodeposition

The actinides were electroplated on stainless steel discs, in ammonium sulphate media at pH 2.5, during 2 hours, according to the habitual technique used in the laboratory [3]. The discs were previously electropolished with a mixture of sulphuric and phosphoric acids, in order to achieve better peaks resolution in the spectra. The electroplated actinides were measured by alpha spectrometry.

## 2.5. Measurement

The alpha spectrometers used for the measurements were:

- 1)  $\alpha$  Alpha Analyst™ -Canberra and
- 2) Octete™PC - EG&G Ortec,  
equiped with the following detectors:
  - 1) Passivated Ion-Implanted Planar Silicon (PIPS) 900 mm<sup>2</sup>, distance 5 mm (Canberra)
  - 2) Ultra™ Ion Implanted Silicon (EG&G Ortec), 900, 1200 mm<sup>2</sup>, distance 5 mm.

The spectra were analyzed using the software PC-based "PROALFA V.9" developed by A.R.N. personnel [4].

## 3. Results and discussion

For testing the applicability of the present procedure, some standard soils were analyzed. Their results and the reference values are listed in table I. The analyzed samples were: soil QAP 0203 (QAP 56) EML-USDOE, QAP 0303 (QAP 58) EML-USDOE, and IAEA-135 Sediment. The chemical yields and the minimum detectable amount of each radionuclide are presented in table II.

Table I. Obtained Values (OV) compared with Reference Values (RV)

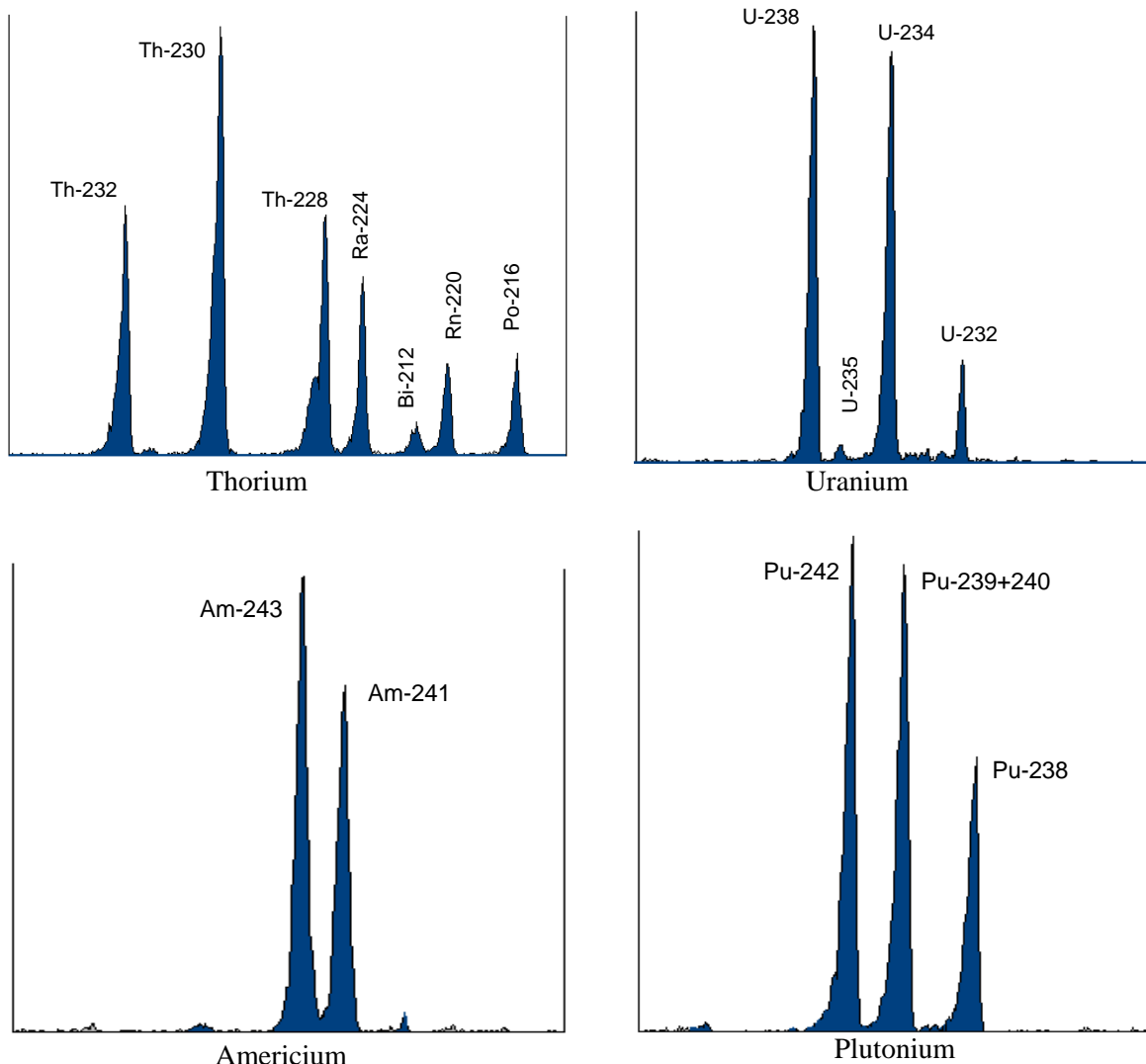
Sample Radio- nuclide	Value	QAP 0203 (56)	IAEA -135 Sediment	IAEA -135 Sediment	QAP 0303 (58)	QAP 0303 (58)
<b>U-234</b> <b>(Bq/Kg)</b>	<b>OV</b>	92.6	28.4	28.7	116	115
	<b>RV</b>	93.88	28.3	28.3	120.0	120.0
<b>U-238</b> <b>(Bq/Kg)</b>	<b>OV</b>	98.2	29.8	29.5	123	120
	<b>RV</b>	96.78	30.0	30.0	125.0	125.0
<b>U-total</b> <b>(Bq/Kg)</b>	<b>OV</b>	198.3	59.6	61.5	245	244
	<b>RV</b>	194.77	59.35	59.35	249.0	249.0
<b>Am-241</b> <b>(Bq/Kg)</b>	<b>OV</b>	---	315	309	15.6	---
	<b>RV</b>	10.927	318	318	13.7	13.7
<b>Pu-238</b> <b>(Bq/Kg)</b>	<b>OV</b>	0.706	44	41	22.7	---
	<b>RV</b>	0.691	43	43	22.38	22.38
<b>Pu-239+240</b> <b>(Bq/Kg)</b>	<b>OV</b>	18.93	230	217	23.4	---
	<b>RV</b>	19.098	213	213	22.6	22.6

Table II. Chemical Yields and Minimum Detectable Amount

	Chemical Yield (%)				Minimum Detectable Amount (Bq/Kg)			
	U	Pu	Am	Th	U total	Pu-239	Am-241	Th-228
<b>QAP 0203 (56)</b>	68	47	21	--	0.57	0.63	0.89	--
<b>IAEA -135 Sediment</b>	51	36	35	52	0.49	0.58	0.91	0.95
<b>IAEA -135 Sediment</b>	64	39	29	46	0.51	0.61	1.1	1.0
<b>QAP 0303 (58)</b>	75	45	25	--	0.43	0.52	1.2	--
<b>QAP 0303 (58)</b>	65	--	--	--	0.59	--	--	--

#### 4. Spectra

The following spectra were achieved applying this procedure.



## **5. Conclusions**

The main advantages of the proposed method are the fast and efficient separation of the actinides, no precipitation is required and low consumption of reagents. The period of time required for the actinides determination is 35-40 hours. It makes possible to determine the activity of uranium, plutonium, americium and thorium in a soil sample without alpha spectral interferences. An additional advantage is the use of lower acid concentrations than the traditional methods. The recoveries are variable depending on the alpha emitter radionuclide and the composition of the soil.

A disadvantage is the high Minimum Detectable Amount, due to the low quantity of soil sample that may be possible to pass through the column without rupture.

This procedure for sequential separation of uranium, thorium, americium and plutonium is easy to apply to other matrixes like, filter and vegetable. If only one of these actinides determinations is required, some steps may be eliminated with care.

## **6. References**

- [1] Dietz, M., Horwitz, E., "Novel chromatographic materials based in nuclear waste processing chemistry", LC.GC.-The magazine of separation science, Vol 11, Nº 6, June 1993.
- [2] Thakkar, A., "Rapid sequential separation of actinides using Eichrom's extraction chromatographic material", Journal of Radioanalytical and Nuclear Chemistry, Vol. 248, Nº2 (2001) 453-456.
- [3] Procedimiento G-01 (15.1), "Electrodeposición de actínidos", Manual de Técnicas de Laboratorio, Autoridad Regulatoria Nuclear, pág. 171, julio 2002.
- [4] "Método de Análisis de Espectros Alfa", Hugo Equillor, Jornadas de Protección Radiológica y Seguridad Nuclear de la SAR, Buenos Aires, Argentina, 9-10 noviembre 2000. Memoria Técnica 2000, Autoridad Regulatoria Nuclear.

# Safety Assessment of Radioactive Waste Management Operations in Type I Facilities

Siraky, G. and Medici, M. A.



# **SAFETY ASSESSMENT OF RADIOACTIVE WASTE MANAGEMENT OPERATIONS IN TYPE I FACILITIES**

Siraky, G. and Medici, M. A.

Nuclear Regulatory Authority

Argentina

## **INTRODUCTION**

Nuclear activity started in Argentina in the early fifties and since then all the peaceful applications of nuclear energy have been developed including nucleoelectricity production. In 1994 the organisation in charge of the regulatory control of nuclear activities, now the Nuclear Regulatory Authority (ARN), became independent from the organisations related with nuclear promotion and Nuclear Power Plants (NPP) operation (mainly National Atomic Energy Commission, CNEA and Nucleoeléctrica Argentina Sociedad Anónima, NASA).

At present, two nuclear power stations with natural and slightly enriched Uranium as fuel and heavy water as coolant and moderator are in operation and one in advanced construction. Concerning other nuclear installations, four research reactors and two critical assemblies are in operation, as well as facilities for radioisotope production, hot cells, a waste management facility and installations for the final disposition of LLRW.

## **REGULATORY FRAMEWORK**

ARN objective is to establish, develop and implement a regulatory system for all nuclear activities performed within the territory of the Argentine Republic.

Law Nº 24804 authorises the ARN to implement such system and vests it with the necessary legal competence to adopt and enforce the appropriate binding rules to regulate and supervise nuclear activities in the Argentine Republic.

## **LICENSING SYSTEM**

In Argentina the licensing system is defined in AR 10.1.1 Basic Standard. This licensing system is applied for all nuclear activities and facilities including those of radioactive waste management.

A main aspect of the regulatory system is the approach adopted where the Responsible Organisation (RO) in charge of the design, construction, commissioning, operation and decommissioning of nuclear installations is fully responsible for the safety, physical protection and safeguards of the installation.

The regulations establish that the construction, commissioning, operation and decommissioning of a Type I Facility<sup>1</sup> cannot be started without the appropriate licenses required by the Responsible Organisation and granted by ARN. The validity of said licenses is subject to the compliance with the conditions set forth in them, as well as with the regulations and requirements of the ARN. Failure to comply with one or more of such regulations, conditions or requirements may cause the ARN to suspend or cancel the validity of such license, in accordance with the existing sanction system.

The regulatory system contemplates licenses for the construction, commissioning, operation and decommissioning of a nuclear installation. Such licenses set out the conditions to which the Responsible Organisation shall be subject at each stage.

After the Responsible Organisation applies for the construction license, a regular interaction starts between the constructor and operator of the proposed installation and the ARN. It is an interactive process whose complexity is consistent with the importance of the demand. Assessment of the capacity of the Responsible Organisation to perform its duties starts in the construction stage.

An operation license is issued when the ARN concludes that the conditions, regulations and specific requirements applicable to the nuclear installation in question are satisfied. Such conclusion is the result of the review of documentation and detailed reports submitted, inspection reports during construction, commissioning activities, and recommendations made by an ad-hoc ARN Commissioning Committee.

The operation license is the document whereby the ARN approves the nuclear installation operation under specific conditions that shall be met by the Responsible Organisation. Since 2000, due to a decision of the ARN Board of Directors, a specific section referred to radioactive waste management in the installations is included in the mentioned license.

At the end of its operational life and at the request of the Responsible Organisation, the ARN approves the decommissioning plan of the nuclear installation and grants a decommissioning license. This document sets out the conditions for the decommissioning of the nuclear installation, and establishes that it is the Responsible Organisation duty to plan and provide the necessary means for its compliance.

Assessments prior to granting any license to a nuclear installation include aspects of quality assurance, construction procedures, operation procedures, provisions for inspections during service, etc, as necessary. Also, the development of emergency plans in coordination with appropriate national, provincial and municipal bodies is required.

<sup>1</sup>

In Argentina, a Type I Facility is an installation or practice that requires a licensing process of more than one step based on the risk that the facility entails. It comprises the following subclasses:

1) Nuclear Power Reactors 2) Research and Production Nuclear Reactors 3) Critical Assemblies 4) Nuclear facilities with critically potential 5) Particle Accelerators with  $E > 1$  MeV (except the medical used accelerators) 6) Irradiation Plants 7) Production plants of open or sealed sources 8) Radioactive Waste Management Facilities 9) Mining and Milling facilities that include the final disposal site of the radioactive waste generated during their operation.

## **REGULATORY AUDITS AND INSPECTIONS**

From the beginning of nuclear activities in the country and in order to verify that nuclear installations comply with the regulatory standards, licenses and requirements in effect, the ARN has performed assessments and different regulatory inspections and audits, with the frequency established as necessary. Its personnel perform these as follows:

*Routine inspections:* are essentially performed by resident inspectors (at NPP) and other inspectors of the ARN. Their objective is to verify that the Responsible Organisation complies with the operation limits and conditions laid down in the operation license.

*Special inspections:* are performed by experts of the ARN in different matters (radiological and RW safety, dosimetry, instrumentation and control, etc.) in coordination with resident inspectors (at NPP). They are performed under certain circumstances or due to the occurrence of specific events in the nuclear installation. They have different purposes such as, for example, to supervise preventive maintenance tasks during scheduled shutdowns at NPP.

*Technical assessments:* are performed by ARN personnel and they consist in the analysis of data collected during inspections or from other sources. For example, assessments of the radiological safety of specific practices at the nuclear installation to detect their potential weaknesses and identify possible measures to reduce doses to personnel.

*Regulatory audits:* are performed in accordance with written procedures and are scheduled to review organisational, operational and procedural aspects related to nuclear and radiological safety.

## **REGULATORY ACTIONS**

In general in all nuclear facilities and particularly in the case of inspections of RWM operations, the validity of a license is subject to the compliance with the conditions established by that license and with the regulations and other documentation issued by the ARN.

The regulatory actions that the ARN may take concerning a particular nuclear installation are originated from:

- The results of regulatory inspections and assessments performed at the facility.
- The knowledge of abnormal events occurred at the installation or at a similar one.
- The result of technical evaluations made by the ARN.

In case of non-compliance of license, regulatory standards, etc., the ARN issues a regulatory document to the Responsible Organisation (RO) in the form of a

**requirement, recommendation or request for additional information**, according to the case. In such document the ARN compels the Responsible Organisation to take the required measures within a specific period. The scope of said documentation is the following:

*Requirement*: is a regulatory order or demand, the Responsible Organisation has to comply with it in the requested manner.

*Recommendation*: is a regulatory order or demand which differs from a requirement in that the Responsible Organisation has certain flexibility to comply with it by means of alternative solutions (i.e. engineering alternatives) which ensure, at least, the same result required by the recommendation. Said alternative solutions must be proposed to the ARN for their assessment.

*Request for additional information*: is a regulatory order or demand whereby more details of the documentation provided are required, for example, the explanation of an statement, the demonstration of the validity of calculations or additional documentation.

As an example of requirements to nuclear facilities, ARN requested the Nuclear Power Plants, a PSA (Probabilistic Safety Analyses) for sources different of the reactor core (i.e. SF and RW management systems). Its results are under ARN evaluation.

## **SAFETY ASSESSMENT OF RADIOACTIVE WASTE OPERATIONS IN TYPE I FACILITIES CARRIED OUT BY ARN**

The safety of nuclear installation operations has to be ensured during the entire lifetime of any Type I facility. Safety Assessments during inspections are undertaken to verify the safety of radioactive waste management operations, according to the related national safety standards consistent with international agreed principles.

During the inspections of Type I facilities, ARN mainly follows the action sheet shown in Figure I to evaluate the safety of the radioactive waste management operations. Each part of that action sheet is performed by different sections of ARN or the Responsible Organisation (RO).

The actions and activities that are carried out by ARN at each stage of the action sheet:

- ASSESSMENT OF RADIOLOGICAL SAFETY OF RWM PROCEDURES**

Procedures should reflect compliance with national radiological standards and the criteria for the safety of waste management. Additionally, it should be ensured that they apply good practices in Radioactive Waste Management operations.

The assessment of radiological safety of RWM procedures ensures not only appropriate and efficient Radioactive Waste Management but also the minimisation of workers doses.

This task is performed by professionals of Safety of Radioactive Waste Management Section.

- **ASSESSMENT OF RWM RADIOLOGICAL SAFETY IN SITU AND OF COMPLIANCE WITH PROCEDURES**

Some of the checked items during these assessment are:

- Occupational dose records
- Conditions of storage of liquid and solid RW
- Keeping of RW inventories
- Contamination level in the facility
- Exposure rate in different working places

This task is performed by inspectors of Type I Facilities with the support of professionals of Safety of Radioactive Waste Management Section and professionals of Dose Evaluation Section.

- **EXAMINATION OF RECORDS OF RW INVENTORIES:**

The checked records are:

- Information about solid LLRW processed (compacted drums, cemented liquid and slurries)
- Information about ILWR stored without foreseen immediate processing (spent resins, spent process filters):
- Information about structural RW stored without foreseen immediate processing:

This checking is performed by inspectors of Type Facilities I in coordination with professionals of Safety of Radioactive Waste Management Section.

- **EXAMINATION OF RESULTS OF TEST ON RW:**

The checked results are:

- Facilities monitoring results
- Environmental monitoring
- RW characterisation

This task is performed by inspectors of Type I Facilities in coordination with professionals of Safety of Radioactive Waste Management Section.

- **EXAMINATION OF RECORDS OF OPERATION AND MAINTENANCE:**

The checked records are:

- Record of analyses
- Operational Records
- Records of stored RW (every three months)
- Records of processed RW (every three months)
- Records of RW generated (every three months)
- Records of modifications on systems and procedures

This checking is performed by inspectors of Type I Facilities in coordination with professionals of Safety of Radioactive Waste Management Section.

- **EXAMINATION OF RECORDS OF FAILURES AND OCCURRENCE OF ABNORMALITIES**

Some of the checked records are:

- a) Deficiency Record (CNE)
- b) Failure Record (CNA)
- c) Radiological Protection Book
- d) Events Book of Radiological Protection
- e) Events Book of Controlled Area

This checking is performed by inspectors of Type I Facilities in coordination with professionals of Safety of Radioactive Waste Management Section.

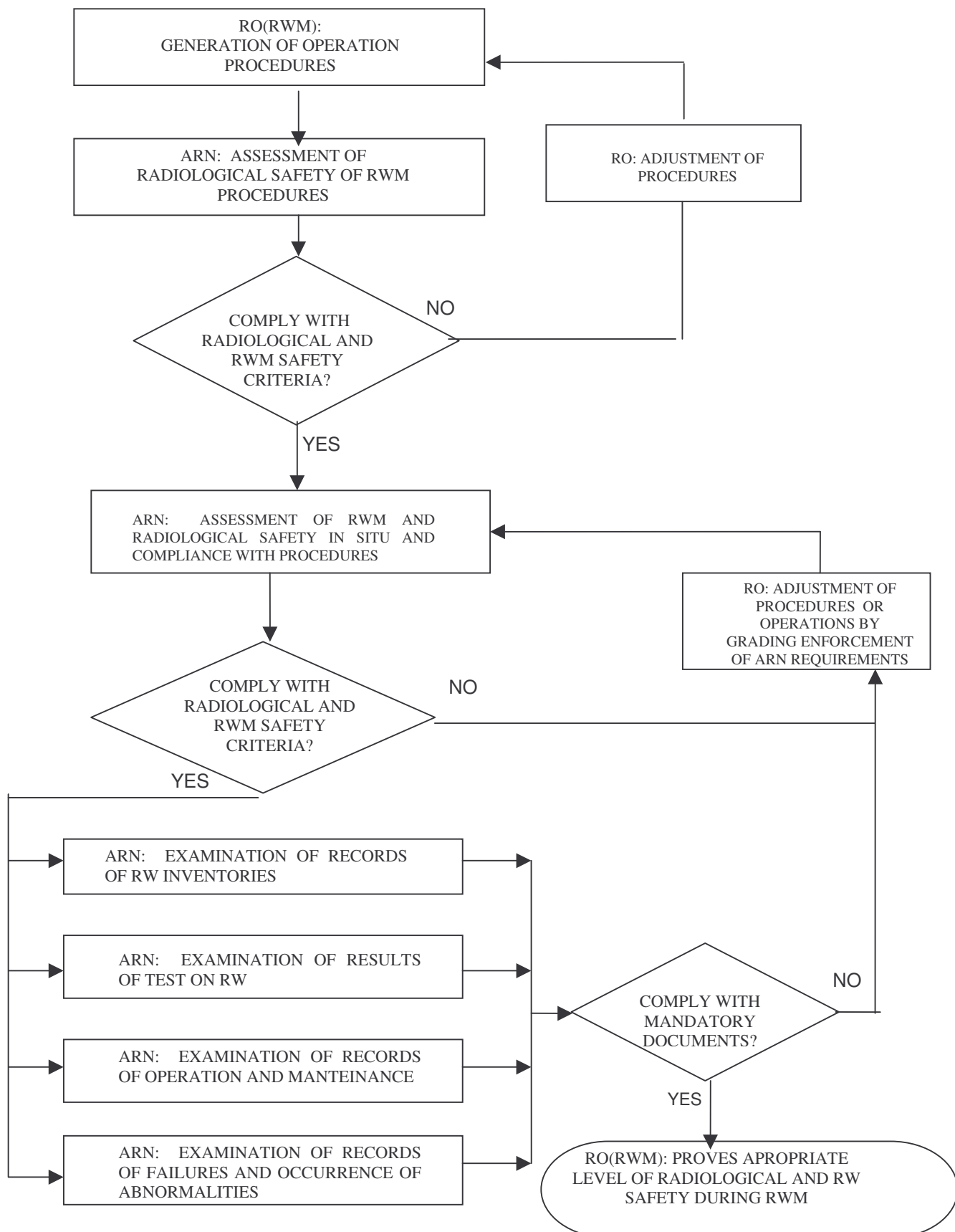
As a result of interactions with the RO, when no compliance with radiological and safety criteria is observed (in relation with standards, procedures, requirements, good practices, etc.), the ARN enforces the RO to adjust procedures or operations.

## **FINAL REMARKS**

The work methodology presented previously, mainly based on the Action Sheet shown in Figure 1 and its results, is under implementation. Once completed ARN will have an improved methodology to gather information in support to its regulatory RWM activities.

We believe that the implemented methodology can be improved and the interaction with SADRWMS will be helpful for such purpose, incorporating not only national experience but also the international one.

**Figure 1: ACTION SHEET FOR SAFETY ASSESSMENT OF RADIOACTIVE WASTE MANAGEMENT OPERATIONS**



## REFERENCES

- [1] Ley No. 24804 – “Ley Nacional de la Actividad Nuclear”, Buenos Aires, Argentina, 1997.
- [2] AUTORIDAD REGULATORIA NUCLEAR, Norma AR 10.12.1, “Gestión de Residuos Radiactivos”, Revisión 1, Buenos Aires, 2002.
- [3] AUTORIDAD REGULATORIA NUCLEAR, Norma AR 10.1.1, “Norma básica de seguridad radiológica”, Revisión 3, Buenos Aires, 2003.
- [4] AUTORIDAD REGULATORIA NUCLEAR, “Informe Anual 2003”, Buenos Aires, 2004.
- [5] “Informe Nacional a la Convención Conjunta sobre Seguridad en la Gestión de Combustible Gastado y sobre Seguridad en la Gestión de Desechos Radiactivos”, Buenos Aires, 2003.
- [6] Siraky Gabriela, “Radioactive Waste Management in Argentina: Present Status” – ISAM - 3<sup>rd</sup> RCM – Sept. 2000
- [7] Siraky, G.; Hernández D. “Regulatory Requirements for the management of radioactive waste in Argentina” – ASAM – 1<sup>st</sup> RCM - Nov. 2002

# On the Radiation Protection of the Environment

Sobehart, L.J ; Clausse, A. and D'Amato, E.



# ON THE RADIATION PROTECTION OF THE ENVIRONMENT

*Sobehart, L.J.<sup>1</sup>; Clausse, A.<sup>2</sup> and D'Amato, E.<sup>1</sup>*

<sup>1</sup> Nuclear Regulatory Authority, Argentina

<sup>2</sup> National Atomic Energy Commission, Argentina

[lsobehar@sede.arn.gov.ar](mailto:lsobehar@sede.arn.gov.ar), [clausse@exa.unicen.edu.ar](mailto:clausse@exa.unicen.edu.ar), [edamato@sede.arn.gov.ar](mailto:edamato@sede.arn.gov.ar)

## Abstract<sup>1</sup>

Over the last decade, substantial advances in what is known as legal protection of the environment, -as a different matter from human being protection- have been made. Some national legislations include serious penalties against environmental damage. It is becoming customary to consider a serious offence any excess in the prescribed limits of radioactive materials release to the environment. What these limits mean, however, is not completely clear nowadays. According to the International Commission on Radiological Protection (ICRP) the standards of environmental control needed to protect man to the degree currently thought desirable will ensure that other species are not put at risk, although, occasionally, individual members of non human species might be harmed. However the use of limits of radioactive releases resulting from the direct application of ICRP recommend limits as legal references for the applicable offences in environmental protection is certainly a misconception. In this paper a conceptual framework for the calculation of legal limits for environmental radioprotection are presented. The approach is based on an ecosystem perspective, assessing the impact of radioactive releases on the ecosystem dynamics and equilibrium. The method is based on functional groups models -i.e. groups of species that are selected from a number of criteria such as play similar rules in the chain of nutrients or have the same radiosensitivity- providing the basis for prescribed limits of the radioactive material release to the environment. The methodology is applied to a system of three functional groups in equilibrium, with is affected by radioactive intrusion. Different impacts on the equilibrium can be identified, depending on the amount of radioactive material released to the environment. It is shown how the concept of equilibrium breakdown can be applied in order to assess the radiological impact.

---

<sup>1</sup> (1) The views expressed remain on the responsibilities of the named authors and do not necessarily reflect those of the government. It is only an academic contribution to the study of this matter.

## 1. Introduction

The need to develop specific methodologies and criteria to support environmental protection decisions, was established because of the growing number of international agreements and policies, as well as national policy statements and regulations related to this specific matter.

In the attempt to resolve this problem, it was noted that at present, there are no internationally agreed criteria or policies that explicitly address protection of the environment from ionizing radiation. Some authors have considered the possibility of developing a system for the radiological protection of the environment that complements the well established anthropocentric system of protection.

Most of the national legal system make some provisions for the protection against pollution, generally including the ionizing radiation.

The excess in the prescribed limits of radioactive materials release to the environment usually it is considered a serious offence, but what these limits mean, however, is not completely clear yet.

In order to answer this question, we study the impact of radioactive releases on the ecosystem dynamics and equilibrium.

The method is based on functional groups models -i.e. groups of species that are selected base on a number of criteria such as playing similar rules in the chain of nutrients or have the same radiosensitivity- providing the basis for prescribed limits of the radioactive material release to the environment.

It is shown how the concept of equilibrium breakdown can be applied in order to assess the radiological impact. In this way, a concept for ecology damage -a more natural to a legal protection reference of the environment- is presented.

## 2. Description

In the functional groups approach, the interaction dynamics of the biotic components of an ecological system could be modeling through the use of balance equations of the general form:

$$\dot{x} = f(x, t, \mu) \quad (1)$$

with  $x \in U \subset \mathbb{R}^n$ ,  $t \in \mathbb{R}^1$ ,  $\mu \in V \subset \mathbb{R}^p$  where  $U$  and  $V$  are open sets on  $\mathbb{R}^n$  and  $\mathbb{R}^p$  respectively. The over dot means  $\frac{d}{dt}$  and we view the variable  $\mu$  as a parameter.

Generally,  $f(x, t, \mu)$  will be a non-linear function of the variables  $x$ ,  $t$  o  $\mu$ .

The vector variable  $x$  could mean the current nutrient density of any specie, i.e. each components of the  $x$  vector could be the carbon biomass density of express in grams of carbon by square meters. So, in order to have biological sense, each component of the vector  $x$  need to be positive.

The variable  $\mu$  represent external factors, and  $p$  is the number of independent relevant parameters under consideration that are needed to define the system.

We can always make a non autonomous equation of the type (1), autonomous by redefining time as a new dependent variable. So, for simplicity, we only study autonomous case.

$$\dot{x} = f(x, \mu) \quad (2)$$

Each point of the phase space  $\Re^n$  is associated with possible state of the ecosystem, and each dimension of the phase space is related with the existences of a specific functional groups.

Generally, as time flows, ecosystems will describe a path in the phase space that finally will converge to one state which does not change in time. Expression (2) allows us to obtain these particular states from the condition:

$$0 = f(\bar{x}, \mu) \quad (3)$$

The solutions  $\bar{x}$  are usually known as equilibrium states. Thus, from (3) the equilibrium states of the ecosystem are known function of the parameters  $\mu$ .

Local stability analysis let us understand the nature of the stability near equilibrium solutions, making proper use of Taylor expansions of (2). So we get a corresponding linear system as:

$$\dot{y} = \frac{d}{dx} f \Big|_{\bar{x}} y \quad (4)$$

It can be proved, that the stability of  $\bar{x}$  is related with the stability of  $y = 0$ .

The derivative of  $f$ -evaluated in  $\bar{x}$ , is a matrix with constant entries, that we can define as  $M(\bar{x})$ . Then, the solution of (4) through a point  $y_0$  at  $t=0$ , can be written as:

$$y(t) = y_0 e^{M(\bar{x})t} \quad (5)$$

From linear analysis, we can find the eigenvalues  $\lambda$  of the matrix  $M(\bar{x})$  from the characteristic equation determined by:

$$\det [M(\bar{x}) - \lambda I] = 0 \quad (6)$$

Where "det" denote determinant and  $I$  is the identity matrix in the  $\Re^{n,n}$  space.

Generally, the eigenvalues will be complex functions of the parameters  $\mu$ :

If all the eigenvalues of the matrix  $M(\bar{x})$  have negative real part, then the solution  $y(t)$  converge to 0, as  $t$  go to  $\infty$ , and the solution at  $y=0$  is said asymptotically stable.

The system whose parameters are in a locally stable region and is started far from equilibrium undergoes a period of transient oscillations before eventually converging to the coexistence steady state.

The system whose parameters are in a locally unstable region, even when it is started very near to equilibrium, can undergo rapid oscillatory divergence from that state. In some cases this divergence does not necessarily diverge indefinitely, instead the system could be settled into a limit cycle.

Only those systems whose phase space path converge to stable state with all his components greater than zero, maintain the original biological diversity on time.

The radiation materials -as other non radioactive pollution substances- affect in different way - not completely known at present- the mortality, fertility, fecundity, morbidity, mutation rates and other factors of the biota component of the ecosystem. In this sense, ionizing radiation exposure affects either eigenvalues and equilibrium solutions of equation (2).

With appropriate models, it is possible to estimate the limits conditions under which an unaffected system can change its original converging path to a stable state with all his components greater than zero, to a new path converging to a less diversified stable state - i.e. unless one component of the stable state equal to zero- or to a new unstable path.

This idea provides a consistent methodology to define protection limits at ecosystem level.

## 2. Three Level System

W.S.C. Gurney and R.M. Nisbet have analyzed the stability behavior of a simple model with three functional groups called P plants, H herbivores and C consumer. This model have a constant primary production  $\phi$  and an interaction of the Holling II type

A Holling II type model assumes that indistinguishable food items are distributed randomly through an environment area. Any animal which is engaged in searching for these items have an specified velocity for capture of items food. When the animal ingested the food, it refrains from searching for more food during a period of time.

The balances equations of this system are as follow:

$$\begin{pmatrix} P \\ H \\ C \end{pmatrix} = \begin{pmatrix} \phi - \delta_p P - \frac{\alpha_H H P}{P + P_0} \\ \frac{\alpha_H H P}{P + P_0} - \delta_H H - \frac{\alpha_C C H}{H + H_0} \\ \frac{\alpha_C C H}{H + H_0} - \delta_C C \end{pmatrix} \quad (7)$$

where

$\phi$  is the biomass production rate

$\delta_p$  is the removing rate of nutrient of plant at the per capita rate

$\delta_H$  is the removing rate of nutrient of herbivore at the per capita rate by respiration or mortality,

$\delta_C$  is the removing rate of nutrient of consumers at the per capita rate,

$\alpha_H$  and  $\alpha_C$  are the attack rate.

$P_0$  and  $H_0$  are parameters related to half-saturation food population.

In order to find the equilibrium states of (7) we have to resolve:

$$\delta_P \bar{P}^2 + (\phi - \delta_P P_0 - \alpha_H \bar{H}) \bar{P} - \phi P_0 = 0 \quad (8a)$$

$$\bar{H} = \frac{\delta_C H_0}{(\alpha_C - \delta_C)} \quad (8b)$$

$$\bar{C} = \left( \frac{\bar{H} + H_0}{\alpha_C} \right) \left[ \frac{\alpha_H \bar{P}}{P + P_0} - \delta_H \right] \quad (8c)$$

As a first approximation, we can think that ionizing radiation affects the primary production rate and the remove rates of the functional groups in a linear way, so:

$$\phi \Rightarrow (\phi - \gamma_\phi D) \quad (9a)$$

$$\delta_P \Rightarrow (\delta_P + \gamma_P D) \quad (9b)$$

$$\delta_H \Rightarrow (\delta_H + \gamma_H D) \quad (9c)$$

$$\delta_C \Rightarrow (\delta_C + \gamma_C D) \quad (9d)$$

Where  $D$  is a measure of the release of radioactive material that produces the exposition to the ionizing radiation of the different functional groups.

In this work we exclude the discussion of how to estimate  $D$  from the source release of radioactive material. For simplicity, we assume that the radioactive material releases impact over each functional group can be modeled from (9) considering  $D$  as global source scalar variable. An alternative approach considering  $D$  as a vector variable may be used.

The first limit condition is the existence of the consumers at the equilibrium state.

From (8c), (9) and  $\bar{C} = 0$

$$(\phi - \gamma_\phi D) = \frac{H_0 (\delta_H + \gamma_H D)(\delta_C + \gamma_C D)}{[\alpha_C - (\delta_C + \gamma_C D)]} + \frac{P_0 (\delta_P + \gamma_P D)(\delta_H + \gamma_H D)}{[\alpha_H - (\delta_H + \gamma_H D)]} \quad (10)$$

If we define

$$A_3 = [-\gamma_\phi \gamma_C \gamma_H + H_0 \gamma_H^2 \gamma_C + P_0 \gamma_C \gamma_P \gamma_H] \quad (11a)$$

$$A_2 = [\gamma_\phi \gamma_C (\alpha_H - \delta_H^0) + \gamma_\phi \gamma_H (\alpha_C - \delta_C^0) + \gamma_\phi \gamma_C \phi_0 - \gamma_H \gamma_C (\alpha_H - \delta_H^0) P_0 + \dots] \quad (11b)$$

$$A_1 = [-\phi_0 \gamma_C (\alpha_H - \delta_H) - \phi_0 \gamma_H (\alpha_C - \delta_C) + \dots] \quad (11c)$$

$$A_0 = [\phi_0 (\alpha_C - \delta_C^0) (\alpha_C - \delta_C^0) - H_0 (\alpha_H - \delta_H^0) \delta_C^0 \delta_H^0 - P_0 (\alpha_C - \delta_C^0) \delta_C^0 \delta_P^0] \quad (11d)$$

we can find  $D_{lim}$  from

$$A_3 D_{lim}^3 + A_2 D_{lim}^2 + A_1 D_{lim} + A_0 = 0 \quad (12)$$

with the additional conditions of

$$D_{lim} > 0 \quad (13)$$

The expression (8 b) is satisfied only if:

$$D_{lim} < \frac{(\alpha_c - \delta_c)}{\gamma_c} \quad (14)$$

From local stability analysis of (7) we will have a characteristic equation of the type:

$$\lambda^3 + B_1 \lambda^2 + B_2 \lambda + B_3 = 0 \quad (15)$$

Where

$$B_1 = \left[ (\delta_p + \gamma_p D) + \frac{\alpha_H P_0 \bar{\bar{H}}}{(\bar{\bar{H}} + H_0)^2} - \frac{\alpha_c \bar{\bar{C}} \bar{\bar{H}}}{(\bar{\bar{H}} + H_0)^2} \right] \quad (16a)$$

$$B_2 = \left[ \left( \frac{\alpha_H^2 P_0 \bar{\bar{H}} \bar{\bar{P}}}{(\bar{\bar{H}} + H_0)^2 (\bar{\bar{P}} + P_0)} \right) + \left( \frac{\alpha_c^2 H_0 \bar{\bar{C}} \bar{\bar{H}}}{(\bar{\bar{H}} + H_0)^3} \right) - \frac{\alpha_c \bar{\bar{C}} \bar{\bar{H}}}{(\bar{\bar{H}} + H_0)^2} \left( (\delta_p + \gamma_p D) + \frac{\alpha_H P_0 \bar{\bar{H}}}{(\bar{\bar{H}} + H_0)^2} \right) \right] \quad (16b)$$

$$B_3 = \left[ \left( (\delta_p + \gamma_p D) + \frac{\alpha_H P_0 \bar{\bar{H}}}{(\bar{\bar{H}} + H_0)^2} \right) \left( \frac{\alpha_c \bar{\bar{H}}}{(\bar{\bar{H}} + H_0)} \right) \left( \frac{\alpha_c H_0 \bar{\bar{C}}}{(\bar{\bar{H}} + H_0)^2} \right) \right] \quad (16c)$$

Here we find  $\bar{\bar{P}}$ ,  $\bar{\bar{H}}$  and  $\bar{\bar{C}}$  from (8) and (9).

The three necessary and sufficient conditions which guarantee the stability of the steady states are:

$$B_1 > 0 \quad (17a)$$

$$B_3 > 0 \quad (17b)$$

$$(B_1 B_2 - B_3) > 0 \quad (17c)$$

These inequalities provide three additional conditions that must be satisfied in order to preserve the original ecosystem diversity.

In the specific case that the parameters of the three level functional groups ecosystem were:

$$\alpha_C = \alpha_H = 1; H_0 = P_0 = 1; \delta_p = \delta_H = 0.1; \delta_c = 0.2; \phi = 0.05; \gamma_p = \gamma_H = \gamma_C = 0.1; \gamma_\phi = 0.025$$

Then the unaffected ecosystem has an equilibrium stable state at:  $\bar{P} = 2.85$ ;  $\bar{H} = 0.25$ ;  $\bar{C} = 0.8$ .

From (12), (13), (14) and (17) it is of legal relevance that the variable D never excess the value 0.32.

#### **4. Conclusions**

The authors share the point of view that standards of environmental control needed to protect man to the degree currently thought desirable -based on the ICRP recommendations- will generally ensure that other species are not put at risk. However, the use of radioactive releases limits resulting from the direct application of ICRP recommended limits, considered as legal references for the applicable offences in environmental protection, is certainly a misconception.

The description of the radioactive material release which impact at ecosystem level, can be analyzed using equilibrium dynamics tools. This approach allows us to define the necessary and sufficient conditions to maintain the system within a stable states region of functional group phase space. Therefore this methodology could provide a basis for prescribed limits of the radioactive material released to the environment from the legal perspective.

Pending on the outcome of the discussion that is taking place, whether it is needed or not to modify the current radiation protection recommended system, the methodology proposed in this paper is a more natural way to establish the legal reference of the radioactive material released to the environment.

#### **5. Reference**

1. A framework for assessing the impact of ionizing radiation on non human species. Annals of the ICRP - Publication 91 Volume 33, No 3 2003, ISSN 0146-06453.
2. W.S.C. Gurney, R.M. Nishet. Ecological Dynamics. Oxford University Press 1998.
3. Ramón Margalef. Ecología.. Ediciones Omega S.A.-Plato 26- 08006 Barcelona. ISBN 84-282-0405-5, Edicion octava, 1995.
- 4 Strand P. Larson, C.M. . Inc. Brechignanc, F. Howard, B.J. Delivering a framework for the protection of the environment from ionizing radiation (Eds) Radioactive Pollutants. Impact on the environment. EDP Sciences, Les Ulis, France, (2001)
- 5 Jones, D.S., Domotor, S.L.: Higley, K.A., et als. Principles and issues in radiological ecological risk assessment. (003). J. Environ. Radioact., 66, 19-39.
- 6 Radiological protection of the environment from the Swedish point of view. J. Radiol. Prot., 22, 235-240.
- 7 ICRP, Recommendation of the International Commission on Radiological Protection, Publication 60. Annals of the ICRP 21. Oxford Pergamon Press (Oxford) (1991).
- 8 IAEA (1992) Effects of ionizing radiation on plant and animals at level implied by current radiation protection standards. International Atomic Energy Agency, Technical Report Series No.332, Vienna.



# The Radioactive Sources Treated as Scrap - Regulatory Aspects, Control and Security

Truppa, W.A. and Cateriano, M.



# THE RADIOACTIVE SOURCES TREATED AS SCRAP - Regulatory aspects, Control and Security

**Truppa, W.A. and Cateriano, M.**

Nuclear Regulatory Authority

Argentina  
e-mail: [wtruppa@sede.arn.gov.ar](mailto:wtruppa@sede.arn.gov.ar)

**Abstract:** The loss of control of a radioactive source may result in a radiological emergency, especially if the source is treated as scrap. This paper presents one case registered in Argentina when a portal radiation monitor detected a radioactive source of Kr-85, that had been used in a nuclear gauge for measurement of thickness. The source, unlabelled and unidentified, was detected by the monitor installed in an important steel mill inside the scrap that was going to be processed. The A.R.N. carried out an investigation to determine the origin and the characteristic of the radioactive source. As a result of the investigation, it was known that the source was originally located at a facility belonging to a company that had gone bankrupt at that moment and had not reported this situation to A.R.N. before. According to the records, the company possessed eleven sources of similar characteristics, located at different facilities placed in the province of Buenos Aires. The search for the sources was carried out with successful result, finding some of the sources. The Regulatory body organized a task group composed of 18 people to audit 362 facilities, to find out other orphan sources. In this way, the A.R.N. applied international criteria for the protection and safety of radiation sources, showing a permanent commitment to strengthen regulatory policies by means of the application of a suitable radiological and physical security control program during the whole lifetime of radioactive sources.

## 1. Introduction

Several incidents or accidents have been reported around the world, regarding to the appearance of radioactive sources, either without regulatory control or because of lack of responsibility of the authorized user, which due to violations of the procedures or human errors can results in risk situations from the radiological point of view, for the workers and particularly for the public in general.[1], [2]

The appearance of a radioactive source is then described, as a result of the lack of control of a licensed company, which went through a difficult financial situation and neither did they not inform the Regulatory Authority, nor did take the necessary actions to guarantee the radioactive protection of the radioactive material. This situation originated the loss of control of the material within the installation.

## 2. Method

Due to the fact that the used radioactive sources, particularly those used in the industry (to measure level, thickness, etc.), form metallic structures, which at the end of their life time could be treated as scrap iron, the radioactive material in these structures, out of lack of control or authorized user negligence might run the same risk the Nuclear Regulatory Authority (A.R.N.) asked for the implementation of a measurement system of the portal monitor type to detect the possible appearance of orphan radioactive sources, within the scrap iron that is processed daily in a steel mill (between 2500 and 3000 tons/day).

During the normal scrap iron entrance in a vehicle that transported it into a steel mill, an operator of the portal detected an increase of the level of bottom radiation, within the material to process. Soon he informed the A.R.N., through the System of Intervention in Radiological Emergencies (S.I.E.R.), whose personnel went to the mill to verify what type of radioactive material had been found.[3] (Fig. 1 and 2)



*FIG. 1 and 2 – Portal monitor detector in steel mill.*

A metal piece without inscriptions or identification that formed a small structure was found. Because the shape and type of support it was at first assumed that the found device came from some industrial use, probably for thickness measurement. The absence of superficial contamination was verified, evaluations of radiological type were made, the device inside a suitable container was arranged and transferred to an authorized repository of radioactive material. (Fig. 3 and 4)

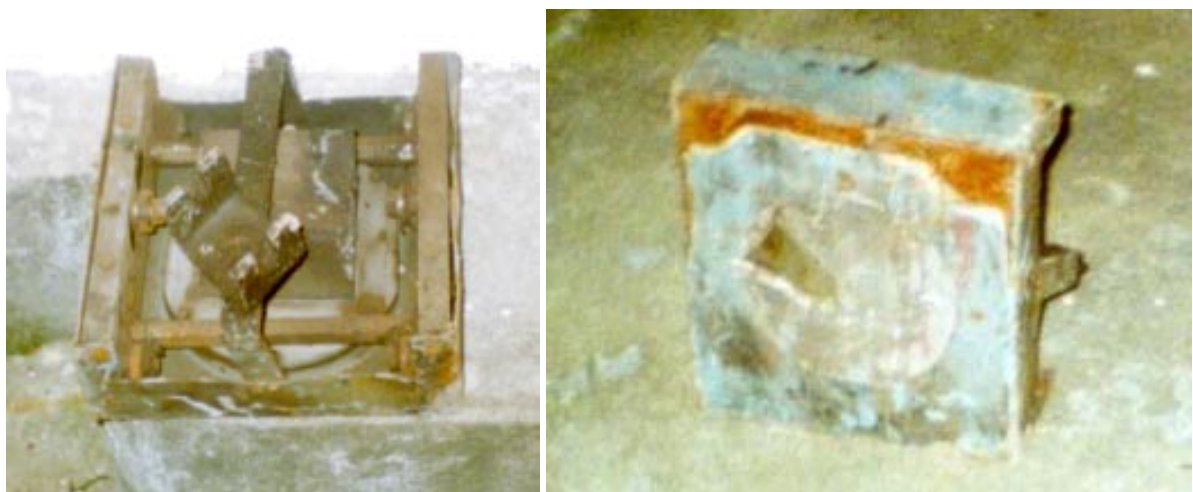


*FIG. 3 and 4 - Detail of the found radioactive source.*

On the following day the radioactive source was transferred to the A.R.N. measurement laboratories for its characterization. Preliminary measurements were made, confirming that the found energy of the radioactive source corresponded to 514 keV .(Fig. 5)

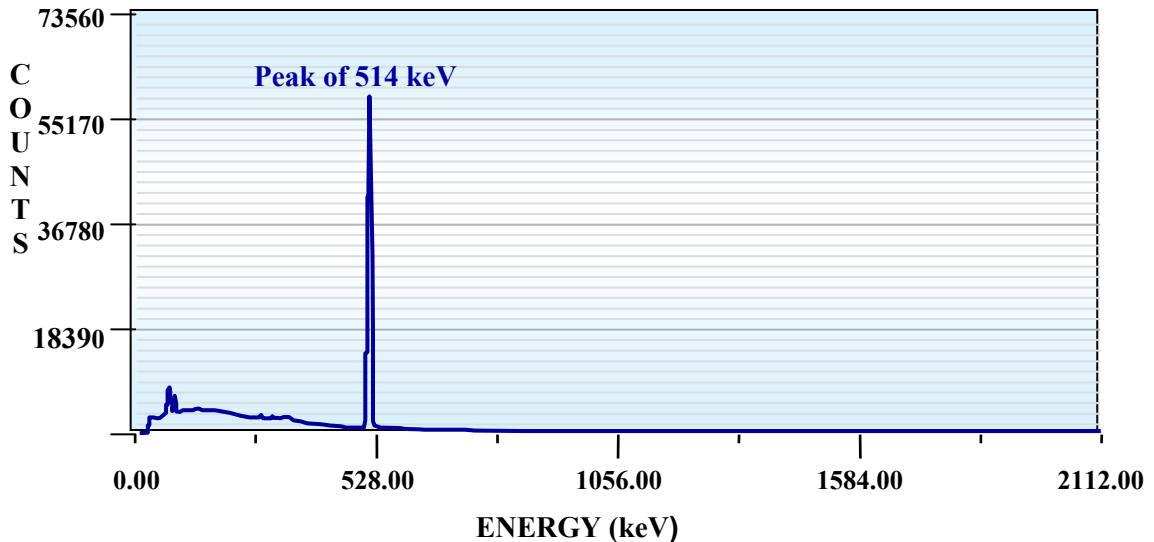


*FIG. 5 - Spectrum generated by the founded radioactive source.*

Afterwards a research in A.R.N files was made among the radioactive sources used in the industry and other aims, in order to establish the possible origin of the source coming to the conclusion that it corresponded to the Kr-85 isotope.

Its activity was calculated in approximately 9,25 GBq at the time it was found.

After the source was identified a search within A.R.N. files to get to know which companies had been authorized to use Kr-85, which was the situation and where they were located. Every authorized company was asked about the state related to their equipment as well as the source they were in charge of. This research lead to a plastic industry which had gone bankrupt and was being dismantled. (Fig. 6 and 7) According to A.R.N. records this facility possessed 12 sources in all.



*FIG. 6 and 7 –The facility in bankruptcy.*

Later on an extensive inspection was made within the estate, where four other radioactive sources, still mounted in their original devices could be located.

The A.R.N. carried out an intense search among companies that were dedicated to make similar products and that used that type of radioactive sources or that could have commercial connection. Due to an information supplied by one of the companies, an inspection was made that lead to an installation that was in phase of assembly and had acquired the remaining sources that belonged to the company in bankruptcy.

As a result of the inspection all the sources that belonged to the company in bankruptcy, could be found. Finally all the equipment and sources found were transferred to the installation to be deposited in an authorized repository for its safekeeping. (Fig. 8)

The radioactive sources inventory were all recovered:

- 8 radioactive sources of Kr-85 (activity between 9,25 and 14,8 GBq).
- 4 radioactive sources of Pm-147 (activity between 2,7 and 5,55 GBq).



*FIG. 8 - Radioactive sources recovered.*

As a result of this irregular circumstance detected by the A.R.N., the following criteria [2],[4] were developed to avoid, in the future, situations of this type:

- A more rigorous policy of control and new measures to detect and respond to situations as the presented in this paper were applied.
- The concepts to be applied by the radiation safety officer in each authorized installation were reinforced, specially those related to the security culture.
- The execution of a plan of management of non used sources without some justification.
- The application of measures of suitable physical protection and radiological security in all the companies that deal with radioactive material.

As a result of the application of these criteria and due to the possibility that other companies might be in a similar situation, the A.R.N. decided to make a regulatory audit of the total amount of facilities that owned sealed sources of industrial use with the intention of verifying the inventory declared by the users, of analyzing the problematic of the area and the degree of radiological security of the facilities in the frame of the effective regulatory policies.

Within the total of sealed radioactive sources of nuclear gauge that are used in the country, the following classification can be made:

**A) Facilities that uses nuclear gauges for industrial purposes:** They are broadly used in companies either to control a productive process or to control the quality of a product. These equipment use diverse radioactive sources with activities that vary between some MBq and several GBq, depending on what purpose the source is going to be used for. (Fig. 9)

**B) Facilities which uses nuclear gauges in the oil activity:** (Fig. 10) it is possible to sub classify them in three groups according to the practices they develop:

**Well loggings:** Measurement of densities of mixtures, sands. and determination of the profile of densities of the walls of the well.

**Well cementation:** In order to measure the density of the cement, nuclear gauges (fixed or movable) are used.

**Inspection of pipes:** the degree of wearing down of the pipes that go down to the well is important since it can affect its production, or even stop it, this is the reason why it is necessary to make an inspection of the pipes every two or three months, in order to verify its thickness.

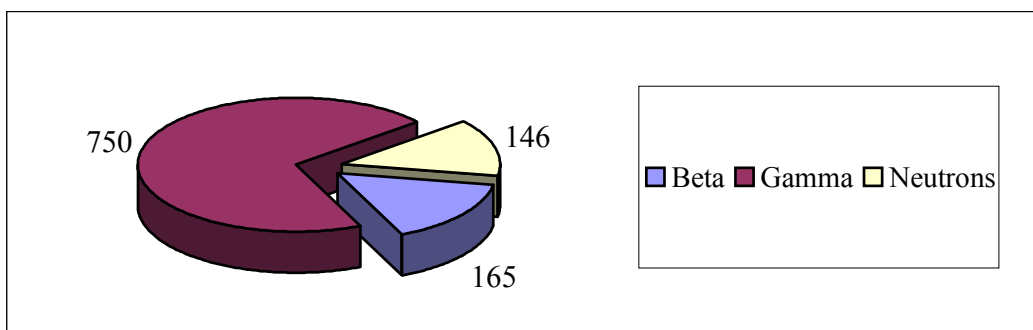


FIG. 9 – Total radioactive sources used in industry uses.

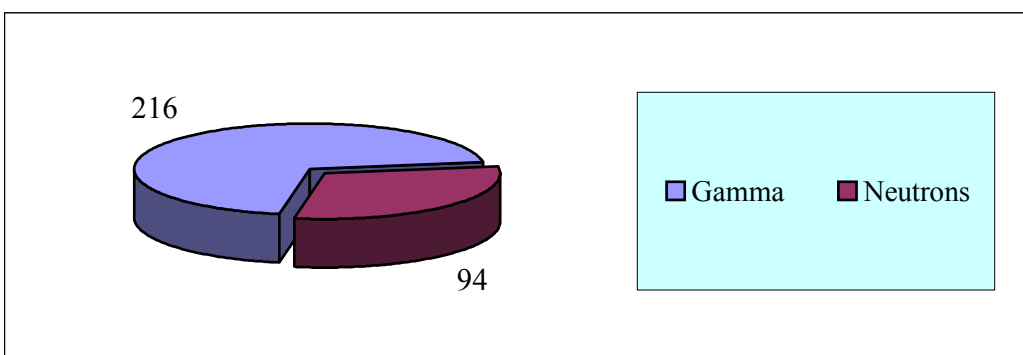


FIG. 10 – Total radioactive sources used in oil uses.

The use of nuclear gauges with encapsulated sources has increased in Argentina during the last years. The A.R.N. has registered 362 industrial companies that use this equipment (16 of them related to the oil activity), 450 radiation safety officer with individual permissions and 390 Operation Licenses, distributed across the country.

In order to fulfill the regulatory audit of the facilities that own sealed radioactive sources for industrial purposes, the Directory of the A.R.N. decided to create a group of inspection made up of 18 inspectors distributed in five work groups.(Fig. 11) Each group corresponding to a different geographical area around the country. This work took approximately 60 days.

In order to carry out this task the uses of land and aerial transport was necessary. 20,000 km by land and 22,000 km by aerial were covered.

The main objectives of this task group were:

- To verify the compliance with regulations and requirements.
- To update the inventory of radioactive sources and equipment.
- To verify the degree of radiological security applied to the radioactive sources in the facilities.
- To inspect the facilities and their services.
- To recover the regulatory control over any orphan radioactive source. This includes keeping in a safe place the radioactive sources, belonging to companies that may have gone bankrupt.
- To make sure that Licensees dispose of or store any disused source at National Atomic Energy Commission facilities.

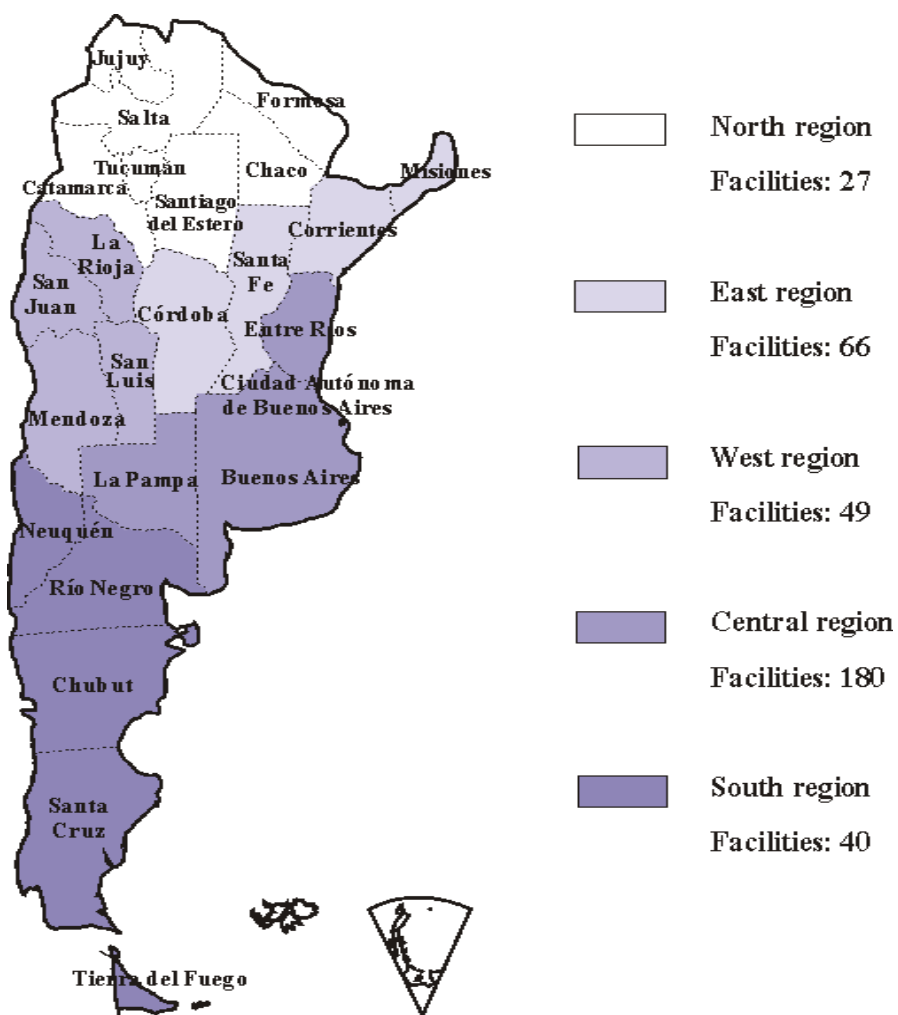


*FIG. 11 - Geographical distribution of facilities.*

The result of the audit showed a total of 362 facilities that use nuclear measurers. The audit was highly satisfactory. All the primary targets were reached. 20 radioactive sources belonging to 5 companies that had gone bankrupt were verified. They were kept under control. The rest of the radioactive sources owned by the companies reported to the inspection group coincided with the data base of the A.R.N. and no orphan sources were detected.

### **3.Conclusions**

As a result of the audit the A.R.N. came to the conclusion that the aspects to emphasize in the future must be:

- To make the maximum effort to maintain the qualification of the personnel involved in the use of radioactive sources and to guide the radiation safety officer to follow concepts of the Safety Culture. [2]
- To require periodic reports to the A.R.N. informing the state of the physical and radiological security of the radioactive sources.
- To require in a short term the disposal of the sources in disuse, its management like radioactive waste and to make the verification of this fulfillment. The A.R.N. will have to take regulatory actions to protect the security of the sources.
- To require the interrelation between the Regulatory Authority and the organisms of border and customs control, in order to prevent and detect possible orphan sources or illicit transport of radioactive material and to pursue mechanisms or appropriate procedures of response.

### **4.References**

- 1 International Atomic Energy Agency (IAEA), “ Security of radioactive sources” TECDOC-1355, Vienna, IAEA, 2003.
- 2 International Atomic Energy Agency (IAEA), “Draft revised Code of conduct on the safety and security of radioactive sources”, Vienna, IAEA, 7 march 2003 – Rev.2.4.a.
- 3 International Atomic Energy Agency (IAEA), ”Generic procedures for assessment and response during a radiological emergency” TECDOC-1162, Vienna, IAEA, 2000.
- 4 Autoridad Regulatoria Nuclear (A.R.N.), Norma Básica de Seguridad AR 10.1.1 - Rev. 3, Buenos Aires, Argentina, 2002. (in spanish)



# Atucha I Nuclear Power Plant

## Achieving a Full Safeguards Approach

Valentino, L.I.; Fernandez Moreno, S.;  
Llacer, C.D. and Bonino, A.D.



# **ATUCHA I NUCLEAR POWER PLANT**

## **ACHIEVING A FULL SAFEGUARDS APPROACH**

Valentino, L.I.; Fernandez Moreno, S.; Llacer, C.D. and Bonino, A.D.

Nuclear Regulatory Authority  
Argentina

### **ABSTRACT**

At Atucha I Nuclear Power Plant (NPP) it has recently been fully attained technical safeguards inspection goals. This is an important accomplishment since the facility had partially attained the safeguards technical goals for some years. Moreover, this situation implied in one occasion that the criterion was not met for the entire State. Nevertheless, it should be stressed that the IAEA, ABACC and ARN have always been able to draw positive safeguards conclusions.

According to IAEA Safeguards Criteria issued in 1991 and in particular since 1995, the facility has attained, only partially, one of the technical inspection goals due to the requirement of having a fuel flow monitor to count and verify by gross defect the fuels discharged from the reactor core before being placed under IAEA and ABACC surveillance at the storage ponds.

Argentina repeatedly stated in different IAEA instances, including its policy-making organs, its opinion that criteria mainly based on one type of OLR<sub>5</sub> could not be easily extrapolated to other OLRs, in particular those already constructed and in operation. Our country nevertheless engaged fully, since the issuing of such criteria, in finding an integral solution to this technical issue.

From ARN viewpoint, the goal has been to find a suitable method to fulfil this requirement without implying substantive construction modifications to the facility, together with having in place appropriate NDA techniques to verify the spent fuel inventory at the ponds of Atucha I before the VIFM were left working. Besides, this NDA method is appropriate in case of a C&S failure.

The paper describes the various attempts for solving this issue that would imply a convenient design, a testing period and the final implementation for safeguards purposes of the selected technical solutions. It is also shown a comparison between the inspection activities performed before the installation of the VIFM (V Irradiated Fuel Monitor) and the ones expected with this system as part of the safeguards approach for this NPP.

### **DESCRIPTION OF ATUCHA I NUCLEAR POWER PLANT (NPP)**

Atucha I NPP is an On Load Pressurised Heavy Water Reactor (PHWR) built in the '70s and in operation since 1974. The power of this NPP is 357 MWe. The reactor started operation with natural uranium fuels but now it works with low enriched uranium fuel assemblies (0,85% U<sup>235</sup>). The core grid capacity is of 252 fuels. Each fuel is formed by 37 rods placed in three concentric circles and with an active length of 5.3 m. The reactor is refrigerated and moderated by D<sub>2</sub>O. In this Plant there are two houses with a total of six pools for storing the spent fuels and two manoeuvring pools, one in each house. The re-fuelling frequency is of 0.72 fuels per day when the reactor is working at full power. There is only one channel between the reactor building and the manoeuvring pools of the two houses and the flow of fuels (fresh, burnt up and semi burnt up) is through it.

Currently, there are approximately 8700 spent fuels in the pool. In the ponds, the fuels are stored in two layers. The fuels are stored in hangers of different design for the upper and the lower layer. Basically, the differences consist of constructive dimensions. Due to that reason, the fuels are not aligned and so placing a detector between the fuels in the lower layer turned into a difficult challenge.

## **DESCRIPTION OF THE PROBLEM**

The technical challenge to fully achieve safeguards goals in a cost-effective manner was the requirement for verifying by gross defect the spent fuels discharge from the core before their storage in the ponds under IAEA/ABACC surveillance.

In addition to that, it was also identified the need of having a suitable NDA technique to re-verify the existing spent fuel inventory at the ponds, at the time of the installation of the flow monitor for spent fuels with long cooling time or those placed in the lower layer of the pond with difficult accessibility.

These NDA techniques would also serve the purpose of re-verifying the spent fuel inventory in case a failure of the C&S system to re-established the continuity of knowledge.

## **CONDITIONS TO SELECT TECHNICAL SOLUTIONS**

To promote a clear understanding of these issues, it should be noted that verifying by gross defect with medium detection probability the spent fuel inventory at every interim inspection could also have fulfilled the safeguards requirements for this facility. However, this would have implied to perform physical inventory verifications every three months and therefore the inspection effort would have been enormous. That has been the main reason for looking for technical solutions to allow maintaining the continuity of knowledge of verified items.

In seeking for techniques to identify an integral solution to this outstanding safeguards issue, the ARN pursues the following approach:

- The methodology or technology to fulfil these safeguards criteria should be such to minimise the intrusiveness in the normal operation of the facility and to avoid any major constructive modifications.
- Such methodology or system should fulfil safeguards objectives for both, ABACC and the IAEA, and be reliable enough to minimise the consequences of a failure.
- To select suitable NDA techniques to re-verify spent fuels stored in the lower layers of Atucha-I ponds or with long cooling times in parallel with the system to measure the spent fuels for gross defect before being placed under C&S.

## **BRIEF REVIEW OF THE COOPERATIVE EFFORTS TO FIND A SOLUTION**

- A feasibility study was required by the IAEA to the Canadian Safeguards Support Programme. Two reports were presented for review to the Argentina Safeguards Support Programme in 1997 and 1999. The ARN and the operator concluded that the Canadian proposal was not adequate for a NPP in operation, due to the fact that big constructive modifications would be needed for its implementation. The ARN proposed a simplified alternative. ABACC decided to join us in this task.
- Based on this simplified alternative, a study carried out by ARN jointly with ABACC was presented to the IAEA in 1999. The proposal tended to fulfil safeguards requirements minimising the facility constructive modifications, which was a very important aspect for a 30 year operating NPP. The IAEA after analysing the proposal informed that it was acceptable in general.
- Later on, the IAEA sent a detailed proposal based on the ARN-ABACC study, but suggesting the use of equipment already approved by the IAEA for routine safeguards purposes (the VIFM). Argentina and ABACC agreed to test the existing equipment and to commence all the tasks needed it for its prompt installation.
- The ARN has also analysed another option consisting in the implementation of an unannounced or short-notice inspections regime complemented by surveillance measures and a mailbox concept.

As it has been mentioned, in addition to the attempts at finding a suitable solution, the testing of the Spent Fuel Attribute Tester (SFAT) and the Spent Fuel Neutron Counter (SFNC) to re-verify spent fuels with long cooling time or difficult to access have been carried out.

## **DESCRIPTION OF THE ADOPTED TECHNICAL SOLUTION**

As previously mentioned, the finding of proper technical solutions to allow achieving a cost-effective safeguards scheme for Atucha I that fully attains the technical goals has been of great importance to Argentina from the very first moment the requirement of having a monitor of the spent fuel flow was issued.

During 2002 ABACC, IAEA and ARN agreed to proceed with ARN-ABACC proposal and to install and test the VIFM suggested by the IAEA. The operator supplied and installed the collimators, supports and piping for this equipment. The VIFM is similar to the one working at Embalse NPP. This system allows the verification by gross defects of fuel flow between the reactor and the ponds. It also included a subsystem of semi submersible cameras.

It was projected the installation of the fuel monitoring system during the first middle of the year 2003 and towards the end of that year the testing period was foreseen to be finished.

For measuring the spent fuels difficult to access stored in the lower layer and for those with long cooling time, a spent fuel neutron counter (SFNC) of suitable dimensions was selected to re-verify this portion of the spent fuel inventory. This was aimed at fulfilling the requirement of verifying the spent fuels already stored before the installation of the system to monitor the flow of spent fuel and at getting a methodology to re-verify the inventory in case of a C&S failure.

In summary, the objectives to be covered during the year 2003 were:

- ❖ To implement the most suitable system to complete the safeguards approach for this NPP.
- ❖ To select complementary methods to the Improved Cerenkov Viewing Device (ICVD) to re-verify the inventory at the storage ponds.

In January 2004, the safeguards goals for Atucha I were fully attained when the activities to re-verify the inventory of spent fuels in the ponds by the IAEA and ABACC were successfully performed. Basically, the tasks consisted of measuring by ICVD and SFNC for gross defect approximately 350 irradiated fuels in the two layers of the storage ponds and the proper functioning of the VIFM was verified and left working for routine safeguards purposes. ARN safeguards inspectors accompanied all these activities.

## **DESCRIPTION OF THE SELECTED MONITORING SYSTEM**

The unattended system already installed consists of gross gamma detectors and a surveillance system semi submerged at the pond, focusing to the transfer channel (See Figure 1). The detectors would be positioned in such a way as to register the direction of each transfer. The underwater cameras would record all the movements through the transfer channel into and out of the bay. The function of these semi submersible cameras is to detect the presence of a possible shielded flask, what might cover the detectors avoiding their readings. The two sets of shielded and collimated gamma detectors would be located adjacent to the tilting mechanism while it is in the horizontal position. One set of detectors was located as close as possible to the transfer exit tube. The second set of detectors was placed downstream, at about a distance of three-quarter of the length of a fuel, still in horizontal position. The advantage of using collimated gamma detectors are to improve the ratio signal-background distinguishing between high irradiated fuels and the low burn up ones and to limit the solid angle of vision of the detectors, necessary condition for fuel direction determination.

The detectors are placed as close as possible to the tilting mechanism for limiting the space for the potential introduction of undeclared detector shielding. Not disturbing the operator procedures and keeping the detectors in a safe location also defined this closest position. The two sets of underwater cameras are directed to the discharge port and to the tilting mechanism, confirming the discharge of the

spent fuel and the gamma detectors remain in the right position and that no special shielding is entered to the pond.

To increase the reliability of the whole system, two independent detectors in each position and two independent cameras were installed.

The digital signals from the gamma detectors and the images from the surveillance cameras are sent to a server that process the data and generate reports and images for a set safeguards period. This server also has redundant functions for power supply and data storage.

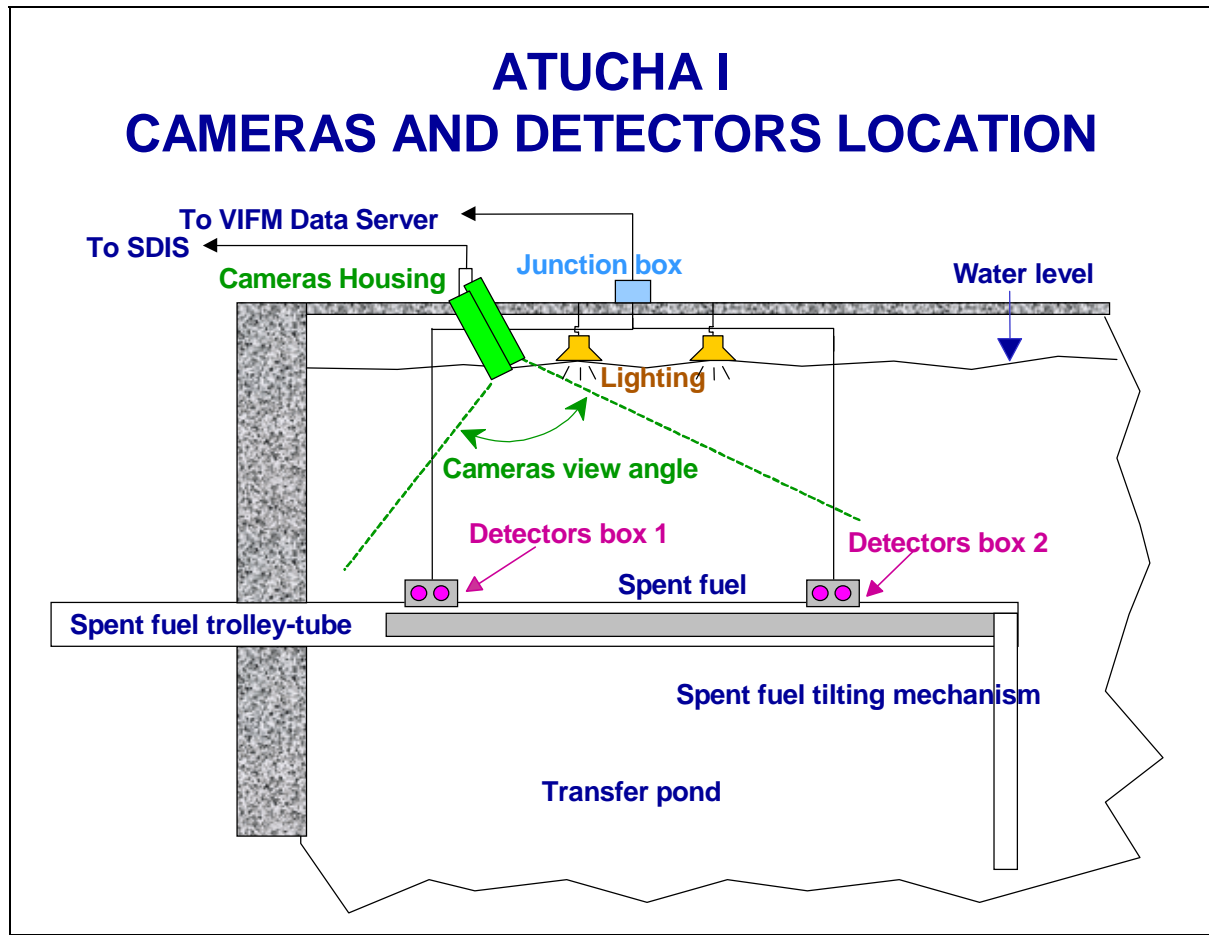


**FIGURE 1**

#### **DESCRIPTION OF THE NDA TECHNIQUES SELECTED TO RE-VERIFY THE SPENT FUEL INVENTORY**

The spent fuels stored in the lower layer of the ponds were mostly inaccessible for in situ measurements because of the limited space between the assemblies. Another feature that had to be considered was the long cooling time of many of the fuels with low burn up that prevented from using the ICVD. Additionally, isolation of the fuels for measurement was extremely difficult due to the number of assemblies and the difficulties in moving and re-arranging the fuels due to safety and operational reasons.

Due to the above-mentioned reasons, several neutron and gamma NDA measurements were made on the spent fuels to develop a gross defect measurement method. Due to the fact that the hangers are not aligned between the lower and upper layer of the ponds a specific device was designed and constructed to drive the neutron detector towards the randomly selected fuel.

### **Spent Fuel Attribute Tester (SFAT)**

Gamma measurement with the standard SFAT on top of the assemblies confirmed that obtaining a prominent  $^{137}\text{Cs}$  peak was not possible. The reasons for this are the distance and amount of attenuating material, separating the active fuel zone from the detector and the low signal level due to the low burn up of the spent fuel.

Another type of gamma measurement was attempted by placing a detector in the gap between assemblies. A special inset was placed inside the housing with a small horizontal hole to try to look for the presence of  $^{137}\text{Cs}$  peak. A very small CdZnTe detector with crystal volume of  $1\text{ mm}^3$  was used to deal with very high gamma flux environmental.  $^{137}\text{Cs}$  peaks were obtained but it was not possible to discriminate individual assemblies as a result of the limited amount of shielding. Increasing the shielding thickness was not possible because of the limited physical size of the gap where the detector was inserted.

### **Spent Fuel Neutron Counter (SFNC)**

The assumption of applying this technique is that the sum of total neutron signal, from low burn up assemblies is linearly correlated to the sum of burn ups of the measured assemblies and that the dominant source of neutrons is  $^{240}\text{Pu}$ . The measured data confirmed that the neutron signal compared to the sum of burn ups was indeed adequately linear. Most of the assemblies had burn ups between 5 to 7000 MWD/TU with very long cooling time (a small number of assemblies with burn up of 11000 MWD/TU). A prototype neutron detector system, which employed a fission chamber (12.7 cm active length, 2.54 cm diameter) and a preamplifier moderated by a polyethylene cylinder (3.5 cm thick polyethylene) was fabricated to use at Atucha. The system was designed to work with MMCA and software widely used by the IAEA. The SFNC was used to collect neutron signals from the assemblies with burn ups of 5000 to 8000 MWD/TU. The measurement results, while limited in the number of data points, showed that the calibration curve was sufficiently linear for the purpose. The detector system was placed 2.4 m below the top of the fuel assemblies and this vertical position was maintained for measurements.

After subsequent field trials, for the re verification of the spent fuels in the ponds, the use of a SFNC and, when applicable, to the irradiated fuel assemblies with low cooling time, an ICVD was defined.

## **SAFEGUARDS ACTIVITIES AT ATUCHA I NPP**

The diversion scenarios were covered by the combination of physical and auditing verification activities, complemented with containment and surveillance measures. The auditing activities are supported by operational and accounting records and reports handled by the operator during the inspections.

As the timeliness verification goal for irradiated fuel is three months, routine inspections are performed with a frequency of 4 inspections per year, 3 interim inspection and 1 Physical Inventory Verification (PIV).

The main changes due to the installation of the VIFM in terms of inspection activities are:

- ❖ Downloading of the images from the surveillance system at the manoeuvring pond in House 1.
- ❖ Taking of the reports of the VIFM system.
- ❖ Comparison between the VIFM reports and the operational records.

## **CONCLUSIONS**

- The testing and installation of the unattended system (VIFM) together with the re-verification of the spent fuel inventory (ICVD and SFNC) has allowed the facility to fully fulfil current Agency and ABACC safeguards requirements.
- It can be drawn that with the performed activities the inspection goals at the facility and at State level will be fully reached and the safeguards approach for this NPP is fully

satisfied. The co-operation between ABACC, IAEA and ARN in the searching for a technological solution helped to obtain in the foreseen time positive results. The co-operation provided by the operator, during the whole process, is also worthy mentioning.

- The identification and successful test and use of the SFNC that allows the verification of the difficult to access spent fuels stored in the lower layer and to those fuels with long cooling time, is available in case a C&S system failure.
- Both, the VIFM system and the SFNC technique did not imply any relevant construction modification to the facility.
- From ARN and Operator's point of view the unattended system is less intrusive than the unannounced inspection regime that ARN had initially studied as a possible option. Nevertheless, in case the VIFM system does not work properly, further consideration might be given to this option if it proves to be cost-effective and once appropriate arrangements between ARN, the Operator, ABACC and IAEA have reached.
- Co-operation is essential to improve safeguards effectiveness and efficiency. To ensure the implementation of cost-effective safeguards, it is important to promote a full understanding of the safeguards requirements and the technical goals and to take due account of the specificities of the facilities. This can be achieved by maintaining a permanent dialogue between the SSACs and the IAEA, and in our case also with ABACC.

## REFERENCES

1. **ALTERNATIVES TO REACH SAFEGUARDS GOALS AT ATUCHA I NUCLEAR POWER PLANT.** PALACIOS E., ORPET P. M., MARZO M - Argentine and Brazilian Accounting and Control Agency (ABACC) VICENS H., VALENTINO L. - Nuclear Regulatory Authority of Argentina (ARN). Presented in the Annual Meeting of the INMM-2000.
2. **SAFEGUARDS CRITERIA 1991- 1995 / 1990-11-21** (including updates).

# Calibración de un sistema de espectrometría multiesfera para campos de neutrones

Carelli, J.L.; Cruzate, J.A.; Papadópolos, S.;  
Gregori, B.N. y Ciocci, L.



# CALIBRACIÓN DE UN SISTEMA DE ESPECTROMETRÍA MULTIESFERA PARA CAMPOS DE NEUTRONES

Carelli, J.L.; Cruzate, J.A.; Papadópolos, S.; Gregori, B.N. y Ciocci, L.

Autoridad Regulatoria Nuclear  
Argentina

En este trabajo se presenta la calibración del sistema espectrométrico de neutrones de la Autoridad Regulatoria Nuclear (ARN) en el Institut de Protection et Sûreté Nucléaire (IPSN), Laboratoire d'Etudes et de Recherches en Dosimetría Externa, Cadarache, Francia.

El sistema multiesfera está compuesto de 9 esferas de polietileno de alta densidad, con un detector gaseoso de  $^3\text{He}$  y la electrónica asociada. La matriz de respuesta energética a neutrones del sistema se obtuvo aplicando el código MCNPX para el rango de energías comprendidos entre térmicos y 100 MeV con secciones eficaces tomadas de la biblioteca ENDF/B-VI. El espectro de neutrones resultante del sistema multiesfera se logró aplicando el código de deconvolución LOUHI82.

En este trabajo se presentan las relaciones entre la respuesta teórica y la experimental obtenidas con las fuentes de AmBe y  $^{252}\text{Cf}$ .

## INTRODUCCIÓN

El conocimiento de la distribución espectral de neutrones es esencial para la evaluación de las magnitudes dosimétricas de aplicación en Protección Radiológica, dosis equivalente personal,  $\text{Hp}(10)$  y la dosis equivalente ambiental,  $\text{H}^*(10)$ . El sistema espectrométrico multiesfera (ME) permite caracterizar, los espectros de neutrones en los ambientes de trabajo, por ej. reactores experimentales y de potencia, aceleradores médicos, tripulaciones en vuelo. La combinación de un detector térmico con esferas moderadoras resulta en un sistema sensible a neutrones en todo el rango energético. La sensibilidad de cada esfera a una energía particular de neutrones depende de su diámetro. La respuesta del conjunto de esferas es la base para obtener información sobre el espectro analizado.

La calibración del ME realizada en el Institut de Protection et Sûreté Nucléaire (IPSN), Laboratoire d'Etudes et de Recherches en Dosimetría Externa, Cadarache, Francia, se llevó a cabo irradiando cada una de las esferas, individualmente, en campos de referencia, de acuerdo a las normas ISO 8529-2 (1). Los campos de radiación utilizados fueron  $^{252}\text{Cf}$ , AmBe, AmBe+Pb,  $^{252}\text{Cf+D}_2\text{O}$ ,  $^{252}\text{Cf+D}_2\text{O}/\text{Cd}$  y campos reales. El trabajo describe los resultados obtenidos para AmBe y  $^{252}\text{Cf}$ .

## ESPECTROMETRÍA DE NEUTRONES

El sistema espectrométrico utilizado está constituido por un detector proporcional de  $^3\text{He}$  de 1.25" de diámetro a una presión de 128kpa, marca Centronic, modelo SP9 y esferas moderadoras de polietileno ( $0.95 \text{ g cm}^{-3}$ ) cuyos diámetros son 3.5", 4.2", 5", 6", 7", 8", 9", 10", 12". El detector se coloca en el centro de cada una de las esferas y tiene asociada una electrónica que permite el análisis del espectro de salida. La integral de los pulsos bajo la curva correspondiente a la reacción  $^3\text{He}(\text{n},\text{p})\text{T}$  son los datos iniciales del sistema para el código de

deconvolución LOUHI82 (2), de forma de obtener la distribución espectral. La esfericidad del sistema y la densidad del material de las esferas fue evaluada en el Instituto Nacional de Tecnología Industrial (INTI) de Argentina.

La matriz de respuesta del ME, mostrada en el Gráfico 1, se obtuvo por medio del código MCNPX 2.1.5E (3) para el rango de energías comprendidas entre térmicos y 100 MeV y la biblioteca de secciones eficaces ENDF/B-VI.

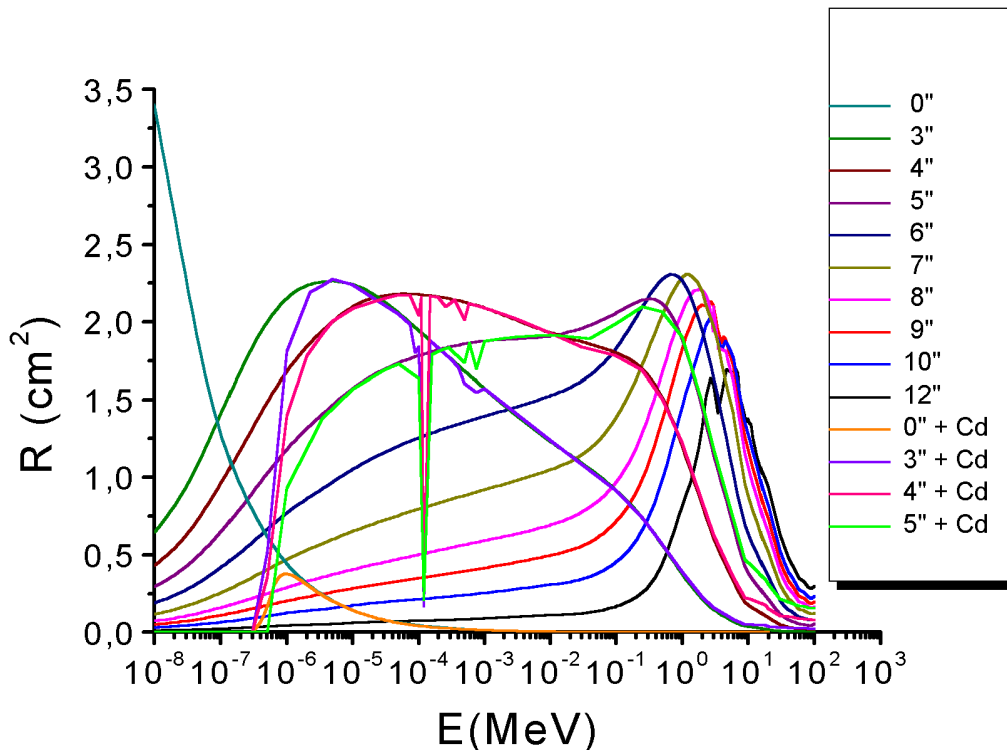


**Gráfico 1:** Matriz de respuesta del sistema ME con He 3.

## CALIBRACIÓN

Se aplicó el protocolo de calibración de Cadarache, consistente en la aplicación de los espectros obtenidos por cálculo y medidas directas. Las irradiaciones se realizaron para el conjunto detector - esfera 5 veces, durante un lapso suficiente para minimizar el error asociado  $((1/n)^{1/2})$ . La fuente (en cada uno de los casos considerados) fue colocada a 75 cm de distancia del centro de la esfera. Se estudió el efecto de la dispersión aplicando el método del cono de sombra.

La respuesta para cada esfera en cada condición de irradiación fue comparada con el correspondiente resultado de aplicar el código MCNPX 2.1.5 E a la simulación de la condición real de irradiación. El gráfico 2 muestra el cociente entre los valores teóricos y experimentales, según se trate de AmBe y  $^{252}\text{Cf}$ . El valor medio del cociente entre respuesta teórica y experimental para el conjunto de esferas es, para el AmBe de  $0.99 \pm 14\%$  ( $n=9$ ,  $\sigma=2$ ); para el  $^{252}\text{Cf}$  es  $1.03 \pm 10\%$  ( $n=9$ ,  $\sigma=2$ ).

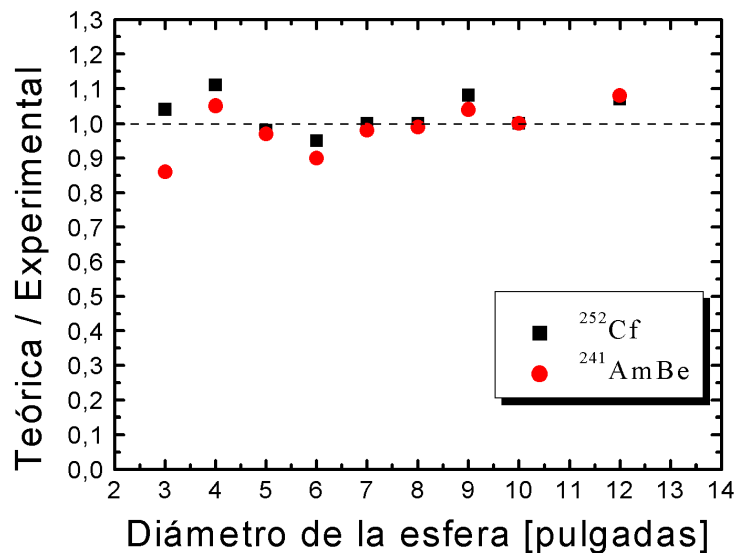


**Gráfico 2:** Comparación entre respuestas teórica y experimental para <sup>252</sup>Cf y AmBe

El programa LOUHI 82 fue aplicado para, a partir de las mediciones de cada esfera, obtener el espectro y la magnitud dosimétrica dosis equivalente ambiental H\*(10). La comparación entre la magnitud H\*(10) obtenida a partir de los datos experimentales y la obtenida del espectro de referencia de la fuente de <sup>241</sup>AmBe según la fluencia informada difieren en menos del 5%. La misma calidad de resultado se obtiene para el <sup>252</sup>Cf.

## CONCLUSIONES

La calibración del ME en el IPSN de Francia permitió validar la metodología teórica aplicada para la caracterización del sistema espectrométrico.

La incertezza en las magnitudes evaluadas a partir de un espectro obtenido por deconvolución es un tema actualmente en discusión y depende fuertemente del código aplicado. El apartamiento en las respuestas de cada esfera particular no reviste mayor incidencia en la incertezza total asociada a las magnitudes dosimétricas.

## REFERENCIAS

- [1] ISO Neutron Reference Radiations for Calibrating Neutron-Measuring Devices Used for Radiation Protection Purposes and for Determining their Response as a Function of Neutron Energy. International Standard ISO 8529-3:1998(E) (International Organization for Standardization, Geneve, Suiza) (1998).
- [2] Routti, J.T. And Sandberg, J.V., General Purpose Unfolding Program LOUHI78 with Linear and Nonlinear Regularisations. Comput. Phys. Commun. 21 (1980) 119-144.

[3] Los Alamos National Laboratory, TPO-E83-G-UG-X-00001, Nov 14, 1999. MCNPX<sup>TM</sup> User's manual, Version 2.1.5, Laurie S. Waters, Editor.

[4] Comisión Internacional de Protección Radiológica "Conversions Coefficients for use in Radiological Protection against External Radiation". Pergamon Press. CIPR Publicación 74. (1997)

# Caracterización de los detectores termoluminiscentes LiF:Mg,Cu,P. Aplicaciones a la dosimetría ambiental

Ciocci, L.; Gregori; B.N.; Papadópolos; S. y Carelli, J.L.



# CARACTERIZACIÓN DE LOS DETECTORES TERMOLUMINISCENTES

## LiF:Mg,Cu,P

### Aplicaciones a la dosimetría ambiental

Ciocci Brazzano, L.; Gregori, B.N.; Papadópolos, S. y Carelli, J.L.

Autoridad Regulatoria Nuclear  
Argentina

En este trabajo se estudian las propiedades termoluminiscentes de los detectores LiF:Mg,Cu,P enriquecido con Li-7 (99,93% de Li-7 y 0,07% de Li-6): optimización del perfil de calentamiento, pérdida de información, límite de detección y respuesta en dosis y en energía. Su desempeño es comparado con el de los detectores LiF:Mg,Ti enriquecido con Li-7 (99,93% de Li-7 y 0,07% de Li-6), que son los utilizados actualmente para dosimetría ambiental por el laboratorio de Dosimetría Física de la Autoridad Regulatoria Nuclear.

## 1. INTRODUCCIÓN

En dosimetría ambiental es necesario medir dosis del orden de los  $10 \mu\text{Gy}$ . Para esto se necesita un detector que posea una alta sensibilidad, como es el caso de los TLD 700H. Es en este contexto que se plantea en la ARN el estudio de estos.

## 2. MÉTODOS Y RESULTADOS

Se utilizaron detectores LiF:Mg,Cu,P enriquecido con Li-7 marca BICRON- HARSHAW (TLD 700H). El equipo utilizado fue un lector manual HARSHAW 3500 QS.

### 1. Optimización del perfil de calentamiento

Se optimizaron velocidad de calentamiento y temperatura máxima de calentamiento, utilizando dos grupos de detectores irradiados a igual dosis. Los parámetros iniciales de prueba se obtuvieron de la literatura. La selección del perfil de calentamiento se realizó con criterios: **minimización en dosis residual (segunda lectura) y aprovechamiento de curva glow.**

Parámetros seleccionados: velocidad de calentamiento:  $15^\circ \text{C/s}$ ; temperatura máxima de calentamiento:  $276^\circ \text{C}$ .

Para irradiación a **altas dosis** (del orden de  $2 \text{ mGy}$ ) se necesitaron hacer hasta **6 lecturas para eliminar la dosis residual**.

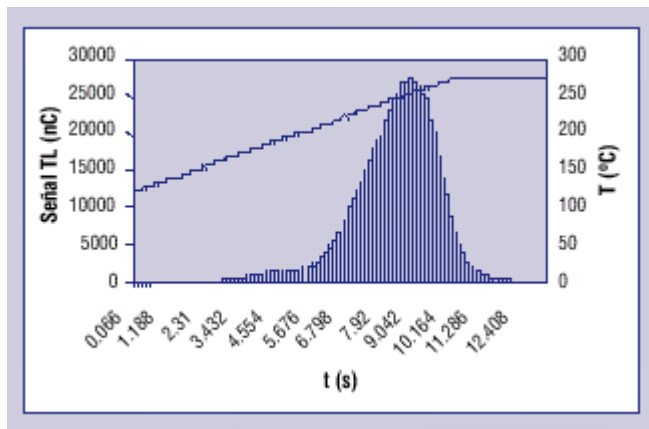


**Figura 1.** Curva glow correspondiente al tratamiento seleccionado

## 2. Respuesta de dosis

Estudio de respuesta en dosis de rango:  $50 \mu\text{Gy} - 120 \text{ mGy}$ . Cálculo del índice de supralinealidad definido como

$$f(D) = \frac{F(D)/D}{F(D_1)/D_1}$$

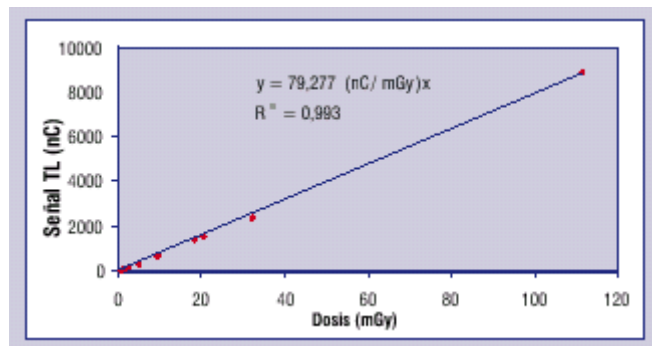


**Figura 2.** Curva de respuesta en dosis

No se encontraron regiones supralineales en el rango estudiado, siendo  $f(D) = 1$ .

## 3. Respuesta en energía

Se estudió la respuesta en energía de los detectores para rayos x con calidades W60, W110, W200; Cs-137 y para radiación  $\beta$  con P-32 ( $E_{\beta\text{máx}} = 1,7 \text{ MeV}$ ).

**Tabla 1**  
Respuesta de energía, relativa a Cs-137  
para RX (calidades W60, W110 y W200) y radiación  $\beta$ .

Calidad ISO	Respuest relativa a Cs-137
W60 (45 keV)	0,41
W110 (79 keV)	0,64
W200 (137 keV)	0,65
Radiación $\beta$	Respuesta relativa a Cs-137
P-32 ( $E_{\beta\text{máx}} = 1,7 \text{ MeV}$ )	1,22

## 4. Pérdida de información

Irradiación de 24 detectores con Cs-137, leídos en grupos de tres con distintos tiempos de almacenamiento (medido desde el momento de la irradiación). Cálculo del cociente entre lectura a tiempo cero con lectura a tiempo de almacenamiento, que varía entre 0 h y 42 días (1008 h).

**Tabla 2**  
Valores de fading obtenidos a distintos tiempos de almacenamiento

Tiempo de almacenamiento (h)	Porcentaje señal inicial (%)
0	100
17,5	98,5
22,7	98,8
67,5	98,3
94,7	104,7
1008	77

## 5. Límite de detección

Se leyó un conjunto de detectores sin irradiar, y se hizo un estudio estadístico de los mismos, encontrando que la expresión más adecuada para calcular el límite de detección era:

$$Ld = 3\sigma$$

Donde  $\sigma$  es la dispersión en las mediciones. El valor encontrado fue  $Ld = (0,440 \pm 0,2) \mu\text{Gy}$

## 6. Comparación de sensibilidades con TLD 700

Sensibilidad TLD 700 H  $\cong 10^*$  Sensibilidad 700

## 3. CONCLUSIONES Y PERSPECTIVAS

En el rango de dosis relevante a estudios ambientales

- no se observan efectos no lineales, por lo que no es necesario aplicar factores de corrección.
- no es necesario hacer más de una lectura para eliminar la dosis residual.

La sensibilidad de estos detectores es aproximadamente 10 veces mayor que la de los TLD700.

Todas estas características de estos detectores los hacen ideales para el trabajo en dosimetría ambiental. Actualmente se están haciendo pruebas de campo con los mismos.

## 4. REFERENCIAS

- [1] Y.S. Horowitz; "LiF:Mg,Ti versus LiF:Mg,Cu,P: the competition heats up"; Rad. Prot. Dosim.; 47; 135-141; (1993).
- [2] J.C. Sáez-Vergara, A.M. Romero; "The influence of the heating system on the hypersensitive thermoluminescent material LiF:Mg,Cu,P (GR- 200)"; Rad. Prot. Dosim.; 66; 431-436; (1996).
- [3] L. Oster, Y.S. Horowitz, A. Horowitz; "Glow curve readout of LiF:Mg,Cu,P (GR200) chips at maximum temperature between 240°C and 280°C: Elimination of the residual signal"; Rad. Prot. Dosim.; 49; 407-411; (1993).
- [4] A. Horowitz, Y.S. Horowitz; "Elimination of the residual signal in LiF:Mg,Cu,P"; Rad. Prot. Dosim.; 40; 265-267; (1992).
- [5] M. Budzanowski et ál.; "The fading of different peaks in LiF:Mg,Cu,P (MCP-N and GR-200A) TL detectors"; Rad. Meas.; 29; 361-364; (1998).
- [6] A.C. Traino et ál.; "Influence on background exposure on TLD minimum dose detection and determination limits"; Rad. Prot. Dosim.; 78; 257-262; (1998).



## **PARTE II**

### **RESÚMENES DE PUBLICACIONES EN REVISTAS**



# CHROMOSOME ABERRATIONS INDUCED IN HUMAN LYMPHOCYTES BY HEAVY CHARGED PARTICLES IN TRACK SEGMENT MODE<sup>\*</sup>

Di Giorgio, M.<sup>1</sup>; Edwards, A.A.<sup>2</sup>; Moquet, J.E.<sup>2</sup>; Finnion, P.<sup>2</sup>; Hone, P.A.<sup>2</sup>; Lloyd, D.C.<sup>2</sup>;  
Kreiner, A.J.<sup>3,4,5</sup>, Schuff, J.A.<sup>3</sup>; Taja, M.R.<sup>1</sup>; Vallerga, M.B.<sup>1</sup>; López, F.O.<sup>2</sup>;  
Burlón, A.<sup>3,4</sup>; Debray, M.E.<sup>3,4</sup> and Valda, A.

<sup>1</sup> Autoridad Regulatoria Nuclear, Argentina

<sup>2</sup> National Radiological Protection Board, Reino Unido

<sup>3</sup> Comisión Nacional de Energía Atómica, Argentina

<sup>4</sup> Escuela de Ciencia y Tecnología, UNSAM, Argentina

<sup>5</sup> CONICET, Argentina

Human blood was irradiated with accelerated ions: 20 MeV  $^4\text{He}$ , 425 MeV  $^{12}\text{C}$  and 1480 MeV and 996 MeV  $^{16}\text{O}$ . For each ion, the blood was exposed to a range of doses as thin specimens in the track segment mode, so that irradiations took place at nearly constant LETs of 31.4, 61, 52 and 69 keV  $\mu\text{m}^{-1}$ , respectively. Lymphocytes were cultured to the first in vitro metaphase, analysed for chromosomal damage and the dicentric aberration frequencies fitted to the linear quadratic model of dose-response. For these high LET radiations, the linear ( $\alpha$ ) yield coefficient predominated and increased with LET, at least up to 60 keV  $\mu\text{m}^{-1}$ . Apart from the 996 MeV oxygen ions, the data indicated the presence of a quadratic ( $\beta$ ) coefficient, statistically consistent with values obtained with low LET radiations. However, the associated uncertainties on the measured  $\beta$  values were large, illustrating the general problem that  $\beta$  is more difficult to measure against a dominating and ever-increasing  $\alpha$  term. The existence or otherwise of a  $\beta$  component of the dose-response at these radiation qualities has important consequences for modelling mechanism of aberrations induction by radiation.

---

\* Publicado en: Radiation Protection Dosimetry Vol. 108, no. 1, p. 47-53, 2004.

**PHARMACOLOGICAL INHIBITION OF DNA REPAIR ENZYMES  
DIFFERENTIALLY MODULATES TELOMERASE ACTIVITY  
AND APOPTOSIS IN TWO HUMAN LEUKAEMIA CELL LINES\***

Dubner, D.L.<sup>1</sup>; Perez, M. del R.<sup>1</sup>; Michelin, S.C.<sup>1</sup>; Bourguignon, M.<sup>2,3</sup>; Moreau, P.<sup>2</sup>;  
Carosella, E.D.<sup>2</sup> and Gisone, P.A.<sup>1,2</sup>

<sup>1</sup> Autoridad Regulatoria Nuclear, Argentina

<sup>2</sup> Commissariat à l'Energie Atomique, Hôpital Saint-Louis, Francia

<sup>3</sup> Faculté de Médecine de Paris-Île-de France Quest et DGSNR, Francia

**Purpose:** To investigate the effect of wortmannin and 3-aminobenzamide (3-AB) on telomerase activity and apoptosis in two human leukaemia cells.

**Materials and methods:** MOLT-4 (p53-wild type) and KGla (p53-null) cells were irradiated with  $\gamma$ -rays (3 Gy at 1.57 Gy min<sup>-1</sup>) and the effects of wortmannin and 3-AB were evaluated. Telomerase activity was measured by polymerase chain reaction and the expression of human telomerase reverse transcriptase, human telomerase RNA and telomerase-associated protein 1 was assessed by reverse transcriptase-polymerase chain reaction. Apoptosis was evaluated by fluorescence microscopy and flow cytometry.

**Results:** A radiation-induced up-regulation of telomerase activity was observed from 4h post-irradiation, coinciding with an accumulation of human telomerase reverse transcriptase mRNA. Apoptosis and G2/M arrest were evident from 4h post-irradiation in MOLT-4 cells. KGla cells exhibited a G2/M block at 24 h post-irradiation and apoptosis increased between 24 and 48 h post-irradiation. 3AB abolished G2/M blockage and enhanced radiation-induced apoptosis in both cell lines, while wortmannin increased apoptosis only in MOLT-4 cells.

**Conclusions:** 3-AB inhibits the radiation-associated telomerase activity increase and enhances apoptosis in MOLT-4 and KGla cells. Wortmannin, which also inhibits the radiation-associated telomerase activity increase in both cell lines, does not modify radiation-induced apoptosis in KGla cells. DNA repair enzymes might be selective targets for enhancing radiosensitivity in certain tumour cells.

---

\* Publicado en: International Journal of Radiation Biology; Vol. 80, no. 8, p. 593-606, 2004.

## **INTEGRATED SAFEGUARDS: EXPECTATIONS AND REALITIES\***

Fernández Moreno, S.

Autoridad Regulatoria Nuclear  
Argentina

The IAEA's safeguards system is a fundamental pillar of the nuclear non-proliferation regime. The existence of credible international safeguards is today more important than ever. In essence, international safeguards constitute a system of confidence building. This concept indicates that the system must be based on international cooperation and it must stand on technical independent competence, expert judgment and non-discriminatory basis and must be widely endorsed by the international community.

In recent years, the IAEA in cooperation with its Member States has significantly progressed in designing and implementing integrated safeguards (IS). A "Conceptual Framework" to combine safeguards measures and technologies has already been established and the IAEA is giving priority to the completion of IS approaches for generic facility types and at the level of the States.

There is a broad range of views and expectations of what IS should be. In general, it has been recognized that IS provides a unique opportunity to design at the level of States a strengthened and more efficient safeguards system. It has also been recognized that IS allows for the greatest degree of adaptation and reduction of traditional safeguards measures and that safeguards implementation and evaluation should be less prescriptive and rigid in comparison to today's approach. Another important aspect of IS is the role of the review and evaluation by the IAEA of all relevant information in drawing safeguards conclusions. The existence of a well-understood, transparent and objective methodology to perform this activity is of fundamental importance to maintain the credibility of the verification system.

The introduction of modern technologies coupled with the intensification of the use of short notice, unannounced inspections, randomization and unpredictability together with the increasing cooperation between the IAEA and the States systems of accounting and control of nuclear materials (single or regional) are important elements of this new safeguards system.

The paper discusses a number of issues and expectations surrounding IS, in particular the analysis of the current state of the development of IS, the expectations of what IS should be and the challenges that still need to be addressed.

---

\* Publicado en: Journal of Nuclear Materials Management; Vol. 32, no. 4, p. 40-43, 2004

# THE EFFECT OF WALL FRICTION IN SINGLE-PHASE NATURAL CIRCULATION STABILITY AT THE TRANSITION BETWEEN LAMINAR AND TURBULENT FLOW\*

Ambrosini, W.<sup>1</sup>; Forgione, N.<sup>1</sup>; Ferreri, J.C.<sup>2</sup>; Bucci, M.<sup>1</sup>

<sup>1</sup> Università di Pisa, Nucleare e della Produzione, Italia

<sup>2</sup> Autoridad Regulatoria Nuclear, Argentina

The present paper is focused on the prediction of stability of single-phase natural circulation in the range of Reynolds numbers characterizing the transition between laminar and turbulent flow. In particular, the predictions obtained by one-dimensional models making use of different assumptions for evaluating wall friction at this transition are discussed, also in front of experimental information from previous investigations.

The starting point of the analysis is the discrepancy observed in the prediction of the linear stability behaviour of an unstable experimental loop obtained by thermal-hydraulic system codes adopting different friction laws. An in-depth investigation of the reasons for such discrepancy is made with the aid of computer programs developed for the one-dimensional linear and non-linear stability analysis of single-phase natural circulation loops. The programs allowed obtaining linear stability maps for the considered loop, which clearly show the effects of the assumptions made in dealing with friction at the transition between laminar and turbulent flow. The available information on the appropriate closure laws for friction in natural circulation, with particular emphasis on the transitional regime, is also discussed. Non-linear effects, coming into play when transient calculations are started far enough from the system fixed point, are shown to have a relevant role in the predicted stability behaviour. Finally, preliminary results obtained by the application of a computational fluid-dynamic code in the analysis of stability in the addressed loop are presented to point out an interesting field of future investigation.

---

\* Publicado en: Annals of Nuclear Energy; Vol. 31, no. 16, p. 1833-1865, 2004

## **THE ROLE OF NITRIC OXIDE IN THE RADIATION-INDUCED EFFECTS IN THE DEVELOPING BRAIN**

Gisone, P.A.<sup>1</sup>; Dubner, D.L.<sup>1</sup>; Perez, M. del R.<sup>1</sup>; Michelin, S.C.<sup>1</sup> and Puntarulo, S.<sup>2</sup>

1 Nuclear Regulatory Authority, Argentina

2 Scholl of Pharmacy and Biochemistry, University of Buenos Aires, Argentina

The immature and adult brain display clear differences in the way they respond to insults. The effects of prenatal irradiation on the developing brain are well known. Both epidemiological and experimental data indicate that ionizing radiation may disrupt developmental processes leading to deleterious effects on post-natal brain functions. A central role of reactive oxygen and nitrogen species (ROS/RNS) as important mediators in both neurotoxicity and neuroprotection has been demonstrated. However; data concerning the role of ROS/RNS in radiation-induced damage in the developing brain are scarce. The goal of this review was to summarize the current studies concerning the role of nitric oxide and its reactive intermediates in activation of signal transduction pathways involved in cellular radiation response, with particular focus on radiation-induced effects in the developing brain.

---

\* Publicado en: In Vivo; Vol. 18, no.3, p. 281-292, 2004

**INCREASED ACTIVITY AND INVOLVEMENT OF CASPASE-3  
IN RADIATION-LNDUCED APOPTOSIS IN NEURAL CELLS PRECURSORS  
\* FROM DEVELOPING RAT BRAIN**

Michelin, S.C.; Perez, M. del R.; Dubner, D.L. and Gisone, P.A.

Nuclear Regulatory Authority  
Argentina

Using primary cultures of neural precursor cells of cortex from developing rat brain, we demonstrated the involvement caspase-3 in the apoptotic process induced by gamma irradiation. The precursor nature of cells was confirmed by nestin and GFAP immunoreactivity and by the capacity of differentiation in neuronal and glial cells after 5 days in culture.

Neural precursors were irradiated with single doses ranging from 0.1 to 4 Gy. Cellular death, determined 24 h post- irradiation (pi) was dose-dependent and the induction of apoptosis was confirmed by nuclear condensation, DNA fragmentation and hypodiploid DNA peak represented by the sub G1 region. For the higher doses apoptosis was evident after 4-6 h pi and increased during 24 h. Caspase-3 activity increased with doses and was maximal at 4-6 h pi with 3 Gy and remained similar with 4 Gy. The protection from radiation-induced apoptosis by caspase-3 inhibitor: zDEVD-fmk, confirmed that this enzyme is involved in the apoptotic mechanism in this system.

The possibility of using this tissue culture system for studying the effects of ionizing radiation on morphological and molecular differentiation w

---

\* Publicado en: Neurotoxicology; Vol. 25, no.3, p. 387,398, 2004

## ÍNDICE DE AUTORES

- Alvarez, D.E. 41  
Ambrosini, W. 308  
Arias, C. 3  
Bergic, R.M. 13  
Biaggio, A.L. 3  
Bomben, A.M. 13, 23  
Bonino, A.D. 283  
Bourguignon, M. 73, 306  
Boutet, L.I. 135  
Bruno, H.A. 135  
Bucci, M. 308  
Burlón, A. 41, 305  
Busto, E. 51  
Canoba, A.C. 145  
Carelli, J.L. 219, 297  
Carosella, E.D. 73, 306  
Cateriano, M. 273  
Ciallella, H.E. 33  
Ciocci Brazzano, L. 219, 297  
Clausse, A. 263  
Cristallini, O. 191  
Cruzaté, J.A. 115, 291  
Chiliutti, C.A. 23  
D'Amato, E. 263  
Davidson, J. 41  
Davidson, M. 41  
Debray, M.E. 41, 305  
Di Giorgio, M. 41, 51, 61, 305  
Dubner, D.L. 73, 105, 183, 306, 309, 310  
Edwards, A.A. 305  
Equillor, H.E. 85, 95, 115, 237  
Fernandez, J.A. 33, 95  
Fernández Moreno, S. 283, 307  
Ferreri, J.C. 308  
Finnon, P. 305  
Forgione, N. 320  
Gavini, R.M. 33, 95, 135  
Gisone, P.A. 73, 105, 175, 183, 306, 309, 310  
Gómez Parada, I. 221  
Gregori, B.N. 115, 291, 297  
Grinman, A.D.R. 95  
Hone, P.A. 305  
Kesque, J.M. 41  
Kreiner, A.J. 41, 305  
Kunst, J.J. 115  
Lerner, A.M. 123  
Lewis, E.C. 33  
Llacer, C.D. 283  
Lloyd, D.C. 305  
López, F.O. 41, 95, 135, 145, 305  
Maceiras, E. 155  
Madariaga, M.R. 123  
Mairal, L. 51  
Marabini, S. 245  
Medici, M.A. 253  
Michelin, S.C. 73, 105, 183, 201, 306, 309, 310  
Moquet, J.E. 305  
Moreau, P. 306  
Mühlmann, M. 165  
Nasazzi, N.B. 3, 165  
Otero, D. 165  
Ozafrán, M.J. 41  
Palacios, M.A. 95  
Papadópolos, S. 115, 291- 297  
Pérez, M. del R. 73, 105, 175, 183, 306, 309, 310  
Puntarulo, S. 183, 309  
Quintana, E.E. 33  
Rivera, E.S. 13  
Robello, E. 105, 183  
Rojas, C.A. 191  
Rojo, A.M. 201  
Rojo, M. 191  
Saavedra, A.D. 155  
Saint Martin, G. 41  
Sardi, M. 51  
Schuff, J.A. 41, 305  
Serdeiro, N.H. 217, 237, 245  
Siraky, G. 253  
Sobehart, L.J. 263  
Somacal, H. 41  
Stoliar, P. 41  
Taja, M.R. 41, 51, 61, 305  
Truppa, W.A. 273  
Valda, A. 41, 305  
Valentino, L.I. 283  
Vallerga, M.B. 41, 51, 61, 305  
Vázquez, M.E. 41  
Waldman, R.M. 123